Quantum chromodynamics at finite temperatures dans densities : a renormalization group resummation of perturbative series

Loïc Fernandez

THÈSE POUR OBTENIR LE GRADE DE DOCTEUR DE L'UNIVERSITÉ DE MONTPELLIER

En Physique Fondamentale

École doctorale i2S

Laboratoire Charles Coulomb: Intéractions fondamentales, astroparticules et cosmologie

Chromodynamique Quantique à températures et densités finies: resommation des séries perturbatives par le groupe de renormalisation.

Quantum Chromodynamics at finite temperatures and densities: a renormalization group resummation of perturbative series.

Présentée par Loïc FERNANDEZ
le 09/12/2022

Sous la direction de Jean-Loïc KNEUR

Devant le jury composé de

Hubert HANSEN, Maître de conférences, Université Claude Bernard Lyon 1	Rapporteur
Urko REINOSA, Chargé de recherche CNRS, CPHT, École Polytechnique	Rapporteur
Sacha DAVIDSON, Directeur de recherche CNRS, LUPM, Université de Montpellier	Présidente du Jury
Rudnei O. RAMOS, Professeur, Université d'état de Rio de Janeiro, Brésil	Examinateur
Jean-Loïc KNEUR, Directeur de recherche CNRS, L2C, Université de Montpellier	Directeur de thèse

UNIVERSITÉ DE MONTPELLIER

LABORATOIRE CHARLES COULOMB MONTPELLIER

À mes parents

Abstract en Français

Cette thèse couvre les recherches conduites à l'université de Montpellier, durant les trois années de contrat financés par l'école doctorale I2S, dans le contexte de la théorie quantique des champs dans un milieu dense et chaud. Cette théorie est un cadre de travail permettant de décrire les champs quantiques à températures et densités finies. Un intérêt spécial est donné au groupe de renormalisation et ses propriétés afin de définir un meilleur schéma de resommation des divergences infrarouges qui affligent la théorie quantique des champs dans un milieu thermal. Nous commençons par définir la méthode dite "renormalization group optimized perturbation theory" (RGOPT), consistant à optimiser la série perturbative en accord avec le groupe de renormalisation, un cadre de travail permettant de resommer les divergences infrarouges, puis nous discutons son application dans différents modèles. Premièrement, l'application au modèle scalaire, plus simple que la chromodynamique quantique (QCD), au troisième ordre perturbatif où nous constatons une forte amélioration de la convergence de la série perturbative ainsi qu'une diminution drastique de la dépendence résiduelle d'échelle de renormalisation. Puis, nous explorons le cas de la QCD à haute densité et température nulle, où nous déterminons une resommation originale à tous les ordres des logarithmes dominants et sous-dominants. La discussion est ensuite étendue pour incorporer l'application de la méthode de resommation RG dans le secteur des quarks, et une première approche à l'extension de ce formalisme au secteur des gluons massifs, décrit par le formalisme Hard Thermal Loop (HTL), est exploré. Finalement, nous discutons une première application de cette méthode de resommation pour la détermination d'une équation d'état pour les étoiles à neutrons.

English Abstract

This Thesis covers research conducted at the University of Montpellier, during the three years of PhD contract financed by the doctorate school I2S, in the context of thermal quantum field theory. This theory is a framework for describing quantum fields in a medium, specifically at finite temperature and/or chemical potential (equivalently, density). A special focus is given to the renormalization group and its properties to define a better resummation scheme for the infrared divergences generically plaguing thermal field theory. We first define and apply a so-called renormalization group optimized perturbation theory (RGOPT), a resummation framework for the infrared divergences, for the specific case of the $\lambda\phi^4$ model at next-to-next-to-leading order, where we found sound results concerning the improvement of the convergence of the series expansion as well as a drastic improvement with respect to the residual arbitrary renormalization scale dependence. Cold and dense quantum chromodynamics is also explored, where we derived an original all order resummation of the leading logarithms as well as the so-called soft next-to-leading logarithms. The discussion is extended so as to include the application of RG resummation in the quark sector at next-to-next-to-leading order, and first developments for the specific case of massive gluons in the context of the Hard Thermal loop perturbation theory. Finally, a preliminary applications of this resummation procedure to the determination of an equation of state for neutron stars are discussed.

Remerciements

Je tiens à remercier mes parents, sans qui il ne m'aurait jamais été donné la chance de pouvoir poursuivre des études en physique théorique. Huit ans plus tôt, nous nous disputions parce qu'ils ne pensaient pas que j'arriverais à terminer mes études. Et pourtant, ils m'ont fait confiance, ils m'ont permis d'apprendre librement et de trouver ma vocation. Aujourd'hui, je finis mes études, non sans mélancolie, car ce fût des merveilleuses années durant lesquelles j'ai appris tant de choses sur le monde dans lequel nous vivons. J'ai même eu la chance de pouvoir à mon tour contribuer, modestement, au domaine. Pour cela, je remercie également l'école doctorale i2S de Montpellier, qui a financé mes recherches pendant ces trois années. Je suis tout particulièrement reconnaissant envers Andrea Parmeggiani qui a du certainement appuyer fortement ma candidature lors de l'évaluation. Grâce à la générosité de mon équipe, j'ai pu me rendre à des nombreuses conférences et écoles d'été après le confinement, pour cela, je leur suis infiniment reconnaissant.

Bien sûr, cela n'aurait jamais pu être possible sans la supervision de Jean-Loïc durant ces trois dernières années. Il y a eu des hauts et des bas de mon côté, le covid-19 n'ayant certainement pas aidé. Mais malgré cela, Jean-Loïc est toujours resté à mes côtés pour m'aider à avancer et à me faire voir la lumière au bout du tunnel. Merci pour tout ces moments partagés ensemble qui auront été si instructifs. À nos après-midi, penchées au-dessus de nos feuilles de calculs à s'arracher les cheveux sur HTL. Nous nous serons bien creusé la tête ensemble pour démêler toutes ces équations, et quel ne fût pas notre bonheur, chaque fois que nous avions une illumination sur le sujet. Finalement, c'est cela qui me plaît le plus dans ce métier et qui me donne envie de continuer.

Ces trois années à Montpellier furent très enrichissantes autant sur le plan professionnel que personnel. J'ai rencontré tellement de personnes incroyables ici avec qui j'ai passé des moments inoubliables. Mes premières rencontres furent certainement les meilleures puisque après tout ce temps nous faisons toujours les quatre cents coups ensembles. Merci à vous Guillaume, Luc, Richard et Matti (classé par ordre de rencontre, pas de malentendu !) pour ces moments formidables. Sans oublier ceux rencontrés en cours de route : Alex, Thomas, Émeline, Lucas...

Merci à toi, Laura, pour m'avoir fait grandir, mais aussi pour m'avoir appris à rester l'enfant joueur qui est en moi. Merci à mes deux meilleurs amis de toujours, Matteo et Charles, avec

qui on refait systématiquement le monde depuis notre canapé. On s'éloigne toujours plus (géographiquement parlant) mais on reste soudés comme au premier jour.

Et enfin, merci Emma pour cette année passée avec toi. La vie peut être assez tumultueuse à mes côtés comme tu t'en es rendue compte, mais tu n'as pas lâchée prise et su garder patience.

Ce n'est certainement pas la fin, seulement le commencement. Le commencement d'un voyage qui débutera dans le grand froid du Nord, à Helsinki, aux côtés de Risto Paatelainen et d'Aleksi Vuorinen.

Je pars de ce pas m'équiper, car certes, l'hiver est rude, mais il apporte toujours ses merveilles avec lui.

Author's publications

The following publications are (partially) included in the printed version of this Thesis. The original versions: (the authors are listed in alphabetical order in accordance with the convention used in particle physics):

- Loïc Fernandez and Jean-Loïc Kneur. All order resummed leading and next-to-leading soft modes of dense QCD pressure. arXiv:2109.02410.
  Accepted in Physical Review Letters.
- Loïc Fernandez and Jean-Loïc Kneur. Renormalization group optimized $\lambda\phi^4$ pressure at next-to-next-to-leading order. Phys. Rev. D, 104:096012, Nov 2021.
  URL: https://link.aps.org/doi/10.1103/PhysRevD.104.096012,
  doi:10.1103/PhysRevD.104.096012
- Loïc Fernandez and Jean-Loïc Kneur. Renormalization group improvement in cold and dense QCD pressure. To be submitted to ArXiv.

The first two publications have been peer-reviewed while the last one will be submitted to ArXiv soon.

Résumé en Français

Introduction

Lors des années 1950, l'invention des chambres à bulles a apporté avec elle la découverte d'un grand nombre de particules, les hadrons, aux propriétés bien différentes. Un tel nombre, qu'il fût vite évident que toutes ces particules ne pouvaient pas être fondamentales, mais plutôt des structures composites, formées d'encore plus petites particules. Cette façon de penser étant motivée par l'histoire de la recherche, et le fait que très souvent, la physique à très petites échelles se révèle plus simple que de prime abord suite à la découverte d'une ou plusieurs symmétries sous-jacentes. Gell-Mann et Zweig furent les premiers à proposer en 1963, indépendamment, un modèle avec une particule plus fondamentale existant en trois saveurs différentes, qui permettaient alors de reconstituer la pléthore de particules hadroniques observées. De ces trois saveurs de quark, les deux premières : *up* et *down* vinrent reconstituer les protons, les neutrons et les pions. Tandis que différents mélanges avec la troisième saveur : *strange* expliquaient les propriétés des kaons. Ce modèle initial fut amélioré à plusieurs reprises durant la décennie qui suivit afin notamment de coller avec la théorie de l'interaction électrofaible. Trois autres quarks vinrent ainsi s'ajouter à l'édifice : le *charm*, le quark *beauty* et enfin le quark *truth*[1]. Cependant, à ce stade, rien n'expliquait pourquoi ces quarks restaient liés au sein des hadrons, ni comment certaines particules composites ne pouvaient même exister puisqu'elles étaient en conflit avec le principe d'exclusion de Pauli. Ce principe stipule que deux particules fermioniques (tels que les quarks) ne peuvent se trouver simultanément *exactement* dans le même état quantique. Ces deux problèmes trouvèrent naturellement leurs réponses en donnant

[1]Il s'agit d'une vieille appellation qui n'a pas perduré, mais elle est préférée par l'auteur. Les quarks sont désormais appelés up, down, strange, charm, bottom and top.

un nouveau nombre quantique aux quarks: la charge de couleur. Ainsi, chacun des quarks pouvait exister sous trois couleurs différentes, par analogie avec la lumière, et l'interaction de ces couleurs permettait d'expliquer les états liés de quarks. Ce nouveau nombre quantique permettait ainsi aux quarks de ne pas être exactement dans le même état quantique, et le principe d'exclusion de Pauli, d'être satisfait. Les gluons émergèrent alors naturellement comme les médiateurs de cette interaction. Une différence fondamentale entre les gluons et les photons (les particules de lumière) est que ces derniers ne possèdent pas de charge électrique (la charge de l'interaction qu'ils véhiculent), tandis que les gluons possèdent une charge de couleur (et une autre d'anti-couleur), ce qui leurs permet d'interagir entre eux. Cette théorie est désormais communément appelée la Chromodynamique Quantique (QCD) et prend tout son sens au sein du formalisme de la théorie quantique des champs. Nous parlons également d'interaction forte pour l'interaction entre hadrons, vue désormais comme une interaction effective, due à celle plus fondamentale de la QCD.

Le confinement de la couleur

Si les quarks n'avaient pas été observés expérimentalement au préalable, c'est que ceux-ci devaient être confinés dans les hadrons (protons, neutrons, pions...). L'interaction doit ainsi croître exponentiellement avec la distance séparant les quarks, expliquant pourquoi nous n'observons jamais de quark libre, et inversement, être presque nulle lorsque les quarks sont très proches les uns des autres. Sinon ils seraient forcés de se condenser en un seul point, ce qui amènerait à une singularité.

Jusqu'à aujourd'hui, il n'y a pas de preuve mathématique rigoureuse de cette propriété de la QCD. Pour cela, il faudrait pouvoir prouver que le potentiel d'interaction croit linéairement avec la distance. En électromagnétisme, ce potentiel (de Coulomb) est bien connu et peut être obtenu en résolvant les équations classiques de la force de Lorentz. En QCD, la résolution des équations classiques de la QCD, une analogie "non abélienne" des équations de Maxwell, est beaucoup plus compliqué dû aux auto-interactions des gluons[2]. Malgré de spectaculaires avancées dans le domaine, la solution nous échappe encore. Ce phénomène est pourtant d'une importance cruciale pour comprendre (en partie) l'origine de la masse dans l'univers observable. Bien que la masse des particules fundamentales (quarks, leptons...) soient générées par leurs interactions avec le champ de Higgs, cette masse ne représente qu'une infime partie de la masse des hadrons. Ainsi, l'énergie mise en jeu dans le confinement des quarks au sein des hadrons, ainsi que le phénomène de brisure de la symétrie chirale, est d'une importance essentielle pour expliquer la masse des hadrons, et par extension, de tous les atomes de l'univers observable.

[2]Une introduction sur ces concepts est présenté entre autre dans les célèbres cours de Feynman sur la chromodynamique quantique. Ceux ci furent en quelques sortes perdus durant des décennies puisque Feynman fût emporté par la maladie avant de les compléter. Un anciant étudiant de Feynman, James M.Cline, publia en 2020 une version originale des "Feynman Lectures on the Strong Interactions". Depuis, nombreuses revues plus modernes, et plus complètes, traitent du sujet.

Un milieu très chaud : le plasma de quarks et de gluons (QGP)

Cependant, ce comportement change sensiblement une fois que l'on chauffe les hadrons, ou qu'un grand nombre d'entre eux se retrouvent compressés dans un faible volume. On parle alors de densités, ou de façon équivalente techniquement pour les calculs, de potentiel chimique très élevé. Après des années de recherches, une transition de déconfinement fut observée dans les grands accélérateurs de particules du LHC au CERN à Genève et du RHIC à Brookhaven. À partir de deux mille milliards de degré Kelvin/Celsius, les quarks et les gluons deviennent tellement énergétiques que les quarks d'un hadron commencent à "voir" ceux d'un autre hadron. Ils peuvent alors interagir ensemble et la notion même d'hadron perd son sens. Ce comportement fut également confirmé par la QCD sur réseau, un modèle de l'interaction forte sur un espace-temps discrétisé qui permet de procéder aux simulations numériques sur des super-calculateurs. Bien que ce domaine du diagramme de phase de la QCD soit désormais bien connu, le domaine des "faibles" températures[3] et très hautes densités demeure plus mystérieux. Les collisionneurs d'ions lourds ne peuvent pour l'instant pas atteindre ce domaine tandis que les calculs sur réseau sont exclus à ce jour à cause du problème dit "du signe". Ce problème a pour origine les quarks avec un potentiel chimique. En tout généralité, il n'est pas toujours possible, pour la description des quarks sur le réseau, d'utiliser une approche stochastique, nécessaire aux calculs sur réseau. Notre meilleur espoir, pour l'instant, de mieux comprendre un tel état de la matière, froid et très compact, se porte alors notamment sur les étoiles à neutrons, ces objets célestes extrêmement compacts, au bord de l'effondrement gravitationnel. La récente détection des ondes gravitationnelles a donné un nouvel essor aux observations astrophysiques. En combinant les informations que nous apportent les ondes gravitationnelles et électromagnétiques, les contraintes sur l'équation d'état de ces étoiles se sont fortement améliorées ces dernières années, nous permettant ainsi de remonter aux variables thermodynamiques de la QCD à très haute densité. Mieux comprendre la structure de ces étoiles à neutrons, c'est à dire, l'état de la matière au fur et à mesure que l'on se rapproche du noyau de l'étoile, permettrait d'affiner notre compréhension du diagramme de phase de la QCD, et donc, de la QCD elle même.

Un aperçu analytique de la physique du QGP

À ces échelles d'énergie, le couplage de l'interaction forte devient de plus en plus petit. Cette propriété de liberté asymptotique nous donne la possibilité d'exploiter la théorie des perturbations afin d'approximer la théorie complète par une succession de corrections. Bien que réussir à résoudre exactement la physique de la QCD est une tâche très difficle à cause de sa trop grande complexité, il nous est néanmoins possible de faire des approximations permettant d'approcher itérativement, au travers de corrections successives, la théorie exacte (non-perturbative). Cer-

[3] Faible vis à vis des $2 * 10^{12}$ degrés

tains effets cependant ne peuvent pas être évalués de cette manière et donc la théorie des perturbations ne pourra jamais exactement reproduire la QCD complète.

Idéalement, nous souhaiterions pouvoir calculer ces corrections perturbatives à des ordres de plus en plus élevés pour affiner notre compréhension du QGP, et ainsi essayer de s'approcher analytiquement le plus possible de la transition de phase. Cependant, même à température et densité zéro, la série perturbative de la QCD ne converge que (très) lentement, voir même ne converge tout simplement pas. Cette divergence n'apparaît qu'à des ordres plus élevés que nous ne pouvons pas atteindre pour l'instant.

Une fois les variables thermodynamiques introduites dans l'équation, la tâche se complique davantage. Non seulement de nouveaux termes correctifs intermédiaires viennent se greffer, mais en plus, pour une température non nulle, l'apparition de modes d'excitations collectifs, non-perturbatifs, pour les gluons viennent stopper net la série perturbative à partir de la troisième correction. En effet, dans le QGP, les corrélations à longues distances des gluons possèdent un caractère intrinsèquement non-perturbatif. Nous parlons d'échelles "dures" (*hard*), pour les particules (quarks et gluons) d'une énergie égale à la température ou de la densité du plasma, d'échelle "douce" (*soft*) et "ultra-douce" (*ultra-soft*) (pour les gluons uniquement) d'énergie bien plus basse que la température du plasma. C'est cette dernière échelle d'énergie qui donne naissance aux modes non-perturbatifs des gluons. La série perturbative naïve est incapable de décrire ces modes qui contribuent avec le même poids à tous les ordres successifs de la théorie perturbative. Ce qui signifie que les corrections que nous calculons ne sont plus réellement des corrections, puisqu'elles contribuent tout autant que les termes qu'elles sont censés corriger.

Heureusement, ces modes non perturbatifs (ultra-soft) disparaissent une fois le plasma refroidi. Néanmoins, il existe toujours dans le milieu des modes d'excitations collectifs à une échelle intermédiaire : les modes *soft*. Pour la physique des hautes densités, la série perturbative converge toujours faiblement, mais mieux qu'à température finie, et ne possède plus d'obstruction intrinsèquement non-perturbative suite à la disparition des modes ultra-soft. Ceci nous motive à repousser le développement perturbatif toujours plus loin afin de pouvoir caractériser au mieux la physique des hautes densités.

Le problème des divergences infrarouges

Ces modes collectifs nous compliquent la tâche, car ils proviennent des divergences infrarouges (IR) apparaissant systématiquement dans les calculs perturbatifs. Ces divergences sont nommées ainsi puiqu'elles traduisent des corrélations à longues distances dans le bain thermique. En opposition aux divergences Ultra-Violette (UV) qui sont elles, des singularités locales. Si nous souhaitons obtenir un résultat analytique, nous devons au préalable traiter le problème de ces divergences IR. Les divergences qui apparaissent dans les calculs intermédiaires ne sont cependant pas toutes indépendantes, et en les regroupant astucieusement et en les resommant,

elles disparaissent naturellement au profit de l'apparition d'une masse effective pour les gluons. Cette masse thermale nous apprends qu'en réalité les gluons se comportent comme des quasi-particules massives lorsqu'ils se propagent lentement dans le plasma. L'utilisation d'une théorie effective de la QCD, avec des gluons effectivement massifs plutôt que de masse nulle, devient alors plus approprié pour décrire la physique du plasma de quarks et de gluons. Introduire cette masse effective au sein même de la théorie nous définit ainsi un schéma de resommation, pour les corrections perturbatives, qui va systématiquement réguler les divergences IR. De plus, l'avantage d'un tel schéma de resommation, est que les corrections successives deviennent effectivement plus petites que les termes qu'elles corrigent, améliorant ainsi la convergence de la série.

Le groupe de renormalisation

Avant de détailler davantage la méthode de resommation, il nous faut d'abord reprendre, brièvement, les concepts clés du groupe de renormalisation, essentiels pour les travaux présentés dans cette thèse. Par construction, la théorie de l'interaction forte nous permet de faire des prédictions sur la physique des quarks et des gluons. Mais pour décrire l'interaction, il faut commencer par introduire un paramètre, le couplage, qui traduit l'intensité des interactions entre ces particules. Ce couplage n'est pas une observable physique. Dans les expériences de collisions de particules, ce que nous observons sont des probabilités que les particules interagissent ou non, et non l'intensité de cette interaction directement. Ainsi, nous pouvons fixer le couplage de notre théorie par ajustement paramétrique ("Fit") grâce aux observations expérimentales. Le résultat d'une expérience à une échelle d'énergie E_1 nous donnera une valeur de ce couplage g_1. Mais ce résultat va dépendre de l'énergie mise en jeu lors des collisions en question. Deux échelles d'énergies différentes, E_1, E_2 donneront deux valeurs différentes pour le couplage: g_1, g_2. Cependant, ces deux valeurs ne sont pas arbitrairement différentes. Sinon, notre approche n'aurait que peu d'intérêt. La façon dont elles sont reliées nous est donnée par le groupe de renormalisation. Ainsi, la connaissance de g_1 à l'échelle d'énergie E_1 nous permet de déterminer (approximativement) la valeur de g_2 à l'échelle E_2. Cette connaissance du couplage et de son évolution est cruciale pour la détermination d'une observable thermodynamique, telle que la pression, à différentes échelles d'énergies (de manière équivalente, à différentes températures et/ou densités).

Resommer la série perturbative

Une des méthodes de resommation des divergences infrarouges qui fut largement utilisée dans la littérature, nommée *Hard Thermal Loop perturbation theory* (HTLpt) permit une meilleure organisation de la série perturbative afin d'affiner les prédictions de la physique du QGP. Mais cette méthode présente parfois des résultats surprenants. Premièrement, la convergence de la

série perturbative n'était pas aussi bonne qu'attendue. Deuxièmement, l'incertitude inhérente due à l'échelle de renormalisation, qui est censée diminuer lorsque nous améliorons le calcul, augmentait progressivement avec les ordres perturbatifs successifs. Autrement dit, la façon dont les échelles d'énergies sont reliées entre elles ne semble pas entièrement correcte dans cette approche, suggérant que le spropriétés du groupe de renormalisation n'ont pas été correctement appréciés.

Récemment, une méthode alternative de resommation de la série perturbative (RGOPT), plus conforme avec les propriétés du groupe de renormalisation, a été développée et donne d'intéressants résultats à températures et densités finis pour QCD ainsi que pour des théories plus simples. Le travail de cette thèse porte donc sur le groupe de renormalisation ainsi que l'application de cette méthode aux ordres perturbatif plus élevés dans le but d'affiner nos connaissances thermodynamiques de la physique du QGP.

La première application de la méthode par l'auteur, concerne le modèle plus simple d'un champ scalaire, contrairement aux quarks et gluons qui sont respectivements des champs (plus compliqués) spinoriels/vectoriels. Notamment, le troisième ordre perturbatifs a été exploré, pour lequel des résultats très concluants sont venus conforter les attentes espérées pour cette méthode de resommation. Autrement dit, la série perturbative est nettement plus convergente, et l'incertitude résiduelle d'échelle de renormalisation a fortement diminuée.

Puis, l'exploration de la QCD à température zéro et à haute densité a été poursuivi. La détermination originale des logarithmes dominants et des logarithmes sous-dominants à *tous* les ordres, ainsi que leur resommation grace au groupe de renormalisation, a été établi, amenant à une nette amélioration comparé à l'état de l'art des calculs du domaine.

Finalement, l'application de la méthode RGOPT pour le secteur des quarks et des gluons est discutée en dernier, notamment les complications rencontrées pour le secteur des gluons. Les premières ébauches de résultat pour l'application à la détermination d'une équation d'état pour les étoiles à neutrons concluent les recherches menées par l'auteur.

Contents

1

Introduction

Quantum Chromodynamics (QCD), the commonly accepted theory of strong interaction, describes the interaction between quarks through the exchange of colored particles, the gluons, in the realm of quantum field theory (QFT). Due to this interaction, the low energy quarks and gluons bound together to form the hadrons, the elementary components of the atoms. QCD possesses genuine non perturbative features such as the confinement that prevents any direct observation of colored particles. At very high energy, more than the QCD scale which is of order $\Lambda_{\mathrm{QCD}} \sim 300\,\mathrm{MeV}$, the strong interaction weakens due to its asymptotic freedom (AF) property, and the (unphysical) shell of the hadrons blurs. This behavior happens at high temperature and/or density and it allows one to use weak coupling expansion in QFT to address the physics of these nearly free quarks and gluons. The state-of-the-art calculations at high temperature and vanishing chemical potential for the free energy is held by lattice QCD simulations (LQCD) which predict a smooth crossover phase transition from a confined phase to a deconfined one [1]. However, owing to the so-called sign problem [2], LQCD is unable to explore mid and high ranges of the chemical potential domain, for $\mu/T \gtrsim 1$, where neutron stars are believed to lies. Moreover, no earth-based experimentation can reach this region of interest, leaving us nearly blind to this physics. At small baryon densities, chiral perturbation theory gives a precise description of the degrees of freedom of QCD whereas perturbative approaches are reliable for very high baryon densities, leaving the mid range, in particular where Neutron Stars (NS) lies, still uncertain. A lot of efforts have been made recently in order to reconnect the two sides of the phase diagram looking forward to obtaining an accurate equation of state (EoS) for compact stellar objects. But due to the (expected) phase transition at this specific order of magnitude for the baryon density, model dependent approaches show huge error uncertainties as they reach an energy scale of the order of Λ_{QCD}.

Our hope resides now in advanced resummation techniques in perturbation theory which could help us to tackle this physics. Introducing such scales (T, μ) makes analytical approaches harder to use, first due to the intrinsic complexity of the calculations in thermal QFT, but also because of the apparition of non-perturbative effects originating from the medium. These non-perturbative effects originates from infrared divergences appearing in Feynman diagram involving bosonic quantum fields. A consistent framework must be defined to address the resummation of such infrared divergences in order to obtain a divergent-free prediction for

the free energy of QCD. A pioneering work by Freedman and McLerran [3; 4; 5] provided the next-to-next-to-leading order (NNLO) pressure for massless quarks at vanishing temperature and finite baryon density (equivalently finite chemical potential). It has been forty years since then and only recently this received an improvement by including corrections from finite quark masses [6] and pushing to a higher order the perturbative corrections [7; 8; 9]. However, infrared divergences appearing at finite temperature and density spoil a naive perturbative expansion, calling for a resummation that thwart the task. Physics of the soft modes, engendered by the temperature and the chemical potential, found a modern descriptions in the realm of Hard Thermal Loop theory used to resum these long-range correlations. While non-perturbative ultra-soft modes, due to the temperature only, is synonym to a break down the naive weak coupling expansion. Fortunately, the ultra-soft modes disappear in the cold and dense case of QCD ($T = 0, \mu \neq 0$) and we are only left with the hard and soft modes. Therefore, one can push to higher orders the weak coupling expansion looking forward to decrease the residual (large) dependence in the renormalization scale observed in the perturbative series as well as refine the precise value of the free energy of QCD.

From the renormalization group properties, we know that the QCD free energy is an invariant of the renormalization group (RG) in the complete theory; but in practice, at finite order of perturbative expansion, this property is only partially realized. Consequently, the resurgence of a remnant renormalization scale dependence is inexorable. However, upon including higher order terms from the expansion, we expect this sensitivity to decrease so as to recover the exact invariance in the limit of full resummation. Nevertheless, it has been observed in the so-called Hard Thermal Loop perturbation theory (HTLpt) framework [10; 11; 12; 13; 14], which relies on the Optimized Perturbation Theory (OPT), that notably at finite temperature, the rather important scale sensitivity increases when successive terms in the weak-coupling expansion are considered. This indicates that the renormalization group properties might not have been addressed properly.

Recently, a modified procedure, Renormalization Group Optimized Perturbation Theory (RGOPT), was developed and aims at resolving this issue [15; 16; 17]. In the present thesis, we explore the application of the RGOPT method in $\lambda\phi^4$ model at next-to-next-to-leading order (NNLO) [18], whose great improvement with respect to standard screened perturbation theory (SPT) motivates us to pursue our efforts in order tor apply the method to gluons in QCD. Due to the high complexity of the HTL framework, first application of RGOPT to NNLO for the naive quark sector is investigated [19], which pushes to next order the previous work from [20].

Another application of renormalization group properties to the sector of massive gluons (in the HTL framework) to determine the leading soft logarithms (LL) and next-to-leading soft logarithms (NLL) at all order, more simply than involved HTL calculations, is presented, based on [21], as well as a resummation formula for the two series. This work goes well beyond the soft sector first evaluated by Gorda et al. [7; 8; 9] using much more involved calculations to determine the second soft leading logarithm of the series. Finally, we present a work in progress to pursue the RGOPT method applied to massive gluons in QCD following previous works in HTLpt [22; 23; 13]. Only one piece is missing in order to complete the result, and we hope to close the calculation very soon.

Before presenting more in depth the HTL formalism and RGOPT approach in chapter 5 and 6 respectively, we will begin with a review of renormalization and the renormalization group in chapter 2. Chapter 3 on the other hand recalls few notions useful for the introduction of QCD in vacuum and in a medium, discussed in chapter 4. Finally, applications to neutron star physics are discussed in chapter 7.

1.1 Bibliography

[1] Y. Aoki, G. Endrodi, Z. Fodor, S. D. Katz, and K. K. Szabo. The Order of the quantum chromodynamics transition predicted by the standard model of particle physics. *Nature*, 443:675–678, 2006, hep-lat/0611014.

[2] Philippe de Forcrand. Simulating QCD at finite density. *PoS*, LAT2009:010, 2009, 1005.0539.

[3] Barry A. Freedman and Larry D. McLerran. Fermions and gauge vector mesons at finite temperature and density. i. formal techniques. *Phys. Rev. D*, 16:1130–1146, Aug 1977.

[4] Barry A. Freedman and Larry D. McLerran. Fermions and gauge vector mesons at finite temperature and density. ii. the ground-state energy of a relativistic electron gas. *Phys. Rev. D*, 16:1147–1168, Aug 1977.

[5] Barry A. Freedman and Larry D. McLerran. Fermions and gauge vector mesons at finite temperature and density. iii. the ground-state energy of a relativistic quark gas. *Phys. Rev. D*, 16:1169–1185, Aug 1977.

[6] Aleksi Kurkela, Paul Romatschke, and Aleksi Vuorinen. Cold Quark Matter. *Phys. Rev. D*, 81:105021, 2010, 0912.1856.

[7] Tyler Gorda, Aleksi Kurkela, Paul Romatschke, Matias Säppi, and Aleksi Vuorinen. Next-to-Next-to-Next-to-Leading Order Pressure of Cold Quark Matter: Leading Logarithm. *Phys. Rev. Lett.*, 121(20):202701, 2018, 1807.04120.

[8] Tyler Gorda, Aleksi Kurkela, Risto Paatelainen, Saga Säppi, and Aleksi Vuorinen. Cold quark matter at N3LO: Soft contributions. *Phys. Rev. D*, 104(7):074015, 2021, 2103.07427.

[9] Tyler Gorda, Aleksi Kurkela, Risto Paatelainen, Saga Säppi, and Aleksi Vuorinen. Soft Interactions in Cold Quark Matter. *Phys. Rev. Lett.*, 127(16):162003, 2021, 2103.05658.

[10] J. P. Blaizot, E. Iancu, and A. Rebhan. On the apparent convergence of perturbative QCD at high temperature. *Phys. Rev. D*, 68:025011, 2003, hep-ph/0303045.

[11] Ulrike Kraemmer and Anton Rebhan. Advances in perturbative thermal field theory. *Rept. Prog. Phys.*, 67:351, 2004, hep-ph/0310337.

[12] Sylvain Mogliacci, Jens O. Andersen, Michael Strickland, Nan Su, and Aleksi Vuorinen. Equation of State of hot and dense QCD: Resummed perturbation theory confronts lattice data. *JHEP*, 12:055, 2013, 1307.8098.

[13] Jens O. Andersen, Najmul Haque, Munshi G. Mustafa, Michael Strickland, and Nan Su. Equation of State for QCD at finite temperature and density. Resummation versus lattice data. *AIP Conf. Proc.*, 1701(1):020003, 2016, 1411.1253.

[14] Najmul Haque, Aritra Bandyopadhyay, Jens O. Andersen, Munshi G. Mustafa, Michael Strickland, and Nan Su. Three-loop HTLpt thermodynamics at finite temperature and chemical potential. *JHEP*, 05:027, 2014, 1402.6907.

[15] J. L. Kneur and A. Neveu. Renormalization Group Improved Optimized Perturbation Theory: Revisiting the Mass Gap of the O(2N) Gross-Neveu Model. *Phys. Rev. D*, 81:125012, 2010, 1004.4834.

[16] Jean-Loic Kneur and Andre Neveu. Chiral symmetry breaking from renormalization group optimized perturbation. *Nucl. Phys. B Proc. Suppl.*, 207-208:232–235, 2010.

[17] Jean-Loïc Kneur and André Neveu. Chiral condensate and spectral density at full five-loop and partial six-loop orders of renormalization group optimized perturbation theory. *Phys. Rev. D*, 101(7):074009, 2020, 2001.11670.

[18] Loïc Fernandez and Jean-Loïc Kneur. Renormalization group optimized $\lambda\phi^4$ pressure at next-to-next-to-leading order. *Phys. Rev. D*, 104(9):096012, 2021, 2107.13328.

[19] Loïc Fernandez and Jean-Loïc Kneur. Renormalization group improvement in cold and dense QCD pressure. *To be submitted to ArXiv.*, 2022.

[20] Jean-Loïc Kneur, Marcus Benghi Pinto, and Tulio Eduardo Restrepo. Renormalization group improved pressure for cold and dense QCD. *Phys. Rev. D*, 100(11):114006, 2019, 1908.08363.

[21] Loïc Fernandez and Jean-Loïc Kneur. All order resummed leading and next-to-leading soft modes of dense QCD pressure. 9 2021, 2109.02410.

[22] Jens O. Andersen, Eric Braaten, Emmanuel Petitgirard, and Michael Strickland. HTL perturbation theory to two loops. *Phys. Rev. D*, 66:085016, 2002, hep-ph/0205085.

[23] Jens O. Andersen, Emmanuel Petitgirard, and Michael Strickland. Two loop HTL thermodynamics with quarks. *Phys. Rev. D*, 70:045001, 2004, hep-ph/0302069.

2

“ À l’échelle d’une carte, le monde est un jeu d’enfant.”
“Scaled to a map, the world is a playground.”

— Laurent Graff

Renormalization

The calculus framework of this thesis is Quantum Field Theory (QFT). While we do not have space for introducing the theory, there is an important part of this thesis based on renormalization group properties that we would like to address carefully. Thus, we assume the reader to be familiar at least with basic concepts of QFT but we will discuss renormalization from basics, followed by the renormalization group.

This chapter is not intended to be exhaustive. There is much more to renormalization and the renormalization group (RG) than what will be addressed here. We only choose the relevant points for our work. An interested reader is referred to reviews such as [1; 2] for the perturbative side of the renormalization group which is the one at hand here.

Our additional goal for this chapter is to motivate the concept of vacuum energy density and related renormalization and anomalous dimension, which is seldom appreciated in the literature, especially in thermal field theory. The notations in this chapter is thought to be self-consistent but some definitions will slightly differ from next chapters. The reason being that some different definitions/conventions were used in the various articles (by the authors or by others). We thus try to set up a clean notation framework for future works.

2.1 Renormalization: a natural procedure

Along the 20th century, QFT has self-imposed as the best tool to describe the microscopic world. The fundamental particles becomes excitations of fields $\phi(x)$ promoted to the operator status: $\hat{\phi}(x)$. Interactions between these fields therefore encode the interactions between the particles. Fields and their interactions are defined by their Lagrangian density integrated over every point in space. Here comes the complication. If we state that two fields can interact at any point in space no matter how far we zoom in, we expect singularities to occur at infinitesimal distances (considering a local theory and no singularities emerging at long distances). The field operator $\hat{\phi}(x)$ is not in general a well-behaved function, but rather it is an operator valued distribution. Products of distributions do not always make sense. Some care is needed to define these properly, and this is in fact the subject of renormalization, in which by appropriate redefinition of the non observable parameters of the theory, we can systematically kill the

divergences. There is however an ambiguity when choosing this redefinition. This redefinition means that we absorb the infinitesimal scale inside the parameters, but where do we draw the line between what should be absorbed and what should not ? Drawing such line is what we call specifying the renormalization scheme. This renormalization scheme depends on the energy scale, or *renormalization scale*, and on the regularization procedure that we choose arbitrarily.

Specifying properly the energy scale will facilitate the description of the observables. It should be of the order of the energy scale at which we evaluate the specific observable otherwise it would lead to unnaturally large quantities. But the predictions must not depend on the choice of this arbitrary energy scale, otherwise we could not make any predictions at all. This constraint is consistently encoded in the renormalization group equation, that we will address after giving a more precise insight in the formalism of renormalization.

One may wonder what would have happened if we did not have infinities in the first place. They are commonly believed to be due to the fact that we do not possess yet a complete knowledge of the Planck scale. But if we had it, it would not mean to throw away the renormalization procedure. Even if we had a natural cut-off scale such as to regulate all the ill-defined integrals appearing in QFT, the theory would still lead to unnaturally large logarithms involving ratio of this intrinsic cut-off (living presumably at the Planck scale) and the momenta of the particles. The renormalization procedure would still allows to absorb these large quantities such as to define a more natural description[1].

2.2 Renormalization

As a concrete example, we will use the massive scalar $\lambda\phi^4$ model to discuss renormalization, not only as a simpler model compared to QCD, but also because it will become handy when discussing our specific work at next-to-next-to-leading order [3]. Starting from the euclidean Lagrangian,

$$\mathcal{L} = \frac{1}{2}(\partial_\mu\phi_0)(\partial_\mu\phi_0) + \frac{1}{2}m_0^2\phi_0^2 + \frac{\lambda_0}{4!}\phi_0^4, \tag{2.1}$$

where index "0" indicates bare quantities, the leading contribution to the self energy (in the vacuum, denoted with index V) in euclidean momentum space is:

$$\Pi_1^V = \frac{\lambda_0}{2}\int\frac{d^4P}{(2\pi)^4}\frac{1}{P^2+m_0^2}, \qquad P=(P_0,\vec{p}), \tag{2.2}$$

In fact, this integral is not properly defined since it blows up when $|P|$ goes to infinity. But this loop itself is not measurable, as discussed previously, the infinity appearing comes from the lack of our knowledge on the infinitesimal distance scale. QFT has to be understood as a low energy effective field theory valid up to some energy scale Λ_{UV}. This scale being roughly the inverse of a lattice spacing in coordinate space which parameterize our threshold of ignorance.

Nevertheless, to make any predictions out of this loop, we must first give a meaning to this integral. To do so, we introduce a regulator. This regulator is certainly not unique and concrete results should be independent of the specific regularization as we wish to remove it ultimately. Specifying a regulator is called a regularization scheme. The most intuitive scheme is simply to cut the integration at a specific UV scale Λ: $\int_0^\infty \mapsto \int_0^\Lambda$. Choosing this regulator, we define a scale that separates between what will be part of the infinity and what is not. Now that we have regulated the divergence, we can renormalize the parameters of the theory

[1] In the sense of naturalness, i.e contributions would be of order one.

to cancel the divergence and then we can remove the regulator. To illustrate more clearly the renormalization procedure, consider the result of Eqn.(2.2) using a cut-off regulator:

$$\Pi_1^V = \frac{\lambda_0}{32\pi^2}\left[\Lambda^2 - m_0^2 \ln\left(\frac{\Lambda^2 + m_0^2}{m_0^2}\right)\right]. \tag{2.3}$$

Which is the first order correction to the propagator: $\frac{1}{P^2+m^2} \mapsto \frac{1}{P^2+m^2+\Pi}$. Upon redefinition of the bare parameters,

$$\phi_0 = \mathcal{Z}\phi_r \ , \ m_0 = \mathcal{Z}_m m_r \ , \ \lambda_0 = \mathcal{Z}_\lambda \lambda_r \tag{2.4}$$

we can define a counterterm δ_m (from $Z_m = 1 + \delta_m$) leading to an extra contribution[2] $2m^2\delta_m$ to Eqn.(2.3). We can use the freedom of defining δ_m to absorb the divergent term. There are infinitely many prescriptions to fix δ_m because we can also choose to absorb arbitrary finite contributions at the same time. As already alluded, specifying what has been absorbed in the counterterms defines a renormalization scheme. Here we absorb the divergent part of Π_1 which is given for $\Lambda \mapsto \infty$:

$$\frac{\lambda}{32\pi^2}\left[\Lambda^2 - m^2 \ln\left(\frac{\Lambda^2}{m^2}\right)\right] + 2m^2\,\delta_m \equiv 0, \tag{2.5}$$

defining a specific δ_m. This is the heart of renormalization: absorbing the ultraviolet (UV) divergences inside the parameter of the theory. Cancellation of UV divergences is essential if a theory is to yield quantitative physical predictions. We can systematically define counterterms such as to absorb the arising divergences at every order. Whether it requires only a finite number of them, we call the theory renormalizable, else it is said to be non-renormalizable.

Our notation is however slightly confusing. As we introduce a (yet unspecified) arbitrary regulator in the theory, we are defining a somewhat different theory dependent of Λ. For the prediction to be independent of the arbitrary choice of Λ, the coupling λ must be dependent of this cut-off scale. Parameters m_r, λ_r redefined in the manner of Eqn.(2.4), called renormalized parameters, now become (renormalization) scale dependent.

What we observe in experiments are solely cross sections, not parameters of the constructed theory. These parameters must be determined experimentally at some energy scale Λ_0, and knowing how they evolve with the energy, we can make a prediction for the cross section at an higher energy scale Λ_1. For a theory of n parameters, we need n of such inputs called renormalization conditions. In QCD, neglecting quark masses to simplify, there is only one scale free to fix associated to the evolution of the coupling, whose renormalization condition leads to the definition of the (renormalization scheme dependent) scale Λ_{QCD}.

Historically and intuitively, it is best to start with the momentum cut off scheme but with the rise of dimension regularization [4; 5; 6] in QFT, it has become evident since then that this scheme is much more powerful and it is widely used in the literature now. It respects gauge invariance, chiral symmetry, Poincaré invariance, as well as being the sole scheme where calculations are tractable in high loop order calculations. Moreover, a cut-off regulator leads to contributions proportional to the scale, see Eqn.(2.5), which ruins intuitive power counting in effective field theory (EFT).

[2]Note that the factor of 2 comes from the definition of $m_0 = \mathcal{Z}_m\, m_r$ instead of $m_0^2 = \mathcal{Z}_m\, m_r^2$ also seen in the literature.

2.2.1 Dimensional regularization and the $\overline{\text{MS}}$ scheme

Dimensional regularization originates from the idea that loop integrals are divergent in four dimensions but not necessarily in smaller ones. So, if we analytically continue our theory in $D = 4 - 2\varepsilon$ dimension instead, no infinities will arise as long as we keep $\varepsilon \neq 0$.

Vector spaces are only defined for integer dimensions so we should not try to take it too literally. It can be given a precise mathematical definition, see e.g [1], but we can just use dimensional regularization as a set of well-established prescriptions. All we need to know is that it exists, it is uniquely defined as long as we axiomatically impose the operator (the would be "D-dimension integration") to satisfy three rules: linearity, scaling and translational invariance. The last two read:

$$\begin{aligned} \int d^D\vec{p}\; f(\vec{p}+\vec{q}) &= \int d^D\vec{p}\; f(\vec{p}) \\ \int d^D\vec{p}\; f(s\,\vec{p}) &= s^{-D}\int d^D\vec{p}\; f(\vec{p}). \end{aligned} \tag{2.6}$$

Following this definition, a very important result is that any scaleless integral vanishes:

$$\int d^D\vec{p}\,(\vec{p})^\alpha \quad , \quad \forall\,\alpha \in \mathbb{R}. \tag{2.7}$$

This can be seen easily from the general result for a one-loop integration,

$$M^{2\varepsilon}\int \frac{d^D\vec{k}}{(2\pi)^D}\frac{(\vec{k}^2)^a}{(\vec{k}^2-M^2)^b} = \frac{iM^{2\varepsilon}}{(4\pi)^{\frac{D}{2}}}\frac{(-1)^{a-b}\,\Gamma(\frac{D}{2}+a)\Gamma(b-a-\frac{D}{2})}{\Gamma(\frac{D}{2})\Gamma(b)}(M^2)^{\frac{D}{2}+a-b} \tag{2.8}$$

upon taking the limit $M \mapsto 0$ (which is valid for $\frac{D}{2}+a-b>0$, but can be analytically continued for more general values).

This framework translates the power or logarithmic UV/IR divergences of the initial integral into poles of gamma functions. Now, upon changing the dimension one has to re-scale the dimension of the parameters in order to keep the Lagrangian density proportional to the inverse D-th power of a length scale. For the coupling, this leads to introduce an arbitrary energy scale:

$$\lambda \mapsto \lambda\, M^{4-D} \tag{2.9}$$

which defines the minimal subtraction scheme (MS). This explain the factor $M^{2\varepsilon}$ inside Eqn.(2.8). Calculations in this scheme lead to inconvenient factor of γ_E (Euler's gamma) and $\ln 4\pi$, terms that we can absorb by changing the renormalization scheme to the so-called modified minimal subtraction scheme ($\overline{\text{MS}}$):

$$M^2 = \bar{M}^2\,\frac{e^{\gamma_E}}{4\pi}. \tag{2.10}$$

We shall work now in this scheme and drop the bar over the M for convenience. As a concrete outcome, now Eqns.(2.3) and (2.5) become:

$$\Pi_1^V = \frac{\lambda_0}{2}\int\frac{d^DP}{(2\pi)^D}\frac{1}{P^2+m_0^2} = -\frac{m_0\,\lambda_0}{32\pi^2\varepsilon} - \frac{\lambda_0\,m_0^2}{32\pi^2}\left(1-\ln\left(\frac{m_0^2}{M^2}\right)\right)+\mathcal{O}(\varepsilon), \tag{2.11}$$

$$2m^2\delta_m = \frac{m^2\,\lambda}{32\pi^2\varepsilon}. \tag{2.12}$$

2.2.2 Weinberg's theorem and renormalizability

So far, we discussed a theory that we implicitly assumed to be renormalizable. But renormalizable theories are only a tiny subset of the available theories at our disposal. A renormalizable theory has the welcome property to only require a finite set of counterterms to be rendered finite, whereas non-renormalizable theory requires a systematic introduction of an infinite set of new counterterms at higher and higher orders to predict finite results. Renormalizable theories were historically preferred, nevertheless, non-renormalizable theories are also powerful tools. The theory of Hard Thermal Loop (HTL), to be addressed in chapter 5, has not yet been proven renormalizable beyond three-loop order and the high-temperature approximation, yet, its predictive power makes it a very standard use in modern thermal field theory.

From power counting argument, we can classify theories in three categories depending on the dimension of their coupling. If the coupling has a dimension $D_i > 0$, the theory is super-renormalizable, if $D_i = 0$ it is renormalizable and if $D_i < 0$ then it is non-renormalizable. A super-renormalizable theory only has a finite number of divergent Feynman diagrams, while a renormalizable theory has an infinity of them at all perturbative orders, but requires only a finite number of counterterms to be regulated.

To prove a theory renormalizable, one need to prove that local counterterms[3] can be written and that only a finite amount of them are needed, with the same form as the original (bare) Lagrangian. The first point was proven long ago by Weinberg [7] as long as the divergences appearing in Feynman diagram are polynomials in its external momenta. The second condition is answered by the above power counting argument for a local field theory. Non-local field theories (such as HTL) does not possess yet a general proof of renormalizability. We will examine the renormalizability of HTL in more details in chapter 5.

2.3 Renormalization Group

"*The renormalization group is one of those brilliant ideas that lets you get something for nothing through clever reorganization of things you already know*" [8].

To clarify immediately, the renormalization group is not a group in the mathematical sense. The renormalization group, as previously mentioned, will ensure that observables are renormalization scale invariant. This designation, sometimes shorten to "scale invariant" is slightly misleading as we should not confuse it with the genuine scale invariance of conformal theories. To avoid any possible confusion we will stick with the designation: "RG invariant" when stating that any observable must be independent of the renormalization scale or explicitly write "renormalization scale".

Mathematically, this requirement can be embedded in the following differential equation, the RG equation,

$$M\frac{d}{dM}\mathcal{O}_i(M, g_1(M), \ldots, g_j(M)) = 0. \tag{2.13}$$

for any observable $\mathcal{O}_i$ dependent of j parameters, typically masses and couplings. The RG equation relates how a change in the renormalization scale M must be compensated by a change in the parameters of the theory such that the prediction remains RG invariant. Pictorially, the RG equation describes a curve of constant physics on the graph above the hyperspace of the parameters of the theory (see Fig.2.1). Wandering away from the curve will result in non RG

[3] In QFT context, we talk about non-local operator as having an inverse dependence on the derivative: ∂^{-1} at tree level. In practical calculations and in Fourier space, such terms leads to non-analytic terms as $\ln(M_1/M_2)$, for two generic (non-renormalization) scale.

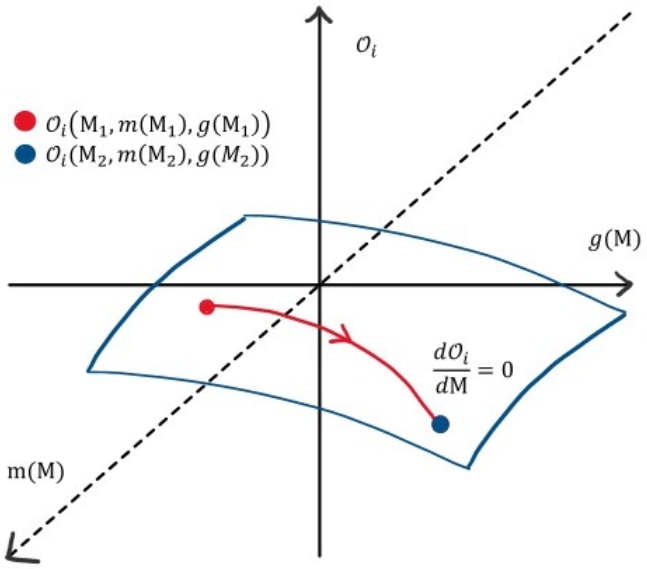

Figure 2.1: RG flow along the curve of constant physics. The M direction has not been drawn.

invariant quantities that we cannot call observables. Thus, we should check for consistency that our final results satisfy, at least perturbatively, the RG equation. If the theory contains only one parameter, e.g λ for massless $\lambda\phi^4$ theory, then Eqn.(2.13) will read explicitly

$$M\frac{d}{dM}\mathcal{O}_i(M,\lambda(M)) = \left(M\frac{\partial}{\partial M} + \beta(\lambda)\frac{\partial}{\partial\lambda}\right)\mathcal{O}_i(M,\lambda(M)), \tag{2.14}$$

where $\beta(\lambda) \equiv M\frac{d\lambda}{dM}$. We will refer to this equation as the "RG reduced equation", since it describes the RG evolution of a massless theory, in opposition to the more general massive RG equation[4],

$$M\frac{d}{dM} = M\frac{\partial}{\partial M} + \beta(\lambda)\frac{\partial}{\partial\lambda} + m\,\gamma_m(\lambda)\frac{\partial}{\partial m}, \quad \gamma_m(\lambda) = \frac{d\ln(m)}{d\ln M}. \tag{2.15}$$

However, for a massive theory, this operator does not encode the complete RG dependence since it is blind to the RG evolution of the vacuum energy. We shall review this point in the eponymous section. In this thesis, we mainly consider 0-point functions, associated to the free energy in thermal field theory, that is why we systematically neglect the anomalous dimension of the fields in the RG operator. To be more complete, if applied to an n-point Green function, the RG operator would pick extra terms: $\sum_{i=1}^{n}\gamma_i$ with $\gamma_i \equiv -M\frac{\partial\phi_i}{\partial M}$.

To understand how the renormalization group invariance occurs in practice, it is good to start with a simple example. Considering the pressure dependent of a mass scale and a coupling λ), the renormalization scale appears in the perturbative expansion inside logarithms according to the following pattern (the first index is for the perturbative order, the second for the power

[4]Note that our convention for γ_m in $\lambda\phi^4$ differs of a minus from our convention in QCD that we will recall in chapter 5.

of the logarithm):

$$\begin{aligned}\frac{\mathcal{P}}{m^4} = -\frac{s_0}{\lambda} + a_{0,1}\ln\left(\frac{\Lambda}{m}\right) &+ a_{1,2}\lambda\ln^2\left(\frac{\Lambda}{m}\right) &+ a_{2,3}\lambda^2\ln^3\left(\frac{\Lambda}{m}\right)\\ a_{0,0} &+ a_{1,1}\lambda\ln\left(\frac{\Lambda}{m}\right) &+ a_{2,2}\lambda^2\ln^2\left(\frac{\Lambda}{m}\right)\\ &+ a_{1,0}\lambda &+ a_{2,1}\lambda^2\ln\left(\frac{\Lambda}{m}\right)\end{aligned} \tag{2.16}$$

The first line, with the dominant logarithm, is called the *leading logarithm* family (LL), while the second line is the first non-logarithmic coefficient $a_{2,0}$ plus the first sub-dominant logarithm family called the *next-to-leading logarithm* family (NLL) and so on and so forth. For this pressure to be RG invariant, the explicit scale dependence inside the logarithms must be compensated by the intrinsic dependence of the parameters $(g(\Lambda), m(\Lambda))$ on the renormalization scale. Working out the RG equation of this generic pressure leads to recursive relations to be satisfied to ensure RG invariance. The very first things that comes out is that we need the first term s_0 since RG invariance requires cancellation between the coupling at order $\mathcal{O}(\lambda^k)$ and the explicit logarithm at order $\mathcal{O}(\lambda^{k+1})$ to be satisfied. This will be discussed in the next section. Restricting the beta function to its leading order contribution also tells us that the renormalization scale cancellation occurs between terms of the leading logarithm family. Therefore, upon resumming the LL and using the leading order running of the coupling and of the mass parameter leads to an exactly renormalization group invariant pressure.

However, we are blind to the precise value of the higher order contributions, and it is hard to estimate the uncertainties associated to these missing terms. Since the RG cancellation occurs between terms of different orders, missing terms from higher order can be traduced by a missing RG cancellation and therefore the appearance of a remnant scale dependence (if we did not resummed logarithm families). Upon varying the remnant scale dependence, we can estimate the uncertainty associated to the missing higher order contributions. Hence, from this simple example we can understand that upon resummation of logarithms families, we can decrease the residual renormalization scale dependence of the pressure (which also incorporates higher order contribution), but to keep track of the missing higher orders non-logarithmic contributions, we must choose higher order running couplings so that the cancellation between the resummation and the running of the parameter mismatch by perturbative corrections.

2.3.1 Renormalization group flow equations

β function: the anomalous coupling dimension

Green functions obtained from the bare Lagrangian depend on the bare parameters obviously independent of the scale M, so the bare parameters satisfy the RG equation:

$$M\frac{d\lambda_0}{dM} = 0. \tag{2.17}$$

Solving Eqn.(2.17) for $\lambda_0 = M^{4-D}\bar{\lambda}_0 = M^{4-D}\lambda\,\mathcal{Z}_\lambda$, it can be expressed in term of the bare coupling:

$$\beta(\lambda) = -\frac{(4-D)\bar{\lambda}_0}{\partial_\lambda\,\bar{\lambda}_0} = -\frac{(4-D)\lambda}{1+\lambda\partial_\lambda\ln\mathcal{Z}_\lambda}. \tag{2.18}$$

We do not have complete knowledge of the beta function in general, rather, only the first few perturbative orders. Due to the truncation error of the intrinsically limited perturbative

series, the beta function is only well defined for a specific range of the coupling, namely when it is sufficiently small so that perturbation theory is valid. To digress slightly, for QCD whose coupling runs to zero at very high energy, there is a Landau pole in the IR sector where the coupling values growth exponentially fast, while for QED it is the opposite. The beta function may or may not have other non trivial zeros $\beta(\lambda^*) = 0$ for specific finite λ^* values. It is possible typically, if there are alternative signs in the perturbative coefficient expansion. In QCD, it appears that every order calculated so far, up to 5-loop, gives a negative sign, so at least for realistic quark flavor numbers, no such fixed points has been found so far. There may be even non-perturbative fixed points, that we ignore the existence, that could be evaluated only through an all order resummation of the series expansion. Fixed points in the theory leads to very interesting physics, as the RG invariance (for a massless theory) becomes trivially satisfied and the theory itself becomes conformally invariant.

Back to $\lambda\phi^4$, expanding in perturbation theory, the first few orders of the beta function reads:

$$\begin{aligned} \beta(\lambda) &= b_0\,\lambda^2 + b_1\,\lambda^3 + \dots \\ b_0 &= \frac{3}{(4\pi)^2} \\ b_1 &= -\frac{17}{3(4\pi)^4} \\ b_2 &= \frac{3915 + 2592\,\zeta(3)}{216(4\pi)^6} \end{aligned} \tag{2.19}$$

Note that the beta function given by Eqn.(2.19) picks up another contribution when applied to bare quantities (see Eqn.(2.18):

$$\beta(\lambda) = -2\varepsilon\,\lambda + b_0\,\lambda^2 + b_1\,\lambda^3 + \dots \tag{2.20}$$

indeed, the beta function is easily evaluated from the counterterm,

$$\mathcal{Z}_\lambda = 1+\delta_\lambda = 1+\delta_{\lambda,1}\lambda+\delta_{\lambda,2}\lambda^2+\dots = 1+\frac{\delta^{(1)}_{\lambda,1}}{\varepsilon}\lambda+\left(\frac{\delta^{(1)}_{\lambda,2}}{\varepsilon}+\frac{\delta^{(2)}_{\lambda,2}}{\varepsilon^2}\right)\lambda^2+\dots = 1+\frac{b_0}{2\varepsilon}\lambda+\mathcal{O}(\lambda^2) \tag{2.21}$$

and Eqn.(2.18):

$$\beta(\lambda) = \frac{(-2\varepsilon)\lambda}{1+\lambda\partial_\lambda \ln(1+\delta_\lambda)} = -2\varepsilon\lambda + 2\delta^{(1)}_{\lambda,1}\lambda^2 + 4\delta^{(1)}_{\lambda,2} + \dots \tag{2.22}$$

Note that $\delta^{(2)}_{\lambda,2}$ is given by $\delta^{(1)}_{\lambda,1}$ and they cancelled out in the above formula. From Eqn.(2.19) at first order in λ, we obtain the leading order RG flow of the coupling:

$$\lambda(M_1) = \frac{\lambda_0}{1 - b_0\,\lambda(M_0)\ln\left(\frac{M_1}{M_0}\right)}. \tag{2.23}$$

This is exactly what we use to specify the coupling parameter. We measure different cross-sections at a given energy scale M_0, trace back what would be the value of $\lambda(M_0)$ that would have given this outcome, and using the running of the coupling, we can predict how the coupling evolve and so on for the cross-section.

γ_m function: the anomalous mass dimension

Just like λ, the mass m is dependent of the renormalization scale M and "runs" (with M) while m_0 is RG invariant. Following the definition in Eqn.(2.15):

$$\gamma_m = \frac{d\ln(m(M))}{d\ln(M)}, \tag{2.24}$$

keeping the same notation as in the last section, we give for completeness the following relations:

$$\begin{aligned} \gamma(\lambda) &= \gamma_0\,\lambda + \gamma_1\,\lambda^2 + \dots \\ \gamma_0 &= \frac{1}{2(4\pi)^2} \\ \gamma_1 &= -\frac{5}{12(4\pi)^4)} \\ \gamma_2 &= \frac{7}{4(4\pi)^6} \end{aligned} \tag{2.25}$$

$$\mathcal{Z}_m(\lambda) = 1 + \delta_m(\lambda) = 1 + \frac{\delta^{(1)}_{m,1}}{\epsilon}\lambda + \dots = 1 + \frac{\gamma_0}{2\varepsilon}\lambda + \mathcal{O}(\lambda^2) \tag{2.26}$$

$$M\frac{dm_0}{dM} = 0, \quad m_0 = m\mathcal{Z}_m \;\mapsto \gamma_m(\lambda) = -\beta(\lambda)\partial_\lambda \ln(1+\delta_m(\lambda)) \tag{2.27}$$

In dimensional regularization, Eqn.(2.5) reads (for the divergence only):

$$-\frac{\lambda\, m^2}{32\pi^2\,\varepsilon} + 2m^2\delta_m = 0 \tag{2.28}$$

Which is satisfied for $\delta^{(1)}_{m,1} = \frac{\gamma_0}{2}$.

Γ_v function: the vacuum energy anomalous dimension

In massive field theory, the leading-order bubble diagram reads, after some algebra,

$$\mathcal{P}_{\rm LO} = \bigcirc = \frac{-1}{2}\left(\frac{e^{\gamma_E}M^2}{4\pi}\right)^{\varepsilon}\int\frac{d^DP}{(2\pi)^D}\ln\left(P^2+m_0^2\right) = \frac{m_0^4}{64\pi^2}\left(\frac{1}{\varepsilon}+\frac{3}{2}-\ln\left(\frac{m_0^2}{M^2}\right)\right). \tag{2.29}$$

Where the momentum integral is easily evaluated in dimensional regularization from Eqn.(2.48) using $\ln(P^2+m_0^2) = \int_0^{m_0^2} dm^2\,\frac{1}{P^2+m^2}$. Here we see two issues emerging:

1. The loop is divergent, and it cannot be absorbed by m_0 renormalization since the latter is necessarily of next order: $m_0 \equiv m\mathcal{Z}_m \simeq m(1-\gamma_0/\varepsilon\,\lambda)$.

2. Even after renormalizing the mass, and naively minimally subtracting the divergent term, the RG equation is in fact not even satisfied already at this leading one-loop order: Acting with the RG operator of Eqn.(2.15) leaves a remnant term $\mathcal{O}(m^4\ln M)$.

Both issues can be addressed upon introducing in the Lagrangian a new operator $\mathcal{E}_0$: the vacuum energy density [9; 10].

This operator does not possess a perturbative expansion expressed in terms of Feynman diagram, thus in the perturbative framework we use, we can only evaluate its contribution

through the RG equation. Following [9; 10; 11; 12; 13], we express its contribution in terms of a perturbative expansion in λ_0, necessarily starting at order $1/\lambda_0$:

$$\mathcal{E}_0 = -\frac{m_0^4}{\lambda_0}\sum_{k=0}^{\infty} s_k\,\lambda_0^k. \tag{2.30}$$

Upon renormalization of this operator: $m_0 = m\,\mathcal{Z}_m,\ \lambda_0 = M^{2\varepsilon}\lambda\mathcal{Z}_\lambda$, (we define $\mathcal{E}_0 = M^{-2\varepsilon}(\mathcal{E} - m^4\mathcal{Z}_v)$ where $\mathcal{E}$ is the same but without the zero index), it generates a counterterms of the same order in λ as in Eqn.2.29. This is a manifestation that perturbative RG invariance occurs from cancellations between terms from the RG equation at order λ^k and the explicit M dependence at the next order λ^{k+1}.

The counterterm $\mathcal{Z}_v$ can be read off directly from the expression of the pressure, namely here, following Eqn.(2.29):

$$\mathcal{Z}_v = \frac{\delta_{v,1}^{(1)}}{\varepsilon}\lambda + \left(\frac{\delta_{v,2}^{(2)}}{\varepsilon^2} + \frac{\delta_{v,2}^{(1)}}{\varepsilon}\right)\lambda^2 + \cdots \simeq \frac{m_0^4}{64\pi^2} \tag{2.31}$$

The coefficients s_n can be determined iteratively from the remnant contribution of the massive RG operator in Eqn.(2.15) applied to the pressure,

$$M\frac{d}{dM}\mathcal{E} \equiv -M\frac{d}{dM}\mathcal{P}(\mathcal{E}=0) \tag{2.32}$$

or, equivalently, by requiring the counterterms to cancel the remnant divergences of the pressure. For $\lambda\phi^4$, the first ones were determined in [14; 3][5]:

$$\begin{aligned}
(4\pi)^2 s_0 &= -\frac{1}{2(b_0 - 4\gamma_0)} = -8\pi^2,\\
(4\pi)^2 s_1 &= -\frac{b_1 - 4\gamma_1}{8\gamma_0(b_0 - 4\gamma_0)} = 1,\\
(4\pi)^2 s_2 &= -\frac{23 + 36\,\zeta(3)}{480\pi^2} \simeq -0.01399,\\
(4\pi)^2 s_3 &= -\frac{-709 + 12\pi^4 - 2628\,\zeta(3) - 5400\,\zeta(5)}{720(16\pi^2)^2}.
\end{aligned} \tag{2.33}$$

For simplicity, we redefine what we called the pressure $\mathcal{P} \mapsto \mathcal{P}^{\rm RGI} = \mathcal{P} + \mathcal{E}$, which will then satisfy the massive RG equation and thus becomes an observable. Equivalently Eqn.(2.32) defines the action of the RG operator on $\mathcal{E}$:

$$\frac{d\,\mathcal{E}}{d\ln M} \equiv \hat{\Gamma}(\lambda)\,m^4. \tag{2.34}$$

$\hat{\Gamma(\lambda)}$, the anomalous dimension of the vacuum energy density, is determined perturbatively $\hat{\Gamma} = \Gamma_0 + \Gamma_1\,\lambda + \ldots$ most easily using the counterterm $\mathcal{Z}_v$ which can be read off directly from the pressure. Together with the RG equation for the bare vacuum energy:

$$\frac{d\mathcal{E}_0}{d\ln M} \equiv 0, \tag{2.35}$$

[5] s_n coefficients were at that time defined with respect to $(4\pi)^2\mathcal{F}$, we prefer now to define them as subtraction to the pressure thus the extra factor of $-1/(4\pi)^2$ with respect to our article [3].

it leads after algebra to:

$$\hat{\Gamma}(\lambda) = M^{-2\varepsilon}\left(\mathcal{E} - m^4 \mathcal{Z}_v\right). \tag{2.36}$$

Using Eqn.(2.34), we can relate the counterterm $\mathcal{Z}_v$ to the subtraction coefficients s_n permitting a simpler evaluation of these coefficients:

$$\hat{\Gamma} = b_0\, s_0 + 4 s_0\, \gamma_0 + (b_1\, s_0 + 4 s_1\, \gamma_0 + 4 s_0\, \gamma_1)\, \lambda + \cdots = -\frac{1}{32\pi^2} + \mathcal{O}(\lambda^2) \tag{2.37}$$

Note that in $\lambda\phi^4$, the coefficient of order λ in $\hat{\Gamma}_v$ is strictly zero. This construction – adding the vacuum energy – will be ultimately very relevant to the determination of a resummation formula for the massive logarithms appearing in hard thermal loop theory. This will be discuss in depth in chapter 5.

2.3.2 Connection with finite temperature field theory

Anticipating slightly our discussion of finite temperature field theory, we can already easily define how the counterterms will depend on the temperature (or the chemical potential): they will not. We discussed divergences in momentum space, but going back to coordinate space, we can understand this statement quite clearly. In coordinate space, divergences originate from singularity at $x = 0$ of the free propagator. Counterterms will then be defined as delta function or derivative of the delta function (thus the notion of locality for counterterms).

As will be discussed later, introducing the temperature in QFT for thermodynamics at equilibrium, means compactifying the time direction integration in the action. The free propagator in coordinate space is not affected by any boundary conditions, thereby its counterterm will remain the same as the $T = 0$ theory [1]. At least, this is true for standard local theory, but maybe not for non-local theories such as Hard Thermal Loop (see chapter 5).

In the context of thermal field theory, the matter contribution decouples from the vacuum contribution, the former coming with an extra factor of $n_B(\vec{p})$ or $n_F(\vec{p})$, respectively the Bose-Einstein/Fermi-Dirac distribution, that decrease exponentially with $\|\vec{p}\| \to \infty$ shielding the term from UV divergences. However, importantly, they lead to IR divergences that we will address in chapter 3. Moreover, even though the counterterms should not depend on T, within higher order calculations, temperature dependent divergences arise at intermediate steps, due to nested (sub)divergences, that are not always easy to disentangle.

2.4 Logs galore

2.4.1 Constraints on the poles

The bare coupling λ_0 contains formally all poles for $\varepsilon \mapsto 0$ that will renormalize the Feynman diagrams. For a renormalizable theory, by definition all these divergences cannot be totally independent. This link can be enlighten through the RG equation. Starting from, cf. Eqn.(2.18),

$$\beta(\lambda,\varepsilon) = \frac{(D-4)\bar{\lambda}_0}{\frac{\partial\bar{\lambda}_0}{\partial\lambda}} \quad , \quad \lambda_0 = M^{2\epsilon}\left(\lambda + \sum_{j=1}^{\infty} d_j(\lambda)\varepsilon^{-j}\right), \tag{2.38}$$

we can solve (formally) the beta function equation for the coefficient d_j for every power of ε. The coefficients $d_j(\lambda)$ are functions that we develop in power of λ. Defining $\beta(\lambda) \equiv -2\varepsilon + \beta^*(\lambda)$, the first orders give,

$$\beta(\lambda,\varepsilon) = -2\varepsilon + 2\left(\lambda\partial_\lambda - 1\right) d_1(\lambda) \;\mapsto\; \beta^*(\lambda) = 2\left(\lambda\partial_\lambda - 1\right) d_1(\lambda). \tag{2.39}$$

Often in perturbative calculations, one drops the factor of ε in the beta function such that we use $\beta(\lambda,\varepsilon) \simeq \beta^*(\lambda)$as $\varepsilon \mapsto 0$, however, forgetting this factor here will lead to wrong results. This equation already tells us that we only need the $1/\varepsilon$ divergences to evaluate the beta function. Then, we determine generically for the order ε^{-j}:

$$2(1-\lambda\partial_\lambda)d_{j+1}(\lambda) + \beta^*(\lambda)\frac{\partial d_j(\lambda)}{\partial\lambda} = 0, \tag{2.40}$$

which means that knowing the beta function, thus the $1/\varepsilon$ divergences at each successive orders, is sufficient to determine every other infinities that the coupling will renormalize. Repeating this procedure for every parameter of the theory, in the end, we only need to calculate the simple poles as well as the finite coefficients to determine exactly an observable at order λ^k. This knowledge will become particularly handy once we discuss cold QCD in chapter 5, since we used a similar reasoning to evaluate and resum every leading and next-to-leading logarithms.

2.5 Renormalization scheme change

For convenience and sensible comparisons, we are working in $\overline{\text{MS}}$, however, the scheme is arbitrary so nothing prevents us from changing scheme at some point. In chapter 6, we will see that changing the scheme will become quite handy. First, a scheme is specified by its (renormalized) parameters, counterterms and renormalization point. Practically, one specifies the renormalization scheme by the renormalization scale and the coefficients of the anomalous dimensions.

Previously, we already mentioned a change of renormalization scheme (RSC) in Eqn.(2.10) when going from the MS scheme to the $\overline{\text{MS}}$ one. This is a specific RSC where only the subtraction point M is modified. There is also a possibility to change the regulator $D = 4-2\varepsilon \mapsto D = 4-\alpha$ keeping the renormalization point unchanged. In practice, it amounts of changing the λ and m. Generically, we will consider a RSC with coefficients that do not depend on the mass. Suppose now that we have a second scheme in which the new mass and coupling are m' and λ', related to the other scheme as a perturbative series :

$$\begin{aligned} \lambda' &= \lambda'(\lambda) = \lambda\left(1 + A_1\,\lambda + A_2\,\lambda^2 + \dots\right), \\ m'^2 &= m^2\mathcal{Z}_m(\lambda) = m\left(1 + B_1\,\lambda + B_2\,\lambda^2 + \dots\right). \end{aligned} \tag{2.41}$$

Using the chain rule, the operator $M\frac{d}{dM}$ in Eqn.(2.15) in the original scheme can be expressed in terms of $M\frac{d}{dM}$ in the new one (see e.g [1; 15]), which leads to:

$$\begin{aligned} b'_0 &= b_0, \\ b'_1 &= b_1, \\ b'_2 &= b_2 - A_1\, b_1 + (A_2 - A_1^2) b_0, \\ b'_3 &= b_3 - 2A_1\, b_2 + A_1^2\, b_1 + (4A_1^3 - 6A_1\, A_2 + 2A_3) b_0, \end{aligned} \tag{2.42}$$

$$\begin{aligned} \gamma'_0 =& \gamma_0, \\ \gamma'_1 =& \gamma_1 + 2b_0\, B_1 - \gamma_0\, A_1, \\ \gamma'_2 =& \gamma_2 + 2B_1\, b_1 + 2(2B_2 - B_1^2) b_0 - \gamma_0\, A_2 - 2A_1\, \gamma_1, \\ \gamma'_3 =& \gamma_3 - A_3\, \gamma_0 - (A_1^2 + 2A_2)\gamma_1 - 3A_1\, \gamma_2 + 2b_2\, B_1 \\ & - 2b_1(B_1^2 - 2B_2) + 2b_0(B_1^3 - 3B_1\, B_2 + 3B_3) \end{aligned} \tag{2.43}$$

We see clearly that γ_0, b_0 and b_1 are RSC invariant, i.e universal quantities.

2.5.1 Dimensional regularization glossary

Working in dimensional regularization, one needs to modify the metric such that its trace gives the right number of dimensions:

$$g^{\mu\nu} g_{\mu\nu} = d \mapsto \gamma_\mu \gamma^\mu = d. \tag{2.44}$$

In $T = 0$ quantum field theory (QFT), we commonly keep the D-dimensional integration measure as $d^D k$ to proceed to integration. However, in HTL theory at finite temperature, as we will see in chapter 5, the integrand is generally dependent on the angle between k_0 and $\vec{k}$, the integrated momentum, so we separate the integration measure:

$$\int d^d k = \int d\Omega_d \int dk\, k^{d-1}, \tag{2.45}$$

where the d dimensional angle reads:

$$d\Omega_d = sin^{d-2}(\phi_{d-1}) sin^{d-3}(\phi_{d-2}) \dots d\phi_1 \dots d\phi_{d-1} \tag{2.46}$$

$$\Omega_d = \int d\Omega_d = 2\pi \prod_{n=2}^{d-1} \left(\int_0^\pi d\phi_n\, sin^{d-1}\phi_n \right) = 2\pi \prod_{n=2}^{d-1} \sqrt{\pi} \left(\frac{\Gamma(\frac{n}{2})}{\Gamma(\frac{n+1}{2})} \right) = \frac{2\pi^{d/2}}{\Gamma(\frac{d}{2})}. \tag{2.47}$$

In the last equation, the integral leading to a factor of $\pi^{d/2}$ is actually an axiom of dimensional regularization. The most common integrals over Euclidean momentum are:

$$\int dk\, \frac{k^a}{(k^2 + \Delta)^b} = \Delta^{\frac{a+1}{2} - b}\, \frac{\Gamma(\frac{a+1}{2}) \Gamma(b - \frac{a+1}{2})}{2\, \Gamma(b)} \tag{2.48}$$

The analytic properties of the gamma function, with well identified poles at negative integers, provides a useful analytic continuation for any a,b values.

2.6 Bibliography

[1] John C. Collins. *Renormalization: An Introduction to Renormalization, the Renormalization Group and the Operator-Product Expansion*. Cambridge Monographs on Mathematical Physics. Cambridge University Press, 1984.

[2] John C. Collins. Renormalization: General theory. 2006, hep-th/0602121.

[3] Loïc Fernandez and Jean-Loïc Kneur. Renormalization group optimized $\lambda\phi^4$ pressure at next-to-next-to-leading order. *Phys. Rev. D*, 104(9):096012, 2021, 2107.13328.

[4] G. 't Hooft. Dimensional regularization and the renormalization group. *Nuclear Physics B*, 61:455–468, 1973.

[5] J. F. Ashmore. A method of gauge-invariant regularization. *Lettere al Nuovo Cimento*, 1972.

[6] C.G. Bollini and J.J. Giambiagi. Lowest order divergent graphs in v-dimensional space. *Physics Letters B*, 40(5):566–568, 1972.

[7] Steven Weinberg. High-energy behavior in quantum field theory. *Phys. Rev.*, 118:838–849, May 1960.

[8] Mattew D. Schwartz. *Quantum Field Theory and the Standard Model*. Cambridge University Press, 2014.

[9] V. P. Spiridonov and K. G. Chetyrkin. Nonleading mass corrections and renormalization of the operators m psi-bar psi and g**2(mu nu). *Sov. J. Nucl. Phys.*, 47:522–527, 1988.

[10] K. G. Chetyrkin, C. A. Dominguez, D. Pirjol, and K. Schilcher. Mass singularities in light quark correlators: The Strange quark case. *Phys. Rev. D*, 51:5090–5100, 1995, hep-ph/9409371.

[11] C. Arvanitis, F. Geniet, M. Iacomi, J. L. Kneur, and A. Neveu. Variational solution of the Gross-Neveu model. 2. Finite N and renormalization. *Int. J. Mod. Phys. A*, 12:3307–3334, 1997, hep-th/9511101.

[12] J. L. Kneur and M. B. Pinto. Scale Invariant Resummed Perturbation at Finite Temperatures. *Phys. Rev. Lett.*, 116(3):031601, 2016, 1507.03508.

[13] Jean-Loic Kneur. Variational quark mass expansion and the order parameters of chiral symmetry breaking. *Phys. Rev. D*, 57:2785–2805, 1998, hep-ph/9609265.

[14] J. L. Kneur and M. B. Pinto. Renormalization Group Optimized Perturbation Theory at Finite Temperatures. *Phys. Rev. D*, 92(11):116008, 2015, 1508.02610.

[15] Jean-Loïc Kneur and André Neveu. α_S from F_π and Renormalization Group Optimized Perturbation Theory. *Phys. Rev. D*, 88(7):074025, 2013, 1305.6910.

[16] C. Ford, D. R. T. Jones, P. W. Stephenson, and M. B. Einhorn. The Effective potential and the renormalization group. *Nucl. Phys. B*, 395:17–34, 1993, hep-lat/9210033.

[17] M.E. Peskin and D.V. Schroeder. *An Introduction To Quantum Field Theory*. Frontiers in Physics. Avalon Publishing, 1995.

[18] G. 't Hooft and M. Veltman. Regularization and renormalization of gauge fields. *Nuclear Physics B*, 44(1):189–213, 1972.

[19] *Quantum Fields in Curved Space*. Cambridge Monographs on Mathematical Physics. Cambridge University Press, author=Birrell, N. D. and Davies, P. C. W., year=1982, collection=Cambridge Monographs on Mathematical Physics.

[20] A. Zee. *Quantum field theory in a nutshell*. 2003.

[21] Oleg Komoltsev and Aleksi Kurkela. How Perturbative QCD Constrains the Equation of State at Neutron-Star Densities. *Phys. Rev. Lett.*, 128(20):202701, 2022, 2111.05350.

3

"A picture is worth a thousand words."
— Confucius

Groups, representations and all sorts of fibers

The modern formulation of particle physics became exponentially greedy in terms of mathematical notions and notations. When tackling the background of the Standard Model (SM), we need tools such as Quantum field Theory (QFT) and Yang-Mills theory which has become the cornerstone of particle physics. None of them is actually completely understood. Practical calculations in Quantum Field Theory remain ill-defined, as we saw in the previous chapter, and the theory is too difficult to be exactly solved, while there is still a missing proof at the heart of Yang-Mills theory concerning its classical solutions. The theory of the strong interaction, Quantum ChromoDynamics (QCD), among other fundamental interaction, is based on QFT and Yang-Mills theories. We will not discuss QFT here, however, we will recall the main concepts at the core of Yang-Mills theory, namely, groups, groups representations and finally fiber bundles.

3.1 Lie Group and representations

3.1.1 Symmetries in nature

It seems a bit ambitious to try to discuss all the symmetries in our surrounding world. And yet, it may be very useful. Obviously, what is man-made is almost always very symmetric, but also the world without our footprint. Flowers have discrete rotational symmetries; trees are cylindrical; leaves have a plane symmetry... Our earth is nearly perfectly spherical, our universe up to its far away confines appears to have a uniformly distributed electromagnetic radiation. This has even motivated mathematician to describe "beauty" in mathematical terms based on symmetry [1; 2]. Not all objects display exact symmetries, but the latter are at least approximate. It seems that stable complex systems are just a gathering of small symmetric constituent blocks assembled in a regular way[3]. Thus, physicists went digging for every possible symmetries, at the microscopic scale, that could help simplifying the description of the world. Knowing all of these symmetries allow to simplify the description of the sub-scale and how the building blocks merge together. At the microscopic scale, this lead to describe matter and its interaction using only symmetry groups. This is the modern formulation of quantum

physics in terms of Quantum Field Theory, group (of symmetry) theory and the gauge principle: the Standard Model.

Group definition

A group G of cardinality n, is a set $\{g_a\}_i$, $i = 1, \ldots, n$ of symmetries, called group elements, which compose together. The composition "o" is inherent to the group and associative:

$$\forall g_1 \in \mathrm{G},\ \forall g_2 \in \mathrm{G},\ (g_1\ o\ g_2) \in \mathrm{G}$$

Every g_a in the group possesses its own inverse in the group such that: $g_a\ o\ g_a^{-1} = \mathbb{1}_{\mathrm{G}}$, where $\mathbb{1}_{\mathrm{G}}$ is the group unitary element, included in $\{g_a\}_i$. If the group composition is *commutative*, thus $g_a\ o\ g_b = g_b\ o\ g_a$, then the group is *Abelian*. Furthermore, the group is said to be simple if it cannot be reduced into direct sum of smaller groups. The group $\mathrm{GL}(n, \mathbb{K}))$ is the group of square matrices of dimension n, invertible, defined on the number field K. J_{pq} is the diagonal matrix consisting of p times one and q times minus one. Then

$$\begin{aligned} \mathcal{O}(p,q) &= \left\{A \in GL(p+q,\mathbb{R}) \middle/ A\ J_{pq} A^t = J_{pq}\right\} \\ SU(N) &\equiv \left\{A \in GL(N,\mathbb{C}) \middle/ A^\dagger A = \mathbb{1}\ \&\ \det(A) = 1\right\} \end{aligned} \tag{3.1}$$

Note that lifting the restriction on the determinant defines the group U(N). Of great importance is the group $\mathcal{O}(1,3)$ which is the Lorentz group encoding rotational symmetry and boost invariance.

Differentiable manifold and Lie groups

Lie groups are continuous groups of symmetries also defined as a differentiable manifold. Thus, we have two pictures for the same objects: an algebraic structure and a geometric structure. This allow to take advantage from both sides.

As the Lie group is locally an euclidean space, in each point of the manifold lies a vector space. At the identity, the vector space is the *Lie algebra* $\mathfrak{g} = T_{\mathbb{1}_{\mathrm{G}}}\mathrm{G}$. Precisely,

$$\mathrm{Lie\ G} = \left\{A \in \mathrm{gl}(n,\mathbb{K}) \;\middle|\; \forall t \in \mathbb{R},\ e^{t\,A} \in \mathrm{G}\right\}. \tag{3.2}$$

From the algebraic structure of the Lie group, the Lie algebra is equipped with an intern composition law, usually wrote "$[,]$" and called "Lie bracket", satisfying:

$$\begin{aligned} &\forall X, Y \in \mathfrak{g} && [X,Y] = -[Y,X] \\ &\forall X, Y \in \mathfrak{g} && [X,[Y,Z]] + [Z,[X,Y]] + [Y,[Z,X]] = 0. \ \text{(Jacobi's identity)} \end{aligned} \tag{3.3}$$

Since we will consider unitary Lie group, whose determinant are equal to one, then the elements of the Lie algebra must be traceless and since $\forall\, \mathrm{G}_1,\ \mathrm{G}_2 \in \mathrm{G} \to \mathrm{G}_1\, o\, \mathrm{G}_2 \in \mathrm{G}$ it implies $\forall\, T_a,\ T_b \in \mathfrak{g} \to [T_a, T_b] \in \mathfrak{g}$ since the commutator is also traceless. The algebra being closed, the Lie bracket defines the *structure coefficients*:

$$[T_a, T_b] = i\, f_{abc}\, T_c \tag{3.4}$$

Lie algebra is said to be the "logarithm of the group G", this is always true by construction but the inverse is not. Indeed, the exponential function cannot reach (it is not surjective), in general, all components of G. It does only if the group G is compact and connected. One last subtlety however, two non isomorphic groups may have isomorphic Lie algebra. For example,

$\mathrm{Lie\,SO(3)} = \mathrm{Lie\,SU(2)}$ but $\mathrm{SO(3)} = \mathrm{SU(2)}/\mathbb{Z}_2$ with $\mathbb{Z}_2 = \{-1, 1\}$ being the second group of congruence. SU(2) forms the covering space of SO(3) and gives the spinor representations of the Lorentz group. There is also the case of SU(3) and $\mathrm{SU(3)}/\mathbb{Z}_3$ which possess the same Lie algebra. The center symmetry $\mathbb{Z}_3$ plays an important role in the confinement of color charges in pure Yang-Mills theory at finite temperature (see chapter 4).

3.1.2 Representation theory on a Hilbert space

Previously, the group action was defined making abstraction of the specific structure upon which it acts. Furthermore, we only defined abstract group elements from their composition without specifying what they were. There are infinitely many different ways to represent the group action, leading to different representations (nevertheless, they are not all linearly independent). For a representation of group elements, we essentially ask for the latter to preserve the inner structure of the group, that is to say that a representation of G on a vector space V is a group homomorphism:

$$\rho : \mathrm{G} \to \mathrm{GL}(V),\ \forall g_1, g_2 \in \mathrm{G} \to\ \rho(g_1\, o\, g_2) = c(g_1, g_2)\, \rho(g_1)\rho(g_2). \tag{3.5}$$

The function $c(g_1, g_2)$ introduced here reminds us that states in the Hilbert space do not necessarily need to transform under representation of the group (that would mean $c(g_1, g_2) = 1$). Quantum states are defined only up to a phase factor, so they only need to transform under projective representations (i.e representation of the covering space).

In practice, there is an infinity of representations, most of them being redundant as they are reducible and can be decomposed into lower dimensional representations ρ_i: $R = \oplus_i \rho_i$. Among all the representations of the group elements, there are two of great importance: the defining (F, also called fundamental) and the adjoint (adj.) representations. The first one is on the vector space $V \cong \mathbb{C}^N$ for $N \in \mathbb{N}^*$, $N = 0$ being the trivial representation, while the adjoint is on the Lie algebra.Denoting respectively D and d for the representations of the Lie group and Lie algebra, for $\mathrm{G} = \mathrm{SU(N)}$, $A \in G$, $\mathfrak{g} = \mathrm{Lie(G)}$ and $a_i \in \mathfrak{g}$:

$$\begin{aligned} D_{\mathrm{F}}(A) = A \qquad &\iff \quad d_{\mathrm{F}}(\mathrm{T_a}) = \mathrm{T_a} \qquad\quad \dim(\mathrm{D_F}) = \mathrm{N} \\ D^{\mathrm{adj.}}_A(a) = A\, a\, A^{-1} &\iff d^{\mathrm{adj.}}_{a_1}(a_2) = [a_1, a_2] \quad \dim(\mathrm{D_{adj.}}) = \mathrm{N}^2 - 1 \end{aligned} \tag{3.6}$$

The Casimir operators of the representation R characterize the representation:

$$\sum_a \mathrm{T^R_a T^R_a} = C_2(R)\mathbb{1} \tag{3.7}$$

and they are dependant on the normalization of the generators of the Lie algebra:

$$\mathrm{Tr}\left(\mathrm{T^R_a T^R_a}\right) = \mathrm{I(R)}\delta_{\mathrm{ab}}. \tag{3.8}$$

We usually set for $\mathrm{SU(3)}$: $T_a = \frac{1}{2}\lambda_a$, where λ_a are the Gell-Mann matrices, recalled explicitly in appendix A. This definition gives:

$$\begin{aligned} I(R = F) = \frac{1}{2} = T_F \ \ , \ \ C_2(R = F) = \frac{N^2 - 1}{2N} = C_F \\ I(R = adj.) = T_A = N = C_2(R = adj.) = C_A \\ d_A \equiv N^2 - 1 \ \ , \ \ d_F \equiv \frac{d_A\, T_F}{C_F} = N \ \ , \ \ f_{acd} f_{bcd} = N\delta_{ab} \end{aligned} \tag{3.9}$$

3.2 Fiber Bundle

3.2.1 Principal Bundle

Every interaction in modern physics is characterized by a gauge symmetry group. Matter fields, gauged under these symmetry groups are then charged under these interactions. The goal now is to define fiber bundles which give a geometrical definition. First, we need to be given a 4-dimensional manifold in which the fields live. Then we need to attach in every point of this manifold a copy of the gauge group to reflect the underlying symmetry of the matter fields. This structure is a fiber bundle. Mathematically, a fiber bundle is a triplet $(\mathcal{P}, \pi, \mathcal{M})$ where $\mathcal{P}$ is called the total space, $\mathcal{M}$ the base, and π is a projection from $\mathcal{P}$ to $\mathcal{M}$. If F is a Lie group, then we call the fiber bundle a *principal bundle*. These are the one we are interested in. Locally, $\mathcal{P}$ is a product space $\mathcal{M} \times \mathcal{F}$ where $\mathcal{F}$ is the *fiber*. However, it may not be the case globally due to non trivial topology, first from the topology of the base space but also due to the fibers. Take the Moëbius strip which is the perfect example (see fig.3.1): locally, $\mathcal{P}$ looks like $\mathbb{R}^2$, but globally, the base space identify to the circle $\mathcal{S}^1$ and not $\mathbb{R}$. Yet, there is at least two total space that relies on the circle: the Moëbius strip and the cylinder. In the first case the fiber can rotate of π around the base space.

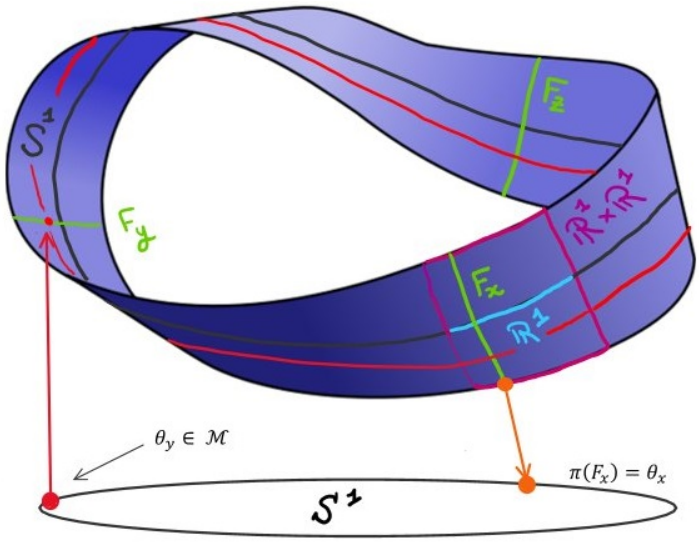

Figure 3.1: the Moëbius strip seen as a fiber bundle. The orange arrow represent the application π while the red one is σ.

To discriminate between the two shapes, we need to introduce a *section* σ. As can be seen on fig.3.1, the section is a *continuous* map from the base to the total space. It associates one point in $\mathcal{M}$ to *one* point on the fiber above $\mathcal{M}$. The section grants us with an origin on the fiber. It is often said that the section is the inverse of π but this is misleading, π projects the whole fiber on $\mathcal{M}$ whereas the section specifies, by an *arbitrary choice*, one point on the fiber. To bo given a section is equivalent to be given a specific topology of $\mathcal{P}$. In physics, this section is related to the gauge fixing condition and the ghost fields that we will explore in the next chapter.

Associated bundle: Bundle of Bundle of...

This structure of a fiber bundle is pretty generic, and we could choose one fiber bundle as being the base space of another bundle. While this seems like self-harming at this point, it is actually of practical use when trying to define the connection on a fiber bundle together with matter field living in a representation of the gauge group, and not the gauge group itself. For a matter field living in a given representation ρ (on the vector space V) of the gauge group, one defines the space where it lives as the associated vector bundle $E = P \times_G V_\rho = P \times V_\rho/\mathrm{G}$.

Connection on a fiber bundle

Consider the point u in the total space P. By definition, it is a point x in $\mathcal{M}$ with a specific referential in the symmetry describes by the Lie group G (or its representation $\rho(\mathrm{G})$ on the fiber F). We would like to transport this referential along a curve in P, as we move from x to

$y \in \mathcal{M}$, keeping the referential parallel to itself in order to compare vectors from two different points in the bundle. This is achieved through the connection which projects the basis vectors onto each other as we move along the curve.

The connection act on vectors from TP (tangent space of P) and takes values in $\mathfrak{g}$. It can be cast on the tangent space of $\mathcal{M}$ via a given section,

$$\begin{array}{c} TP \xrightarrow{\mathcal{A}} \mathfrak{g} \\ \sigma \uparrow\downarrow \ \pi \\ T\mathcal{M} \underset{\mathcal{A}}{\rightarrow} \mathfrak{g} \end{array} \tag{3.10}$$

such that the connection is a 1-form on $\mathcal{M}$ instead of P. We see here that we need a section to define the connection form on the base space. In physicist language, this means that we will need ghost fields so that the gauge fields may be described on space-time. Unfortunately, the theory of connection would lead us way too far from thermal quantum field theory at this point, thus we will restrain from discussing these notions more deeply. Only we need to know is:

We will consider trivializable principal bundle which means that it can locally be expressed as a product space. So, we can define locally a 1-form along the natural local coordinates of 1-forms dx^μ. Since the connection takes values in the lie algebra, we can expand it in terms of the generators of the Lie algebra (in any representation). In a given representation ρ it reads:

$$\rho(\mathcal{A}) = \mathcal{A}^a_\mu \, \rho(X_a) dx^\mu. \tag{3.11}$$

For convenience, we will write $\rho(X_\alpha) = X^R_\alpha$ for a given representation R from now on.

3.3 Bibliography

[1] Jean-Paul Delahaye. La beauté mise en formules. *Pour la science*, (455), 2015.

[2] George David Birkhoff. *Aesthetic measure*. Cambridge, Mass., Harvard University Press, 1933.

[3] François Gieres. About symmetries in physics, December 1997.

[4] Anthony Zee. *Group Theory in a Nutshell for Physicists*. Princeton University Press, 2016.

[5] Sydney Coleman. *Aspects of symmetry*. Cambridge University Press, 1985.

[6] Adam Marsh. *Gauge Theories and Fiber Bundles: Definitions, Pictures, and Results*. ArXiv, 2016.

[7] Robert Coquereaux. *Espaces fibrés et connexions*. Centre de Physique théorique, Luminy, Marseille, 2002.

[8] Hidenori Fukaya. Why is quantum gravity so difficult (compared to QCD)?, March 2020.

[9] Tohru Eguchi, Peter B. Gilkey, and Andrew J. Hanson. Gravitation, gauge theories and differential geometry. *Physics Reports*, 66(6):213–393, 1980.

[10] John C. Baez. *Gauge fields, knots, and gravity*. K & E series on knots and everything. World Scientific, Singapore ; New Jersey, 1994. Includes index.

4

"Color! What a deep and mysterious language, the language of dreams."
— Paul Gauguin

Quantum Chromodynamics in a medium

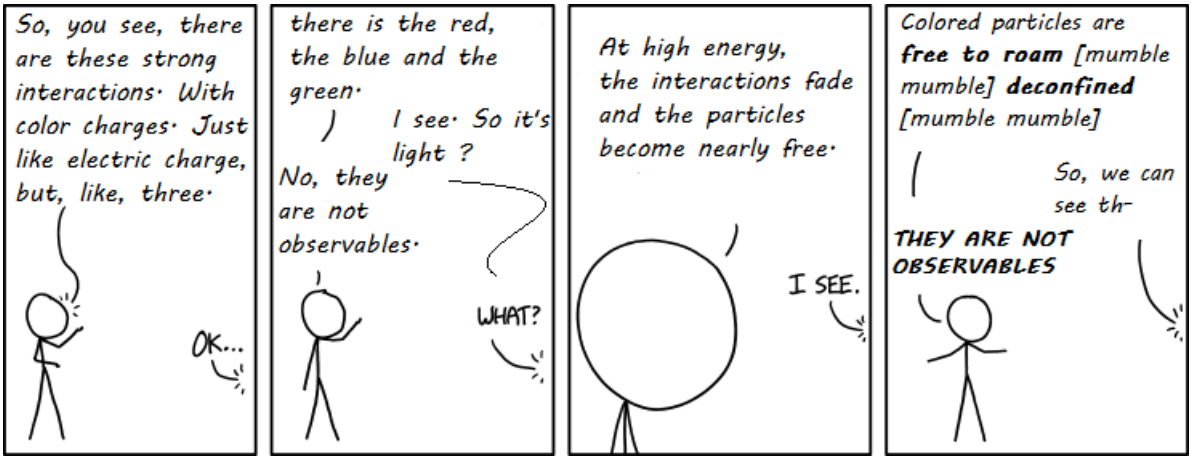

Adapted from `https://xkcd.com/1489/`

4.1 Hadrons, baryons, mesons, quarks and gluons ?

In the 1950s, the invention of the bubble chambers lead to the discovery of a large number of particles in high-energy collision experiments: the hadrons. So many of them that it became unreasonable for particle physicists to think of them as the most elementary ones. In fundamental physics, we are looking for simplification and unification. Physicists were also guided by the fact that some particles could not even possibly exist as they were not satisfying the Pauli exclusion principle. To reconcile theory and experiments, Gell-Mann [1] and Zweig [2] proposed independently in 1963 a model of smaller particles existing in three flavors which could explain the observed abundance of Hadrons. Protons, neutrons and pions could therefore be explained with the first two flavors: *up* and *down*, while the *strange* quark was required to explain the properties of the Kaons. In 1968, a scaling in deep-inelastic electron-nucleon scattering was observed implying a point-like substructure that was given the name of "*partons*" [3; 4]. Partons were later identified to be the quarks (and gluons) of the Gell-Mann and Zweig model.

Quark flavor	mass	Charge (QED)
up	$2.16^{+0.49}_{-0.26}\,\mathrm{MeV/c^2}$	$+\frac{2}{3}e$
down	$4.67^{+0.48}_{-0.17}\,\mathrm{MeV/c^2}$	$+\frac{-1}{3}e$
strange	$93^{+11}_{-5}\,\mathrm{MeV/c^2}$	$+\frac{-1}{3}e$
charm	$1.27^{+0.02}_{-0.02}\,\mathrm{GeV/c^2}$	$+\frac{2}{3}e$
bottom	$4.18^{+0.03}_{-0.02}\,\mathrm{GeV/c^2}$	$+\frac{-1}{3}e$
top	$172.76^{+0.30}_{-0.30}\,\mathrm{GeV/c^2}$	$+\frac{2}{3}e$

Table 4.1: Current quark masses [13] at $M \simeq 2\mathrm{GeV}$ and charge with respect to QED.

Gell-Mann also discussed a theory of interacting quarks through the exchange of gluons, the mediator of the interaction, which also resolved the issue that the wave function of the three quarks in the baryon Δ^{++} could not be anti-symmetric without an extra quantum number. This charge, which comes in three different types in contrast with electromagnetism, was given the name of *color* by loose analogy with the three fundamental colors of the visible spectrum of light. Therefore, three-particle composite objects described the baryons while particle/anti-particle described the mesons. The nascent theory was thus named *Quantum Chromodynamics* (QCD). Just a year after the birth of QCD by Gell-Mann and Zweig, Glashow and Bjorken [5] proposed to introduce a new flavor: the *charm* quark in order to obtain a better description of the weak interactions, the latter having the same number of families for the quarks and the leptons. This was later reinforced [6] since an additional quark could explained the suppression of neutral current processes (GIM mechanism) involving change in the strange isospin. Soon after, in 1974, it was discovered independently by two teams [7; 8]. Yet, Kobayashi and Maskawa, following an old idea of Cabbibo [9] predicted in 1973 that it required a new pair of quarks in order to reproduce CP violation in weak interactions. While the first one, the *beauty* quark (commonly named *bottom* now) was observed at Fermilab [10] in 1977, physicists at that time had to wait until 1995 [11; 12] for the discovery of the last one: the *truth* quark (called *top* now). Quantum numbers and presently known masses for the quarks are summarized in Table.(4.1). Even though the proton was believed since long to be composed of two up and one down quarks, quantum field theory predicts that in addition there is an infinite number of quark/antiquark pairs that could emerge from the vacuum. Thus, it has been argued that the proton could have a sizable intrinsic component of the lightest heavy quark, the charm quark. Recently, an evidence at the statistical three sigma level for this intrinsic charm quark inside the proton was reported [14]. This now demands to be confirmed by another group.

The strong interactions is confined inside the core of the Hadrons since color charge has never been observed directly until now. This suggests that only "white" composite particles exist as bound states. Yet, this confinement property of QCD has not been proven rigorously mathematically for all values of the coupling, even though it has been observed, at finite temperature, on lattice computations of the theory [15; 16]. In 1973, Politzer [17], Gross and Wilczek[18] showed that the only-renormalizable force at long distance and decreasing at short distance was of Yang-Mills types [19]. In this theory, the leading order contribution in perturbation theory to the beta function that drives the coupling evolution with the energy scale is, in appropriate units,

$$\beta = -\frac{g^4}{32\pi^2}\left(\frac{11}{3}N_c - \frac{2}{3}N_f\right) + \mathcal{O}(g^6). \tag{4.1}$$

Where N_c is the number of colors, specifically, three for QCD. For $N_f \leq 33/2$, the beta function is negative leading to a logarithm fall off of the coupling at high energy, i.e. at short distances. In this range, quarks and gluons become nearly free particles, able to roam outside hadrons, although the confinement property still holds strictly (quarks and gluons never appear in isolation).

Due to this asymptotic freedom property, it seems reasonable to pursue a weak coupling expansion at high energy. However it is well known for a while that the perturbative series is presumably not convergent in QCD, but only a so-called asymptotic series [20][1]. However, it is believed that the perturbative series will converge for the first N terms before diverging. The precise value of N is unknown but roughly of the order of the inverse of the coupling. See [21] for a detailed argument. We will assume that the instabilities of the series arise at a much higher order than what will be addressed in this thesis.

4.1.1 Color screening and asymptotic freedom, an intuitive picture

The relative sign between the number of colors N_c and the number of flavors N_f in the beta function states that gluons and quarks operate oppositely in the screening of the bare charge. Same color quarks repel each others, while for quarks of different colors it is slightly more complicated. They can either attract each others, or, there is a possibility that they exchange their colors and the this is a repulsive channel. Averaging over the color charge, quarks repel each others while they are attracted to anti-quarks, similarly to QED. Even though the interaction between quarks are slightly more complicated than in QED, they give the same positive screening that tends to make us see a smaller charge as we move away from a color charge. On the contrary, as we move forward the central quark, we penetrate the screening cloud of virtual quark-antiquark pairs and gluons and we see a greater fraction of the true color charge. However, as gluons carry a pair of charge/anti-charge, the picture is totally modified. Penetrating the screening cloud, we see less and less gluons, carriers of a charge. This contribution being stronger, it drives the beta function to be negative. Overall, we see less and less of the charge as we move in, explaining the asymptotic freedom of QCD.

4.2 Yang-Mills theory and the gauge principle

Now, moving on to QCD, we assign to the quarks a color charge and the three colored fields are embedded in a color multiplet living in the fundamental representation **3** of SU(3). The six flavors of quark fields are described as elements of the trivial bundle P whose base space is space-time and the fiber is the fundamental representation of the (global) symmetry $\mathrm{SU}_{\mathrm{color}}(3)$. Upon using the gauge principle, thus requiring the symmetry to be preserved locally, gluon fields emerge as the connection in the adjoint representation on the fiber bundle. This connection is well-defined if and only if we give a specific section on the fiber bundle as discussed in the last part of chapter 3 (see Fig.3.1). This section, a gauge fixing term, is called the ghost fields in QCD terminology. We will see below how ghost emerge in the Faddeev-Popov procedure.

Gauging the quark fields under the SU(3) symmetry using the minimal coupling procedure and expanding the gluon fields on the fundamental representation of $SU(3)$:

$$\partial_\mu \to \mathcal{D}_\mu^{(\mathcal{A})}\psi \equiv (\partial_\mu - ig\mathcal{A}_\mu)\,\psi, \qquad \mathcal{A}_\mu = \mathcal{A}_\mu^a\, T_{\mathrm{F}}^a, \tag{4.2}$$

[1]Strictly speaking, the argument was developed for QED as QCD was not yet invented, however, the generalization holds.

with the $N_c \times N_c$ matrices T_F^a of the fundamental representation. For a local gauge transformation[2] $U(x) = e^{i\,g\,\alpha_a(x)T^a}$, which acts on $\psi \to U(x)\psi$, the transformation law of the gluons in the adjoint representation:

$$A'_\mu = UA_\mu U^{-1} + \frac{i}{g}U(\partial_\mu U^{-1}) \Rightarrow \mathcal{D}_\mu^{(A')}U^R = U^R\mathcal{D}_\mu^{(A)} \tag{4.3}$$

makes the Lagrangian for quarks explicitly gauge invariant under both global and local transformations:

$$\mathcal{L}_q = \bar{\psi}_{\alpha,j,f}\left(i\gamma^\mu(\mathcal{D}_\mu^{(\mathcal{A})})_{jk} - m_f\,\delta_{j,k}\right)\psi^\alpha_{k,f}. \tag{4.4}$$

Greek indices α denotes spinor indices while μ is for Lorentz vector indices. Latin letter except f are used for color indices while f is for the flavor. On top of that, we include the Yang-Mills Lagrangian for the gluon fields:

$$\mathcal{L}_{\rm YM} = -\frac{1}{4\,\mathrm{I(R)}}\mathrm{Tr}\,(F^{\mu\nu}F_{\mu\nu}) = -\frac{1}{4}F^{\mu\nu}_a F^a_{\mu\nu}\ , \quad F^a_{\mu\nu} = \partial_\mu\mathcal{A}^a_\nu - \partial_\nu\mathcal{A}^a_\mu + g\,f^{abc}\mathcal{A}^b_\mu\mathcal{A}^c_\nu. \tag{4.5}$$

The coefficients related to representations are given in chapter 3. Finally, from these two Lagrangian terms, we construct the one for QCD:

$$\mathcal{L}_{\rm QCD} = \sum_{f=1}^{N_f}\bar{\psi}_{\alpha,j,f}\left(i\gamma^\mu(\mathcal{D}_\mu^{(\mathcal{A})})_{jk} - m_f\,\delta_{j,k}\right)\psi^\alpha_{k,f} - \frac{1}{4}F^{\mu\nu}_a F^a_{\mu\nu}. \tag{4.6}$$

Where we added different mass terms m_f for each flavor of quarks. The Lagrangian in Eqn.(4.6) only contains information about the strong interaction, not from the electroweak sector. In particular, the masses present in the Dirac terms are not truly static in the context of the full Standard Model, but rather dynamically generated by the spontaneous breaking of the electroweak symmetry via the Yukawa interactions between quarks and the Higgs field. One final last step is to perform a Wick rotation $t \to \tau = i\,t$, for later convenience, which leads to the Euclidean action:

$$\mathcal{S}_{\rm QCD} = \int d^D x \quad \left(\frac{1}{4}F^a_{\mu\nu}F^{\mu\nu}_a + \sum_f^{N_f}\bar{\psi}_f\left(\gamma^\mu\mathcal{D}_\mu + m_f\right)\psi_f\right). \tag{4.7}$$

Note that to obtain this expression we redefined the following quantities [22]:

$$\begin{aligned} &\tilde{\gamma_0} \equiv \gamma^0\ ,\ \tilde{\gamma_k} \equiv -i\gamma^k \\ &A^a_0 \to i\tilde{A}^a_0 \end{aligned} \tag{4.8}$$

4.2.1 Quantization of YM gauge theory: path-integral approach

In this thesis, we shall use only the Feynman's path integral approach to the quantization of QCD as it is more straightforward to introduce the temperature and density in the theory afterwards. Assuming implicit product over spinor, vector and color indices in the measure, the naive partition function for QCD reads:

$$\mathcal{Z} = \mathcal{N}\int\mathcal{D}\mathcal{A}\int\mathcal{D}\bar{\psi}\mathcal{D}\psi\ e^{-\mathcal{S}_{\rm QCD}}. \tag{4.9}$$

[2]Einstein's summation rule is understood for every repeated indices.

However, this naive partition function leads to a non-invertible operator $K_{\mu\nu}$ for the gluons quadratic terms so we cannot define a propagator. Mathematically, this is because we did not specify a section yet, thus the projection π from the total space to the base space, taking $\mathcal{A} \in P \to \mathcal{A}_\mu dx^\mu \in \mathcal{M}$ (see Eqn. 3.10) is not invertible. Equivalently, in a more physical picture, this is because we have a redundancy in the gauge space configurations along the so-called gauge orbit $\mathcal{O}_\mathcal{A}$ (the fiber) and we need to introduce a gauge fixing term to define a propagator for the gluons.

Letting $\mathbb{A}$ be the configuration space of the gauge field that is integrated over in Eqn.(4.9), we rewrite $\mathbb{A} = \mathcal{O}_\mathcal{A} \times \mathbb{A}/\mathcal{O}_\mathcal{A}$ to separate the degrees of freedom, with $\mathbb{A}/\mathcal{O}_\mathcal{A} = \mathcal{G}$ being the orbit space. To eliminate the redundancy in the gauge space, we introduce a generalized gauge fixing term $f(A) = B$, where B is a given field independent of A . This defines a gauge slicing not necessarily perpendicular to the gauge orbits (see fig.(4.1)). For the rest of this thesis, we will assume that this equation admits a unique solution for each gauge orbit. Then, we can follow the Faddeev-Popov procedure [23] to implement the gauge slicing term inside $\mathcal{Z}$. To begin with, we insert a factor of unity in the functional integral in the form:

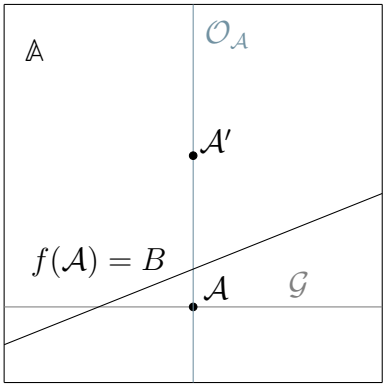

Figure 4.1: Gauge configurations

$$1 = \Delta^\mathcal{A}_{\text{FP}} \int_{\mathcal{O}_\mathcal{A}} \mathcal{D}U \; \delta(f(\mathcal{A}^U) - B)), \quad \Delta^\mathcal{A}_{\text{FP}} = \frac{\delta f(\mathcal{A}^U)}{\delta U}. \tag{4.10}$$

Using Grassmann fields $c, \bar{c}$ and associated properties of Gaussian-like integrals, we may rewrite this determinant in terms of the ghost fields:

$$\Delta^\mathcal{A}_{\text{FP}} = \int \mathcal{D}\bar{c}\mathcal{D}c \, e^{-\mathcal{S}_{\text{ghost}}(\mathcal{A},\bar{c},c)}. \tag{4.11}$$

Having introduced an arbitrary field B, we average on this condition with a gaussian weight $\exp\left(\frac{1}{2\xi}\int d^D x \text{Tr}B^2\right)$, that we integrate over, where ξ a gauge fixing parameter. Ultimately, physical observables should be independent of the gauge fixing condition , thus, should be independent of ξ. The delta function kills the B-integration leading to $B \to f(\mathcal{A})$. From this construction, the integration over the (infinite) gauge orbit volume factorizes and defines a new integration constant $\mathcal{N}'$. Finally, we are left with the standard expression for the (Faddeev-Popov) QCD path integral :

$$\mathcal{Z} = \mathcal{N}' \int \mathcal{D}\mathcal{A}\mathcal{D}\bar{c}\mathcal{D}c\mathcal{D}\bar{\psi}\mathcal{D}\psi \; e^{-\mathcal{S}_{\text{YM}} - \mathcal{S}_{\text{fix.}} - \mathcal{S}_{\text{ghost}} - \mathcal{S}_q} \tag{4.12}$$

$$\mathcal{S}_{\text{ghost}} \equiv \int d^D x \int d^D y \; \bar{c}^a(x) \frac{\delta f_a(\mathcal{A}^U(x))}{\delta U^b(y)}\Big|_{\alpha=0} c^b(y) \; , \; \mathcal{S}_{\text{fix.}} = \frac{1}{2\xi}\int d^D x \; \text{Tr}(f(\mathcal{A}(x))^2). \tag{4.13}$$

The infinite constant $\mathcal{N}'$ cancels between the numerator and the denominator of the following expression when considering expectation values of observables:

$$\langle \mathcal{O} \rangle = \frac{\int \mathcal{D}\mathcal{A}\mathcal{D}\bar{c}\mathcal{D}c\mathcal{D}\bar{\psi}\mathcal{D}\psi \; \mathcal{O}(\mathcal{A}, \ldots, \psi) \; e^{-\mathcal{S}_{\text{YM}} - \mathcal{S}_{\text{fix.}} - \mathcal{S}_{\text{ghost}} - \mathcal{S}_q}}{\int \mathcal{D}\mathcal{A}\mathcal{D}\bar{c}\mathcal{D}c\mathcal{D}\bar{\psi}\mathcal{D}\psi \; e^{-\mathcal{S}_{\text{YM}} - \mathcal{S}_{\text{fix.}} - \mathcal{S}_{\text{ghost}} - \mathcal{S}_q}} \tag{4.14}$$

We started from a gauge invariant Lagrangian and ended with a path integral which is explicitly not due to the Faddeev-Popov gauge fixing term. This might seems contradictory at first.

However, practical calculations show that observables remain independent of the gauge fixing parameter ξ. Even with the gauge symmetry being explicitly broken, there is still a hidden global symmetry remaining in the theory: the BRST symmetry [24]. This symmetry puts a lot of constraints on the gauge theory. First, it ensures that the ghosts are excluded from the physical asymptotic states when performing calculations. Second, since it is preserved by higher order loop calculations, it prevents introduction of counterterms which might spoil renormalizability. For a proof of QCD's renormalization, see [25; 26]. BRST also ensures that the expectation value of a gauge invariant functional does not depend on the choice of gauge fixing condition.

Gribov ambiguity

We assumed earlier that a solution to the gauge slicing equation existed and that it was unique. This was quite a strong assumption. It was first Gribov [27] who realized that actually it turns out to be wrong in general. It appears that multiple solutions exist for this equation: the Gribov copies. But the assumption we used is well justified at weak coupling values where the degeneracy disappears.

4.2.2 Symmetries of QCD

Chiral symmetry

Fermions, described by Dirac spinors, live in the spinor representation of the Lorentz group $\mathrm{SO}^+(1,3) \cong \mathrm{SU}(2) \oplus \mathrm{SU}(2)$ that decomposes into two irreducible representations of SU(2). Their charge is $(1/2,0)\oplus(0,1/2)$ and are called the left and right Weyl spinors. Accordingly, we introduce the projection operators $\mathcal{P}_R = \frac{1+\gamma^5}{2}$, $\mathcal{P}_L = \frac{1-\gamma^5}{2}$, and decompose ψ into $\mathcal{P}_{L,R}\,\psi = \psi_{L,R}$ such that $\psi = \psi_L + \psi_R$. Each of these Weyl spinors are invariant under respectively U(1) left and right symmetry:

$$\begin{aligned} &\mathrm{U(1)_L} : \psi_L \to e^{i\,\theta_L}\psi_L \quad \& \quad \psi_R \to \psi_R, \\ &\mathrm{U(1)_R} : \psi_L \to \psi_L \qquad\quad \& \quad \psi_R \to e^{i\,\theta_R}\psi_R, \end{aligned} \tag{4.15}$$

expressing that the two spinors decouple and operate separately. In the massless quark approximation, considering that QCD does not discriminate between the massless flavors of quarks, we can embed the quarks inside a ($\mathrm{N_f}$ dimensional) fundamental representation of $\mathrm{SU(N_f)}$ symmetry, while anti-quarks live in the anti-fundamental one. Proceeding for both left and right Weyl spinors, the multiplets are invariant under both $\mathrm{SU(N_f)_L}$ and $\mathrm{SU(N_f)_R}$ group of transformations. The whole chiral group is then $\mathrm{U(N_f)_L} \otimes \mathrm{U(N_f)_R}$. This symmetry can be decomposed into:

$$\frac{\mathrm{SU(N_f)_L} \otimes \mathrm{SU(N_f)_R}}{\mathbb{Z}_{\mathrm{N_f}}} \otimes \mathrm{U(1)_L} \otimes \mathrm{U(1)_R}. \tag{4.16}$$

This group transformation can be recast in an equivalent form:

$$\frac{\mathrm{SU(N_f)_V} \otimes \mathrm{SU(N_f)_A}}{\mathbb{Z}_{\mathrm{N_f}}} \otimes \mathrm{U(1)_V} \otimes \mathrm{U(1)_A}, \tag{4.17}$$

where the diagonal vector subgroup characterizes chiral transformations satisfying $\theta_L = \theta_R$ while the axial one satisfes $\theta_L = -\theta_R$. Charm, bottom and top quark are far from massless while up, down and to some extend strange have relatively small masses compared to hadronic scale $\sim \mathcal{O}(1\,\mathrm{GeV})$. The chiral symmetry is only approximately relevant for the first three flavors of quarks.

Although this is a symmetry of the Lagrangian, it is not a symmetry of QCD. First because it is broken explicitly by quark masses, so it is at most an approximate symmetry, but most importantly because of non perturbative effects. The chiral symmetry $\mathrm{SU(3)_A}$ is spontaneously broken by the quark condensate $\langle\bar{\psi}\psi\rangle$[28; 29], while $\mathrm{U(1)_A}$ is explicitly broken by the, instanton induced, chiral anomaly [30]. Breaking of the axial SU(3) symmetry leads to the generation of eight massless Goldstone bosons, the pions, the kaons and the meson η. The spontaneous breaking of the symmetry is mainly responsible for the mass of the proton and the neutron. The remaining $\mathrm{U(1)_V}$ symmetry is identified to $\mathrm{U(1)_B}$, the conservation of baryon number. The remaining symmetries are:

$$\mathrm{SU(N_f)_V} \otimes \mathrm{U(1)_B} \tag{4.18}$$

and remain exact. Notably, because $\mathrm{SU(N_f)_A}$ is broken, no opposite parity partner of the pseudo-Goldstone bosons are observed.

Conformal symmetry

The Lagrangian of QCD possesses yet another symmetry which is broken at the quantum level: conformal transformations. Conformal invariance reflects, among other things, the invariance under dilatation of space-time coordinates. Even in absence of quark masses, quantum corrections typically require to introduce a regularization parameter that defines a length scale in the theory. The latter is not compatible with conformal transformation except at particular values of the parameter: the fixed point of the RG equation. Precisely, restoration of conformal invariance requires the trace of the energy-momentum tensor to vanish. The latter one being directly related to the beta function, in the following (non-perturbative) relation :

$$T^{\mu}_{\mu} = \frac{\beta(g)}{2g^2} F^a_{\mu\nu} F^{\mu\nu}_a + (1+\gamma_m) \sum_q \bar{q}\, m_q\, q \tag{4.19}$$

No fixed point for the beta function (assuming massless quarks) has been found so far, but due to asymptotic freedom, QCD must be asymptotically conformally invariant.

4.2.3 Limits of perturbative QCD

Even if the QCD perturbative series would converge ultimately, it would not encode other genuinely non-perturbative features of QCD. To cite some of them:

Instantons: They are classical solutions to the Lagrange equation, maximizing the Gaussian weight in the partition function. They are responsible, by quantum tunneling, of "jumps" from one vacuum to another. The instanton effect allowed 't Hooft [31] to solve the $\mathrm{U(1)_A}$ puzzle which was that there was no explicit breaking mechanism of $\mathrm{U(1)_A}$ therefore, since the symmetry was not observed (i.e no opposite parity partner) it could only be spontaneously broken with an associated Goldstone boson, again, not observed. Instantons explicitly break the $\mathrm{U(1)_A}$ symmetry and the puzzle was resolved. In QCD, their effects are reliably computed only at short distances (equivalently at high temperature or chemical potential) but in this domain they are always dominated by perturbative corrections [32]. Moreover, light quarks greatly suppress instanton [33], so we will not consider their effects in this thesis as we are working mostly with massless flavors of quarks .

Quark condensate: The chiral quark condensate $\langle\bar{q}\,q\rangle$ is a main order parameter of spontaneous chiral symmetry breaking for massless quarks. As such it is intrinsically nonperturbative, indeed vanishing at any finite order of (ordinary) perturbative QCD in the chiral limit. In this framework, the quark condensate can be evaluated only through effective QCD models

[34], Lattice techniques (see for a recent review [35]), or possibly through RG resummation techniques [36].

4.3 QCD in a thermal bath

Soon after the advent of Quantum Chromodynamics as the theory of strong interaction, it became clear that there should be a qualitative change in the properties of hadronic matter as the temperature or density increases. At low-energy, due to confinement, quarks and gluons are stuck inside hadronic matter forming a dilute system of composite particles. In a very dense system, however, such extended composite particles would overlap, and quarks and gluons would start to interact with quarks and gluons from other hadrons. Likewise, at very high temperature, thermal excitations from the medium tend to break the bound between quarks and gluons. A phase transition from hadron gas to this plasma of quarks and gluons (QGP) requires a very large amount of energy not commonly seen in nature. It is believed that this transition could have occurred soon after the big bang, or still commonly today in the core of neutron stars, or occurring during high energy heavy ion collisions. Recently, after tremendous efforts, it was observed experimentally at the Relativistic Heavy Ion Collider (RHIC) of Brookhaven [37] and at the Large hadron Collider (LHC) of CERN [38; 39] for a critical temperature of roughly $T_c \sim 150$MeV and vanishing chemical potential. This critical temperature is associated to the deconfinement transition as well as the restoration of chiral symmetry. Both on the theoretical side and the experimental one, the high temperature and vanishing chemical potential part of the phase diagram is well understood. In a now bedrock article [40], the Lattice QCD community observed the QGP phase transition, in a realistic setup, and predicted a smooth crossover transition between the two phases. However, it is expected to qualitatively change in the opposite regime, namely, vanishing temperature and high chemical potential. This domain of the phase diagram remains very mysterious and is subject to many studies and conjectures. The only thing we know for sure at the moment is the first order liquid-gas transition taking place at one nuclear saturation density n_0 from a gas of nuclei to a liquid of nuclear matter[41; 42]. A first order phase transition is believed to occur, due to the restoration of the chiral symmetry at an energy scale yet unknown. But it is likely to be at some density existing inside Neutron Stars (NS) so that the latter could become probe for that physics. Additionally, the chiral transition and the deconfinement one may not take place at the same energy scale anymore. This would allow the possibility to have an exotic Quarkyonic state [43]. At even higher baryon density, the quark near the Fermi surface become correlated in Cooper pairs and form a state of color superconductivity(CSC)[44; 45]. A conjectured phase diagram is given in fig. (4.2) illustrating the previous discussion, but there is much more at hand concerning the horizontal axis than what has been discussed.

At the moment, we remain nearly blind to this region of physics. While we do not have yet experiments running in the vanishing temperature and high chemical potential side of the phase diagram, lots of efforts are made in this direction [46; 47]. Concerning Lattice QCD, due to the so-called sign problem [48] (see below for a short description), LQCD is hampered to pursue Monte-Carlo simulations hence cannot give us a glimpse of this physics. On top of that, the method relies on imaginary time formalism; thus only static observable may be addressed. Our best hope at the moment, for experimental observations, comes from the sky and the rapidly developing domain of gravitational wave physics conjointly used with information coming from the light spectrum. This will be discussed further in chapter 7. The need to quantitatively understand the physics of high temperature and chemical potential both at real and imaginary time is consequent in particle and nuclear physics as well as in cosmology. On the theory

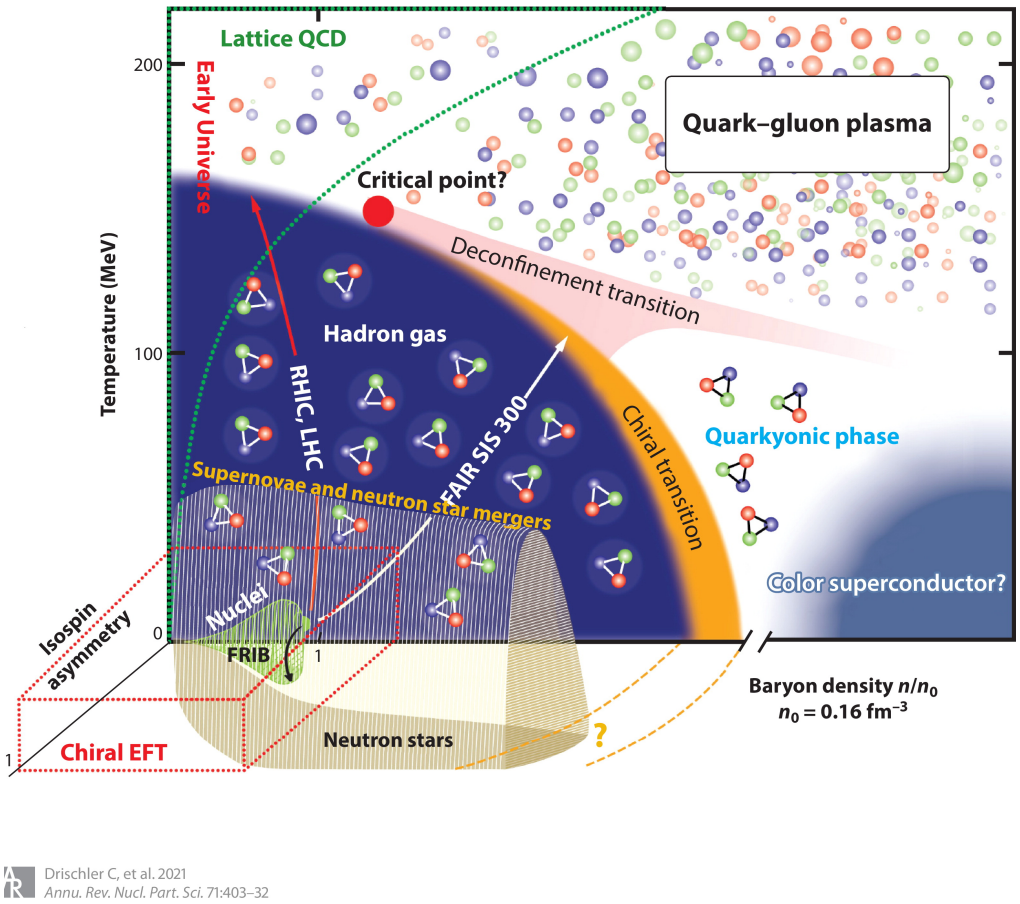

Figure 4.2: A theorized QCD phase diagram. Source: [49].

side, at the moment, weak coupling expansion methods is our best option to tackle this region motivating us to pursue efforts in this direction.

A recurrent issue in thermal perturbative calculations, however, is the appearance of infrared divergences caused by long range correlations inside the medium. One needs to perform somehow a resummation of these IR divergences at all loop orders to reach a result valid at some specific order in g. The lack of convergence of the series expansion is even stronger at finite temperature due to the breakdown of the naive perturbative expansion. Inevitably, the weak expansion fades at g^6 order due to the famous Linde problem [50]. Collective excitations of the chromomagnetic modes at the scale g^2T, appearing at g^6 order, cannot be calculated perturbatively since every n-loop diagrams, $n \geq 4$, will contribute to this coefficient [51; 52; 53; 54; 55; 22]. For an overview of the QGP see also [56].

4.3.1 Sign problem

This section would probably deserve it own thesis as it is possibly the most challenging problem of LQCD now that computational power has exponentially grown during the last decades. A more thorough description of LQCD can be found in classic papers [57; 58; 59] and we will restrict here only to a short overview of the sign problem. The argument is adapted from [48].

The starting point of Lattice QCD is to consider the Euclidean path integral in Eqn.(4.9) discretized on a space time lattice. The exponential factor is a highly oscillating function that we do not know how to evaluate in closed form. The integration is carried out using stochastic method.

Aside from the complications of high dimensional integration, discretizing fermions on a lattice, considering small mass for the fermions and assessing the relevant gauge configurations, this works perfectly fine. As long as we work with zero chemical potential, of course.

For fermions, we know how to integrate the path integral in closed form. This is exactly how we introduced the ghosts fields in the first place. This leads to a factor $\det\left(\not{D} + m + \mu\gamma_0\right)$. Because of $\gamma_5 \not{D} \gamma_5 = \not{D}^\dagger$, this operator satisfies:

$$\gamma_5 \left(\not{D} + m + \mu\gamma_0\right) \gamma_5 = \left(\not{D} + m - \mu^*\gamma_0\right)^\dagger . \tag{4.20}$$

With the star denoting the complex conjugate operation. Ultimately, this means:

$$\det\left(\not{D} + m + \mu\gamma_0\right) = \det{}^*\left(\not{D} + m - \mu^*\gamma_0\right). \tag{4.21}$$

which constraints the determinant to be real only for $\mathrm{Re}(\mu) = 0$.If we consider now an even number of flavors with the same mass and chemical potential, then the determinant is positive definite and Monte-Carlo techniques apply.

In the general case, the determinant is imaginary and with an imaginary determinant, it is no longer possible to use importance sampling methods as we can no longer give a probabilistic interpretation of the integrand; the very basics of lattice simulations. Many researches are pursued to circumvent this issue, a more detailed overview is given in [48].

4.4 In medium QFT

In thermal quantum field theory, the concept of asymptotic states fade since any state is subject to thermal interactions. One must instead define mixture of microscopic pure states as the new vacuum state of the theory. This is consistently incorporated inside the density matrix operator. For micro-states $|i\rangle$ (not necessarily orthogonals) with probability $p_i(t_0)$, this operator reads:

$$\hat{\rho}(t_0) \equiv \sum_i p_i(t_0) \left|i\right\rangle \left\langle i\right| . \tag{4.22}$$

Then any expectation values of observables can be expanded on this basis:

$$\langle \hat{\mathcal{O}}(t_0) \rangle = \mathrm{Tr}\ \rho(\hat{t_0}) \mathcal{O}(\hat{t_0}). \tag{4.23}$$

We will be interested only in static observables such as the pressure, so we can directly express the density matrix operator at equilibrium, using the grand canonical ensemble:

$$\hat{\rho}_{\mathrm{eq.}} = \frac{e^{-\beta\left(\hat{\mathrm{H}} - \mu_{\mathrm{i}}\hat{\mathrm{N}}_{\mathrm{i}}\right)}}{\mathcal{Z}}, \quad \mathcal{Z} = \mathrm{Tr}\, e^{-\beta\left(\hat{\mathrm{H}} - \mu_{\mathrm{i}}\hat{\mathrm{N}}_{\mathrm{i}}\right)}. \tag{4.24}$$

Where $\hat{H}$ is the Hamiltonian operator, $\hat{N}_i$ the conserved charge operator, $\beta \equiv 1/T$ the inverse of the temperature and $\mathcal{Z}$ the partition function. The quantity μ_i, the chemical potential for a flavor i, is a Lagrange multiplier determining the mean number of particles of type i in the system. The density matrix $\hat{\rho}$, or equivalently, the partition function $\mathcal{Z}$, contains all the thermodynamic properties of the system. For example, the pressure, particle number, entropy,

and energy density are, in the infinite-volume limit, given by

$$\begin{aligned} \mathcal{P} &= \frac{\partial\,(T\,\ln\mathcal{Z})}{\partial V}, \quad & N_i &= \frac{\partial\,(T\,\ln\mathcal{Z})}{\partial\mu_i}, \\ \mathcal{S} &= \frac{\partial\,(T\,\ln\mathcal{Z})}{\partial T}, \quad & E &= -\mathcal{P}V + TS + \mu_i N_i. \end{aligned} \tag{4.25}$$

Inserting the field basis closure relation in this trace, it can be expressed in terms of path integrals [55; 22]. From here, the previously developed formalism of path integral quantization of QCD using the Faddeev-Popov procedure becomes very handy.

4.4.1 Imaginary time formalism

This formalism is particularly well suited for the determination of bulk thermodynamic quantities which are time independent.

The Faddeev-Popov path integral in Eqn.(4.12) and the normalization constant in Eqn.(4.24) can be identified assuming we apply to Eqn.(4.12) the right transformations. First, the analogy between the Boltzmann factor and the exponential of the action suggests that we should identify the euclidean action with $\beta\,\hat{H}$, meaning that the imaginary time integration becomes restricted to $(0,\beta)$. Second, the cyclicity of the trace in the partition function (and the commutating/anti-commutating nature of bosonic/grassmannian fields) induce that bosonic/fermionic fields must respect periodic/anti-periodic boundary conditions respectively.

In the imaginary time formalism, the resulting modification in the Feynman rules is to trade the usual Fourier transform of the time component for a Fourier series on the so-called Matsubara frequencies. The chemical potential μ_i, associated with the conservation of the quark number, can be readily introduced in the Lagrangian using Legendre transformation. This appears as an extra term $\mu_i\,\bar{\psi}\gamma_0\psi$ inside the Lagrangian. Finally, the partition function reads (defining $d = D-1 = 3-2\varepsilon$):

$$\mathcal{Z} = \int_{\text{p.}} \mathcal{D}\mathcal{A} \int_{\text{a.p.}} \mathcal{D}\bar{\psi}\mathcal{D}\psi \int_{\text{p.}} \mathcal{D}\bar{c}\mathcal{D}c\; e^{-\int_0^\beta d\tau \int d^d x\; \left(\mathcal{L}_{\text{FP}} + \sum_i \bar{\psi}_f \mu_i \gamma^0 \psi_f\right)}. \tag{4.26}$$

Importantly, despite their Grassmann nature, the ghost fields satisfy periodic (p.) instead of antiperiodic (a.p.) boundary conditions, owing to the fact that the original matrix determinant is purely bosonic. Going in momentum space, the Matsubara frequencies take very different values for bosons and fermions:

$$\omega_B = 2\pi\, n\,\mathrm{T}\,, \qquad \tilde{\omega}_F = (2n+1)\pi\,\mathrm{T} - i\,\mu_i\,, \qquad n \in \mathbb{Z}, \tag{4.27}$$

that leads to crucial differences in the IR sector for the bosons and the fermions.

This construction with Matsubara frequencies is obviously at the cost of the real-time parameter required to describe out-of-equilibrium systems. This problem can be cured by carrying an analytic continuation from Euclidean to Minkoswki space. It is however possible to avoid using the imaginary time formalism. This requires to introduce a specific contour in the complex plane, known as the Schwinger-Keldysh contour, allowing calculations for two operators acting at different times.

The real-time formalism is out of the scope of this thesis as we only use imaginary time formalism, much more convenient for our purpose. More information can be found in [51; 60].

Feynman rules in euclidean space at finite temperature and density are recapitulated in the appendix A.

Center symmetry of $\mathrm{SU(N_c)}$

Among all gauge transformations, there is one especially simple.:

$$\mathcal{Z}_N = e^{i\frac{2\pi}{N}k}\mathbb{1}, \quad k = 0, 1, \ldots, N-1. \tag{4.28}$$

It is not possible for the integer k to change continuously between two different space-time points, consequently, center symmetries are only global symmetries.

Although this is a symmetry of the full QCD Lagrangian, at finite temperature, due to the compactification of time, this is no longer true [31; 61; 62]. Because gauge fields and quark fields satisfy different boundary conditions, the center symmetry will act differently on them. For a gauge transformation which does not satisfy this periodicity $U(\vec{x}, \beta) = U_{b.c} \neq U(\vec{x}, 0)$, the gluons in the adjoint representation are invariant while the quarks in the fundamental representation are not:

$$\begin{aligned} \mathcal{A}'_\mu(\vec{x}, \beta) &= U^\dagger_{b.c}\mathcal{A}_\mu(\vec{x}, \beta)U_{b.c} = \mathcal{A}_\mu(\vec{x}, \beta) = \mathcal{A}_\mu(\vec{x}), \\ \psi'(\vec{x}, \beta) &= U_{b.c}\psi(\vec{x}, \beta) = -U_{b.c}\psi(\vec{x}, 0) \neq -\psi(\vec{x}, 0). \end{aligned} \tag{4.29}$$

The global $\mathcal{Z}_n$ center symmetry of QCD is spoiled by any fields in the fundamental representation at finite temperature. However, the center symmetry in pure Yang-Mills is still present, but, it happens to be spontaneously broken at high-energy. Despite the fact that the pure Yang-Mills theory does not incorporate all effect of QCD, it is believed to capture non-trivial features of it through the non-abelian interactions. In particular, unlike the physical QCD case, the deconfinement transition appears here as a genuine phase transition, associated with the breaking of the center symmetry. An order parameter [63] for the $\mathcal{Z}_N$ symmetry breaking is the Polyakov loop:

$$\mathcal{L}_P(\vec{x}) \equiv \mathrm{Tr}\,\mathcal{P}\,\exp\left\{\int_0^\beta d\tau\,\mathcal{A}_0(\tau, \vec{x})\right\}. \tag{4.30}$$

$\mathcal{P}$ here is the path ordering operator. The object inside the trace is the Wilson line which, constructed from gluon fields, obviously transforms in the adjoint representation. From the cyclic property of the trace and the transformation law of the adjoint representation (4.3), the Polyakov loop is a gauge invariant quantity.

At very high temperature, the theory is weakly coupled, and naively we would think that $\mathcal{L}_P \to 1$. Instead, the allowed vacua exhibit a N-fold degeneracy:

$$\langle\mathcal{L}_P\rangle = e^{\frac{2\pi i}{n}k}\mathcal{L}_0, \quad \mathcal{L}_0 \xrightarrow[T\to\infty]{} 1 \tag{4.31}$$

At zero temperature, due to the confinement, the Polyakov loop must vanish $\mathcal{L}_0 \to 0$. Crossing the critical temperature T_c, the center symmetry is spontaneously broken and the Polyakov loop select one specific vacuum. This is different from the physical QCD case where a smooth crossover between the two states takes place [64; 65]. In the context of low energy effective model of QCD such as the Nambu-Jona-Lasinio (NJL) model [66], this Polyakov loop can be introduced at tree level in order to treat the chiral symmetry breaking/restoration as well as the deconfinement transition within a single model (PNJL) [67]. This is particularly powerful to scan the QCD phase diagram at finite temperatures and densities, looking for the critical endpoint of QCD [68].

4.4.2 QCD pressure at leading order

First things first, thermal field theory calculations can become much more complicated than its zero temperature counterpart. Before going more in depth of the Hard Thermal Loop theory and its involved calculations, we start by giving some well known results as a warm up and a useful tool to setup notations.

Notably, bosonic Matsubara frequencies are denoted P while fermionic ones are $\{P\}$ as it is standard in the literature. The free energy $\mathcal{F}$ is given by[3] $\mathcal{F} = \lim_{V\to\infty} \frac{-1}{V\beta} \ln \mathcal{Z}$ and is the opposite of the pressure $\mathcal{P} = -\mathcal{F}$.

Once reduced to scalar integrals, the QCD pressure for free gluons and N_f flavors of equal mass quarks is given by the sum of the following three contributions :

$$\begin{aligned}
\mathcal{P}_q &= 2N_f\, N_c \sum\!\!\!\!\!\!\int_{\{P\}} \ln\left(P^2 + m^2\right), \\
\mathcal{P}_{gl.} &= -d_A \sum\!\!\!\!\!\!\int_{P} \left(\frac{(d+1)}{2} \ln P^2 - \frac{1}{2}\ln(\xi) \right), \\
\mathcal{P}_{gh.} &= d_A \sum\!\!\!\!\!\!\int_{P} \ln P^2.
\end{aligned} \tag{4.32}$$

Where, in dimensional regularization,

$$\sum\!\!\!\!\!\!\int_{P/\{P\}} = T \sum \left(\frac{e^{\gamma_E} M^2}{4\pi} \right)^{\varepsilon} \int \frac{d^d P}{(2\pi)^d} \tag{4.33}$$

$d = 3 - 2\varepsilon$ and γ_E is the Euler gamma constant. The sum integral on ξ is independent of the temperature and scale free, therefore, it vanishes in dimensional regularization and it is a crosscheck that we do have a gauge invariant observable.

The final task now is to evaluate the two sum integrals:

$$\begin{aligned}
\sum\!\!\!\!\!\!\int_{P} \ln P^2 &= T \sum_n \int \frac{d^d \vec{p}}{(2\pi)^d} \ln\left(\omega_B^2 + \vec{p}^{\,2}\right), \\
\sum\!\!\!\!\!\!\int_{\{P\}} \ln\left(P^2 + m^2\right) &= T \sum_n \int \frac{d^d \vec{p}}{(2\pi)^d} \ln\left(\tilde{\omega}_F^2 + \vec{p}^{\,2} + m^2\right).
\end{aligned} \tag{4.34}$$

Proceeding to the sum, the general method is to identify $T\sum$ with the poles of a weighting function f_w and via the residue theorem to rewrite the sum as a contour integral. Before doing so, we will simplify the sum by differentiating with respect to $|\vec{p}|$ such as to avoid contour

[3] $V\beta$ here is the volume of space time. In any Feynman diagrams, there is an overall delta functions and a Kronecker delta that appears and give a factor of $V\beta$ cancelling the one in the free energy definitions. Thus, we systematically neglect to write this factor.

integration around the branch cut of the logarithm.

$$\begin{aligned}
\sum\!\!\!\!\!\!\int_P \ln P^2 &= \underbrace{\frac{2\pi^{d/2}}{(2\pi)^d\Gamma(d/2)}\left(\frac{e^{\gamma_E}M^2}{4\pi}\right)^{\frac{3-d}{2}}}_{H(d)}\int dp\, p^{d-1}\int_0^p 2dp_1\, p_1\, T\sum_n \frac{1}{\omega_B^2+\vec{p_1}^{\,2}},\\
&= H(d)\int dp\, p^{d-1}\int_0^p 2dp_1\, p_1\,\frac{1}{2p_1}\left(1+2\,n_B(p_1)\right),\\
&= H(d)\int dp\, p^{d-1}\left(p-2\,T\ln\left(1-e^{-\beta\, p}\right)\right),\\
&= -2\,T\,H(d)\int dp\, p^{d-1}\sum_n \frac{e^{-n\,\beta\, p}}{n} = -2\,T\,H(d)\sum_n\left(\frac{T}{n}\right)^d\Gamma(d),\\
&= -2\,T^{d+1}\,H(d)\,\Gamma(d)\zeta(d+1),\\
&\overset{d=3}{=} -\frac{\pi^2T^4}{45}.
\end{aligned} \tag{4.35}$$

This is a very standard calculation [22], more information on how we went from the first to the second line is given in appendix A. One might be interested in introducing a mass in Eqn.(4.35), $\ln P^2 \to \ln(P^2+m^2)$. Actually, it is not known how to evaluate this massive sum integral in closed form for both non-vanishing temperature and mass. Upon isolating the zero Matsubara mode, we can proceed to a systematic expansion in mass in different limits $m/T \to \infty$ or $m/T \to 0$ to include corrections. In the latter, it reads :

$$\sum\!\!\!\!\!\!\int_P \ln\left(P^2+m^2\right) \simeq -\frac{\pi^2T^4}{45}+\frac{m^2T^2}{12}-\frac{m^3T}{6\pi}-\frac{m^4}{(2\pi)^2}\left(\ln\left(\frac{m\,e^{\gamma_E}}{4\pi T}\right)-\frac{3}{4}\right)+\frac{2\,m^6\zeta(3)}{3(4\pi)^4T^2}+\mathcal{O}(\frac{m^8}{T^4}). \tag{4.36}$$

Where the non-analytic term comes from the $n=0$ mode.

The second sum integral in Eqn.(4.34) is however much more challenging. For simplicity, we will restrict here to $T,\mu \neq 0$ and $m=0$:

$$\begin{aligned}
\sum\!\!\!\!\!\!\int_{\{P\}} \ln P^2 = \frac{2^{1-d}T^{d+1}}{\pi^{d/2}\Gamma(d/2)}\Big(&\frac{(\frac{\mu}{T})^{d+1}}{d(d+1)}-\Gamma(d)(1+(-1)^d)\mathrm{Li}_{d+1}(-e^{-\mu/T})\\
&+\sum_{n=1}\frac{(-1)^{n+1}}{n^{d+1}}\left(\Gamma(d,\frac{n\mu}{T})e^{\frac{n\,\mu}{T}}-(-1)^d\Gamma(d,-\frac{n\,\mu}{T})e^{-\frac{n\,\mu}{T}}\right)\Big)
\end{aligned} \tag{4.37}$$

Where Li is the polylogarithm function. The derivation is quite similar except that we must be careful when expanding the logarithm in power series. This expansion is not justified for any p and separation of the integral in two regions is required. Again, using high temperature expansion, mass correction terms can be included [22].

Then, in $d=3$ dimensions, omitting here at the moment a divergent but T,μ-independent contribution, the free density pressure for QCD reads:

$$\mathcal{P}_{QCD}(m_f=0) = \frac{\pi^2T^4}{90}\left\{2d_A+\frac{7}{2}N_f\,N_c+N_f\frac{\mu^2/T^2}{6}+N_f\frac{\mu^4/T^4}{12\pi^2}\right\}. \tag{4.38}$$

At $T=0$, a closed form including the mass of the quarks can be evaluated and will be the topic of the section "Cold & Dense" in the next chapter.

4.4.3 Infrared divergences of thermal field theory.

While the UV sector of (massless) QCD is well known from $T = \mu = 0$, and dictated by the beta function, in medium QCD suffers from additional infrared divergences. Fermions do not make any trouble since the Matsubara modes never take zero value, but it does for the bosons. Moreover, fermions have a mass term that protect them from developing IR divergences which is not the case for bosons. Accumulating massless bosonic propagators inside a Feynman diagram will accordingly lead to new IR divergences.

How bad could be these divergences ? It depends. Some of them are easily recognized to be related, and we can find a resummation scheme such that in the end it leads to a finite result. They are the divergences occurring at the so-called soft scale and reflect the apparition of long-range interactions in the medium, which cannot be consistently reproduced by a naive weak coupling expansion. However, there are also divergences which require to resum every single Feynman diagrams, starting at four loop order, to regulate the divergences. These intrinsically non-perturbative contributions at the ultra-soft scale [50] is responsible for the inevitable break down of perturbation theory at finite temperature.

This is easily understood regarding the contributions of every scale at hand in the theory. For the non-zero mode, the 4-vector $P = (\omega_n^{F/B}, \vec{p})$, necessarily takes value at the **hard scale** πT, but for the zero mode of the bosons, it may also takes values at the **soft scale** $P = (0, g\,T)$ or at the **ultra-soft scale** $P = (0, g^2\,T)$, where it is assumed that every components of $\vec{p}$ is of the order of the concerned scale. By power-counting arguments, static gluons will contribute to the pressure as $\int dp\, p^3 n_B(p)$ hence for a generic scale $P = (0, g^n\,T)$, the outcome is [51]:

$$\int dp\, p^3\, n_B(p) \sim (g^n\,T)^4 n_B(g^n\,T) \sim \frac{g^{4n}\,T^4}{(g^n)} \sim g^{3n} T^4. \tag{4.39}$$

Corrections from higher orders would be to add a loop of gluons, corresponding by power-counting as an extra factor $g^2 n_B(p)$. Proceeding similarly, this corrections gives contribution of the order $g^2/(g^n T) \sim g^{2-n} T$. For $n \geq 2$, this correction is of the same perturbative orders in the weak coupling expansion as the quantity it corrects. Contributions from the ultra-soft and higher scales are therefore purely non-perturbative. Nevertheless, it should be noted that while there is also a similar soft scale $g\,\mu$ at zero temperature but finite chemical potential, there is no ultrasoft scale, which is purely a finite temperature contribution. This is precisely why at finite μ the perturbative expansion suffers less instability than its counterpart at finite T. At zero temperatures, the gluons do not fill the medium; they only appear through quantum mechanical processes, and so cannot form a condensate at small wavelengths resulting in non-perturbative physics. Another at first intriguing result from Eqn.(4.39) is that the soft scale gives contributions with odd power in g at finite temperature, thus non-analytic in $\alpha_s \sim g^2/4\pi$. These odd powers in the weak expansion arise solely from the $n = 0$ Matsubara mode, which cannot be isolated at $T = 0$, $\mu \neq 0$ hence are not present at $T = 0$, $\mu \neq 0$. A more complete power-counting argument (see [55]) refines this picture to also include logarithm dependence in the coupling. To summarize, the pressure in QCD at $T \neq 0$, $\mu \neq 0$ takes the following form:

$$\mathcal{P} = \# + \#g^2 + \#g^3 + g^4(\#\ln g + \#) + \#g^5 + g^6(\#\ln g + \#). \tag{4.40}$$

While at zero temperature but finite chemical potential,

$$\mathcal{P} = \# + \#g^2 + g^4(\#\ln g + \#) + g^6(\#\ln^2 g + \#\ln g + \#) + \ldots \tag{4.41}$$

Note the doubling of the logarithm that appears at finite chemical potential and at order g^6.

Nearly every coefficient displayed here was calculated during the last forty years or so. Only the full coefficient of $\#g^6 \ln g + \#g^6$ at $T = 0, \mu \neq 0$ which requires a full four loop calculations remains unknown. A schematic overview of the contribution to the domain is given in Table(4.2).

	$T = 0$, $\mu \neq 0$	$T \neq 0$, $\mu = 0$	$T \neq 0$, $\mu \neq 0$
g^0	Stefan Boltzmann		
g^2	Freedman & McLerran [69; 70; 71](1977)	Shuryak [72](1978)	Kapusta [54](1979)
g^3		Kapusta [54](1979) ($m_f \neq 0$)	
$g^4 \ln g$	Freedman & McLerran [69; 70; 71]*(1977)	Toimela [73](1983)	Toimela [73](1983)**
g^4	Freedman & McLerran [69; 70; 71]*(1977), Baluni [76](1978), Kurkela et al.($m_f \neq 0$)[78](2010)	Arnold & Zhai [74] (1994)	Vuorinen [75](2003)** Ipp et al. [77](2006)
g^5		Zhai & Kastening [79](1995)	Vuorinen [75](2003)**
$g^6 \ln^2 g$	Gorda et al.(2018) [80]		
$g^6 \ln g$	Not yet determined***	Kajantie et al. [81](2003)	Vuorinen [75](2003)**
g^6	Not yet determined***	Non perturbative [82; 83; 84; 85]	Non perturbative [86]

Table 4.2: State-of-the-art calculations for standard QCD in medium. This results stands for massless quarks otherwise stated. *Note that for this work the g^4 order was not evaluated in the covariant gauge. **These results were obtained in the framework of EQCD whose range of applicability stands for $4\mu_f < T$.***While the hard and mixed sector have not been evaluated yet, the soft sector has been completed last year [87; 88].

Identifying and resumming the IR divergent diagrams can be very tedious and the convergence of the strict pQCD series evaluated in that way is extremely poor. This is how it was originally done, resumming the so-called ring diagrams (or Daisy diagrams) but more refined framework has been found since then. By identifying the origin of the IR bad behavior we can be more efficient and realize that this resummation can be realized using a massive theory framework. But here come the first difficulty: we do not know how to introduce a mass term for the gluons. What have been done mostly in the literature is to use the Hard Thermal Loop framework, that naturally incorporates, among other things, a gauge invariant mass term for the gluons at tree level. This Lagrangian has the welcome property to reproduce the gluons self-energy in the static limit and provide a framework where we can organize the degrees of freedom using kinematic arguments. But this Lagrangian comes at the cost of the non-locality and it is technically very involved to conduct loop calculations. Another option at hand would be to use the Curci-Ferrari model [89; 90; 91] where one simply add a more naive mass term. Benefits of this framework are that calculations are much easier, the model is known to be renormalizable and it takes into account the Gribov copies. The price to pay however is to loose the gauge invariance. In this thesis we will work exclusively in the HTL framework and let the second for possible future investigation.

4.4.4 Electrostatic QCD and effective field theory

EQCD

Many of the works mentioned in table (4.2) were realised using an effective field theory for static QCD relevant at very high temperature. This theory relies on the observation that in this region, the integration on the time direction become asymptotically zero and we end up with a three dimensional theory instead. This suggests carrying the integration over these hard degrees of freedom (non-static fields necessarily live at the hard scale) and define a dimensionally reduced 3D effective field theory (EFT): Electrostatic QCD (EQCD). This theory now reflects the physics of the soft mode and their interactions where the hard modes are incorporated as shift in the Wilson coefficients. These are just the coefficients multiplying the operators in the Lagrangian, as we will explore below. Just like for any EFT, it requires to incorporate in the Lagrangian every possible operator satisfying the symmetries of the theory. Power counting arguments will then tell which of these operators are relevant or not. This new theory of massive electric fields can be further integrated such as to describe the physics of the spatial chromomagnetic gauge field A_i. As alluded before, this theory is now purely non-perturbative, containing the ultra soft scale. However, it can be evaluated on the lattice (see table 4.2).

While this theory is highly valuable at high temperature, its applicability undeniably disappears at zero temperature due to its construction. However, the arguments used to construct the EFT are worth to take some time for further investigations. It will be particularly important for the discussion of cold and dense QCD in the next chapter.

Effective Field theory, brief overview

If one is interested in making prediction out of a certain theory, which we will call the UV theory, one may encounter the possible appearance of multiple intrinsic scales while pursuing calculations of the perturbative corrections. In QCD at finite temperature, these scales are the one we discussed: hard, soft and ultra-soft which are determined by the medium. On top of that, considering N_f degenerate flavors of massive quarks also add N_f scales inside the picture. Generally, calculations involving multiple scales are much harder than with only one scale. An EFT construction allow to disentangle the contributions from a specific scale such that practical calculation in this constructed EFT will only contain one less scale than in the original theory. Iterating the procedure allow to define successive EFT successively disentangling contributions from each scale. For instance the EQCD effective theory described the soft modes of QCD at high temperature but still possesses the ultra soft scale.Further integrating out the soft modes of EQCD gives an EFT describing the chromo-magnetic sector (the ultra-soft scale). Knowing the exact contribution of each scale may not be relevant since they do not necessarily weight the same in the perturbative expansion. If we wish to predict the result of a scattering experiment of Hadrons at an energy $\sqrt{s} = 1\,\mathrm{GeV}$, knowing the exact structure of the contribution of the up quark or of the gauge boson W is irrelevant since these mass scales are far away from the center energy of the experiment. The mass of the up quark can be neglected while the exchange of the boson W can be efficiently described by a local point-like operator. One particularly powerful consequence of using an EFT to describe the UV theory, is the resummation of the large logarithm involving the ratio of two mass scales of different magnitudes. The perturbative corrections $A\,g^k$ are no longer small even when $g \ll 1$ if it is multiplied by such large logarithms. Therefore, it becomes crucial to resum such logarithms, and it can be achieved using the renormalization group in the EFT. This will be the topic of the next chapter in HTL.

To illustrate the principles of an EFT, we will do a short digression and discuss the principles

of EFT in a simpler toy model that will only involve one-loop integration and two different mass scales. All principles can be directly applied to QCD too, but the formalism is more involved. So the simple picture is to consider a UV theory containing only two scales, an IR mass scale m and an UV mass scale M with $m \ll M$. We wish to disentangle the contribution from the IR scale to a certain observable we are looking for. So, if a certain matrix element of the UV theory is $\mathcal{M}_{\text{UV}}$ (for instance $\phi\phi \to \phi\phi$ scattering), we would like to have an EFT description, which should be obviously simpler, that would reproduce perturbatively $\mathcal{M}_{\text{UV}}$ in the limits $m/M \ll 1$ and $p_i/M \ll 1$, where p_i is the set of external momenta. We will neglect this last complication here (see e.g [92]) :

$$\mathcal{M}_{\text{EFT}} \simeq \mathcal{M}_{\text{UV}}((m^2/M^2)^{k-1}) + \mathcal{O}\left(\left(\frac{m^2}{M^2}\right)^k\right). \tag{4.42}$$

Where k should be chosen accordingly to the perturbative order we are looking for. This equation is called the *matching* in the vocabulary of EFT.

Let's consider the following Lagrangian:

$$\mathcal{L}_{\text{UV}} = \frac{1}{2}\left[(\partial_\mu\phi)^2 - m_L^2\phi^2 + (\partial_\mu H)^2 - M^2\phi^2\right] - \frac{\lambda_0}{4!}\phi^4 - \frac{\lambda_1}{3!}\phi^3 H. \tag{4.43}$$

The calculation of the matrix element can be carried out in the UV theory using the exact propagator of the heavy field, then taking the limits discussed previously. Or, equivalently, the propagator of the heavy field can be expanded:

$$\frac{1}{k^2 - M^2} = -\frac{1}{M^2}\left(1 + \frac{k^2}{M^2} + \frac{k^4}{M^4} + \dots\right) \tag{4.44}$$

and we define an effective Lagrangian with a point-like interaction that must reproduce perturbatively the UV theory. This procedure is called integrating out the field H. To write the Lagrangian for the EFT, we must add every operators that respect the original symmetries of the UV theory. Higher order operators involving partial derivatives are redundant and can be eliminated by field redefinition (fore more details see the review from [93]).

In the EFT Lagrangian, we only have a light field ϕ (different from the one in the UV theory), therefore :

$$\mathcal{L}_{\text{EFT}} = \frac{1}{2}\left[(\partial_\mu\phi)^2 - m^2\phi^2\right] + \hat{\mathcal{O}}_{d\geq 4} \tag{4.45}$$

where the higher dimensional operators are suppressed by higher powers of the UV scale :

$$\hat{\mathcal{O}}_{d\geq 4} = C_4\hat{\mathcal{O}}_{d=4} + \frac{C_5}{M}\hat{\mathcal{O}}_{d=5} + \frac{C_6}{M^2}\hat{\mathcal{O}}_{d=6} + \dots \simeq -C_4\frac{\phi^4}{4!} - \frac{C_6}{M^2}\frac{\phi^6}{6!}, \tag{4.46}$$

While operators of dimension less than four are called relevant, the operators of dimension higher than four are called irrelevant due to this scaling. They organize as higher order contributions in practical calculations. This core concept of an EFT construction is called the power counting argument. Simply by looking at the dimension of an operator (and the number of loops), we know at which orders this contributions will enter. For operators of dimension four, called marginal, the classical dimension cannot tell whether they are relevant or not. Only through the computation of the anomalous dimensions we can answer this question. The coefficients C_i are called the Wilson coefficients and are determined, order by order, by the matching condition such that it correctly reproduces the matrix element of the UV theory. Since the UV

scale has been integrated out, there is only one scale that can appear in Feynman diagrams which drastically simplify the picture. If the theory contains more scales, for instance three scales $m_1 \ll m \ll M$, the procedure can be iterated, however, there is one subtlety in the matching procedure (see [94] for a concrete example). Indeed, the matching in Eqn.(4.42) has to be proceeded for a renormalization scale of the order of the UV scale $\Lambda \sim M$. This determine the Wilson coefficients of the first EFT (let's call it EFT1) at the scale $\Lambda \sim M$, now using the RG equations, we can evolve the Wilson coefficients of EFT1 down to the scale $\Lambda \sim m$ where we can now integrate the light field of mass m. This defines a second EFT (EFT2) with new Wilson coefficients containing only the super-light field of mass m_1. These new Wilson coefficients can be determined in terms of the Wilson coefficients of EFT1 but the matching has to be done at the renormalization scale $\Lambda \sim m$ this time. For each EFT, the Wilson coefficients are determined at the scale where the corresponding field has been integrated out.

But, the matching in Eqn.(4.42) still requires to evaluate the matrix element in the complete UV theory, then to take the limit $m \ll M$ to get the Wilson coefficients, so what would be the benefit of an EFT construction (beside summing the large logarithms) if we already have to evaluate the exact contribution ? First, the Wilson coefficients are universal, once determined, it is done, so one could fix the Wilson coefficients using one calculation in the full UV theory then use the EFT to make other predictions. Second, this full theory calculations is actually not needed. The beauty of an EFT construction is that it allows to dissociate a complicated calculations into easier steps. To understand that, we need first to study the divergences that appear in EFT.

Since the UV scale has been integrated out, the UV behavior of the theory has been modified, therefore the UV divergences of the UV theory and of the EFT are completely different and each of them need to be renormalized by appropriate counterterms. Such that Eqn.(4.42) is understand after renormalization. But, integrating out an UV scale has no effects on the IR behavior of the theory. This sector is left unchanged while constructing the EFT such that the full theory and the EFT will display the same IR divergences and non-logarithmic contributions in the IR scale. We can use this to our advantage to avoid the evaluation of the exact matrix element in the full theory. Consider the following difference :

$$\mathcal{M}^{\text{ren.}}_{\text{UV}} - \mathcal{M}^{\text{ren.}}_{\text{EFT}} = (\mathcal{M}^{\text{ren.}}_{\text{UV}} - \mathcal{M}^{\text{ren.}}_{\text{EFT}}) \,|_{\text{Expanded in the IR scales}}, \tag{4.47}$$

The notation *ren.* is to remind us that we have to renormalize the UV divergences first. The argument below is completely generic and applies to any theory and any object, whether they are observables or not. Because the two theories have the same IR sector, in the above difference one can do the expansion in the IR scale (or all the IR scales if there is more than one IR scale in the theory) without affecting the result. The exact evaluation of the UV matrix element is not required, but only its expansion in the IR scales, breaking down an intrinsic two-scale calculations into two, much more simple, one-scale calculation: : the EFT calculation and the matching. The last term $\mathcal{M}_{\text{EFT}} \,|_{\text{exp.}}$ is always a scaleless integral since both the UV and the IR scale has been expanded out. But it is useful to remember that even though it is zero, because $1/\varepsilon_{\text{UV}} - 1/\varepsilon_{\text{IR}}$ appears, the UV divergence is renormalized thus the IR divergence is used to cancel the exact same IR divergence of the expanded UV theory.

As a concrete example, the matching at tree and loop order of the EFT Lagrangian in Eqn.(4.45) to the UV Lagrangian requires :

$$m_L = m \tag{4.48}$$

Because we want the two point function to match in the theory. The 4-point green function of

the light field on the other hand gives :

$$C_4^{\text{tree}} = \lambda_0, \quad C_6^{\text{tree}} = 0, \tag{4.49}$$

where we introduced a notation to remember that the Wilson coefficients are modified by higher order contributions when we match at higher loop orders.

$$C_i = C_i^{\text{tree}} + C_i^{\text{1L}} + C_i^{\text{2L}} + \dots \tag{4.50}$$

The matching of this theory at loop order is discussed in [95]. Quoting the result adapted to our notation:

$$C_6^{\text{1L}} = -20\lambda_1^2, \quad C_4^{\text{1L}} = (4!)\frac{\lambda_1^2}{(3!)^2}\frac{1}{16\pi^2}\left(\ln\frac{\Lambda^2}{M^2} + 1\right). \tag{4.51}$$

Connection to Cold and Dense QCD

The entire previous discussion was completely generic. All the arguments presented there will apply to the context of EFT using the so-called Hard Thermal Loop theory to be presented in the next chapter. In Cold and Dense QCD, the two scales are given by the medium. The UV scale is the chemical potential μ and called the hard scale while the IR scale is called the soft scale and given by the Debye mass $m_E^2 \sim \#\alpha_s\mu^2$. The expansion in the IR scale with respect to the UV scale thus becomes $m^2/M^2 \overset{QCD}{\to} \#\alpha_s$ such that the small mass expansion is the perturbative expansion. For this reason, we need the EFT to match the full calculation only at the relevant order at which the latter is originally (perturbatively) calculated, namely up to unknown higher orders.

4.5 Bibliography

[1] Murray Gell-Mann. A Schematic Model of Baryons and Mesons. *Phys. Lett.*, 8:214–215, 1964.

[2] G. Zweig. *An SU(3) model for strong interaction symmetry and its breaking. Version 2*, pages 22–101. 2 1964.

[3] E. D. Bloom, D. H. Coward, H. DeStaebler, J. Drees, G. Miller, L. W. Mo, R. E. Taylor, M. Breidenbach, J. I. Friedman, G. C. Hartmann, and H. W. Kendall. High-energy inelastic $e - p$ scattering at 6ř and 10ř. *Phys. Rev. Lett.*, 23:930–934, Oct 1969.

[4] M. Breidenbach, J. I. Friedman, H. W. Kendall, E. D. Bloom, D. H. Coward, H. DeStaebler, J. Drees, L. W. Mo, and R. E. Taylor. Observed behavior of highly inelastic electron-proton scattering. *Phys. Rev. Lett.*, 23:935–939, Oct 1969.

[5] B.J. Bjørken and S.L. Glashow. Elementary particles and SU(4). *Physics Letters*, 11(3):255–257, 1964.

[6] S. L. Glashow, J. Iliopoulos, and L. Maiani. Weak interactions with lepton-hadron symmetry. *Phys. Rev. D*, 2:1285–1292, Oct 1970.

[7] J. E. Augustin, A. M. Boyarski, M. Breidenbach, F. Bulos, J. T. Dakin, G. J. Feldman, G. E. Fischer, D. Fryberger, G. Hanson, B. Jean-Marie, R. R. Larsen, V. Lüth, H. L. Lynch, D. Lyon, C. C. Morehouse, J. M. Paterson, M. L. Perl, B. Richter, P. Rapidis, R. F. Schwitters, W. M. Tanenbaum, F. Vannucci, G. S. Abrams, D. Briggs, W. Chinowsky, C. E. Friedberg, G. Goldhaber, R. J. Hollebeek, J. A. Kadyk, B. Lulu, F. Pierre, G. H. Trilling, J. S. Whitaker, J. Wiss, and J. E. Zipse. Discovery of a narrow resonance in e^+e^- annihilation. *Phys. Rev. Lett.*, 33:1406–1408, Dec 1974.

[8] J. J. Aubert, U. Becker, P. J. Biggs, J. Burger, M. Chen, G. Everhart, P. Goldhagen, J. Leong, T. McCorriston, T. G. Rhoades, M. Rohde, Samuel C. C. Ting, Sau Lan Wu, and Y. Y. Lee. Experimental observation of a heavy particle j. *Phys. Rev. Lett.*, 33:1404–1406, Dec 1974.

[9] Makoto Kobayashi and Toshihide Maskawa. CP-Violation in the Renormalizable Theory of Weak Interaction. *Progress of Theoretical Physics*, 49(2):652–657, 02 1973, https://academic.oup.com/ptp/article-pdf/49/2/652/5257692/49-2-652.pdf.

[10] S. W. Herb, D. C. Hom, L. M. Lederman, J. C. Sens, H. D. Snyder, J. K. Yoh, J. A. Appel, B. C. Brown, C. N. Brown, W. R. Innes, K. Ueno, T. Yamanouchi, A. S. Ito, H. Jöstlein, D. M. Kaplan, and R. D. Kephart. Observation of a dimuon resonance at 9.5 gev in 400-gev proton-nucleus collisions. *Phys. Rev. Lett.*, 39:252–255, Aug 1977.

[11] S. Abachi et al. Observation of the top quark. *Phys. Rev. Lett.*, 74:2632–2637, 1995, hep-ex/9503003.

[12] F. Abe et al. Observation of top quark production in $\bar{p}p$ collisions. *Phys. Rev. Lett.*, 74:2626–2631, 1995, hep-ex/9503002.

[13] Particle Data Group. Review of Particle Physics. *Progress of Theoretical and Experimental Physics*, 2020(8), 08 2020, https://academic.oup.com/ptep/article-pdf/2020/8/083C01/34673722/ptaa104.pdf. 083C01.

[14] Richard D. Ball, Alessandro Candido, Juan Cruz-Martinez, Stefano Forte, Tommaso Giani, Felix Hekhorn, Kirill Kudashkin, Giacomo Magni, and Juan Rojo. Evidence for intrinsic charm quarks in the proton. *Nature*, 608(7923):483–487, 2022, 2208.08372.

[15] M. Okamoto et al. Equation of state for pure SU(3) gauge theory with renormalization group improved action. *Phys. Rev. D*, 60:094510, 1999, hep-lat/9905005.

[16] F. Karsch. Lattice QCD at high temperature and density. *Lect. Notes Phys.*, 583:209–249, 2002, hep-lat/0106019.

[17] H. David Politzer. Reliable Perturbative Results for Strong Interactions? *Phys. Rev. Lett.*, 30:1346–1349, Jun 1973.

[18] David J. Gross and Frank Wilczek. Ultraviolet behavior of Non-Abelian Gauge Theories. *Phys. Rev. Lett.*, 30:1343–1346, Jun 1973.

[19] C. N. Yang and R. L. Mills. Conservation of Isotopic Spin and Isotopic Gauge Invariance. *Phys. Rev.*, 96:191–195, Oct 1954.

[20] F. J. Dyson. Divergence of perturbation theory in quantum electrodynamics. *Phys. Rev.*, 85:631–632, Feb 1952.

[21] Mario Flory, Robert C. Helling, and Constantin Sluka. How I Learned to Stop Worrying and Love QFT. 1 2012, 1201.2714.

[22] Mikko Laine and Aleksi Vuorinen. *Basics of Thermal Field Theory*, volume 925. Springer, 2016, 1701.01554.

[23] L.D. Faddeev and V.N. Popov. Feynman diagrams for the yang-mills field. *Physics Letters B*, 25(1):29–30, 1967.

[24] C. Becchi, A. Rouet, and R. Stora. The abelian higgs kibble model, unitarity of the s-operator. *Physics Letters B*, 52(3):344–346, 1974.

[25] G. 't Hooft and M. Veltman. Regularization and renormalization of gauge fields. *Nuclear Physics B*, 44(1):189–213, 1972.

[26] J. Zinn-Justin. Renormalization of gauge theories. In H. Rollnik and K. Dietz, editors, *Trends in Elementary Particle Theory*, pages 1–39, Berlin, Heidelberg, 1975. Springer Berlin Heidelberg.

[27] V.N. Gribov. Quantization of non-abelian gauge theories. *Nuclear Physics B*, 139(1):1–19, 1978.

[28] Y. Nambu and G. Jona-Lasinio. Dynamical model of elementary particles based on an analogy with superconductivity. i. *Phys. Rev.*, 122:345–358, Apr 1961.

[29] Yoichiro Nambu and G. Jona-Lasinio. DYNAMICAL MODEL OF ELEMENTARY PARTICLES BASED ON AN ANALOGY WITH SUPERCONDUCTIVITY. II. *Phys. Rev.*, 124:246–254, 1961.

[30] Gerard 't Hooft. How Instantons Solve the U(1) Problem. *Phys. Rept.*, 142:357–387, 1986.

[31] Gerard' T. Hooft. *Does Quantum Chromodynamics Imply Confinement?*, pages 19–31. Springer US, Boston, MA, 1984.

[32] David J. Gross, Robert D. Pisarski, and Laurence G. Yaffe. QCD and Instantons at Finite Temperature. *Rev. Mod. Phys.*, 53:43, 1981.

[33] Curtis G. Callan, Roger Dashen, and David J. Gross. Toward a theory of the strong interactions. *Phys. Rev. D*, 17:2717–2763, May 1978.

[34] M BUBALLA. NJL-model analysis of dense quark matter. *Physics Reports*, 407(4-6):205–376, feb 2005.

[35] Y. Aoki et al. FLAG Review 2021. *Eur. Phys. J. C*, 82(10):869, 2022, 2111.09849.

[36] Jean-Loïc Kneur and André Neveu. Chiral condensate from renormalization group optimized perturbation. *Phys. Rev. D*, 92(7):074027, 2015, 1506.07506.

[37] Miklos Gyulassy. The QGP discovered at RHIC. In *NATO Advanced Study Institute: Structure and Dynamics of Elementary Matter*, pages 159–182, 3 2004, nucl-th/0403032.

[38] Ulrich Heinz and Maurice Jacob. Evidence for a new state of matter: An assessment of the results from the cern lead beam programme, 2000.

[39] Berndt Muller, Jurgen Schukraft, and Boleslaw Wyslouch. First Results from Pb+Pb collisions at the LHC. *Ann. Rev. Nucl. Part. Sci.*, 62:361–386, 2012, 1202.3233.

[40] Y. Aoki, G. Endrodi, Z. Fodor, S. D. Katz, and K. K. Szabo. The Order of the quantum chromodynamics transition predicted by the standard model of particle physics. *Nature*, 443:675–678, 2006, hep-lat/0611014.

[41] M. D'Agostino, M. Bruno, F. Gulminelli, F. Cannata, Ph. Chomaz, G. Casini, E. Geraci, F. Gramegna, A. Moroni, and G. Vannini. Nuclear liquid-gas phase transition: Experimental signals. *Nuclear Physics A*, 749:55–64, 2005. Phase transitions in strongly interacting matter. Proceedings of the 18th Nuclear Physics Division Conference of the EPS.

[42] J. B. Elliott, P. T. Lake, L. G. Moretto, and L. Phair. Determination of the coexistence curve, critical temperature, density, and pressure of bulk nuclear matter from fragment emission data. *Phys. Rev. C*, 87:054622, May 2013.

[43] Larry McLerran and Robert D. Pisarski. Phases of cold, dense quarks at large N(c). *Nucl. Phys. A*, 796:83–100, 2007, 0706.2191.

[44] D. Bailin and A. Love. Superfluidity and superconductivity in relativistic fermion systems. *Physics Reports*, 107(6):325–385, 1984.

[45] Mark G. Alford, Andreas Schmitt, Krishna Rajagopal, and Thomas Schäfer. Color superconductivity in dense quark matter. *Rev. Mod. Phys.*, 80:1455–1515, 2008, 0709.4635.

[46] Gert Aarts. Introductory lectures on lattice QCD at nonzero baryon number. *J. Phys. Conf. Ser.*, 706(2):022004, 2016, 1512.05145.

[47] David Tlusty. The RHIC Beam Energy Scan Phase II: Physics and Upgrades. In *13th Conference on the Intersections of Particle and Nuclear Physics*, 10 2018, 1810.04767.

[48] Philippe de Forcrand. Simulating QCD at finite density. *PoS*, LAT2009:010, 2009, 1005.0539.

[49] Slavko Bogdanov et al. Snowmass 2021 Cosmic Frontier White Paper: The Dense Matter Equation of State and QCD Phase Transitions. In *2022 Snowmass Summer Study*, 9 2022, 2209.07412.

[50] Andrei D. Linde. Infrared Problem in Thermodynamics of the Yang-Mills Gas. *Phys. Lett. B*, 96:289–292, 1980.

[51] Jacopo Ghiglieri, Aleksi Kurkela, Michael Strickland, and Aleksi Vuorinen. Perturbative Thermal QCD: Formalism and Applications. *Phys. Rept.*, 880:1–73, 2020, 2002.10188.

[52] PETER ARNOLD. QUARK-GLUON PLASMA AND THERMALIZATION. *International Journal of Modern Physics E*, 16(09):2555–2594, oct 2007.

[53] Ulrike Kraemmer and Anton Rebhan. Advances in perturbative thermal field theory. *Rept. Prog. Phys.*, 67:351, 2004, hep-ph/0310337.

[54] Joseph I. Kapusta. Quantum Chromodynamics at High Temperature. *Nucl. Phys. B*, 148:461–498, 1979.

[55] Joseph I. Kapusta and Charles Gale. *Finite-Temperature Field Theory: Principles and Applications*. Cambridge Monographs on Mathematical Physics. Cambridge University Press, 2 edition, 2006.

[56] K. Yagi, T. Hatsuda, and Y. Miake. *Quark-gluon plasma: From big bang to little bang*, volume 23. 2005.

[57] Zoltan Fodor and Christian Hoelbling. Light Hadron Masses from Lattice QCD. *Rev. Mod. Phys.*, 84:449, 2012, 1203.4789.

[58] F. Karsch. Lattice QCD at high temperature and density. *Lect. Notes Phys.*, 583:209–249, 2002, hep-lat/0106019.

[59] Christof Gattringer and Christian B. Lang. *Quantum chromodynamics on the lattice*, volume 788. Springer, Berlin, 2010.

[60] Michel Le Bellac. *Thermal Field Theory*. Cambridge Monographs on Mathematical Physics. Cambridge University Press, 1996.

[61] Urko Reinosa. Perturbative aspects of the deconfinement transition – physics beyond the faddeev-popov model, 2020.

[62] Robert D. Pisarski. Notes on the deconfining phase transition, 2002.

[63] Nathan Weiss. Effective potential for the order parameter of gauge theories at finite temperature. *Phys. Rev. D*, 24:475–480, Jul 1981.

[64] Szabocls Borsanyi, Zoltan Fodor, Christian Hoelbling, Sandor D. Katz, Stefan Krieg, and Kalman K. Szabo. Full result for the QCD equation of state with 2+1 flavors. *Phys. Lett. B*, 730:99–104, 2014, 1309.5258.

[65] Szabolcs Borsanyi, Zoltan Fodor, Matteo Giordano, Jana N. Guenther, Kornél Kapás, Sandor K. Katz, Kalman K. Szabó, Attila Pasztor, Israel Portillo, and Claudia Ratti. Searching the QCD critical endpoint with lattice simulations. *EPJ Web Conf.*, 235:02004, 2020.

[66] S. P. Klevansky. The nambu—jona-lasinio model of quantum chromodynamics. *Rev. Mod. Phys.*, 64:649–708, Jul 1992.

[67] Kenji Fukushima. Chiral effective model with the Polyakov loop. *Phys. Lett. B*, 591:277–284, 2004, hep-ph/0310121.

[68] Pedro Costa, M. C. Ruivo, C. A. de Sousa, and H. Hansen. Phase diagram and critical properties within an effective model of QCD: the Nambu-Jona-Lasinio model coupled to the Polyakov loop. *Symmetry*, 2:1338–1374, 2010, 1007.1380.

[69] Barry A. Freedman and Larry D. McLerran. Fermions and gauge vector mesons at finite temperature and density. i. formal techniques. *Phys. Rev. D*, 16:1130–1146, Aug 1977.

[70] Barry A. Freedman and Larry D. McLerran. Fermions and gauge vector mesons at finite temperature and density. ii. the ground-state energy of a relativistic electron gas. *Phys. Rev. D*, 16:1147–1168, Aug 1977.

[71] Barry A. Freedman and Larry D. McLerran. Fermions and gauge vector mesons at finite temperature and density. iii. the ground-state energy of a relativistic quark gas. *Phys. Rev. D*, 16:1169–1185, Aug 1977.

[72] Edward V. Shuryak. Theory of Hadronic Plasma. *Sov. Phys. JETP*, 47:212–219, 1978.

[73] T. Toimela. The next term in the thermodynamic potential of QCD. *Physics Letters B*, 124(5):407–409, 1983.

[74] Peter Brockway Arnold and Cheng-Xing Zhai. The Three loop free energy for pure gauge QCD. *Phys. Rev. D*, 50:7603–7623, 1994, hep-ph/9408276.

[75] A. Vuorinen. The Pressure of QCD at finite temperatures and chemical potentials. *Phys. Rev. D*, 68:054017, 2003, hep-ph/0305183.

[76] Varouzhan Baluni. Non-abelian gauge theories of fermi systems: Quantum-chromodynamic theory of highly condensed matter. *Phys. Rev. D*, 17:2092–2121, Apr 1978.

[77] A. Ipp, K. Kajantie, A. Rebhan, and A. Vuorinen. Pressure of deconfined QCD for all temperatures and quark chemical potentials. *Phys. Rev. D*, 74:045016, Aug 2006.

[78] Aleksi Kurkela, Paul Romatschke, and Aleksi Vuorinen. Cold Quark Matter. *Phys. Rev. D*, 81:105021, 2010, 0912.1856.

[79] Cheng-xing Zhai and Boris M. Kastening. The Free energy of hot gauge theories with fermions through g**5. *Phys. Rev. D*, 52:7232–7246, 1995, hep-ph/9507380.

[80] Tyler Gorda, Aleksi Kurkela, Paul Romatschke, Matias Säppi, and Aleksi Vuorinen. Next-to-Next-to-Next-to-Leading Order Pressure of Cold Quark Matter: Leading Logarithm. *Phys. Rev. Lett.*, 121(20):202701, 2018, 1807.04120.

[81] K. Kajantie, M. Laine, K. Rummukainen, and Y. Schröder. Pressure of hot QCD up to $g^6 \ln(1/g)$. *Phys. Rev. D*, 67:105008, May 2003.

[82] Guy D. Moore. Pressure of hot QCD at large N(f). *JHEP*, 10:055, 2002, hep-ph/0209190.

[83] A. Gynther, A. Kurkela, and A. Vuorinen. The N(f)**3 g**6 term in the pressure of hot QCD. *Phys. Rev. D*, 80:096002, 2009, 0909.3521.

[84] A. Hietanen, K. Kajantie, M. Laine, K. Rummukainen, and Y. Schroder. Plaquette expectation value and gluon condensate in three dimensions. *JHEP*, 01:013, 2005, hep-lat/0412008.

[85] F. Di Renzo, M Laine, V Miccio, Y Schröder, and C Torrero. The leading non-perturbative coefficient in the weak-coupling expansion of hot QCD pressure. *Journal of High Energy Physics*, 2006(07):026–026, jul 2006.

[86] Andreas Ipp and Anton Rebhan. Thermodynamics of large-n_f QCD at finite chemical potential. *Journal of High Energy Physics*, 2003(06):032–032, jun 2003.

[87] Tyler Gorda, Aleksi Kurkela, Risto Paatelainen, Saga Säppi, and Aleksi Vuorinen. Soft Interactions in Cold Quark Matter. *Phys. Rev. Lett.*, 127(16):162003, 2021, 2103.05658.

[88] Tyler Gorda, Aleksi Kurkela, Risto Paatelainen, Saga Säppi, and Aleksi Vuorinen. Cold quark matter at N3LO: Soft contributions. *Phys. Rev. D*, 104(7):074015, 2021, 2103.07427.

[89] Urko Reinosa. QCD at finite temperature and density from the Curci-Ferrari model. *PoS*, LC2019:074, 2020.

[90] Marcela Peláez, Urko Reinosa, Julien Serreau, Matthieu Tissier, and Nicolás Wschebor. A window on infrared QCD with small expansion parameters. *Rept. Prog. Phys.*, 84(12):124202, 2021, 2106.04526.

[91] Duifje Maria van Egmond, Urko Reinosa, Julien Serreau, and Matthieu Tissier. A novel background field approach to the confinement-deconfinement transition. *SciPost Phys.*, 12(3):087, 2022, 2104.08974.

[92] Andrzej J. Buras. Weak hamiltonian, cp violation and rare decays, 1998.

[93] Adam FALKOWSKI. Lectures on effective field theories, Jan 2019.

[94] Aneesh V. Manohar. Effective field theories. In *Perturbative and Nonperturbative Aspects of Quantum Field Theory*, pages 311–362. Springer Berlin Heidelberg.

[95] Aneesh V. Manohar. Introduction to Effective Field Theories. In *Effective Field Theory in Particle Physics and Cosmology: Lecture Notes of the Les Houches Summer School: Volume 108, July 2017*. Oxford University Press, 04 2020.

5

Hard Thermal Loop theory

An alternative method for performing a high-temperature resummation based on the Hard Thermal Loop (HTL) effective theory is discussed. While the beginning of this chapter is mainly a review of textbook material, the last section contains our original contribution [1] that relies on the HTL picture and formalism.

5.1 One ring to resum them all

For static observables, the perturbative series suffers from IR divergences that occur due to the bosonic Matsubara zero mode. Naively, defining an EFT for this mode works perfectly as a resummation scheme. In practice, this is the content of EQCD that we briefly described in sec.4.4.4. However, for non-static observables, we need all Mastubara modes in order to proceed to analytic continuation, suggesting that we should incorporate all modes at tree level. As it turns out, all of these can be collected into a compact effective action which is manifestly gauge invariant [2; 3; 4; 5; 6]. It started from the observation that an arbitrary number of insertions of the self-energy of the gluons are perturbatively of the same order, if the gluon momentum is soft. This non-perturbative behavior then requires to resum all hard loops to specify a specific perturbative order. This Lagrangian was thus dubbed *Hard Thermal Loop*. In this description, the static leading order contributions to the self-energy of quarks and gluons are included in the Lagrangian, in addition to resummed vertices which are necessary in order to maintain gauge invariance. For a complete proof of this statement, see [7]. This effective Lagrangian allows for a consistent definition of the propagation and the interactions of the collective modes living at the soft scale. Connection of this effective description for quasi-particles with a kinetic picture for the underlying hard modes is discussed in depth in [8]. It should be emphasized that HTL does not incorporate any information about the ultra-soft scale which remains irremediably non-perturbative. For more properties of HTL, see [9; 10; 11; 12].

HTL renormalizability has not been proven at arbitrary orders yet. Until now, its renormalizability has been established at LO (m_g^4), or equivalently NNLO (α_s^2), in [13], and then we extended the proof of renormalization to NLO ($\alpha_s\, m_g^4$), equivalently NNNLO α_s^3 [1].

To motivate the effective Lagrangian for HTL, it is better to start with a more schematic

picture of the perturbative series. Following the power counting in Eqn.(4.39), we expect the first IR divergences to appear at order g^3 at finite temperature. This is indeed the case, and it originates from the ring diagram in Fig.(5.1) with only two insertions of the self-energy. Upon resumming all of the ring diagram with an arbitrary number of self-energy, it leads to a finite result whose starting contribution is at order g^3. Higher order contributions to the ring refine this picture and give $g^4 \ln g$, g^5 and so on[1]. If the momentum flowing in the loop is hard, i.e $\|\vec{p}\| \sim T$ (or $\|\vec{p}\| \sim \mu$), this resummed diagram is perturbative and it can be re-expanded. But when the momentum is soft, i.e $\|\vec{p}\| \sim gT$ (or $\|\vec{p}\| \sim g\mu$), every single insertion contributes at the same order. This motivates to resum the static infrared limit of the self-energy and to define an EFT using this self-energy. At finite T or μ, we are often only interested in matter contributions to the self-energy so we will split the latter (M) from the vacuum contribution (V).

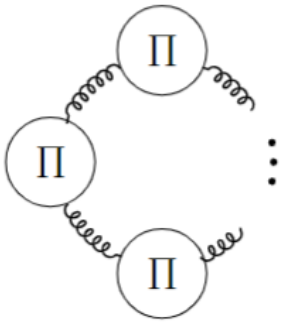

Figure 5.1: Ring diagrams

Since the divergences arise from the static and infrared limit $k_0 = 0$, $\|\vec{k}\| \to 0$, we expand the self-energy in power of the external momentum and define successive approximations in terms of this parameter. At finite temperature, it requires to select first the mode $n = 0$ for the momentum K running through the loop and then expanding in $\|\vec{k}\|$. At zero temperature and finite chemical potential, since the mode zero cannot be isolated, it reads (the label indicates the first, second order contributions etc.) [14; 15] :

$$\begin{aligned}\Pi_{\rm QCD}(K,\Phi) =& \Pi_1(K,\Phi) + \Pi_2(K,\Phi) + \dots \\ =& \left(\Pi_1^{\rm HTL}(0,\Phi) + K^2\,\Pi_0^{\rm pow.}(0,\Phi) + \mathcal{O}(K^4)\right) \\ &+ \left(\Pi_2^{\rm NLO}(0,\Phi) + \mathcal{O}(K^2)\right) + \mathcal{O}(g^4).\end{aligned} \tag{5.1}$$

Where Φ is the four dimensional angle: $\tan\Phi = |\vec{k}|/K_0$. The leading order is what we call the HTL contribution while the next contributions constitute higher dimensional operators that are beyond our current scope.

In this thesis we will only work with the first HTL correction, which happens to be sufficient to address consistently up to $g^4 \ln g$ order in cold and dense QCD.

5.2 HTL formalism

We shall now define more precisely the formalism of HTL. The notation follows mostly [16; 17].

At zero temperature, there are only two tensors relevant due to the Lorentz invariance : $\delta^{\mu\nu}$ and $K^\mu K^\nu$. But at finite temperature, the introduction of a thermal bath breaks explicitly the Lorentz invariance. Introducing the rest frame for the thermal bath (in Euclidean) $N^\mu = (-i, 0)$, now the general basis decomposition is extended. Since the gluons satisfy the Ward identity, $P_\mu \Pi^{\mu\nu} = 0$, they are D-dimensional transverse and the decomposition simplifies. Introducing convenient projection operators on longitudinal and transverse modes in D and d dimensions:

$$\begin{aligned}T^{\mu\nu}(\hat{K}) &\equiv \delta^{\mu i}\delta^{\nu j}\left(\delta^{ij} - \hat{k}^i\hat{k}^j\right), \\ L^{\mu\nu}(\hat{K}) &\equiv \delta^{\mu\nu} - \hat{K}^\mu\hat{K}^\nu - T^{\mu\nu}(\hat{K}),\end{aligned} \tag{5.2}$$

[1]It continues to higher orders, as we will discuss in the context of cold and dense QCD, but at finite temperature these contributions are not very meaningful due to the presence of the ultra-soft scale and associated non-perturbative corrections.

with $\hat{K} = K/|K|$ and $\hat{\mathbf{k}} = \mathbf{k}/|\mathbf{k}|$, then, the HTL self energy tensor decomposes into:

Figure 5.2: Gluon self energy at leading order

$$\Pi^{\mu\nu}(K) = T^{\mu\nu}(\hat{K})\Pi_T(K) + L^{\mu\nu}(\hat{K})\Pi_L(K), \tag{5.3}$$

Evaluation of the self-energy requires the calculations of the Feynman diagrams presented in appendix A.1.5 and depicted in fig.(5.2). Using the decomposition in Eqn.(5.1), the leading order contribution (HTL) reads after some algebra (see [9; 11] for a detailed derivation):

$$\Pi^{\mu\nu}(K) = m_g^2 \int_{\hat{\mathbf{v}}} \left(\delta^{\mu 0}\delta^{\nu 0} - \frac{iK_0}{K\cdot V} V^\mu V^\nu \right) \tag{5.4}$$

where $V^\mu \equiv (-i, \hat{\mathbf{v}})$ is a lightlike vector, with $\hat{\mathbf{v}}$ a d-dimensional unit vector. The integration measure is, (with $z_v \equiv \hat{\mathbf{k}}\cdot\hat{\mathbf{v}}$):

$$\int_{\hat{\mathbf{v}}} \equiv \frac{w(d)}{2} \int_{-1}^{1} dz_v (1-z_v^2)^{\frac{d-3}{2}}, \quad w(d) \equiv \frac{\Gamma(\frac{d}{2})}{\Gamma(\frac{3}{2})\Gamma(\frac{d-1}{2})}, \tag{5.5}$$

where $w(d)$ is a weight factor, such that $\int_{\vec{v}} 1 \equiv 1$. From this self-energy, Braaten and Pisarski [2; 3] were able to find explicitly gauge invariant effective actions :

$$\begin{aligned} \mathcal{L}_{YM}^{\text{HTL}} &= \frac{m_E^2}{2} \text{Tr} \int_{\hat{\mathbf{v}}} F^{\alpha\beta} \frac{v_\beta v^\gamma}{(v\cdot D_{\text{adj.}})^2} F_{\gamma\alpha}, \\ \mathcal{L}_{\text{q}}^{\text{HTL}} &= m_q^2 \int_{\hat{\mathbf{v}}} \bar{\psi} \frac{\not{v}}{(v\cdot D_{\text{F}})^2} \psi. \end{aligned} \tag{5.6}$$

The parameter m_E and m_q are the Debye screening mass for gluons and quarks. A derivation of the specific case $d = 3$ for m_E is given in appendix A.1.5. The general result in d dimension is, (see for example [10]) :

$$\begin{aligned} m_E^2 =& g^2 \left((d-1)^2 N_c \sum\!\!\!\!\!\!\int_K \frac{1}{K^2} - 2(d-1) N_f \sum\!\!\!\!\!\!\int_{\{P\}} \frac{1}{P^2} \right) \\ \overset{d=3}{=}& g^2 \left(N_f \left(\frac{T^2}{6} + \frac{\mu^2}{2\pi^2} \right) + \frac{N_c T^2}{3} \right). \\ m_q^2 =& -3C_F\, g^2 \sum\!\!\!\!\!\!\int_{\{P\}} \frac{1}{P^2} \\ m_q^2 \overset{d=3}{=}& \frac{g^2}{4}\frac{C_F}{2} \left(T^2 + \frac{\mu^2}{\pi^2} \right) \end{aligned} \tag{5.7}$$

We have given $\mathcal{L}_q^{\text{HTL}}$ for completeness, but we systematically neglect it in this thesis[2] as we consider massless quarks; or massive quarks but through the usual mass term $m^2\bar{\psi}\psi$. Taking into account the quarks in the HTL framework will be part of a future work in the realm of Hard Thermal Loop perturbation theory (HTLpt) (presented in chapter 6). In addition to the

[2]Because the calculations are not available yet.

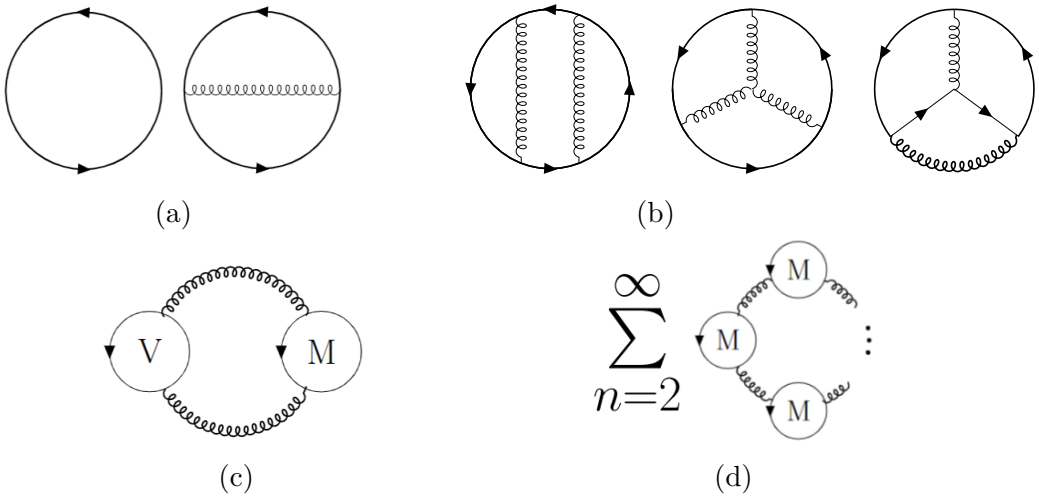

Figure 5.3: Feynman diagrams for the pressure at NNLO

two resummed propagators in Eqn.(5.6), there are also resummed vertices for the three-gluon and four-gluon self-interaction notably required for the evaluation of the two loop pure gauge HTL diagram in fig.(5.4a). The relatively involved expressions for these vertices can be found in [13; 18]. For our calculation in this chapter and the next one, they will not be necessary since we only evaluate the quark sector whose vertex do not require a resummation (if we neglect the quark HTL Lagrangian). There are two interesting limits of the HTL self-energy. First, The static limit where $K_0 \to 0$ in (5.4) gives:

$$\Pi^{\mu\nu} = m_g^2 \delta^{\mu 0}\delta^{\nu 0} \tag{5.8}$$

From here, we see that the chromo-electric field (component 00) is screened by the Debye mass while the spatial chromomagnetic field does not develop a thermal mass. This expresses the blindness of HTL to the ultra-soft scale and the absence of genuine chromo-magnetic field screening in the EFT. The second limit $K_0 \neq 0,\ \vec{k} \to 0$ leads to :

$$\begin{aligned} \Pi_T &\to \frac{m_E}{3} \\ \Pi_L &\to \frac{m_E}{3} \end{aligned} \tag{5.9}$$

and it corresponds to plasma oscillations.

Importantly, the HTL self-energy develops an imaginary part when $K_0 < \|\vec{k}\|$ and it is related to the physics of Landau damping: space-like gauge fields may lose energy to hard particles in the plasma. More information about the HTL formalism can be read off from appendix B. From now one, we will define an EFT for HTL and therefore replace $m_E \to m_g$. This must be now considered as a parameter of the EFT. Furthermore, the definition of the complete HTL Lagrangian is :

$$\mathcal{L}_{\text{HTL}} \equiv \mathcal{L}_{\text{YM}} + \mathcal{L}_{\text{YM}}^{\text{HTL}}. \tag{5.10}$$

Where $\mathcal{L}_{\text{YM}}^{\text{HTL}}$ contributes to modify (non-locally) the gluon propagator.

5.3 Cold & Dense QCD

Now we turn our focus on the specific case of zero temperature and high chemical potential. There are three main differences between perturbative computations carried out at high and low temperatures. First, in many regards the latter resembles the strict $T = 0$ case, and it is possible to dodge the finite temperature formalism. The second difference comes from the IR sector of the theory. Whereas it is possible to isolate the Matsubara zero modes at finite temperature, it is no longer possible now. Distance between the matsubara modes are proportional to the temperature, therefore, when we lower the temperature, an infinity of modes collapses on the zero mode and it becomes impossible to use a dimensionally reduced effective field theory for them. And finally, the absence of the ultra-soft scale makes the weak-coupling expansion in principle well-defined to arbitrary orders in the coupling g.

Lacking of dimensionally reduced EFT, the recent approach in zero temperature calculations is to use HTL as an effective field theory following the principles detailed in sec.4.4.4. Since the temperature has been removed, we also talk about Hard Dense Loop (HDL) instead [19]. Recently, the first higher order correction to the time-honored calculation of cold and dense QCD pressure up to 3-loop order [20] was derived using this HTL framework [21; 22; 23]. Freshly this year, the latter authors also discussed further improvement in the mixed sector (see below) of QED at NNNLO [15; 24].

The complete calculations up to and including $\alpha_s^2 \ln \alpha_s$ for the resummed ring graph, of the cold quark matter pressure by FreedMann and McLerran [20], later refined to include temperature effects [25], is given by:

$$\mathcal{P}_{\alpha_s^2}^{\text{C.Q.M}} = \mathcal{P}_f \left\{ 1 - \frac{2}{\pi}\alpha_s - \frac{N_f}{\pi^2}\alpha_s^2 \ln \alpha_s - 0.874355\, \alpha_s^2 - 2d_A \frac{(11N_c - 2N_f)}{3(4\pi)^2} \ln\left(\frac{M_h}{\mu}\right) \alpha_s^2 \right\}, \tag{5.11}$$

with $\alpha_s = g^2/(4\pi)$, $\mu_q = \mu = \mu_B/3$, M_h the arbitrary renormalization scale, and $\mathcal{P}_f = N_c\, N_f \mu^4/(12\pi^2)$ is the free gas pressure of quarks of Eqn.(4.32). The first and second coefficient correspond respectively to the leading and next-to-leading order depicted in fig.(5.3a). The next term, $\alpha_s^2 \ln \alpha_s$, comes from the IR sector of the set of ring diagrams (5.3d) in pQCD. The remnant coefficients originate from the set of perturbatively calculated three loop diagram (5.3b and 5.3c). At zero temperature, only the quark loop gives a non zero contribution to the gluon self-energy, and since the Vacuum-Vacuum diagram (VV) is a chemical potential independent contribution, it is neglected[3]. It should be noted that recently, a more convenient way to carry loop integration with a chemical potential has been developed, the so-called "cutting rules" [26], however only valid for standard QCD propagators, in particular not for HTL modified one, which were greatly valuable for the very involved calculation of the contribution of quark masses to $\mathcal{P}_{\text{C.Q.M}}$ at NNLO [27].

5.3.1 HTL Effective Field Theory (EFT)

Following the definition of the EFT presented earlier in section 4.4.4, one can formulate [28] an EFT to consistently describes the soft modes. The precise Lagrangian will be discussed later, for now, we will consider the different contributors. In this scheme, three kinematic regions emerge. The soft region, defined by the HTL Lagrangian, incorporates resummed propagator/vertices of the gluons and contains the physics of the collective modes in the plasma. On the opposite

[3]Actually, once the renormalization scale is identified to the chemical potential, it is no longer medium independent. This contribution has been neglected in the literature and we stand on this ground for this chapter. We will fully appreciate this contribution in the next chapter.

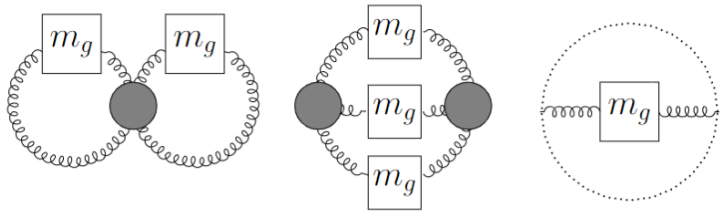

(a) Soft contribution at N^{3}LO

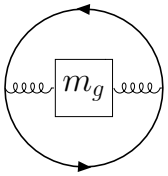

(b) Mixed contribution at N^{3}LO

Figure 5.4

side, the hard region contains unresummed quarks and gluons whose momenta are of the order of the chemical potential. Up to order $\alpha_s^2 \ln \alpha_s$, these are the only two kinematic regions appearing, but as we go to α_s^3 order, the two regions start to talk to each others. This mixed region is recognizable by the presence of both resummed and unresummed propagators. For a comprehensive overview of the different kinematic regions, see [22; 24].

In this reformulation, the IR behavior of the ring sum (soft gluons) becomes the one loop HTL diagram (5.5) while the UV (hard gluons) can be re-expanded perturbatively. While the full contribution is finite, this separation in terms of kinematic region introduces a UV divergence in the resummed loop which should cancel against an IR divergence of the hard kinematic region. This one loop HTL diagram reproduce the already known result for the

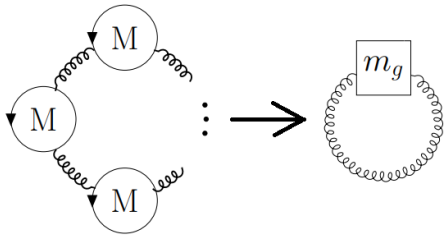

Figure 5.5: Ring in HTL formalism

$\alpha_s^2 \ln \alpha_s$ coefficient, it was evaluated exactly for $T \to 0$ in [29], while the next order $\mathcal{O}(\varepsilon)$ coefficient, necessary for renormalization as we will see explicitly below, was evaluated first by ourselves (to our knowledge) in [1], we obtained:

$$\begin{aligned} \mathcal{P}^{\text{Soft}}_{\text{Ring},\alpha_s^2} \equiv \mathcal{P}^{\text{HTL}}_{\text{LO}} =& \frac{d_A\, m_g^4}{(8\pi)^2}\left[\frac{1}{2\varepsilon} + C_{11} - L + \varepsilon\left(L^2 + C_{21}L + C_{22}\right)\right] \\ \equiv& m_g^4\left[-\frac{a_{1,0}}{2\varepsilon} + a_{1,0}L + a_{1,1} + \mathcal{O}(\varepsilon)\right] \end{aligned} \tag{5.12}$$

where $C_{11} \sim 1.17201$, $L = \ln\left(\frac{m_g}{M_s}\right)$. In the second line we also introduced a convenient notation that will become handy later. We obtain $C_{21} = -2C_{11}$, $C_{22} \simeq 2.16753$. Next, the hard contribution is given by the expression called p_3^b in [25]; it was evaluated in another scheme than dimensional regularization at that time. While determining its full contribution, in dimensional regularization, at order $\mathcal{O}(\varepsilon)$ is not trivial, its divergence can be easily extracted. Assuming quarks to have the same chemical potential:

$$\mathcal{P}^{\text{Hard}}_{\text{Ring},\alpha_s^2} = \frac{-d_A\, \alpha_s^2\, N_f^2\, \mu^4}{32\pi^4\varepsilon}\left(\frac{e^{\gamma_E} M_h}{4\pi}\right)^{3\varepsilon} + \frac{d_A\, N_f^2 \alpha_s^2}{(192\pi^4)}\left(19 - 2\pi^2 - 16\ln 2 - 6\ln(N_f)\right). \tag{5.13}$$

As expected, the two contributions of Eqns.(5.12) and (5.13) sum to a finite result, providing

that one identifies $m_g^2 \to m_E^2 \equiv 2\frac{N_f}{\pi}\alpha_s\mu^2$. The sum of the two kinematic regions in Eqns.(5.12) and (5.13) reproduces the known coefficient at α_s^2 from Eqn.(5.11). On top of that, the soft sector at N^{3}LO, whose diagrammatic representation is given in fig.(5.4a) reads [21; 22; 23] :

$$\mathcal{P}^{\text{soft}}_{\alpha_s^3} = \frac{\alpha_s\, N_c\, d_A m_g^4}{(8\pi)^2}\left(\frac{m_g}{M_s}\right)^{-4\varepsilon}\left(\frac{p_{-2}}{4\varepsilon^2}+\frac{p_{-1}}{2\varepsilon}+p_0\right), \tag{5.14}$$

where,

$$p_{-2} = \frac{11}{6\pi},\;\; p_{-1} \simeq 1.50731(19),\;\; p_0 \simeq 2.2125(9). \tag{5.15}$$

The complete mixed sector appearing at α_s^3 has not been evaluated for QCD yet, but was recently completed for QED [24], where it is a bit more simple since only abelian interaction needs to be accounted. Therefore, we will not include the contribution of the diagram (5.4b) in our analysis. The last piece, the hard sector at N^{3}LO, remains entirely unknown at present. Notice in Eqn.(5.14), besides M_h, the different scale M_s introduced in [23; 22][4]. This scale is not truly a renormalization scale of QCD (the only one being M_h) but was introduced as a "factorization scale" that separates the kinematic region soft/hard. At α_s^2 it consistently disappears. However, the situation is slightly more complicated at α_s^3 since there is still some missing contributions involving this factorization scale.

5.4 Matching the cold and dense QCD pressure

Now that we have defined all the relevant pieces for a complete EFT based calculation, we will collect them together so that it will, hopefully, become clear how one recovers the pressure in Eqn.(5.11), originally calculated in standard QCD, long before HTL was developped. The diagrammatic expansion of the pressure is shown explicitly in Eqn.(5.16).

$\mathcal{P}_{\text{QCD}} =$ 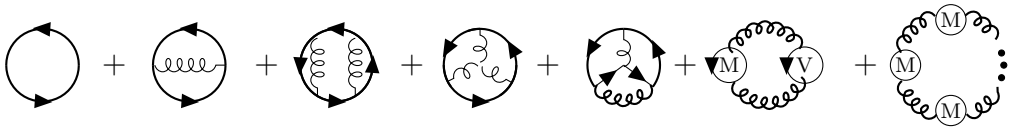

(5.16)

The concrete question now is to understand what we should incorporate into our EFT Lagrangian in order to perturbatively reproduce this pressure. The starting idea is that we wish to describe to soft modes using an EFT since we wish to determine and resum these logarithms. Therefore, the EFT must incorporate the Lagrangian written in Eqn.(5.10). One cannot simply add the quarks in the picture since they are the carrier of the hard scale and so we would end up with the exact same problem: having two scales in the same theory. One way around, is to define an EFT just for the soft modes, and to add perturbatively the hard contributions using the following identity:

$$\mathcal{P}_{\text{QCD}} = \mathcal{P}_{\text{EFT}} + (\mathcal{P}_{\text{QCD}} - \mathcal{P}_{\text{EFT}})\,|_{\text{exp. IR scale}}, \tag{5.17}$$

where one simply add and subtract the EFT contribution and do the expansion in the IR scale in the second quantity, as we have discussed in section 4.4.4. The EFT thus solely means the one loop HTL diagram of fig.(5.5) while $\mathcal{P}_{\text{QCD}}\,|_{\text{exp. IR scale}}$ incorporates the LO, NLO and NNLO pure hard contributions displayed in Eqn.(5.16) where the ring sum has to be redeveloped to

[4]Our M_s scale corresponds to Λ_h in [22]

order α_s^2.

This works perfectly fine at the leading order in the EFT (i.e α_s^2) so we will focus on this approach first. At higher orders, by construction it would also be correct, but it is unclear how one should define the Wilson coefficients of the higher order operators. Another option, is to add the quark kinematic term but without the covariant derivative. Thus to match the QCD pressure would means to incorporate the NLO and NNLO hard contributions inside the Wilson coefficient of this operator. This is easily generalized to any order and correctly dissociate the hard and soft scales. Moreover it allows to define the right RG properties at NNNLO to correctly determine the next-to-leading soft logarithms. Our first approach, slightly more naive, will ensure we correctly resum the leading soft logarithms but only partially resum the next-to-leading ones. For the mixed sector, to be hopefully evaluated soon, its contributions is included in the EFT picture as higher order operators (for QED see [30]), but this is currently beyond our scope.

In this picture, the contribution from the HTL EFT is simply Eqn.(5.12) where, in order to recover the $\alpha_s^2 \ln \alpha_s$ coefficient, it requires to match m_g with the d-dimensional Debye mass :

$$m_g^2 = \frac{2g^2 N_f \mu^2}{\pi^2} \left(\frac{e^{\gamma_E} M_s}{4\pi\mu} \right)^{\varepsilon}, \tag{5.18}$$

Moreover, it also requires to identify the two scale $M_h = M_s$ to correctly match the QCD pressure as was explained previously. The reason being that explicit dependence on M_s cancels, as it should but intrinsic dependence inside the couplings remains and the matching has to be done at the hard scale.

Now considering the next N^{3}LO order (α_s^3), we do not have the hard nor the mixed sectors yet. Thus, neither the (UV) divergences of (5.14) nor its factorization scale cancel explicitly as they should, to let only $\ln^p \alpha_s$ terms ($p = 1, 2$). In absence of such explicit cancellations, since the soft terms can be treated as a separate m_E-dependent sector, to avoid large logarithms it appears sensible to choose[24] $M_h \sim \mathcal{O}(\mu)$ and $M_s \sim \mathcal{O}(m_E)$, but keeping $\alpha_s(M_h \sim \mathcal{O}(\mu))$ to remain reasonably perturbative. It has been argued in [21; 23] that the final factor for the finite p_{-2} term should be $2p_{-2} \to p_{-2}$ instead, due to the cancellation with presently unknown hard contributions, and it is indeed the correct coefficient at $\alpha_s^3 \ln(\alpha_s)$. In our renormalized framework, this occurs consistently upon considering the consequence of the renormalization of the gluon mass at this order. Moreover, it also implies modifications to p_{-1} and p_0 as we shall see below.

Thus, the state-of-the-art result (before our original work, to be presented next), for the cold and dense QCD pressure reads:

$$\begin{aligned} \mathcal{P}_{\alpha_s^3}^{\text{C.Q.M}} =& \mathcal{P}_f \left\{ 1 - \frac{2}{\pi}\alpha_s - \frac{N_f}{\pi^2}\alpha_s^2 \ln \alpha_s - 0.874355\, \alpha_s^2 - 2d_A \frac{(11N_c - 2N_f)}{3(4\pi)^2} \ln\left(\frac{M_h}{\mu}\right) \alpha_s^2 \right\} \\ &+ \frac{N_c d_A \alpha_s m_g^4}{(8\pi)^2} \left(p_{-2} \ln^2 \frac{m_g}{M_s} - 2p_{-1} \ln \frac{m_g}{M_s} + p_0 \right), \end{aligned} \tag{5.19}$$

with $m_g^2 = m_E^2$ as in Eqn.(5.18).

5.4.1 The anomalous mass dimension of the gluons

Despite the non-local HTL Lagrangian, the NNLO perturbative HTL calculations give new m_g-dependent UV divergences and related counterterms having a seemingly standard renor-

malizable form (5.12)(5.14). The gluon's mass in the EFT has to be treated as a standard Wilson coefficient which undergoes the renormalization procedure and develops an anomalous dimension. The anomalous dimension of the HTL operator is what we call the anomalous mass dimension of the gluon.

Within $T \neq 0$ HTL calculations, the divergences from $m_g \neq 0$ occur in two-loop order $\alpha_s(m_g^2 T^2, m_g^3 T^3)$ terms, and the corresponding (unique) one-loop counterterm $\Delta\, m_g$ was obtained first in [16]. Using this Δm_g and the standard relation between bare mass m_g^B, $\mathcal{Z}_{m_g}$ counterterm at leading order:

$$m_g^B \equiv m_g\, \mathcal{Z}_{m_g} \simeq m_g \left(1 - g^2 \frac{\gamma_0^g}{2\varepsilon}\right) \tag{5.20}$$

we easily identify

$$\gamma_0^g = \frac{11 N_c}{3(4\pi)^2} \equiv b_0^g. \tag{5.21}$$

Namely, the LO interactions from HTL that contribute to renormalize m_g give a divergent contribution identical to the one defining b_0^g, the pure gauge LO beta function coefficient. Although striking, this equality of pure gauge b_0^g and γ_0^g is merely a one-loop order accident. Incidentally, it is worth noting that the same result (5.21) was obtained independently from a localizable, *renormalizable* gauge-invariant setup for a (vacuum) gluon mass[31]. This is not a coincidence since, recalling the discussion of chapter 2, these universal RG quantities are vacuum quantities independent of T, μ. The two-loop order γ_1^g, has also been calculated from the same $T = \mu = 0$ formalism, with the result[32] $(4\pi)^4 \gamma_1^g = 77 N_c^2/12$. Furthermore, the mass renormalization within Eqn.(5.12), $\mathcal{P}_{\rm LO}^{\rm HTL}(m_g \to m_g Z_{m_g})$, generates additional terms that combine with genuine two-loop contributions in Eqn.(5.14), as it is standard in renormalizable theory calculations.

Importantly, the unwanted nonlocal $\ln(m_E/M_s)/\varepsilon$ divergence in Eqn.(5.14) exactly cancels in those combinations. While (local) remnant divergences after mass renormalization are renormalized by vacuum energy $\mathcal{E}_0$ counterterms, always necessary in a massive theory. According to Weinberg's theorem, such local counterterms prove the renormalizability of the $T = 0$ HTL pressure at NLO $\alpha_s m_g^4$, i.e. NNNLO α_s^3. In other words, combining the results (5.14) from [23] with our renormalized HTL-EFT framework, we could prove HTL renormalizability at N^{3}LO at least for the pressure.

Remark that renormalizing m_g in Eq.(5.12) also modify the *finite* coefficients in Eq.(5.14), as

$$\begin{aligned} 2p_{-2} \to p_{-2}, \qquad p_{-1} \to p_{-1} - \frac{8\pi\gamma_0^g}{N_c}(C_{11} - \frac{1}{4}) \simeq p_{-1} - 0.5381, \\ p_0 \to p_0 - \frac{8\pi\gamma_0^g}{N_c}(C_{22} - \frac{C_{11}}{2}) \simeq p_0 - 0.9229. \end{aligned} \tag{5.22}$$

For clarity, we will call these modified coefficients $p_{-1}^{\rm ren.}$, $p_0^{\rm ren.}$.

5.4.2 Vacuum-energy induced subtraction terms in HTL-EFT

Earlier in chapter 2, we thoroughly explained how one must include an extra operator $m^4\mathbb{1}$– the vacuum energy contribution– in the Lagrangian when considering massive theories, in order to define a RG invariant perturbation series. As we move in the massive gluon framework of HTL, we should add this operator in the Lagrangian. Nevertheless, it is defined perturbatively with an analytical power dependence in the mass. It seems reasonable to think that the re-expansion

entering the matching contribution to the full QCD calculation, see (5.17), leaves it unchanged and thus it would cancel out:

$$\mathcal{P}_{\rm HTL} - \mathcal{P}_{\rm HTL}\big|_{m_g^2 \ll \mu^2} \to \mathcal{E}_0(m_g, M) - \mathcal{E}_0'(m_g, M) = 0. \tag{5.23}$$

Where $\mathcal{E}_0(m_g, M) = -m_g^4(M)/g(M)^2 \sum_i s_i\, g^{2i}$. However, the matching procedure in Eqn.(5.23) might be a strong assumption, since this operator's contribution derives solely from RG properties, and we do not have a clear diagrammatic expansion for it. The matching procedure requires the series solely to match perturbatively, order by order, with the full theory result. One way to go around is to subtract perturbatively only the spurious contribution from this vacuum energy.

The benefits are twofold. First, the vacuum energy genuinely operates the same way, by construction from RG invariance, as the factorization scale cancellation would: it cancels the spurious M_s scale dependence left. Since the calculations at α_s^3 are incomplete, we can use this contribution to effectively cancel the soft scale dependence there, anticipating from relatively cheap calculations, the expected cancellation in the full calculation at order α_s^3 not presently available. This procedure, used in [1], shows sizeable improvement with respect to both hard (M_h) and spurious factorization scale (M_s) dependence. Second, to introduce the implicit resummation formula for the LL and NLL series that we will discuss later, it is necessary to think of the pressure as including the subtraction terms (from the vacuum energy $\mathcal{E}_0$), implying in particular to start at order $1/g^2$. Though the vacuum subtraction term are not needed to obtain a resummation formula for the LL and NLL, since these two are not related. But it allows a much more compact formula.

We should note carefully, however, that it is only because of the matching procedure to the full theory that the operator in Eqn.(5.23) vanishes. Specifically, upon considering finite temperature and HTLpt framework, the latter to be discussed in the next chapter, no such matching procedure are required by construction, thus the operator $\mathcal{E}_0$ remains and plays an important role.

For these reasons, we will introduce a somehow different matching procedure and relax the constraint in Eqn.(5.23) and only insure that we fully reproduce the known perturbative order (α_s^2), but keeping higher order RG induced terms.

To begin with, instead of solving perturbatively the RG equation to determine $\mathcal{E}_0$, as we did in section 2.3.1 , we integrate the differential equation (see Eqn.(2.34)) :

$$M \frac{d\,\mathcal{E}_0}{d\ln M} \equiv \hat{\Gamma}_0^g(g) m_g^4, \tag{5.24}$$

which leads to,

$$\mathcal{E}_0(g(M), m_g(M)) = \mathcal{E}_0(g(M_0, m(M_0)) + \int_{g^2(M_0)}^{g^2(M)} dx\, m_g^4(M_0) \left\{ \frac{\hat{\Gamma}_0^g(x)}{\beta(x)} \exp\left(-4 \int_{g^2(M_0)}^{x} dy\, \frac{\gamma_m^g(y)}{\beta(y)} \right) \right\}. \tag{5.25}$$

Here, M_0 is an initial scale (different from M), that we identify as a boundary condition. This equations reflects the fact that the vacuum energy also needs a renormalization condition, just like we define $\Lambda_{\overline{MS}}$ for the coupling. After expanding the gamma and beta functions and

proceeding to some algebra, we find :

$$\mathcal{E}_0(g(M_h), m_g(M_h)) = \mathcal{E}_0(g(M_0), m_g(M_0)) - \Bigg\{ m_g^4(M)\left(\frac{s_0^g}{g^2(M)} + s_1^g\right) - m_g^4(M_0)\left(\frac{s_0^g}{g^2(M_0)} + s_1^g\right) + \mathcal{O}(m_g^4\, g^2)\Bigg\}. \tag{5.26}$$

To get there, we have identified the NLO running mass expansion :

$$m_g(M) \simeq m_g(M_0)\left(\frac{g^2(M)}{g^2(M_0)}\right)^{\frac{\gamma_0^g}{2b_0^g}}\left(1 + \frac{2}{(b_0^g)^2}(b_0^g\,\gamma_1^g - b_1^g\gamma_0^g)g^2(M_0) + \mathcal{O}(g^4)\right), \tag{5.27}$$

and the perturbative solution to the RG equation in Eqn.(5.24):

$$\Gamma_0^g = -s_0^g(b_0^g - 2\gamma_0^g),\ \Gamma_1^g = 4\gamma_0^g s_1^g - 2s_0^g(b_1^g - 2\gamma_1^g). \tag{5.28}$$

Even though the gluon mass is matched to α_s after the matching, in the EFT it remains an arbitrary parameter at first the runs according to its anomalous dimension. Only after can it be identified to α_s. Next, we choose M_0 (a fix boundary scale) to be equal to the central value of the hard scale M_h, such that we calibrate correctly for higher orders to the massless QCD pressure.

The spurious contribution at α_s^2 order that must be subtracted is:

$$\begin{aligned} -\frac{s_0^g\, m_g^4(M_h)}{g^2(M_h)} + \frac{s_0^g\, m_g^4(M_0)}{g^2(M_0)} &\simeq \mathcal{P}_f \frac{2N_f}{\pi^2}\alpha_s^2(M_0)\frac{b_0}{b_0^g}\ln\left(\frac{M_0}{M_h}\right) + \mathcal{O}(\alpha_s^3). \\ \mathcal{P}^{\text{match.}} &\equiv \mathcal{P}_f \frac{2N_f}{\pi^2}\alpha_s^2(M_0)\frac{b_0}{b_0^g}\ln\left(\frac{M_0}{M_h}\right) \end{aligned} \tag{5.29}$$

The $b_0 \equiv \frac{1}{14\pi^2}(\frac{11}{3}N_c - \frac{2}{3}N_f)$ factor originates from the running of the full QCD coupling which is taken at $N_f \neq 0$ consistently for the complete QCD pressure. The factor of $(b_0^g)^{-1}$ is, in contrast, the pure gauge LO beta function coefficient, see Eqn.(5.33), due to s_0^g that is driving the soft sector including only pure glue diagrams.

Let us summarize the procedure for the sake of clarity :

1. The massive sector in isolation is not RG invariant already at LO, thus one needs to add the vacuum energy contribution $\mathcal{E}_0 \overset{g<<1}{\simeq} -m_g^4\, s_0^g/g^2 + \dots$ to restore the RG invariance ; $\mathcal{P} \to \mathcal{P}^{\text{R.G.I}} \equiv \mathcal{P} + \mathcal{E}_0(M_h)$.

2. Matching the massive EFT theory (HTL here) to the full theory (QCD) seems to require to remove this last contribution to correctly reproduce the full theory :
$\mathcal{P}^{\text{R.G.I}} \to \mathcal{P}^{\text{R.G.I}} - \mathcal{E}_0'(M_h)$ since the renormalization group invariance under M_h is acting differently in the full theory.

3. An exact matching thus means:
$\mathcal{E}_0(M_h) = \mathcal{E}_0'(M_h)$.

4. We relax this constraints so that we only perturbatively reproduces the full theory but keeps higher order vacuum energy induced terms that anticipates the (still missing) soft

scale cancellation at $\mathcal{O}(\alpha_s^3)$:

5. In the end, what is used in the numeric is :
$\mathcal{P} = \mathcal{P}^{\text{resum}}_{\text{pert.}} - m_g(M_h)^4\, s_0^g/g^2(M_h) + m_g(M_0)^4 s_0^g/g^2(M_0) - \mathcal{P}^{\text{match.}}$

Where $\mathcal{P}^{\text{resum}}_{\text{pert.}}$ contains all other perturbatively determined contributions (possibly resummed).

5.5 Massive Leading and next-to-leading soft logarithms in Cold and Dense QCD

The derivation of (5.14) in [22] required highly involved HTL computations. The coefficient of the $\alpha_s^3 \ln^2 \alpha_s$ term, among other things, required clever identification of the relevant kinematic regions. From renormalization group properties, we could derive this same logarithm in a much simpler way [1], as well as all coefficients of the leading logarithms at all orders. Moreover, using the coefficient p_{-1} from Eqn.(5.14) as the first NLL, we carry the same procedure to determine and resum all next-to-leading soft logarithms to all orders.

Note however that, while the coefficients of the leading logarithms originate solely from the pure soft sector of HTL, the next-to-leading logarithm receive corrections at $\mathcal{O}(\alpha_s^3)$ already from the mixed sector which is not accounted by HTL itself (see (5.1) and explanations around). This is because such logarithms can only originate from resummed gluon lines and only one resummed propagator appears in the mixed sector. Nevertheless, the soft contribution for the NLL series is well-accounted by the resummation formula that we derived. This formula can be easily generalized when the full p_{-1} coefficient, including mixed soft-hard contributions, will be available in the future.

5.5.1 Schematic picture

Since we introduced a new operator (HTL) in the Lagrangian, the RG invariance requires to consider its anomalous dimension within the RG operator. In our case, it means first considering also an anomalous mass dimension for the gluons. To distinguish this anomalous dimension from the one of the quark, we denote γ_m^g such function.

In a massive theory, it is evident that the coefficients of the poles in dimensional regularization are directly related to the coefficient of the logarithm involving the renormalization scale M and the mass m. The pole of order n: $1/\varepsilon^n$ produces after renormalization a logarithm $L^n \equiv \ln(M/m)^n$.

Pictorially, we can visualize the pressure in massive theory as having the following expansion:

$$\begin{aligned}\frac{\mathcal{P}^{\text{RGI}}}{m_g^4} = \frac{a_{0,0}}{g^2} &+ a_{1,0}\, L &&+ g^2\, a_{2,0} \quad L^2 &&+ \dots \text{ LL} \\ &+ a'_{1,1} &&+ g^2\, a_{2,1} \quad L^1 &&+ \dots \text{ NLL} \\ & &&+ g^2\, a'_{2,2} \quad L^0 &&+ \dots\end{aligned} \tag{5.30}$$

Precise definitions of the coefficients appearing here will be discussed in the next sections. Moreover, as the definitions will be scattered along the text, a summary is given in the very last section. The first line is the Leading-Logarithm (LL) series, while the second is the next-to-LL (NLL) and so on. Following section 2.4.1, the coefficient $a_{1,0}$, proportional to the one-loop

order simple pole, is related to all the leading divergence appearing at higher orders. These coefficients determining the leading logarithm series, it is the generator of the LL series. As we move to the next order radiative corrections, we only need to evaluate both the two-loop (in HTL) order coefficients $a_{2,1}$, generator of the NLL series, and the "finite"[5] coefficient $a_{2,2}$. Note the subtraction coefficients in Eqn.(5.30), reflected in particular in the first term $a_{0,0}$, do not contribute to the recurrence relations between the logarithm series, but are necessary to deduce the resummation formula. We shall first work out the recurrence relations for the LL and NLL and then, take care of the matching to the full QCD pressure at α_s^2 order. The prime on coefficients $a_{n,n}$, for $n \geq 1$, in Eqn.(5.30) reminds us to include the subtraction term: $a'_{n,n} = a_{n,n} - s_n^g$. The first subtraction term s_0^g defines the coefficient $a_{0,0} = -s_0^g$.

Defining formally the full series as,

$$\mathcal{P}^{\mathrm{RGI}} = \frac{m_g^4}{g^2} \sum_{p=0}^{\infty} (g^2)^p \sum_{l=0}^{p} a_{p,l} \ln\left(\frac{m_g}{M}\right)^{p-l}, \tag{5.31}$$

and acting with the RG operator on it, we can work out, after some algebra, recursive relations between logarithms of the same series. Explicitly, the RG operator reads in our convention:

$$\begin{aligned} M\frac{d}{dM} &= M\frac{\partial}{\partial M} + \beta(g)\frac{\partial}{\partial g^2} - m_g\,\gamma_m^g(g)\frac{\partial}{\partial m_g}, \\ \beta(g) &\equiv \frac{d\,g^2}{d\ln M} = -2b_0^g\,g^4 - 2b_1^g\,g^6 + \ldots \\ \gamma_m^g(g) &\equiv -\frac{d\ln m_g}{d\ln M} = \gamma_0^g\,g^2 + \gamma_1^g\,g^4 + \ldots \end{aligned} \tag{5.32}$$

With b_0^g, b_1^g, the pure gauge contributions reading:

$$(4\pi)^2\,b_0^g = \frac{11N_c}{3},\ (4\pi)^4\,b_1^g = \frac{34N_c^2}{3}. \tag{5.33}$$

Considering g fixed, and identifying same order terms, one obtain :

$$\mathrm{LL}: \qquad -p\,a_{p,0} = (4\gamma_0^g + 2b_0^g(p-2))\,a_{p-1,0}, \quad p \geq 1 \tag{5.34}$$

$$\mathrm{NLL}: \quad (1-p)a_{p,1} = (4\gamma_0 + 2b_0^g(p-2))\,a_{p-1,1} + (4\gamma_1 + 2b_1^g(p-3))\,a_{p-2,0} + \gamma_0^g(p-1)a_{p-1,0} \tag{5.35}$$

The first series is rather straightforward as it only relates the logarithm at order $k+1$ to the coefficient of the logarithm of the same family at order k. The NLL series, however, is much more involved as it has the same property but also includes two coefficients from the LL series at order k and $k-1$. Feeding this expressions with the input $a_{1,0}$ and $a_{2,1}$, we can obtain the desired coefficients at any order p.

It would be fine, if we could somehow resum all these logarithms together, instead of working them one by one, such as to obtain a compact formula which upon re-expansion would give the right coefficients. This was done long ago [33] using a method that we shall review now.

[5] In opposition to the coefficients of the Logarithms which originates from the divergences.

5.5.2 Resummation of the LL and NLL series

Consider the definition of the γ_m^g function in Eqn.(5.32). It can be formally integrated using the separation of variables method:

$$m_g(M_1) = m_g(M_h) \exp\left\{ - \int_{g^2(M_h)}^{g^2(M_1)} dg^2 \frac{\gamma_m^g(g)}{\beta(g)} \right\}. \tag{5.36}$$

If we impose the specific boundary condition $M \equiv m_g(M)$ for $M_1 = M$, we will define an implicit formula encoding the RG resummation at all orders for this mass term. Note that we avoid the notation M_0 for the lower boundary term to avoid confusion with the one in Eqn.(5.25). Specifically, this boundary condition is exactly the scale at which we want to evaluate the pressure, so as a foreshadowing, we directly chose M_h.

LL series

After integration at leading order in g^2 of Eqn.(5.36), using b_0^g, γ_0^g in Eqn.(5.32), it reads:

$$\frac{m_g(M_1)}{m_g(M_h)} = \left(\frac{g^2(M_1)}{g^2(M_h)} \right)^{\frac{\gamma_0^g}{2b_0^g}}. \tag{5.37}$$

Using the specific boundary conditions: $M_1 \equiv m(M_1)$, and using the one-loop running of $\alpha_s = g^2/4\pi$ (Eqn.(49) in appendix A), we come to the final result:

$$M_1 = \frac{m_g(M_h)}{\left(1 + b_0^g \, g^2(M_h) \ln\left(\frac{M_1}{M_h}\right)\right)^{\gamma_0^g/2b_0}}. \tag{5.38}$$

Further defining:

$$f_1 = 1 + b_0^g \, g^2(M_h) \ln\left(\frac{M_1}{M_h}\right) \equiv \frac{g^2(M_h)}{g^2(M_1)}. \tag{5.39}$$

one can write compactly :

$$M_1 \equiv m_g(M_h) f_1^{-\frac{\gamma_0^g}{2b_0^g}}. \tag{5.40}$$

In order to relate this result to the pressure, naturally we would think to take $\mathcal{P} \sim M_1$ to get the resummation of the LL since $\mathcal{P} \simeq m_g^4$. However, as we discussed at length in chapter 2, the renormalization group invariant (RGI) quantity is $\mathcal{P}^{\rm RGI}$ which starts at order $\frac{1}{g^2}$ for RG consistency. Therefore, we write: $\mathcal{P}^{\rm RGI} \simeq \frac{M_1^4}{g^2(M_1)}$, identifying $M_1 = m_g$, which after some algebra leads to:

$$\mathcal{P}_{\rm LL}^{\rm RGI} = -\frac{s_0^g \, m_g(M_h)^4}{g^2(M_h)} f_1^{1-4\frac{\gamma_0}{2b_0}}. \tag{5.41}$$

In fact, one can alternatively recover the sole LL series without any RG subtraction contribution, substituting: $-s_0^g \to a_{1,0} g^2 \ln\left(\frac{m_g}{M_h}\right)$ in Eqn.(5.41):

$$\mathcal{P}_{\rm LL}^{\rm RGI} = a_{1,0} m_g(M_h)^4 \ln\left(\frac{m_g}{M_h}\right) f_1^{1-4\frac{\gamma_0}{2b_0}}. \tag{5.42}$$

However, without the the RG substraction contribution in the first place, one could not have guessed (or difficultly) the extra -1 power in the previous equation. This last formula makes

it clear that $a_{1,0}$ is the actual generator of the LL formula. Nevertheless, it is interesting to recast results as in Eqn.(5.41) with s_0^g as the generator for this series since s_0^g is actually also determined by $a_{1,0}$ via the RG equation, see previous derivation of chapter 2. Generalizing to higher order, it turns out that the coefficient s_n can be seen partially as a generator of the N$^{\text{n}}$LL. We will explain carefully below why it is not the full generator of the N$^{\text{n}}$LL series (these ones being $a_{n,1}$ the single logarithm coefficient at order $(g^2)^n$).

NLL series

While contributions from coefficient $a_{p-1,0}$ and $a_{p-2,0}$ to the NLL, see Eqn.(5.35), can be taken into account formally upon expanding to higher orders Eqn.(5.38), the contribution from $a_{p-1,1}$ requires to modify the Ansatz for the pressure. Denoting $g^2(M_i) \to g_i^2$ as well as $m_g(M_i) \equiv m_{g,i}$ for simplicity, at next order we have:

$$m_{g,1} = m_{g,h} \exp\left\{ \int_{g_h^2}^{g_1^2} dg^2 \frac{\gamma_0^g g^2 + \gamma_1^g g^4}{2b_0^g g^4 + 2b_1^g g^6} \right\}. \tag{5.43}$$

After exact integration and some algebra:

$$m_{g,1} = m_{g,h} \left(\frac{g_1^2}{g_h^2}\right)^{\frac{\gamma_0^g}{2b_0^g}} \left(\frac{1+\frac{b_1^g}{b_0^g}g_1^2}{1+\frac{b_1^g}{b_0^g}g_h^2}\right)^{-\frac{\gamma_0^g}{2b_0^g}} \left(\frac{1+\frac{b_1^g}{b_0^g}g_1^2}{1+\frac{b_1^g}{b_0^g}g_h^2}\right)^{\frac{\gamma_1^g}{2b_1^g}}. \tag{5.44}$$

Now, we can identify $M_2 \equiv m_g(M_2) = M_1$, $f_2 \equiv \frac{g_h^2}{g_1^2}$, that leads to :

$$M_2 = m_g(M_h) f_2^{-\frac{\gamma_0^g}{2b_0^g}} (R)^{\frac{\gamma_1^g}{2b_1^g} - \frac{\gamma_0^g}{2b_0^g}}, \qquad R = \frac{1+\frac{b_1^g}{b_0^g}g_h^2 f_2^{-1}}{1+\frac{b_1^g}{b_0^g}g_h^2}. \tag{5.45}$$

which generalizes Eqn.(5.38) to NLO and is an exact relation. In Eqn.(5.45), the exact two-loop running of the coupling ratio f_2 is an implicit function given by:

$$f_2 = 1 + +2b_0^g\, g_h^2 \ln\left(\frac{M_2}{g_h^2}\right) + \frac{b_1^g}{b_0^g} g_h^2 \ln(f_2) + \frac{b_1^g}{b_0^g} g_h^2 \ln\left(\frac{1+\frac{b_1^g}{b_0^g}g_h^2 f_2^{-1}}{1+\frac{b_1^g}{b_0^g}}\right) \tag{5.46}$$

whose first order terms after re-expansion reads:

$$f_2 = 1 + \left[2b_0^g\, g_h^2 + 2(b_1^g - \gamma_0^g b_0^g) g_h^4\right] \ln \frac{m_g(M_h)}{M_h} + \mathcal{O}(g^6). \tag{5.47}$$

Eq.(5.47) gives numerically good approximations as long as the coupling is not too large ($\alpha_s \equiv \frac{g^2}{4\pi} \lesssim 0.5$) as will be approximately the case in our practical application to cold and dense pressure. Introducing new convenient notations,

$$A_0 = \frac{\gamma_0^g}{(2b_0^g)},\ A_1 = \frac{\gamma_1^g}{(2b_1^g)},\ B = 4(A_1 - A_0), \tag{5.48}$$

now we can define our Ansatz for the pressure, incorporating exactly the NLL series :

$$\mathcal{P}_{\rm NLL} = \frac{-s_0^g\, m_g(M_h)^4}{g^2(M_h)\, f_2^{4A_0-1}}[R(f_2)]^B \left(1 - \frac{a'_{1,1}\, g^2(M_h)}{s_0^g\, f_2} - \frac{a'_{2,2}\, g^4(M_h)}{s_0^g\, f_2^2} + \dots\right). \tag{5.49}$$

In this formula, using the exact relation Eqn.(5.46) the re-expansion reproduces the LL, NLL series of Eqn.(5.35) to all orders as well as the first finite coefficient $a_{1,1}$. From this formula it is not immediately transparent what precisely is the generator of the NLL series. At first, it looks like $a'_{1,1}$ is the generator. But, by RG construction, s_1^g is also proportional to $a_{1,1}$ such that the difference, $a'_{1,1}$, is independent of $a_{1,1}$. Moreover, s_1^g is actually determined by $a_{2,1}$, so here we find back the actual NLL generator. In our case we obtain explicitly :

$$\begin{aligned} s_0^g =& -\frac{a_{1,0}}{2(b_0^g - 2\gamma_0^g)} \\ s_1^g =& a_{1,1} + \frac{a_{2,1}}{4\gamma_0^g} + \frac{a_{1,0}}{4} + \frac{s_0^g}{4\gamma_0^g}(b_1^g - 2\gamma_1^g), \end{aligned} \tag{5.50}$$

where we also added s_0^g for completeness. The term $-\frac{a'_{2,2} g(M_h)^4}{s_0^g\, f_2^2}$ in Eqn.(5.49) incorporates the finite term $a_{2,2}$ and the next order RGI subtraction s_2^g (yet unknown[6]). Upon integrating to the next order the gamma function it would generate the NNLL series.

Alternatively, we can derive an exact and more compact formula in terms of explicitly RG invariant quantities more convenient than the implicit formula (5.46). Defining the two-loop RG invariant mass,

$$\hat{m}_g = 2^C m_g (2b_0^g\, g_h^2)^{-A_0}(1 + b_1^g\, g_h^2/b_0^g)^{A_0 - A_1}, \tag{5.51}$$

$$F_2 \equiv \frac{f_2}{2b_0^g\, g_h^2}, \tag{5.52}$$

and the exact two-loop running coupling, given as an implicit $g^2(M)$ solution of:

$$\Lambda_{\overline{MS}} = M_h e^{-1/(2b_0^g g_h^2)}(b_0^g\, g_h^2/(1 + b_1^g\, g_h^2/b_0^g))^{-C}, \tag{5.53}$$

where $C = b_1^g/(2(b_0^g)^2)$ one obtains after some algebra :

$$\mathcal{P}_{NLL} = -2b_0^g\, s_0^g\, 2^{-4C} \hat{m}_g^4\, F_2^{1-4A_1}(C + F_2)^{4(A_1 - A_0)} \left(1 - \frac{a'_{1,1}}{2s_0^g b_0^g F_2} - \frac{a_{2,2}}{s_0^g\,(2b_0^g F_2)^2}\right). \tag{5.54}$$

F_2 can be easily determined for given $g^2 = 4\pi\alpha_s$ values, then plugged into Eqn.(5.54) for m_g values given from Eqn.(5.51).

5.6 Results

As a concrete outcome of this construction, the coefficient $a_{2,0}$ for the LL at α_s^3 can be easily extracted from Eqn.(5.34):

$$a_{2,0} = -2\gamma_0^g\, a_{1,0} = \frac{N_c\, d_A\, p_{-2}}{(4\pi)(8\pi)^2}. \tag{5.55}$$

[6]Determining s_2^g require evaluation of the simple divergence of the three-loop HTL theory. Only last year the two-loop order was completed involving impressive efforts to achieve the task thus three loops is completely out of our scope for now.

It reproduces independently and exactly the result from [23] in a straightforward manner. The important feature required to obtain it from the above simple RG relations is having identified the gluons anomalous mass γ_0^g. The LL series simplifies even more since $\gamma_0^g = b_0^g$, thus every successive order can be obtained from :

$$a_{p,0} = (-2\gamma_0^g)^p \, a_{1,0}, \tag{5.56}$$

which is now trivially recognized as a simple geometric series.

The resummed NLL and LL series in Eqn.(5.49) obviously incorporate the first LL $a_{1,0}\alpha_s^2 \ln \alpha_s$ and the finite term $a_{1,1}$. But this contributions are already accounted for by the pressure at α_s^2 in Eqn.(5.19). To avoid double-counting, one must carefully subtract these two terms. The α_s^2 order being complete, the matching to the pressure necessitates to also remove the contributions from any spurious subtraction terms up to and including the α_s^2 order. However, as explained around Eqn.(5.29), we can keep s_0^g and s_1^g contributions at α_s^p, $p \geq 3$ for they are anticipating the soft-hard cancellation mechanism.

Collecting all the pieces from Eqns.(5.18)(5.19)(5.29)(5.47)(5.49), our final expression for the pressure incorporating all order LL, NLL resummation is :

$$\begin{aligned}\mathcal{P}_{\rm NLL}^{\rm C.Q.M} =& \mathcal{P}^{\rm C.Q.M} - \frac{s_0^g \, m_g(M_h)^4}{g^2(M_h)\, f_2^{4A_0-1}} [R(f_2)]^B \left(1 - \frac{a'_{1,1}\, g^2(M_h)}{s_0^g \, f_2} - \frac{a_{2,2}\, g^4(M_h)}{s_0^g \, f_2^2}\right) \\ & - m_g^4 \left(a_{1,1} + a_{1,0} \ln\left(\frac{m_E}{M_h}\right)\right) - \mathcal{P}_f \frac{2N_f}{\pi^2} \alpha_s^2(M_0) \frac{b_0}{b_0^g} \ln\left(\frac{M_0}{M_h}\right).\end{aligned} \tag{5.57}$$

Note that if one wants to get the same results but restricted to the LL only, upon replacing the NLL series in Eqn.(5.57) by the LL series in Eqn.(5.42), the coefficient $-m_g^4 a_{1,1}$ of Eqn.(5.57) must be removed too. Compact formula are given in Eqn.(5.66) in the last section, convenient to reproduce more easily the results. We discussed previously that the ignorance of α_s^p, $p \geq 3$ hard contributions incites to take $M_s \sim \mathcal{O}(m_E)$ in order to avoid large logarithms. But the resummation in Eqn.(5.57) relate M_h and M_s : if we had exact renormalization group invariance, we could choose any $M_s \sim m_E < M < M_s$.

5.6.1 Numerical results and comparisons

In Fig.5.6a and 5.6b the RGI LL and NLL resummed pressures from Eqn.(5.57) are compared to the present state-of-the-art Eqn.(5.19 as function of $\mu_B = 3\mu$. The central scale values $M_h = 2\mu$ and the $\mu \leq M_h \leq 4\mu$ remnant scale dependence are illustrated for the different quantities (using in Eqns.(5.11),(5.57) the exact NLO QCD running coupling $\alpha_s(M_h)$ in Eqn.(5.53) with $\Lambda_{\overline{MS}}$). As a concrete value, we use $\alpha_s(M = 1.5\,\text{GeV}) = \text{g}^2/4\pi = 0.326$. The equivalent in terms of $\Lambda_{\overline{\rm MS}}$ can be found in appendix A.1.9. For sensible comparisons we also adopt the minimal sensitivity [34] determined soft scale in [23], $M_s \sim 0.275 m_E$.

Note first that the sole LL resummation with $-s_0^g \to a_{1,0} g^2 \ln m_g/M_h)$ gives a sizeably reduced scale dependence, compared to the NNLO pressure Eq.(5.11) at $\mathcal{O}(\alpha_s^2)$, as resummed LL induces *positive* $\alpha_s^{p\geq 3}$ contributions partly cancelling the negative α_s^2 coefficient in Eq.(5.11). However, this effect is approximately cancelled once including p_{-1}, p_0 α_s^3-order terms from Eqs.(5.15),(5.22). Next, for the LL and NLL RGI pressures, deviations from the state-of-the-art ("NNLO + soft N^{3}LO" in Fig.5.6b) are noticeable. The central scale ($M_h = 2\mu$) RGI pressure is slightly higher for fixed μ values, with very moderate differences between (RGI) LL and NLL pressures. Importantly, the remnant scale dependencies of the RGI pressures are reduced as compared to the NNLO + soft N^{3}LO results: only slightly for the LL pressure, due

to cancellations with p_{-1}, p_0 $\mathcal{O}(\alpha_s^3)$ terms, but significantly for the NLL pressure, both for M_h and M_s variations, due to extra cancellations from $\alpha_s^{p\geq 3}$ terms induced in (5.49). Concerning possible M_0 variations, for fixed M_h they give much smaller uncertainties than M_h variations in Fig.5.6b, as can be seen from fig.(5.7a).

5.6.2 Conclusions

In conclusion, we have obtained compact explicit expressions for the all order resummation of both leading logarithms and and soft next-to-leading logarithms series contributions to the cold and dense QCD pressure, that goes well beyond previously established results in the literature. The renormalization group resummation construction moreover gives clearly improved residual scale dependence with both the hard scale and the spurious soft scale. This result is expected to improve control towards lower μ_B values to match with the extrapolated equation of state from the nuclear matter density region. The next step now, is to work in a realistic set up, namely, including different chemical potential for the quarks a well as the strange quark current mass in order to more realistically describe the equation of state for neutron star. Investigation of neutron star equation of state will be part of chapter 7. Before that, we will discuss another resummation scheme in the next chapter for the series as well as corrections from massive quarks to the pressure.

5.6.3 Summary of all coefficients required for $\mathcal{P}^{\rm C.Q.M}_{\rm NLL}$.

$$\gamma_0^g = \frac{1}{(4\pi)^2}\left(\frac{11\,N_c}{3}\right), \quad \gamma_1^g = \frac{1}{(16\pi^2)^2}\left(\frac{77}{12}N_c^2\right). \tag{5.58}$$

$$b_0^g = \frac{1}{(4\pi)^2}\left(\frac{11\,N_c}{3}\right), \quad b_1^g = \frac{34\,N_c^2}{3(4^p i)^4}. \tag{5.59}$$

$$C_{11} = \frac{(1.17201\ d_A)}{(8\pi)^2}, \quad C_{21} = 2\,C_{11}, \quad C_{22} = 2.16753. \tag{5.60}$$

$$s_0^g = -\frac{a_{1,0}}{2(b_0^g - 2\gamma_0^g)} = \frac{-d_A}{2(8\pi)^2 b_0^g}, \quad s_1^g = a_{1,1} + \frac{a_{2,1}}{4\gamma_0^g} + \frac{a_{1,0}}{4} + \frac{s_0^g}{2\gamma_0^g}(b_1^g - 2\gamma_1^g) \tag{5.61}$$

$$a_{0,0} = -s_0^g, \quad a_{10} = -\frac{d_A}{(8\pi)^2}, \quad a_{11} = \frac{d_A\,c_{11}}{(8\pi)^2}. \tag{5.62}$$

$$a_{20} = \frac{N_c\ d_A}{(4\pi)(8\pi)^2}p_{-2}, \quad a_{21} = \frac{N_c\,d_A}{(4\pi)(8\pi)^2}(-2p_{-1}^{\rm ren.}), \quad a_{22} = \frac{d_A\ N_c}{(4\pi)(8\pi)^2}p_0^{\rm ren.}. \tag{5.63}$$

$$a'_{2,1} = a_{2,1} - s_1^g.$$

$$A_0 = \frac{\gamma_0^g}{2b_0^g}, \quad A_1 = \frac{\gamma_1^g}{2b_1^g}, \quad B = 4(A_1 - A_0). \tag{5.64}$$

Practical compact formula

For the LL series:

$$\mathcal{P}^{\rm LL}_{\alpha_s^{p\geq 3}} = \mathcal{P}^{\rm C.Q.M}_{\alpha_s^2} + \mathcal{P}_f\left(\frac{2N_f}{\pi^2}\right)\left(\frac{1}{8\pi b_0^g}\left[\frac{\alpha_s}{1+8\pi b_0^g\alpha_s\ln\frac{m_E}{M_s}} - \alpha_s(M_0)\right] + \alpha_s^2\ln\frac{m_E}{M_s} - \alpha_s^2(M_0)\frac{b_0}{b_0^g}\ln\frac{M_0}{M_h}\right), \tag{5.65}$$

while for the NLL series :

$$\begin{aligned}\mathcal{P}^{\rm NLL}_{\alpha_s^{p\geq 3}} =& \mathcal{P}^{\rm C.Q.M}_{\alpha_s^2} + \mathcal{P}_f\left(\frac{2N_f}{\pi^2}\right)\left(\frac{1}{8\pi b_0^g}\left[\frac{\alpha_s}{f_2}\left(\frac{1+\frac{51}{22\pi}\frac{\alpha_s}{f_2}}{1+\frac{51}{22\pi}\alpha_s}\right)^{-59/68}\left(1+\frac{d_1\,\alpha_s}{f_2}+\frac{d_2\,\alpha_s^2}{f_2^2}\right)\right]\right.\\ &\left.+\alpha_s^2\left(\ln\frac{m_E}{M_s}+d_3\right)+d_4\,\alpha_s^2(M_0)-\alpha_s^2(M_0)\frac{b_0}{b_0^g}\ln\frac{M_0}{M_h}\right),\end{aligned} \tag{5.66}$$

where $\alpha \equiv \alpha_s(M_h)$ and,

$$\begin{aligned} d_1 \simeq 3.29659 \equiv (\frac{-4\pi}{s_0^g})a'_{1,1},\;\; d_2 =& \simeq 6.77276 \equiv -(\frac{(4\pi)^2}{s_0^g})a_{2,2},\\ d_3 \simeq -1.17201 \equiv C_{11},\;\; d_4 &\simeq -0.711003 \equiv 8\pi^2 s_1^g. \end{aligned} \tag{5.67}$$

And the truncated f_2 defined in Eqn.(5.46) reading explicitly :

$$f_2 = 1+\left(\frac{11}{2\pi}\alpha_s - \frac{19}{8\pi^2}\alpha_s^2\right)\ln\frac{m_E}{M_s}+\mathcal{O}(\alpha_s^3). \tag{5.68}$$

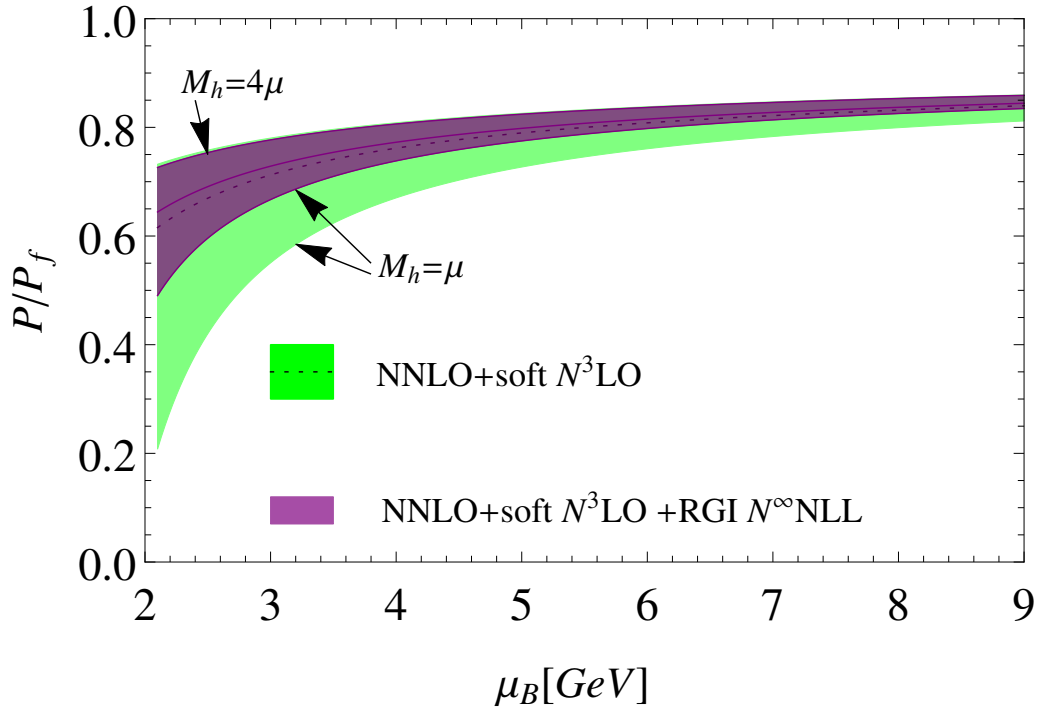

(a)

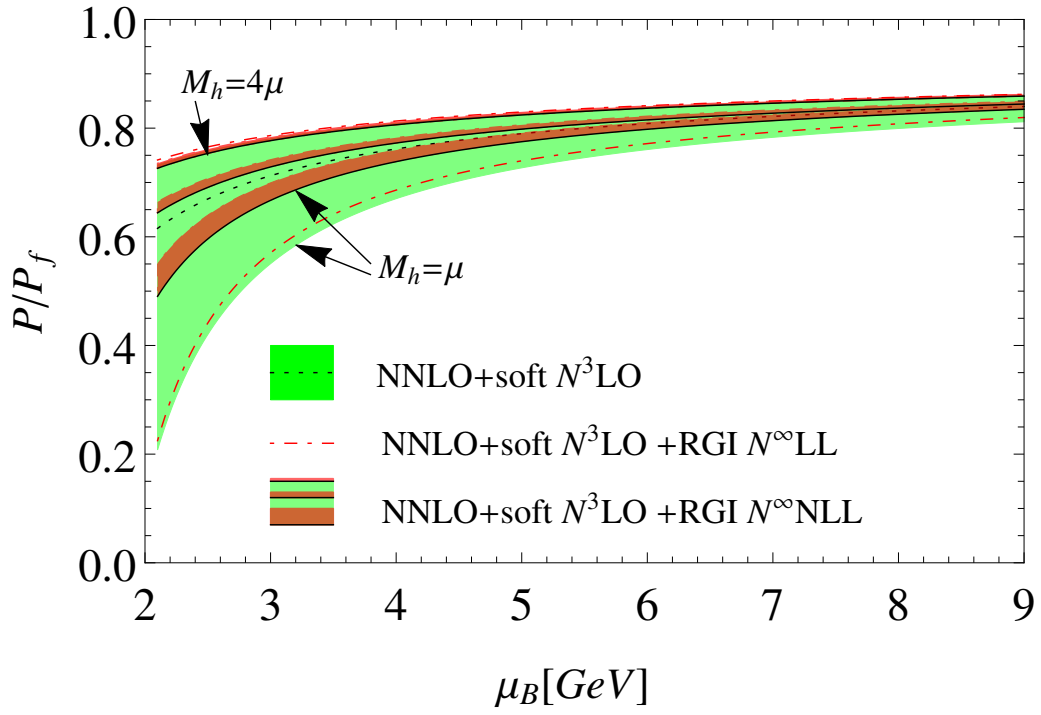

(b)

Figure 5.6: NNLO+ soft N^{3}LO in Eqn.(5.19) versus NNLO+soft N^{3}LO+RGI LL, NLL resummed pressures, as functions of $\mu_B = 3\mu$, with $\mu \leq M_h \leq 4\mu$. We follow the prescription in [23]: $M_s \simeq 0.275 m_E$. $M_0 = 2\mu$. For the RGI NLL resummed pressure, M_s variation within $[M_s/2, 2M_s]$ are shown in addition as darker bands.

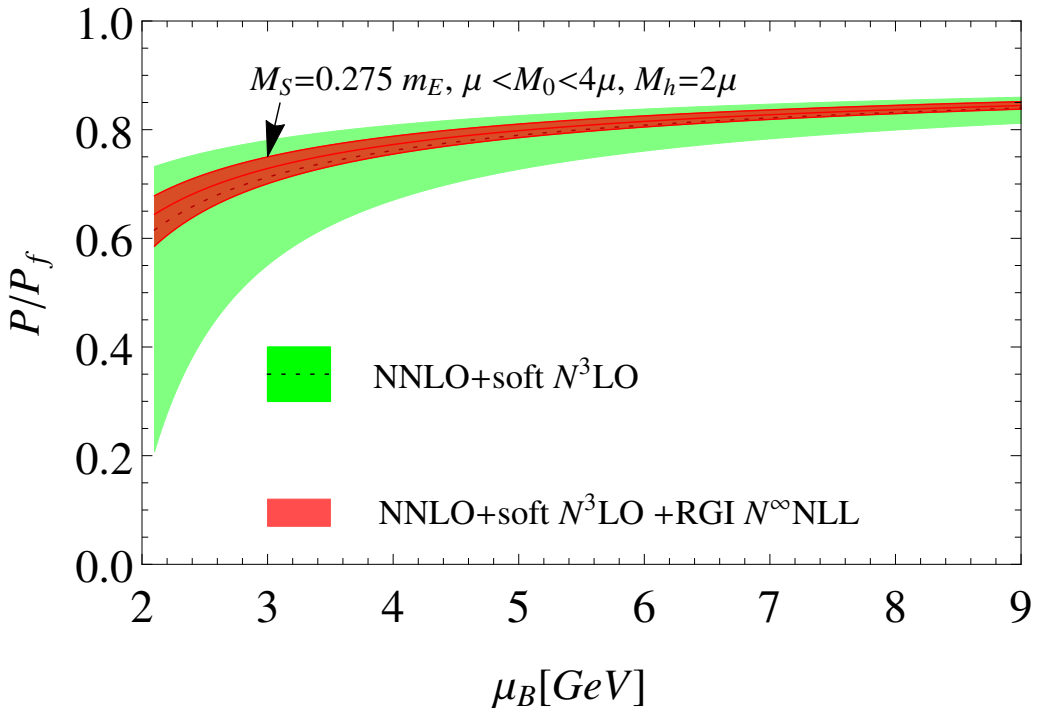

(a)

Figure 5.7: NNLO+ soft N^{3}LO in Eqn.(5.19) versus NNLO+soft N^{3}LO+RGI LL, NLL resummed pressures, as functions of $\mu_B = 3\mu$. We follow the prescription in [23]: $M_s \simeq 0.275 m_E$. With $M_h = 2\mu$ and $\mu \leq M_0 \leq 4\mu$.

5.7 Bibliography

[1] Loïc Fernandez and Jean-Loïc Kneur. All order resummed leading and next-to-leading soft modes of dense QCD pressure. *Accepted in Phys. Rev. Lett.*, 9 2021, 2109.02410.

[2] Eric Braaten and Robert D. Pisarski. Soft amplitudes in hot gauge theories: A general analysis. *Nuclear Physics B*, 337(3):569–634, 1990.

[3] Eric Braaten and Robert D. Pisarski. Simple effective Lagrangian for hard thermal loops. *Phys. Rev. D*, 45:R1827–R1830, Mar 1992.

[4] J. Frenkel and J.C. Taylor. High-temperature limit of thermal QCD. *Nuclear Physics B*, 334(1):199–216, 1990.

[5] J. Frenkel and J. C. Taylor. Hard thermal QCD, forward scattering and effective actions. *Nucl. Phys. B*, 374:156–168, 1992.

[6] J. C. Taylor and S. M. H. Wong. The Effective Action of Hard Thermal Loops in QCD. *Nucl. Phys. B*, 346:115–128, 1990.

[7] R. Kobes, G. Kunstatter, and A. Rebhan. Gauge dependence identities and their application at finite temperature. *Nucl. Phys. B*, 355:1–37, 1991.

[8] Jean-Paul Blaizot and Edmond Iancu. The Quark gluon plasma: Collective dynamics and hard thermal loops. *Phys. Rept.*, 359:355–528, 2002, hep-ph/0101103.

[9] Michel Le Bellac. *Thermal Field Theory.* Cambridge Monographs on Mathematical Physics. Cambridge University Press, 1996.

[10] Michael Strickland. *Relativistic Quantum Field Theory, Volume 3.* 2053-2571. Morgan Claypool Publishers, 2019.

[11] Mikko Laine and Aleksi Vuorinen. *Basics of Thermal Field Theory*, volume 925. Springer, 2016, 1701.01554.

[12] Joseph I. Kapusta and Charles Gale. *Finite-Temperature Field Theory: Principles and Applications.* Cambridge Monographs on Mathematical Physics. Cambridge University Press, 2 edition, 2006.

[13] Jens O. Andersen, Emmanuel Petitgirard, and Michael Strickland. Two loop HTL thermodynamics with quarks. *Phys. Rev. D*, 70:045001, 2004, hep-ph/0302069.

[14] Stefano Carignano, Cristina Manuel, and Joan Soto. Power corrections to the HTL effective Lagrangian of QED. *Phys. Lett. B*, 780:308–312, 2018, 1712.07949.

[15] Tyler Gorda, Aleksi Kurkela, Juuso Österman, Risto Paatelainen, Saga Säppi, Philipp Schicho, Kaapo Seppänen, and Aleksi Vuorinen. Degenerate fermionic matter at N^3LO: Quantum Electrodynamics. 4 2022, 2204.11893.

[16] Jens O. Andersen, Eric Braaten, Emmanuel Petitgirard, and Michael Strickland. HTL perturbation theory to two loops. *Phys. Rev. D*, 66:085016, 2002, hep-ph/0205085.

[17] Najmul Haque, Aritra Bandyopadhyay, Jens O. Andersen, Munshi G. Mustafa, Michael Strickland, and Nan Su. Three-loop HTLpt thermodynamics at finite temperature and chemical potential. *JHEP*, 05:027, 2014, 1402.6907.

[18] Jacopo Ghiglieri, Aleksi Kurkela, Michael Strickland, and Aleksi Vuorinen. Perturbative Thermal QCD: Formalism and Applications. *Phys. Rept.*, 880:1–73, 2020, 2002.10188.

[19] Cristina Manuel. Hard dense loops in a cold nonAbelian plasma. *Phys. Rev. D*, 53:5866–5873, 1996, hep-ph/9512365.

[20] Barry A. Freedman and Larry D. McLerran. Fermions and gauge vector mesons at finite temperature and density. iii. the ground-state energy of a relativistic quark gas. *Phys. Rev. D*, 16:1169–1185, Aug 1977.

[21] Tyler Gorda, Aleksi Kurkela, Paul Romatschke, Matias Säppi, and Aleksi Vuorinen. Next-to-Next-to-Next-to-Leading Order Pressure of Cold Quark Matter: Leading Logarithm. *Phys. Rev. Lett.*, 121(20):202701, 2018, 1807.04120.

[22] Tyler Gorda, Aleksi Kurkela, Risto Paatelainen, Saga Säppi, and Aleksi Vuorinen. Cold quark matter at N3LO: Soft contributions. *Phys. Rev. D*, 104(7):074015, 2021, 2103.07427.

[23] Tyler Gorda, Aleksi Kurkela, Risto Paatelainen, Saga Säppi, and Aleksi Vuorinen. Soft Interactions in Cold Quark Matter. *Phys. Rev. Lett.*, 127(16):162003, 2021, 2103.05658.

[24] Tyler Gorda, Aleksi Kurkela, Juuso Österman, Risto Paatelainen, Saga Säppi, Philipp Schicho, Kaapo Seppänen, and Aleksi Vuorinen. Soft photon propagation in a hot and dense medium to next-to-leading order. 4 2022, 2204.11279.

[25] A. Vuorinen. The Pressure of QCD at finite temperatures and chemical potentials. *Phys. Rev. D*, 68:054017, 2003, hep-ph/0305183.

[26] Ioan Ghisoiu, Tyler Gorda, Aleksi Kurkela, Paul Romatschke, Matias Säppi, and Aleksi Vuorinen. On high-order perturbative calculations at finite density. *Nucl. Phys. B*, 915:102–118, 2017, 1609.04339.

[27] Aleksi Kurkela, Paul Romatschke, and Aleksi Vuorinen. Cold Quark Matter. *Phys. Rev. D*, 81:105021, 2010, 0912.1856.

[28] Aleksi Kurkela and Aleksi Vuorinen. Cool quark matter. *Phys. Rev. Lett.*, 117(4):042501, 2016, 1603.00750.

[29] Sylvain Mogliacci, Jens O. Andersen, Michael Strickland, Nan Su, and Aleksi Vuorinen. Equation of State of hot and dense QCD: Resummed perturbation theory confronts lattice data. *JHEP*, 12:055, 2013, 1307.8098.

[30] Stefano Carignano, Margaret E. Carrington, and Joan Soto. The htl lagrangian at nlo: The photon case. *Physics Letters B*, 801:135193, 2020.

[31] M. A. L. Capri, D. Dudal, J. A. Gracey, V. E. R. Lemes, R. F. Sobreiro, S. P. Sorella, and H. Verschelde. A Study of the gauge invariant, nonlocal mass operator Tr integer d**4 x F mu nu (D**2)**-1 F mu nu in Yang-Mills theories. *Phys. Rev. D*, 72:105016, 2005, hep-th/0510240.

[32] M. A. L. Capri, D. Dudal, J. A. Gracey, V. E. R. Lemes, R. F. Sobreiro, S. P. Sorella, and H. Verschelde. Quantum properties of a non-Abelian gauge invariant action with a mass parameter. *Phys. Rev. D*, 74:045008, 2006, hep-th/0605288.

[33] Jean-Loic Kneur. Variational quark mass expansion and the order parameters of chiral symmetry breaking. *Phys. Rev. D*, 57:2785–2805, 1998, hep-ph/9609265.

[34] P. M. Stevenson. Optimized perturbation theory. *Phys. Rev. D*, 23:2916–2944, Jun 1981.

6

Renormalization Group Optimized Perturbation Theory

In this chapter, we will discuss other resummation schemes, first the *optimized perturbation theory* (OPT), then we will introduce an extension incorporating renormalization group properties: *renormalization group optimized perturbation theory* (RGOPT), first in the $\lambda\phi^4$ model at finite temperature [1], then in cold and dense QCD [2]. Application of the OPT approach to the specific case of Hard Thermal Loops goes by the name of *Hard Thermal Loop perturbation theory* (HTLpt) and will be part of the last section of this chapter, including the first developments of RGOPT on HTLpt.

6.1 The need to reorganize the perturbative series

We already discussed in depth how the naive weak expansion breaks down at finite temperature and density. This is not the only issue of the perturbative series in a medium. It appears that the series is also very poorly convergent, specifically at finite T, and that higher order contributions are not so small with respect to lower orders, even when pushed to the highest perturbative order available. Furthermore with increasingly sizeable remnant scale dependence, at least specially at $T \neq 0$. Accordingly many efforts have been devoted in the past to overcome the generically observed issues of poor perturbation theory convergence. Apart from the most important case of QCD, the above mentioned behavior is generic for any thermal quantum field theory, thus, it seems desirable to have if possible a framework which would incorporate the same physics, namely quasi-particle degrees of freedom, in a more systematic way in order to improve the convergence of the series. Various approximations attempting to more efficiently resum thermal perturbative expansions have been developed and refined over the years, typically the optimized perturbation theory (OPT) [3; 4], sometimes called linear delta-expansion (LDE) [5], or also better known under the name of screened perturbation theory (SPT) [6; 7; 8; 9] in the thermal community. But also the non-perturbative renormalization group (NPRG)[10] approach or the two-particle irreducible (2PI) formalism [11; 12; 13]. The former one, OPT, being the subject of our focus.

6.1.1 Optimized perturbation theory

OPT is a reorganization of the weak-coupling expansion based on a variational approach. A physical quantity, typically, the pressure $\mathcal{P}$ in our context, is then expressed as the variational minimum of a thermodynamic potential $\mathcal{P}(T, \mu, g; m_i)$ [1] that depends on one or more variational mass parameters that are collectively denoted by m_i and a generic coupling g. Remark that adding a Gaussian mass term does not change the polynomial structure of the theory so that the process is compatible with the usual renormalization procedure. At least in theories where mass terms do not spoil gauge invariance, so it is not so simple for QCD. In the thermal field theory context, these variational mass parameters are the equivalent of the thermal mass presented earlier in Eqn.(5.7). The idea is to "add and subtract" such variational parameters, one being treated as an interaction term while the other modifies the free propagator. This can be conveniently generalized as the following modification :

$$\mathcal{P}(T, \mu, g, m_i) \to \mathcal{P}(T, \mu, \delta\, g, m_i\,(1-\delta)). \tag{6.1}$$

upon identifying $\delta = 1$, we recover the original massless interacting theory, while $\delta = 0$ is the non-interacting theory incorporating the massive quasi-particles degrees of freedom. The trick now is to perform a re-expansion in δ, with respect to both the coupling *and* the mass, at the same perturbative order than the original perturbative expression, and subsequently taking the limit $\delta \to 1$. If we were able to calculate the perturbative series at all order, this procedure would trivially remove the contribution from m to the perturbation series and leaves no differences with the original calculation. But, due to the specific truncation at finite orders of perturbative series, this leaves a remnant non-trivial dependence in m, that reshuffles the perturbative expansion. Notably, at leading order the OPT has the welcome property of exactly reproducing large-N results [14; 15] for simpler models with an O(N) symmetry. Since the full results (at all order) does not depend on such variational parameters, the best approximation at finite perturbative order is the one that minimizes the dependence on these non-physical parameters, the one where it is the less rapidly varying [3; 16]:

$$\frac{\partial \mathcal{P}(T, \mu, g, m_i)}{\partial m_i}\Big|_{m_i = \hat{m}_i} \equiv 0, \quad \forall\, m_i. \tag{6.2}$$

The application of this OPT procedure to the specific case of the HTL Lagrangian (HTLpt), see [17] for a review, as compared to perturbation theory, the NNLO HTLpt predictions in Refs.[18; 19; 20; 21] are very close to the lattice results for temperatures down to $T \simeq 2T_c$ (the critical temperature). Unfortunately, there is a serious issue, also plaguing standard thermal perturbation theory but not sensibly reduced in OPT: namely the sensitivity to the arbitrary renormalization scale is observed to substantially increase when higher orders are considered. Even a moderate scale variation of a factor 2 dramatically affects the pressure and related thermodynamical quantities by relative variations of order 1 or more. It appears that the lack of renormalization group (RG) invariance is more basically rooted within the HTLpt approach that definitely calls for further improvements.

[1] We will not distinguish these two functions in the following even though they are strictly speaking different.

6.1.2 Renormalization group optimized perturbation theory

More recently, OPT at vanishing temperatures and densities was extended to the so-called renormalization group optimized perturbation theory (RGOPT) [15; 22]. The basic novelty is that it restores perturbative RG invariance at all stages of calculations, in particular when fixing the variational mass parameter, by solving the (mass) optimization prescription as well as the RG equation. An important feature of the approach is that it also incorporates consistently the RG properties of the vacuum energy density defined in chapter 2 and reviewed for HTL EFT in chapter 5. At vanishing temperatures and densities, it has given precise first principle determinations [22] of the basic QCD scale ($\Lambda_{\overline{MS}}$) or related coupling α_s, and of the quark condensate [23; 24]. The RGOPT was extended at finite temperatures for the scalar $\lambda\phi^4$ model in [25; 26] and for the non-linear sigma model (NLSM) in [27], showing how it substantially reduces the generic scale dependence and convergence problem of thermal perturbation theories at increasing perturbative orders. More recently the RGOPT in the quark sector contribution to the QCD pressure was investigated at NLO, for finite densities and vanishing temperatures [28], and at finite temperature and density [29; 30], leading to drastic improvements with respect to both perturbative QCD and HTLpt, specially at nonzero temperature.

The heart of the method relies on three main modifications to the standard OPT. The first one is to incorporate consistently for a massive theory, the vacuum energy and its anomalous dimensions, necessary both for renormalization as well as for restoration of the perturbative RG invariance as explained in chapter 2. Secondly, one applies a *modified* delta expansion rather than the original one in Eqn.(6.1):

$$g \to \delta g \ , \ m_i \to m_i(1-\delta)^{a_i}. \tag{6.3}$$

Where a_i are at first arbitrary parameters, to be next determined by enforcing the delta-expansion to be consistent with RG invariance. Since the underlying goal is to reproduce the massless pressure, *after* the delta expansion $\delta \to 1$ is carried out, we impose the pressure to satisfy the reduced (massless) RG equation :

$$\left(M\frac{\partial}{\partial M} + \beta(g)\frac{\partial}{\partial g}\right)\mathcal{P} = 0. \tag{6.4}$$

This equation determines at leading order once and for all the values of the a_i coefficients with $a_i = \#\frac{\gamma_{0,i}}{b_0}$ [2]. Once the a_i are fixed, the RG equation at higher order, is not satisfied anymore, which gives alternative prescription, different from Eqn.(6.2), to determine variationally the parameters m_i of the theory, incorporating some higher order RG properties. If one considers alternatively the *full* RG equation, incorporating the anomalous mass dimension, this leads to three possible prescriptions (not all independent) that may be used to determine the parameters :

$$\begin{gathered}
\frac{\partial\mathcal{P}(T,\mu,g,m_i)}{\partial m_i}\Big|_{m_i=\hat{m}_i} \equiv 0 \\
\left(M\frac{\partial}{\partial M} + \beta(g)\frac{\partial}{\partial g}\right)\mathcal{P} = 0 \\
\left(M\frac{\partial}{\partial M} + \beta(g)\frac{\partial}{\partial g} + \sum_i m_i\,\gamma_{m,i}\frac{\partial}{\partial m_i}\right)\mathcal{P} = 0.
\end{gathered} \tag{6.5}$$

[2] Since this determination depends of the specific convention for the beta and gamma function, we will specify their precise values later

We speculate that if one could calculate to all orders the solutions of those different prescriptions, the solutions would presumably converge towards a unique, non-perturbatively dressed mass $\hat{m}$. As it happens [15] in the large-N limit of the O(N) Gross-Neveu model, where the original perturbative series is known to all orders.

Inherently to many variational methods beyond the lowest order, solutions to this equation, non-analytic in m_i, are often complex valued. While physical quantities of interest, in our context the pressure, are obviously real. This is admittedly a technical burden of such methods, but the occurrence of complex variational solutions has no deeper physical meaning. Rather, it may be viewed to some extent as an accident of the specific $\overline{\text{MS}}$ scheme in which the original perturbative coefficients were calculated, given that nonreal solutions are often expected upon exactly solving nonlinear equations. At the same time we wish to maintain these relations as exact as possible in order to capture RG resummation properties beyond perturbation theory. A crude escape could be simply to take the real part of the solutions, but that potentially loses some of the sought RG properties.

Having multiple perturbatively equivalent prescriptions becomes handy in the search of real valued solutions. Notably, since we are interested in thermodynamic quantities at different energy scales, it may be possible that on a specific subregion ($T, \mu \in [a, b]$ for generic a, b) of interest, one prescription gives real valued solutions that become complex elsewhere. One solution to circumvent this issue is to simply take the Debye screening mass, instead of a variationally determined parameter, as is indeed prescribed in HTLpt [19; 21] but by doing so, we loose some of the benefits of the method namely, the RG consistent construction. Another option is to proceed to a perturbative renormalization scheme change (RSC), provided that non-real solutions are not far away from being real. The formalism of RSC introduce at the end of chapter 2 will become particularly useful.

Having in mind that the all order perturbative expansion is renormalization scheme independent, and that only the partial sum is scheme dependent, we will use the freedom to change the unphysical scheme for another one whose slightly different coefficients might lead to recover real solutions.

Importantly, keeping $a_i = \gamma_{0,i}/b_0$ at higher orders further guarantees that the only acceptable solutions are those matching [22] the perturbative asymptotic freedom (AF) behavior for $g \to 0$ at $T = 0$. This simple but compelling criterion often selects a unique solution, even at five-loop order so far explored [24], in contrast with the related OPT/SPT approaches where using solely Eqn.(6.2) generates an increasing number of possible solutions at increasing orders.

6.1.3 Application at leading order in $\lambda\phi^4$ model

As a concrete example, let us investigate the application of the method at leading order for the specific case of the $\lambda\phi^4$ model. At leading order, the free energy (equivalently minus the pressure) including a mass term is :

$$\mathcal{F}_0 = \frac{1}{2}\sum\!\!\!\!\!\!\int_P \ln\left(\mathbf{P}^2 + m_0^2\right) = -\frac{1}{8(4\pi)^2} m_0^4 \left(\frac{2}{\varepsilon} + 3 + 2\ln\frac{M^2}{m_0^2}\right) - \frac{T^4}{2(4\pi)^2} J_0\left(\frac{m_0}{T}\right). \tag{6.6}$$

To restore the RG invariance and renormalize the UV divergence of Eqn.(6.6), we add the perturbatively determined vacuum energy:

$$\mathcal{E}_0(\lambda_0, m) = -\frac{m_0^4}{\lambda_0}\sum_{k\geq 0} s_k \lambda^k = -\frac{s_0\, m_0^4}{\lambda_0} - s_1\, m_0^4 + \mathcal{O}(\lambda_0). \tag{6.7}$$

Where,

$$s_0 = \frac{1}{2(b_0 - 4\gamma_0)} = 8\pi^2, \qquad s_1 = \frac{(b_1 - 4\gamma_1)}{8\gamma_0\,(b_0 - 4\gamma_0)} = -1 \tag{6.8}$$

Note that, the vacuum subtraction terms (s_n) are calculated with respect to :

$$M\frac{d\mathcal{E}(\lambda, m)}{dM} \equiv -M\frac{d}{dM}\left((4\pi)^2\mathcal{F}_0(\mathcal{E}\equiv 0)\right), \tag{6.9}$$

using the following definition for the beta and gamma functions:

$$\begin{aligned} \beta(\lambda) =& \frac{d\lambda}{d\ln M} = b_0\,\lambda^2 + b_1\lambda^3 + \ldots \\ \gamma_m(\lambda) =& \frac{d\ln m}{d\ln M} = \gamma_0\,\lambda + \gamma_1\,\lambda^2 + \ldots \end{aligned} \tag{6.10}$$

with relevant values at LO: $(4\pi)^2 b_0 = 3$, $(4\pi)^2\gamma_0 = 1/2$. Hence, the RG reduced equation defined in Eqn.(6.4) gives the universal RG coefficient :

$$a = \frac{\gamma_0}{b_0} = \frac{1}{6}. \tag{6.11}$$

After performing the modified delta expansion $\mathcal{F}(m^2 \to m^2\,(1-\delta)^{2a}\,;\quad \lambda \to \delta\lambda)$, only the s_0 term is non-trivially affected which yields, after taking the limit $\delta \to 1$:

$$(4\pi)^2\mathcal{F}_0^{\delta^0} = m^4\left[-\frac{s_0}{\lambda}(1 - 4\frac{\gamma_0}{b_0}) - \left(\frac{3}{8} + \frac{1}{4}\ln\frac{M^2}{m^2}\right)\right] - \frac{T^4}{2}J_0(\frac{m}{T}). \tag{6.12}$$

The standard (dimensionless) thermal integrals appearing in Eq.(6.12) and below are given by

$$J_n(x) = 4\frac{\Gamma[1/2]}{\Gamma[5/2-n]}\int_0^\infty dt \frac{t^{4-2n}}{\sqrt{t^2+x^2}}\,\frac{1}{e^{\sqrt{t^2+x^2}} - 1}\,, \tag{6.13}$$

where $t = p/T$ and $x = m/T$. The other relevant integrals can be easily related by employing derivatives such as

$$J_{n+1}(x) = -\frac{1}{2x}\frac{\partial}{\partial x}J_n(x)\,. \tag{6.14}$$

Also, a high-T expansion,

$$J_0(x) \simeq \frac{16}{45}\pi^4 - 4\frac{\pi^2}{3}x^2 + 8\frac{\pi}{3}x^3 + x^4\left[\ln\left(\frac{x}{4\pi}\right) + \gamma_E - \frac{3}{4}\right] + \mathcal{O}(x^6)\,, \tag{6.15}$$

is often useful as a rather good approximation as long as $x \lesssim 1$, i.e., $m \ll T$.

At this leading order, the reduced RG equation is satisfied exactly, while the mass optimization Eq.(6.2) determines a nontrivial dressed thermal mass as follows. One can conveniently express results in terms of the one-loop renormalized self-energy including all the relevant T-dependence, Σ_R, reading explicitly

$$\Sigma_R = \gamma_0\lambda\left[m^2\left(\ln\frac{m^2}{M^2} - 1\right) + T^2 J_1\left(\frac{m}{T}\right)\right]. \tag{6.16}$$

Since

$$T\frac{\partial}{\partial m^2}\sum\!\!\!\!\!\!\int \ln\left(\omega_n^2 + \omega_{\mathbf{p}}^2\right) = 2\frac{\Sigma_R}{\lambda}, \tag{6.17}$$

the exact solution of the OPT Eq.(6.2) gives the mass-gap equation:

$$\hat{m}^2 = (4\pi)^2\, b_0\, \Sigma_R(\hat{m}^2), \tag{6.18}$$

which at this leading nontrivial order is exactly (one-loop) RG-invariant, being only dependent on b_0. To illustrate more transparently the latter property, it is convenient to use the above high-T expansion $m/T \equiv x \ll 1$ of $J_n(x)$ [3]. In this case the OPT Eq. (6.2) is a simple quadratic equation for x, with the unique physical ($x > 0$) solution:

$$\hat{x} = \frac{\hat{m}^{(1)}}{T} = \pi\frac{\sqrt{1 + \frac{2}{3}\left(\frac{1}{b_0\lambda} + L_T\right)} - 1}{\frac{1}{b_0\lambda} + L_T} \simeq \pi\, b_0\lambda + \mathcal{O}(\lambda^2) \tag{6.19}$$

with $L_T \equiv \ln[M\, e^{\gamma_E}/(4\pi T)]$. The corresponding one-loop RGOPT pressure reads

$$\frac{P^{(1)}}{P_0} = 1 - \frac{15}{4\pi^2}\hat{x}^2 + \frac{15}{2\pi^3}\hat{x}^3 + \frac{45}{16\pi^4}\left(\frac{1}{b_0\lambda} + L_T\right)\hat{x}^4 + \mathcal{O}(\hat{x}^6), \tag{6.20}$$

where $P_0 = (\pi^2/90)T^4$ is the ideal gas pressure. Eqs. (6.18)-(6.20) involve clearly an all order dependence in λ, and are *exactly* RG-invariant, upon using for $\lambda \equiv \lambda(M)$ the "exact" (one-loop) running:

$$\frac{1}{\lambda(M)} = \frac{1}{\lambda(M_0)} - b_0 \ln\frac{M}{M_0} \tag{6.21}$$

since $1/(b_0\lambda(M)) + L_T$ is M-independent. Accordingly Eqs. (6.19) and (6.20) only depend on the single parameter $b_0\lambda(M_0)$, where M_0 is some reference scale, typically $M_0 = 2\pi T$.

Eq. (6.20), perturbatively re-expanded, gives for the first few orders

$$P^{(1)}/P_0 \simeq 1 - 5\alpha/4 + 5\sqrt{6}\alpha^{3/2}/3 + 5(L_T - 6)\alpha^2/4 + \mathcal{O}(\alpha^{5/2}) \tag{6.22}$$

where $\alpha \equiv b_0\lambda$. Note that Eq.(6.22) contains the nonanalytic term $\lambda^{3/2}$, originating from the

[3] At one-loop order this approximation is actually valid at the 0.1% level even for $x1$, sufficient for our purpose since the RGOPT one-loop solution $\hat{m}/T$ happens to always lies in this range.

bosonic zero mode resummation, here readily obtained from RG properties. Expanding at higher orders Eq.(6.19) it is easily seen that it entails nonanalytic terms $\lambda^{(2p+1)/2}, p \geq 1$ at all orders. It is worth stressing that Eqs. (6.18)-(6.20) correctly reproduce at all orders the $O(N)$ scalar model large N-results (*e.g.* Eq. (5.7) of [31]), as can be checked upon identifying the correct large-N $b_0 = 1/(16\pi^2)$ value [31]. Accordingly, at one-loop order, although RGOPT essentially relies on the very first one-loop graph of Fig.2.29, augmented by the optimized RG construction as above described, it happens to correctly resum the whole set of 'foam' graphs as illustrated in Fig.6.1.

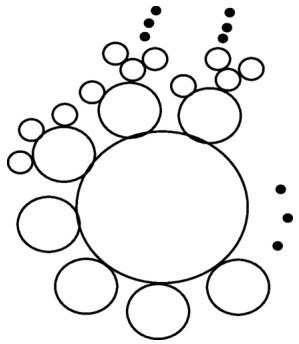

Figure 6.1: The graphs being resummed at first nontrival RGOPT order.

6.2 Renormalization group optimized $\lambda\phi^4$ pressure at next-to-next-to-leading order

This part reports on the original work [1] pursued by the author. We refer to the article for further details and only quote the results.

6.2.1 NNLO massive free energy

The contribution up to three-loop order to the free energy comes from the set of graphs in Fig (6.2) and read

$$\begin{aligned}\mathcal{F}_0^{3l} = -\frac{\lambda_0^2}{48}\Bigg[3\left(\sum\!\!\!\!\!\!\int_p \frac{1}{\mathbf{p}^2+m_0^2}\right)^2 \sum\!\!\!\!\!\!\int_q \frac{1}{(\mathbf{q}^2+m_0^2)^2} \\ + \sum\!\!\!\!\!\!\int_{pqr} \frac{1}{(\mathbf{p}^2+m_0^2)(\mathbf{q}^2+m_0^2)(\mathbf{r}^2+m_0^2)((\mathbf{p}+\mathbf{q}+\mathbf{r})^2+m_0^2)}\Bigg] \\ + \mathcal{F}_0^{3l,\mathrm{ct}},\end{aligned} \tag{6.23}$$

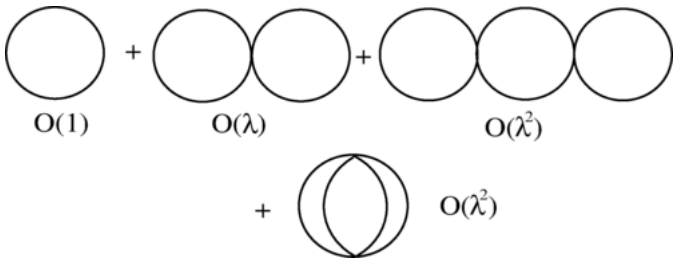

Figure 6.2: Free energy diagrams up to NNLO in $\lambda\phi^4$ model

With the contribution at NLO being [8] (using $L = \frac{M^2}{m^2}$) :

$$(4\pi)^2 \mathcal{F}^{NLO} = \mathcal{E}_0 - \frac{1}{8} m^4 (3 + 2L) - \frac{1}{2} T^4 J_0(\frac{m}{T}) + \frac{1}{8} \frac{\lambda}{16\pi^2} \left[(L+1)m^2 - T^2 J_1(\frac{m}{T}) \right]^2 . \quad (6.24)$$

The NNLO contribution involves the additional genuine three-loop second integral in (6.23), first calculated in [32]. After algebra, the complete three-loop contribution can be expressed as[8].

$$\begin{aligned} F_{3l} = -\frac{1}{48} (\frac{\lambda}{16\pi^2})^2 \Big[& m^4 \left(5L^3 + 17L^2 + 41/2 - 23 - 23/12\pi^2 + 2\zeta(3) + c_0 + 3(L+1)^2 J_2(\frac{m}{T}) \right) \\ & - m^2 T^2 J_1(\frac{m}{T}) \left(12L^2 + 28L - 12 - \pi^2 - 4c_1 + 6(L+1) J_2(\frac{m}{T}) \right) \\ & + T^4 \left(3(3L + 4 + J_2(\frac{m}{T})) J_1^2(\frac{m}{T}) + 6K_2(\frac{m}{T}) + 4K_3(\frac{m}{T}) \right) \Big] \end{aligned} \quad (6.25)$$

where

$$c_0 = 275/12 + 23/2\zeta(2) - 2\zeta(3); \quad c_1 = -59/8 - 3/2\zeta(2), \quad (6.26)$$

and it involves two extra irreducible two-loop $K_2(m/T)$ and three-loop $K_3(m/T)$ integrals, given explicitly in ref.[32], reproduced for self-containedness in Appendix D.

If not including the RG invariance restoring subtractions in Eq.(6.7), note that the lack of RG invariance from unmatched leading $m^4 \ln M$ terms remains largely screened at one- and two-loop orders of the thermal expansion for sufficiently small coupling, since perturbatively $m^4 \sim \lambda^2$. This explains why the remnant scale dependence of SPT remains nevertheless quite moderate at NLO. Conversely it partly explains why a very sizeable scale dependence plainly resurfaces at three-loop λ^2 order in SPT[8]. In contrast the RGOPT scale dependence is expected to further improve at higher orders: being built on perturbative RG invariance of the free energy at order $m^4 \lambda^k$ for *arbitrary* m, the mass gap exhibits its dominant remnant scale dependence as $\hat{m}^2 \sim \lambda T^2 (1 + \cdots + \mathcal{O}(\lambda^{k+1} \ln M))$, thus the dominant scale dependence in the free energy, coming from the leading term $-s_0 \, m^4/\lambda$, is expected to appear first only at $\mathcal{O}(\lambda^{k+1})$. However, this formally expected trend may be partly spoiled, first by large perturbative coefficients (generically growing at higher orders), or by the well-known thermal PT issues due to infrared divergent bosonic zero modes. It is thus important to investigate more explicitly the outcome of our construction at NNLO, where standard thermal PT starts to badly behave, to delineate the RGOPT scale dependence improvement that can be actually obtained. Concern-

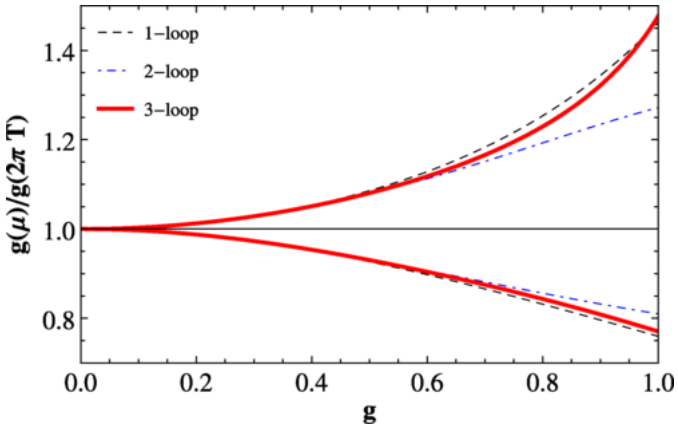

Figure 6.3: Relative scale dependence at successive orders of the running coupling in the ϕ^4 model, with $g \equiv \sqrt{\lambda/24}$ and $\pi T \leq \mu \leq 4\pi T$ at one, two- and three-loop orders.

ing the ϕ^4 model moreover, the peculiar sign alternating beta-function coefficients b_i from one- to three-loop orders imply that considering the running coupling alone, its three-loop order has a comparatively worse scale dependence than the two-loop order, as is illustrated in Fig.6.3. This feature tends to partly counteract the benefits of our RG-improved construction, when comparing three-loop with two-loop order. [4]

Applying the variational modification from Eq.(6.3)(6.11) to the complete thee-loop free energy, sum of Eq.(6.24) and Eq.(6.25), expanded consistently now to order δ^2, and taking $\delta \to 1$, gives after algebra :

$$\begin{aligned}(4\pi)^2\mathcal{F}_0^{\delta^2} = \mathcal{E}_0^{\delta^2} - \frac{m^4}{8}\left(3 + 2\,L + 8(\frac{\gamma_0}{b_0})^2(L + J_2)\right) - \frac{T^4}{2}J_0 \\ + \frac{m^2\Sigma_R^2}{\gamma_0\lambda}\frac{\gamma_0}{b_0}\left(\frac{\gamma_0}{b_0} - \frac{3}{2}\right) + \frac{m^2}{32\pi^2 b_0}\Sigma_R(L + J_2) \\ + \frac{\Sigma_R^2}{128\pi^2\gamma_0\lambda} + F_{3l}\end{aligned} \tag{6.27}$$

where we again conveniently expressed results in term of the one-loop Σ_R defined in (6.16), and with:

$$\mathcal{E}_0^{\delta^2} = -m^4\left(\frac{14}{81}\frac{s_0}{\lambda} + \frac{2}{9}s_1 + \frac{1}{3}s_2\lambda + s_3\lambda^2\right), \tag{6.28}$$

and the three-loop order contribution, designated by F_{3l} in Eq.(6.27), is already given in the original expression (6.25), this term being not affected at δ^2 order.

The explicit expressions at NNLO for the RG and OPT Eqs.(6.2), (6.4) can be obtained easily from (6.27) (we refrain to give their explicit form, being quite involved and not particularly telling). At this stage without examining further constraints one may a priori use any of the three possible (but not independent) prescriptions for the NNLO dressed optimized mass $\bar{m}(\lambda, T)$: the OPT Eq.(6.2), or the (massless) RG Eq.(6.4), or the full RG equation with the anomalous mass dimension. One may also exploit the freedom to incorporate the highest order subtraction term s_3 or not, the latter being formally a three-loop contribution, but depending on four-loop order RG coefficients, and not necessary for perturbative NNLO RG invariance. The latter flexibility happens to give a relatively simple way to circumvent the annoyance of possibly non-real NNLO solutions, that appear only at relatively large couplings in the $\lambda\phi^4$ model. The outcome is that, in order to maximize the range of coupling g and scale M where real solutions are obtained, it is appropriate to take simply $s_3 = 0$ if using the OPT Eq.(6.2), and $s_3 \neq 0$ when using the RG (6.4). On the other hand at NNLO the full RG gives no real solutions for the relevant case of $M = 4\pi T$, for a large coupling range.

Fig. 6.4 illustrates our two different prescriptions thus retained at NNLO, namely the OPT (with $s_3 = 0$) and RG (with $s_3 \neq 0$). As seen, despite giving quite different functions of the coupling, they have very similar and very moderate scale dependence. Similarly to NLO the RG solution is generically giving a slightly better scale dependence than the OPT one, since the former embeds more directly the perturbative RG properties.

Fig. 6.5 illustrates the corresponding pressures obtained from the two alternative OPT and RG mass prescriptions [5]. As one can see, despite the quite different $\overline{m}$ in Fig. 6.4 the resulting

[4] We mention that in QCD the analogous behavior is expected to be better, since the first three beta function coefficients have the same sign.

[5] At NNLO we use the exact expressions of all thermal integrals: in particular the high-T approximations of the two-loop $K_2(x)$ and three-loop $K_3(x)$ integrals are not a good approximation.

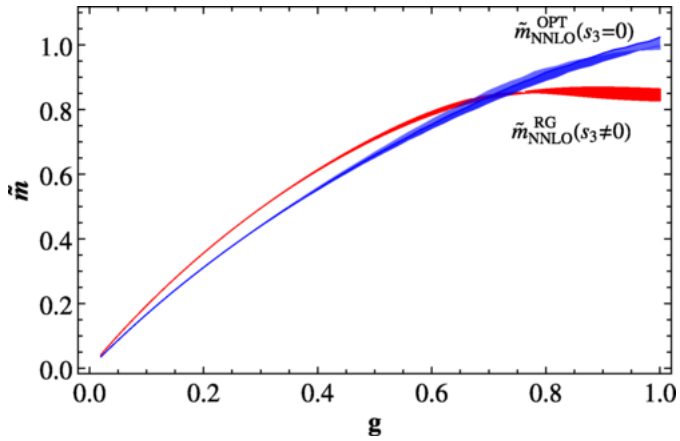

Figure 6.4: NNLO (three-loops) $\overline{m}$ from the OPT Eq.(with $s_3 = 0$) and RG Eq (with $s_3 \neq 0$) as a function of rescaled reference coupling g, with scale dependence $\pi T \leq \mu \leq 4\pi T$.

OPT and RG pressures are very close and similar in shape, and have very comparable and very moderate scale dependence. The latter feature will be better appreciated when being compared with NNLO PT or SPT below.

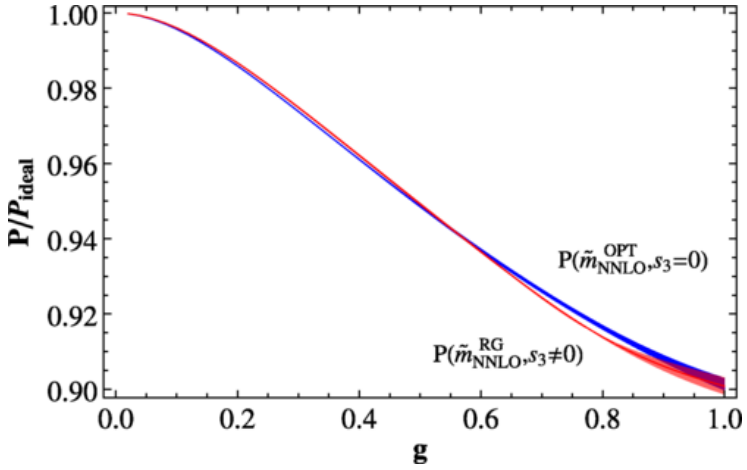

Figure 6.5: Comparison of NNLO pressure P/P_{ideal} for the $\overline{m}$ OPT and RG prescriptions (with $s_3 = 0$ and $s_3 \neq 0$ respectively), as a function of $g \equiv \sqrt{\lambda/24}$, with $\pi T \leq \mu \leq 4\pi T$

Finally, we illustrate our main results at successive LO, NLO, and NNLO in Fig. 6.6, compared with both PT and SPT. The NNLO PT, namely with successive terms up to $\mathcal{O}(\lambda^2)$, has a substantially larger remnant scale dependence than the $\mathcal{O}(\lambda^{3/2})$ PT in Fig. 6.5. Concerning the SPT at NNLO we only show the results from using the same prescription as in [8] namely,

$$m^2_{SPT} = \Sigma_R. \tag{6.29}$$

In contrast one can see that the RGOPT pressure is extremely stable from LO to NLO and NNLO, and has a very moderate remnant scale dependence. Actually, the improvement from NLO to NNLO is quite moderate, that we understand as the counter effect from the worsening NLO running coupling as above explained. At any rate it appears drastically improved as compared to PT and SPT.

Overall, although ϕ^4 model is much simpler than QCD, it has a simpler IR behavior, calling for resummation. Our RGOPT results here give us some reasonable hint that RGOPT applied to thermal QCD, within appropriate description of thermally dressed gluon mass, might give similarly improved scale dependence at higher orders, in contrast with the HTLpt approach.

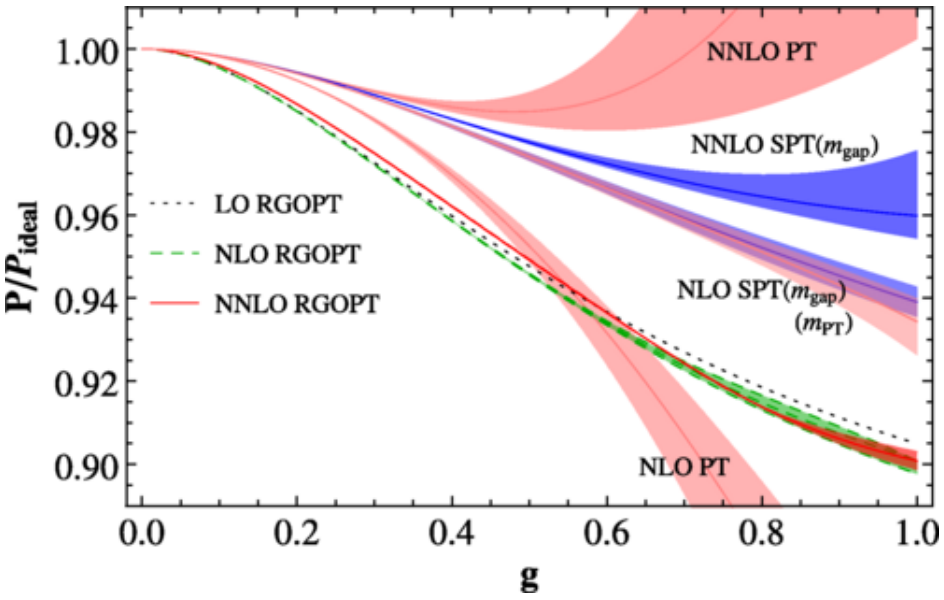

Figure 6.6: RGOPT pressure at successive LO,NLO,NNLO orders versus NLO,NNLO PT and NLO,NNLO SPT pressures, with $\pi T \leq \mu \leq 4\pi T$, ($g \equiv \sqrt{\lambda/24}$).

6.3 Review of LO and NLO in RGOPT Cold & Dense QCD

Let us now switch to the RGOPT construction applied to complete QCD, restricted here to the cold and dense regime. The relevant Feynman diagrams at NNLO for cold and dense QCD are:

$\mathcal{P}_{\rm QCD} =$ 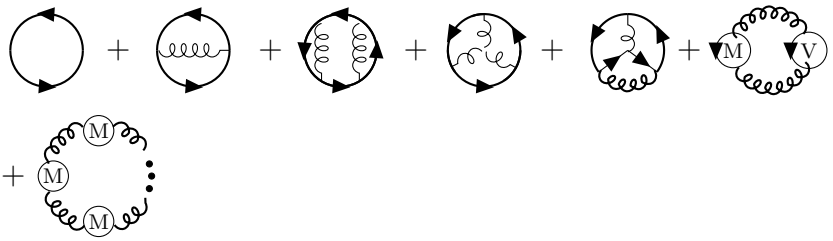

(6.30)

The convention for the renormalization group functions at hand are:

$$\beta(g) = -2b_0 g^2 - 2b_1 g^3 + \mathcal{O}(g^4) \tag{6.31}$$

$$\gamma_{m,q}(g) = \gamma_{0,q} g + \gamma_{1,q} g^2 + \mathcal{O}(g^3) \tag{6.32}$$

$$\gamma_{m_g,g}(g) = \gamma_{0,g} g + \gamma_{1,g} g^2 + \mathcal{O}(g^3) \tag{6.33}$$

which gives, upon solving the RG reduced equation in (6.4), the value of the coefficient:

$$a_q = \frac{\gamma_0}{2b_0} = \frac{4}{9}. \tag{6.34}$$

Before going to our work at NNLO, we first review the RGOPT results that were obtained[28] considering three massless flavors of quarks, up to NLO order-g (defining for convenience in this section $g = 4\pi\alpha_S$), corresponding to the first two graph on Figure 6.30, in the limit of vanishing temperatures and finite baryon densities. With the genuine mass of the quarks being zero, we take $\mu_s = \mu_u = \mu_d$, as we will review in the next chapter upon considering beta equilibrium in neutron stars. At this order, there is still no gluons in the medium as they formally enter at the NNLO through the Ring diagrams. This simplifies drastically the approach as we do not have to use HTLpt yet to address a medium-dressed mass term for the gluons, i.e at NLO the gluons can still be considered massless. The expression of the pressure for the quark sector is given in appendix A up to NNLO. At leading order, the RG equation being already used for fixing $a_q = \gamma_0^q/(2b_0)$, we solve $\tilde{m}_{LO}$ using equation 6.2 applied on 37, after the delta expansion of Eqn.(6.3). For illustration, we give the LO mass gap that was obtained in [28]:

$$\tilde{m}_{LO}^2 = \mu^2 \left(\frac{\sqrt{1 + 4c\left(\tilde{m}_{LO}, \mu, g\right)} - 1}{2c\left(\tilde{m}_{LO}, \mu, g\right)} \right). \tag{6.35}$$

With:

$$c\left(\tilde{m}_{LO}, \mu, g\right) = \left(\frac{1}{2b_0 g} - \frac{1}{2} + L_\mu \right)^2 \quad , \quad L_\mu = \ln\left(\frac{\mu + p_F}{M} \right) \quad , \quad p_F = \sqrt{\mu^2 - m^2} \tag{6.36}$$

Applying the procedure (6.3) to perturbative expression at NLO 39, the following expression for the RGOPT pressure for a single flavor is obtained:

$$\begin{aligned} P_f^\delta(m,\mu) =& Nc\frac{m^4}{(4\pi)^2 b_0 g} + \frac{N_c}{12\pi^2}\left[\mu p_F\left(\mu^2 - \frac{5}{2}m^2\right) + \frac{3}{2}m^4\left(L_\mu - \frac{3}{4}\right)\right] - N_c\frac{m^4}{(4\pi)^2}\left(\frac{\gamma_0}{b_0}\right)\left(\frac{1}{b_0 g}\right) \\ &+ m^4\left(2\frac{\gamma_0}{b_0} - 1\right)s_1 + N_c\frac{m^2}{8\pi^2}\left(\frac{\gamma_0}{b_0}\right)^2(1 - 2L_\mu) + 2\mu\, p_F] - \frac{g\, d_A}{4(2\pi)^4}\Big[m^4\left(\frac{1}{4} - 4\,L_\mu + 3L_\mu^2\right) \\ &+ \mu^2(\mu^2 + m^2) + m^2\mu\, p_F(4 - 6L_\mu)\Big] \end{aligned} \tag{6.37}$$

Where $d_A = N_c^2 - 1$ and $N_c = 3$. Already at this order [28], it has been found that no real solution existed on the full domain of interest so that a Renormalization Scheme Change (RSC) was needed. Invoking the invariance under RSC of the observable, we are free to slightly change the scheme, to a one close to $\overline{\text{MS}}$, such that a comparison remains relevant but modifying the coefficient of the RG equation to possibly recover real solutions. Practically, it consist of applying the RSC before the delta modified expansion:

$$m \to m\left(1 + B_2\, g^2\right) \tag{6.38}$$

Where B_2 is at first an arbitrary variationnal parameter. Now we have to solve $\{\tilde{m}, \tilde{B}_2\}$ simultaneously. In order to fix B_2, one needs, however, to use a definite prescription. Following[28], one notes that the closest real solution arises when the two independent RG and OPT equations intersect first, namely hen their respective tangent vectors are collinear. The latter easily translates into a vanishing determinant, the f_{RSC} equation:

$$f_{RSC} = \frac{\partial f_{RG}}{\partial g}\frac{\partial f_{OPT}}{\partial m} - \frac{f_{RG}}{\partial m}\frac{\partial f_{OPT}}{\partial g} \equiv 0 \tag{6.39}$$

Since the latter also depends non-trivially on B_2, one solves it in conjunction with the RG equation for $(\tilde{B}_2, \tilde{m})$. It can be checked a posteriori that $\tilde{B}_2 g^2$, driving the RSC, represents a reasonably perturbative deviation from the original $\overline{\text{MS}}$ scheme.

6.4 RGOPT pressure at next-to-next-to-leading order

6.4.1 RG resummed quarks and perturbative gluons

Now pursuing on at NNLO, we have to take into account the new three loop diagrams in Eqn.(6.30). As already explained, we will first study the gluons only perturbatively, using the result for the ring diagram Eqn.[33]. We apply the procedure in Eqn.(6.3) to the quark sector of Eqn.(36) where the ring diagram, represented in Fig (6.30), takes the value in Eqn.(42). Upon using the PMS prescription Eqn.(6.2) or the reduced RG equation in Eqn.(6.4) to determine $\tilde{m}$ we found no real solutions in the full domain of interest for $\mu \in 0.5, 2.5$ GeV but only in a subregion $\mu \in 1.0, 2.5$GeV for the RG equation. It is actually a double root at $\mu = 1$ GeV being complex for values of μ below one GeV, and two distinct real solutions for values above. It then motivated us to introduce again a RSC in order to obtain real solutions on the full domain. To be consistent at NNLO, we modify the scheme only at order δ^2:

$$m \to m\left(1 + B_3\, g^3\right) \tag{6.40}$$

Due to the g^3 term, this modification enters solely through the term $-m^4 s_0/g$, producing an extra contribution to the pressure, $\sim -4m^4 s_0 B_3 g^2$. By construction B_3 is also a variationnal parameter, and its solution will encode non-trivial coupling dependence: $B_3 \to \tilde{B}_3(g)$. Similarly to NLO, we can recover a real solution by requiring the condition above, Eq.(6.39), to be satisfied, now solved for $(\tilde{B}_3, \tilde{m})$. We chose to use the three loop order running coupling recalled in appendix A. Actually, another conceptually simpler way to recover a real $\tilde{m}$ solution is to truncate the RG equation to lower orders, noting that the higher order RG terms are strictly beyond the actual (NNLO) perturbative pressure expansion $\sim g^2$. In this way, one certainly loses some effects from higher RG order content, but at the benefit of a much simpler prescription as compared to Eq. (6.39). Moreover, it turns out that the two different prescriptions actually give very similar $\tilde{m}$: this is illustrated in Fig. 6.7. Moreover, quite remarkably we notice that both solutions tend asymptotically for sufficently large μ towards the standard (LO) Debye screening mass:

$$m_{Debye}^2 = \frac{g}{6\pi^2}\mu^2, \tag{6.41}$$

as illustrated in Fig.(6.8). Next, in Fig.6.8 we illustrate the scale dependence of the RG solution as compared to the one of the perturbative Debye mass, Eq.(6.41). Already at this stage, as it was expected, the RG dependence seems to have significantly dropped going from a purely perturbative Debye mass to the variational RG-determined mass. Accordingly, the pressure is expected to exhibit reduced scale dependence upon using the RG determined mass. It is precisely the case as can be observed in figure 6.9. However, the RGOPT pressure tends to be lower than the NNLO pressure for a given μ, which is due to relatively large $\tilde{m}_{RG}$, see Fig. 6.7. Alternatively, since the RG variational mass tends asymptotically to m_{Debye}, we could use the latter as another possible prescription: this is illustrated in Fig.6.10, where one can see that the resulting pressure is closer to the standard NNLO one, but at the price of not so much improved scale dependence. Finally, it is worth to combine our RGOPT results in the quark sector with the recently derived all order resummed HTL soft logarithmic dependence in the pure glue sector[34], that are discussed in chapter 5. More explicitly, we add to the NNLO

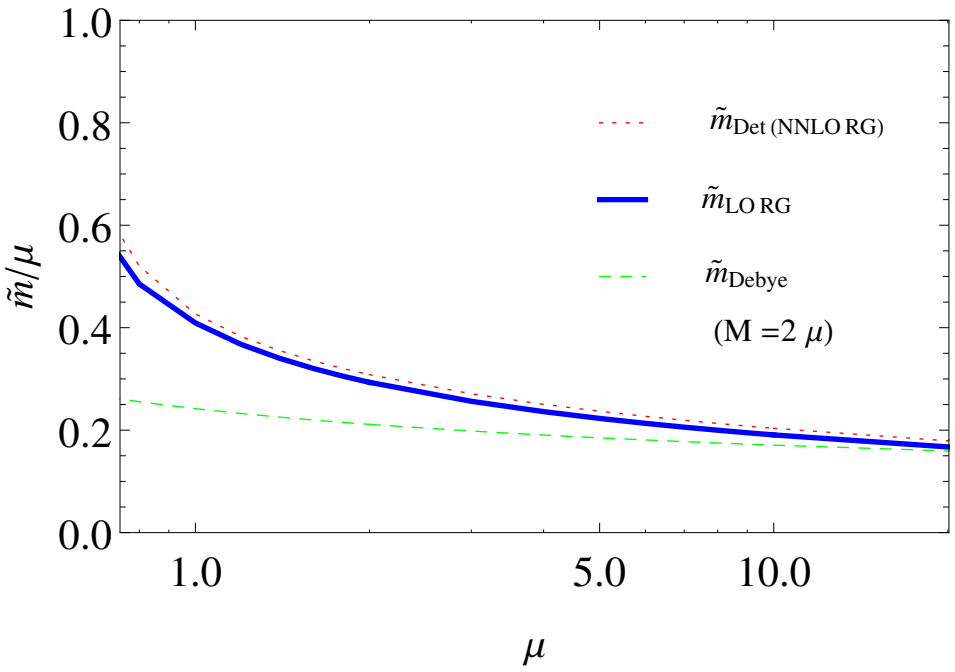

Figure 6.7: Solution to the RG equation at NNLO, for the central scale $M = 2\mu$, from Eq. (6.39) or from LO truncated RG (black, plain), compared to the standard LO Debye quark mass (purple, dotted).

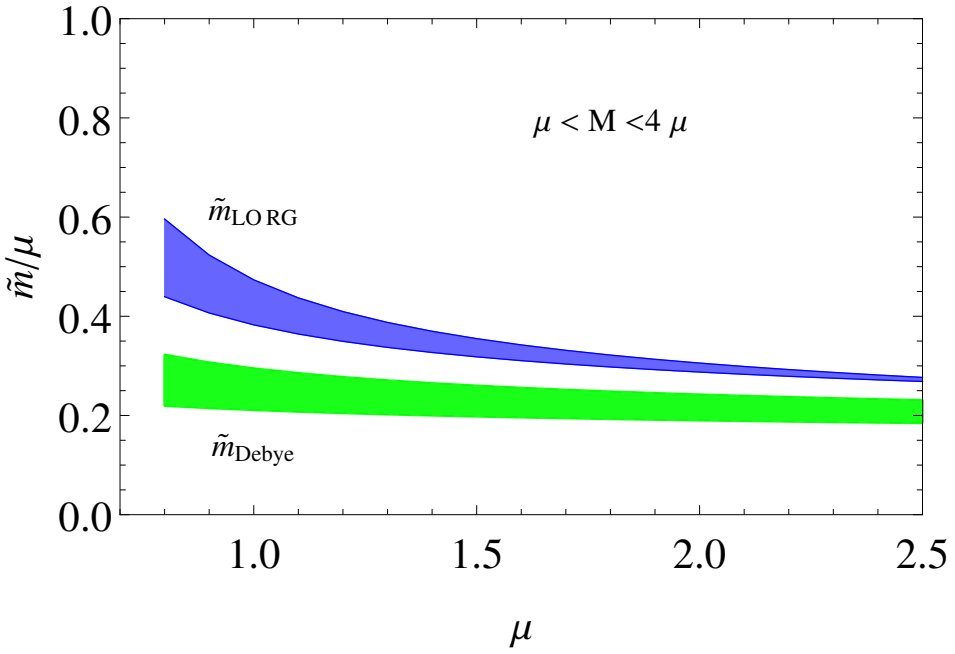

Figure 6.8: Remnant scale dependence of the RG-determined mass $\tilde{m}_R G(M)$ for $M \in \{\mu, 4\mu\}$ as compared with the LO Debye mass.

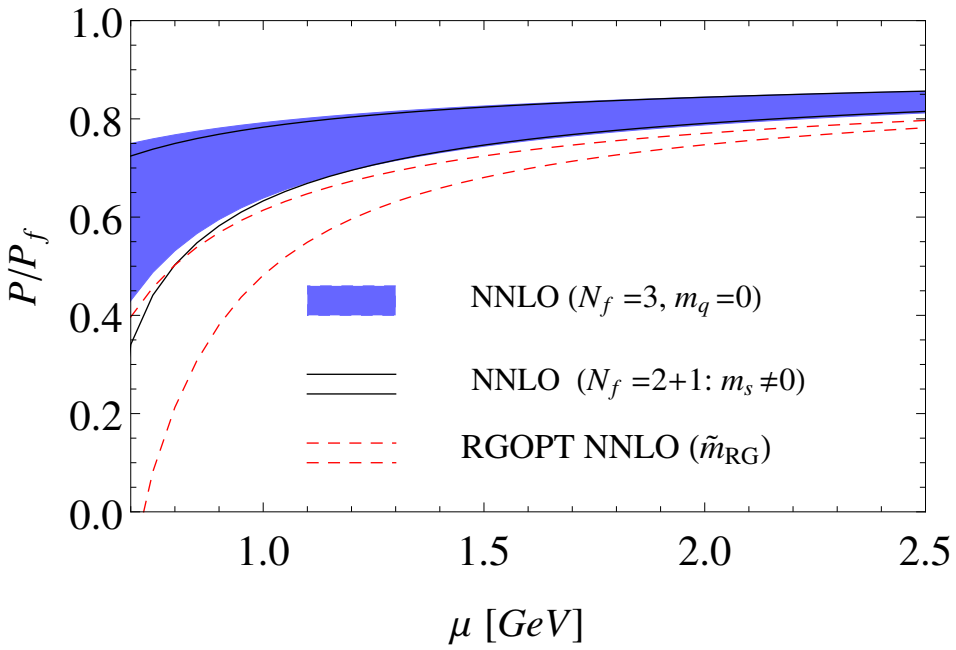

Figure 6.9: RGOPT pressure compared to NNLO pQCD pressure (massless and massive quarks as indicated) for three different scales $M = X\ 2\mu$ with $X \in \{\frac{1}{2}, 1, 2\}$

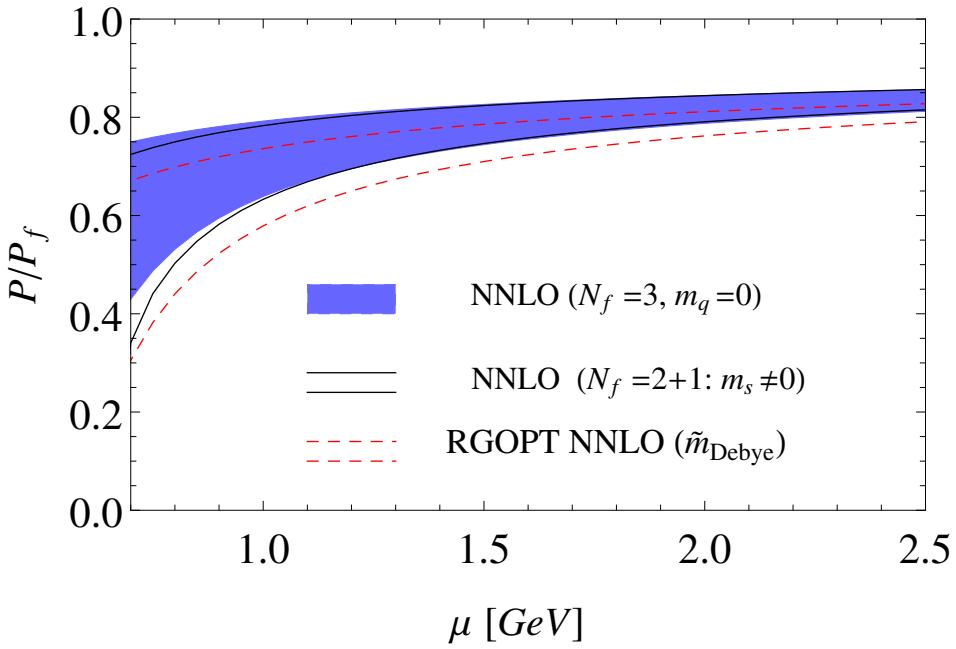

Figure 6.10: RGOPT pressure using m_{Debye} compared to NNLO pQCD pressure (massless and massive quarks as indicated) for three different scales $M = X\ 2\mu$ with $X \in \{\frac{1}{2}, 1, 2\}$

massive quark expression the expression for higher order LL, NLL given in Eqn.(5.66). This is illustrated in Fig.6.11 and Fig.6.12 respectively, where a visible scale dependence improvement is obtained in addition from the gluon resummed sector.

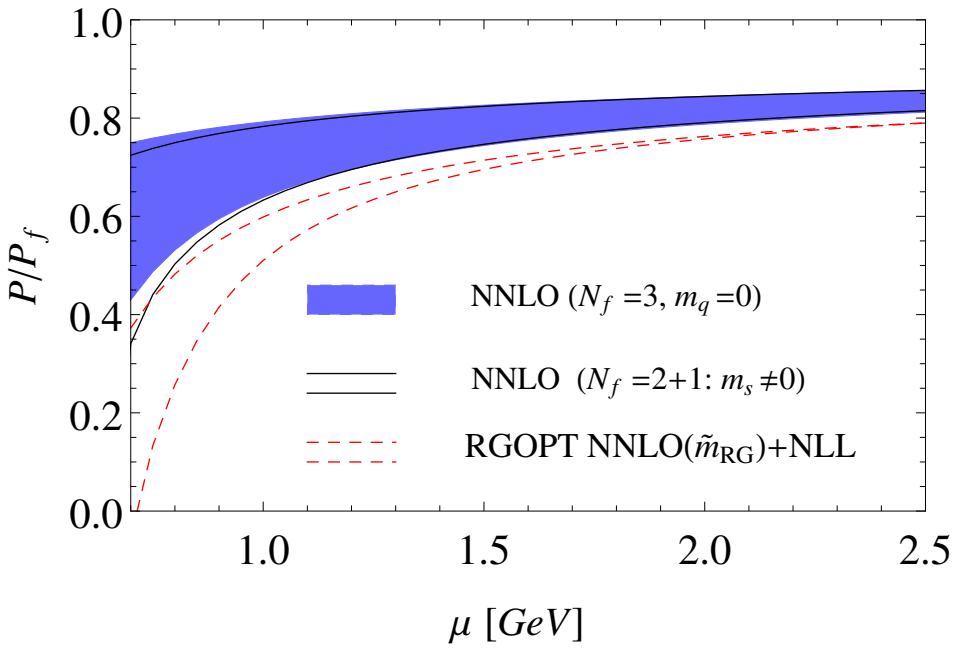

Figure 6.11: RGOPT pressure using $\tilde{m}_{RG}$ and adding NLL-resummed HTL glue pressure, compared to NNLO pQCD pressure (massless and massive quarks as indicated) for three different scales $M = X\ 2\mu$ with $X \in \{\frac{1}{2}, 1, 2\}$

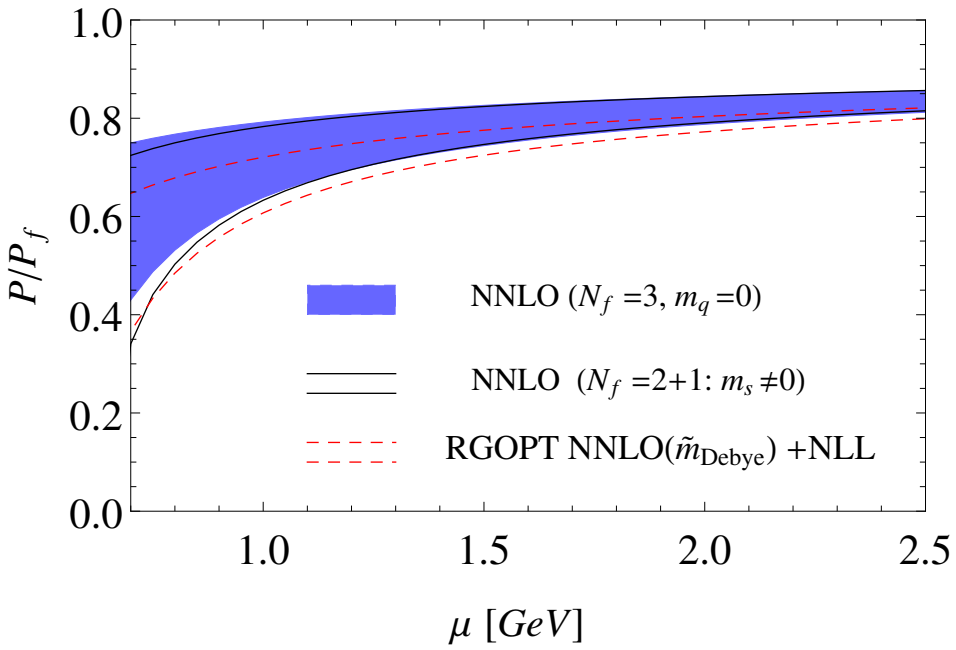

Figure 6.12: RGOPT pressure using m_{Debye} and adding NLL-resummed HTL glue pressure, compared to NNLO pQCD pressure (massless and massive quarks as indicated) for three different scales $M = X\ 2\mu$ with $X \in \{\frac{1}{2}, 1, 2\}$

This closes our analysis on the renormalization group improvement of the naive quark sector (not HTL) with sound result displaying good improvement with respect to the NNLO state-of-the-art. Notably, the result for the pressure obtained seems to drop towards zero slightly less faster than NLL thus suggesting interesting results once the equation of state will be considered. For that matter, see chapter 7.

6.5 HTLpt framework for gluons in cold and dense QCD

Having explored the RGOPT approach to the quark sector, we will focus now on the gluon sector and the applicability of the renormalization group improved HTLpt approach. Namely, we will consider massless quarks in interactions with the HTL resummed gluon propagator. At LO and NLO, the pressure is given by the set of diagrams given in Eqn.(6.42) :

$\mathcal{P}_{\rm QCD} =$ 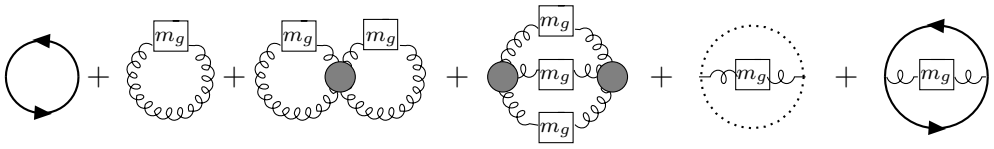 (6.42)

We already calculated in chapter 5 the subtraction coefficient s_0^g and s_1^g for the gluon so we can readily incorporate them in the picture. Now, what differs from the HTL effective field theory picture of the last chapter, is that we do not need a matching procedure anymore. The delta expansion will ensure that we will consistently address the degrees of freedom of the massless pressure and so the vacuum energy is not spurious anymore. Consequently, that means that we have to consider its renormalization, a point that we omitted in the last chapter since it essentially cancelled in the matching procedure. Following the general steps we introduce in section 6.1.1 and 6.1.2, we start with the mass renormalization for the gluons, the coupling renormalization, which enters only at NNLO so not needed here, then after this multiplicative renormalization we proceed to the additive multiplication of the vacuum energy. Details on the notations and the renormalization of the vacuum energy operator can be found in chapter 6 and in [34].

Following previous definitions of the gluon gamma function and beta function, we can determine via the RG reduced equation the coefficient a^g for the gluons which reads:

$$a^g = \frac{\gamma_0^g}{2b_0}. \tag{6.43}$$

Here, b_0 stands for the complete LO beta function coefficient while γ_0^g is no longer equals to b_0^g since we have now introduced the quarks in the picture, but rather $\gamma_0^g = b_0$. Therefore, we have the trivial result for the gluon sector:

$$a^g = \frac{1}{2}. \tag{6.44}$$

Meaning that the naive "add and subtract" tricks as was used in HTLpt for simplicity, appears in retrospect to be RG-consistent for the gluon sector. Now, it is important to remember that

the gluon mass parameter undergo the modified delta expansion, thus it has be treated as a variational parameter, blind to its precise physical origin (at first) as a dynamically generated thermal mass. Since the gluons do not possess a chemical potential, at $T = 0$, $\mu \neq 0$, their contributions (in HTL) is proportional to m_g^4 and thus, a priori, medium independent. In order to obtain a solution to the mass gap equation (6.2) which depends on the thermodynamical variable μ, like it is the case for the Debye mass, one needs to go one order higher than the leading order, to get a mixing in the Feynman diagrams between the quark and the gluon sector. Then, a term $\#\alpha_s m_g^2 \mu^2$ will arise naturally from the calculations, and lead to a nontrivial solution to the mass gap equation which effectively dependent on the parameter of the medium. Such term naturally arise from the mixed sector, namely the last diagram in Eqn.(6.42).

This diagram has already been evaluated at finite temperature [35] as well as in the limit of high temperature and small chemical potential [21] in a naive mass expansion m_g^2. However, no such calculation has been pursued at strictly zero temperature and finite chemical potential. This lead to us to investigate this calculation such as to apply the RGOPT method to the gluon sector.

Naively, one would think that the calculation at zero temperature is simpler than the one at finite temperature since at zero temperature, the Bose-Einstein distribution vanishes and the Fermi-Dirac distribution of the quarks either vanished or goes to a theta function cutting the momentum integration up to the Fermi sphere. Unfortunately, it appears that it is still very involved. By-passing this issue required the use of Mellin-Barnes transformation and contour integration over generalized Hypergeometric functions. The calculation is very closed to be completed now, only one last piece of an integral needs further crosschecking as we are not confident on this specific contribution. The detailed derivation of this diagrams is given in appendix B, while useful mathematical reminder and relations over the Mellin-Barnes method and the generalized Hypergeometric function are given in appendix C.

The formal expression for this diagram, expanded in m_g^2 reads[35]:

$$\begin{aligned}\mathcal{P}_{3qg}^{(hh)} =& -\frac{d_A N_f}{2} m_E^2 g^2 \sum\!\!\!\!\!\!\int_{\{PQ\}} \left[\frac{d+1}{d-1}\frac{1}{P^2Q^2r^2} - \frac{4d}{d-1}\frac{q^2}{P^2Q^2r^4} - \frac{2d}{d-1}\frac{P\cdot Q}{P^2Q^2r^4}\right]\mathcal{I}_R \\ &- \frac{d_A N_f}{2} m_E^2 g^2 \sum\!\!\!\!\!\!\int_{\{PQ\}} \left[\frac{3-d}{d-1}\frac{1}{P^2Q^2R^2} + \frac{2d}{d-1}\frac{P\cdot Q}{P^2Q^2r^4} - \frac{d+2}{d-1}\frac{1}{P^2Q^2r^2}\right. \\ &\qquad \left. + \frac{4d}{d-1}\frac{q^2}{P^2Q^2r^4} - \frac{4}{d-1}\frac{q^2}{P^2Q^2r^2R^2}\right].\end{aligned} \tag{6.45}$$

Where

$$\mathcal{I}_R = \frac{w(\epsilon)}{2}\int_{-1}^{-1} dc(1-c^2)^{-\epsilon}\frac{iR_0}{iR_0 - \|\vec{r}\|\,c} = \frac{w(\epsilon)}{2}\left\langle \frac{iP_0}{iP_0 - p\,c}\right\rangle_c, \qquad w(\epsilon) = 2^{2\epsilon}\frac{\Gamma(2-2\epsilon)}{\Gamma(1-\epsilon^2)} \tag{6.46}$$

While our current results for it is given by :

$$-\frac{d_A m_g^4 g^2 N_f \mu^2}{256\pi^4\varepsilon} - \frac{d_A m_g^4 g^2 N_f \mu^2}{64\pi^4}\ln\left(\frac{M}{\mu}\right) - \frac{d_A m_g^4 g^2 N_f \mu^2}{512\pi^2} - \frac{3\,d_A g^2 m_g^2 \mu^2 \ln(2)}{128\pi^4} + \frac{89\,d_A\,g^2 m_g^2 N_f \mu^2}{28800\pi^4}. \tag{6.47}$$

This diagrams seems to possess, at first, a spurious double pole $1/\varepsilon^2$. We obtained, with certainty, that the coefficient of this double pole is zero. This is a very nice crosscheck since we know it must not have a double pole otherwise this diagram would possess a double logarithm which can only arise from the pure soft sector [36]. We also have crosschecked in multiple

different ways the simple pole complete structure and the associated logarithm arising. Only the finite coefficient $\mathcal{O}(\varepsilon^0)$, of interest, remains unknown at present. Notably, the unnatural coefficient appearing in the last term suggest that, indeed, the last piece is probably incorrect.

6.6 Bibliography

[1] Loïc Fernandez and Jean-Loïc Kneur. Renormalization group optimized $\lambda\phi^4$ pressure at next-to-next-to-leading order. *Phys. Rev. D*, 104(9):096012, 2021, 2107.13328.

[2] Loïc Fernandez and Jean-Loïc Kneur. Renormalization group improvement in cold and dense QCD pressure. *To be submitted to ArXiv.*, 2022.

[3] P. M. Stevenson. Optimized perturbation theory. *Phys. Rev. D*, 23:2916–2944, Jun 1981.

[4] Hirofumi Yamada. Spontaneous symmetry breaking in QCD. *Z. Phys. C*, 59:67–76, 1993.

[5] Anthony Duncan and Moshe Moshe. Nonperturbative physics from interpolating actions. *Physics Letters B*, 215(2):352–358, 1988.

[6] Rajesh R. Parwani. Resummation in a hot scalar field theory. *Phys. Rev. D*, 45:4695, 1992, hep-ph/9204216. [Erratum: Phys.Rev.D 48, 5965 (1993)].

[7] F. Karsch, A. Patkos, and P. Petreczky. Screened perturbation theory. *Phys. Lett. B*, 401:69–73, 1997, hep-ph/9702376.

[8] Jens O. Andersen, Eric Braaten, and Michael Strickland. Screened perturbation theory to three loops. *Phys. Rev. D*, 63:105008, Apr 2001.

[9] Jens O. Andersen and Lars Kyllingstad. Four-loop Screened Perturbation Theory. *Phys. Rev. D*, 78:076008, 2008, 0805.4478.

[10] Jean-Paul Blaizot, Andreas Ipp, and Nicolas Wschebor. Calculation of the pressure of a hot scalar theory within the Non-Perturbative Renormalization Group. *Nucl. Phys. A*, 849:165–181, 2011, 1007.0991.

[11] J. P. Blaizot, Edmond Iancu, and A. Rebhan. Approximately selfconsistent resummations for the thermodynamics of the quark gluon plasma. 1. Entropy and density. *Phys. Rev. D*, 63:065003, 2001, hep-ph/0005003.

[12] J. Berges, Sz. Borsanyi, U. Reinosa, and J. Serreau. Renormalized thermodynamics from the 2PI effective action. *Phys. Rev. D*, 71:105004, 2005, hep-ph/0409123.

[13] M. E. Carrington, B. A. Meggison, and D. Pickering. The 2PI effective action at four loop order in φ^4 theory. *Phys. Rev. D*, 94(2):025018, 2016, 1603.02085.

[14] Sunil K. Gandhi, H. F. Jones, and Marcus B. Pinto. The delta expansion in the large N limit. *Nucl. Phys. B*, 359:429–440, 1991.

[15] J. L. Kneur and A. Neveu. Renormalization Group Improved Optimized Perturbation Theory: Revisiting the Mass Gap of the O(2N) Gross-Neveu Model. *Phys. Rev. D*, 81:125012, 2010, 1004.4834.

[16] P. Stevenson. *Renormalized Perturbation Theory and Its Optimization by the Principle of Minimal Sensitivity.* 08 2022.

[17] Jens O. Andersen and Michael Strickland. Resummation in hot field theories. *Annals Phys.*, 317:281–353, 2005, hep-ph/0404164.

[18] Jens O. Andersen, Lars E. Leganger, Michael Strickland, and Nan Su. NNLO hard-thermal-loop thermodynamics for QCD. *Phys. Lett. B*, 696:468–472, 2011, 1009.4644.

[19] Jens O. Andersen, Lars E. Leganger, Michael Strickland, and Nan Su. Three-loop HTL QCD thermodynamics. *JHEP*, 08:053, 2011, 1103.2528.

[20] Sylvain Mogliacci, Jens O. Andersen, Michael Strickland, Nan Su, and Aleksi Vuorinen. Equation of State of hot and dense QCD: Resummed perturbation theory confronts lattice data. *JHEP*, 12:055, 2013, 1307.8098.

[21] Najmul Haque, Aritra Bandyopadhyay, Jens O. Andersen, Munshi G. Mustafa, Michael Strickland, and Nan Su. Three-loop HTLpt thermodynamics at finite temperature and chemical potential. *JHEP*, 05:027, 2014, 1402.6907.

[22] Jean-Loïc Kneur and André Neveu. α_S from F_π and Renormalization Group Optimized Perturbation Theory. *Phys. Rev. D*, 88(7):074025, 2013, 1305.6910.

[23] Jean-Loïc Kneur and André Neveu. Chiral condensate from renormalization group optimized perturbation. *Phys. Rev. D*, 92(7):074027, 2015, 1506.07506.

[24] Jean-Loïc Kneur and André Neveu. Chiral condensate and spectral density at full five-loop and partial six-loop orders of renormalization group optimized perturbation theory. *Phys. Rev. D*, 101(7):074009, 2020, 2001.11670.

[25] J. L. Kneur and M. B. Pinto. Renormalization Group Optimized Perturbation Theory at Finite Temperatures. *Phys. Rev. D*, 92(11):116008, 2015, 1508.02610.

[26] J. L. Kneur and M. B. Pinto. Scale Invariant Resummed Perturbation at Finite Temperatures. *Phys. Rev. Lett.*, 116(3):031601, 2016, 1507.03508.

[27] Gabriel N. Ferrari, Jean-Loic Kneur, Marcus B. Pinto, and Rudnei O. Ramos. Asymptotically Free Theory with Scale Invariant Thermodynamics. *Phys. Rev. D*, 96(11):116009, 2017, 1709.03457.

[28] Jean-Loïc Kneur, Marcus Benghi Pinto, and Tulio Eduardo Restrepo. Renormalization group improved pressure for cold and dense QCD. *Phys. Rev. D*, 100(11):114006, 2019, 1908.08363.

[29] Jean-Loïc Kneur, Marcus Benghi Pinto, and Tulio E. Restrepo. QCD pressure: Renormalization group optimized perturbation theory confronts lattice. *Phys. Rev. D*, 104(3):L031502, 2021, 2101.02124.

[30] Jean-Loïc Kneur, Marcus Benghi Pinto, and Tulio E. Restrepo. Renormalization group improved pressure for hot and dense quark matter. *Phys. Rev. D*, 104(3):034003, 2021, 2101.08240.

[31] I. T. Drummond, R. R. Horgan, P. V. Landshoff, and A. Rebhan. Foam diagram summation at finite temperature. *Nucl. Phys. B*, 524:579–600, 1998, hep-ph/9708426.

[32] Jens O. Andersen, Eric Braaten, and Michael Strickland. The Massive thermal basketball diagram. *Phys. Rev. D*, 62:045004, 2000, hep-ph/0002048.

[33] Aleksi Kurkela, Paul Romatschke, and Aleksi Vuorinen. Cold Quark Matter. *Phys. Rev. D*, 81:105021, 2010, 0912.1856.

[34] Loïc Fernandez and Jean-Loïc Kneur. All order resummed leading and next-to-leading soft modes of dense QCD pressure. *Accepted in Phys. Rev. Lett.*, 9 2021, 2109.02410.

[35] Jens O. Andersen, Emmanuel Petitgirard, and Michael Strickland. Two loop HTL thermodynamics with quarks. *Phys. Rev. D*, 70:045001, 2004, hep-ph/0302069.

[36] Tyler Gorda, Aleksi Kurkela, Paul Romatschke, Matias Säppi, and Aleksi Vuorinen. Next-to-Next-to-Next-to-Leading Order Pressure of Cold Quark Matter: Leading Logarithm. *Phys. Rev. Lett.*, 121(20):202701, 2018, 1807.04120.

7

Neutron Stars

Having now spent a lot of time and ink on the formalism of perturbation theory, we will turn to a topic a bit more down to earth. Or let's say down the stars. This chapter is merely an introduction to neutron stars and certainly not exhaustive, it presents first application of the RGOPT approach to the neutron stars [1]. It is perhaps not so surprising that a special interest has been progressively given in this thesis to the case of cold and dense QCD regarding the ever growing interest of the community in the physics of neutron stars (NS). It appears that we are at the dawn of multi-messenger astronomy which will teach us a lot about celestial corpses in extreme conditions. Since 2016, and the discovery of gravitational waves (GW), the study of NS has taken another leap forward. Combining information from GW, electromagnetism and neutrino physics, it provides a deeper insight in the physics of compact stellar objects. Notably, the special event of GW170817 [2; 3], first merger of two neutron stars, opens a new path to determining neutron stars properties.

Considering that we cannot reproduce, yet, such conditions in heavy ion collisions, it is even more thrilling since it is completely new physics. Especially, NS resides partially (conjecture) in the region of interest, namely, near the theoretical first order phase transition at finite chemical potential between a chirally broken phase and a restored one, see Fig.(4.2). Although at zero temperature and finite chemical potential, the picture is slightly different since it might be possible that formation of diquark pairs still breaks the chiral symmetry. Such pairs arise from QCD color-magnetic interactions and are very similar to Bardeen-Cooper-Schrieffer (BCS) condensate of electron pairs in superconductor [4].

7.1 Neutron stars, from the core to the crust

In the very core of the neutron stars, it might be possible that deconfined matter exists [5] (see [6] for recent developments), while the outer crust is composed of a dilute gas of nucleons. In the core, a stiff equation of state (EoS) is required for stability of the NS, i.e, preventing the gravitational collapse. A stiff EoS means that the pressure ($\mathcal{P}$) versus energy density (ε) ratio is high and it is particularly hard to compress the quark matter. This reflects in a high value of the speed of sound $c_s^2 = \mathcal{P}/\varepsilon$. Intuitively, this is just like in seismology where we know

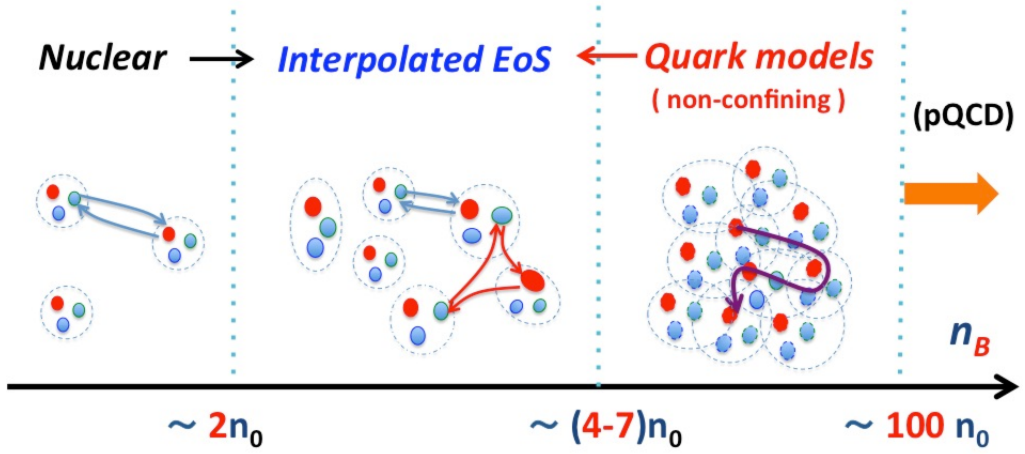

Figure 7.1: Schematic picture of the transition from nuclear to deconfined quark matter with increasing density. n_0 is the nuclear saturation density, the typical density of heavy atoms. While n_B is the baryon density related to the baryon chemical potential $\mu_B = 3\mu_q$, μ_q the chemical potential, used in last chapter, for a single quark. See text below for further description of the different states of matter. Source [10]

that seismic waves travel faster where the rigidity of the material is greater. Such stiffness of the EoS is required in order to support the NS and prevent gravitational collapse. On the contrary, the outer crust, of dilute gas, can be "easily" compressed and is thus described by a soft equation of state. Recombining the two equation of states, soft to stiff, is theoretically very challenging, but it seems to be what nature prefers in view of the latest observations of NS masses. Specifically, the existence of neutron stars of mass greater than two solar masses[7; 8; 9] is not very compatible with soft equations of states that incorporate hyperons in nuclear models. The apparition of strange hadrons around twice nuclear saturation density softens the EoS and puts an upper constraint on the maximum stable star mass. Additionally, pQCD tends to soften the EoS in the core of NS and suggests that at intermediate baryon density regime a phase transition involving a stiff EoS.

Describing hadrons and quarks degrees of freedoms within the same framework is a particularly difficult task. The conventional approach is to regard the nuclear and quark matter as distinct phases and evaluate both energy density to determine which state is preferred. Recombination of the two phases using bitangent Maxwell construction leads to a first order phase transition from nuclear to quark matter [10].

A schematic picture of the different states of matter in function of the baryon density inside the star is depicted in 7.1. The relevant scale is the nuclear saturation density $n_0 = 0.16\,\text{nucleons by fm}^3$, the typical density inside atoms. Below 2 n_0, the relevant degrees of freedom for QCD are hadrons whose exchange are well described by mesons. At such low densities, the equation of state is well described by low energy effective QCD, such as chiral effective field theory [11] or pNJL model [12; 13; 14] . Going to higher densities, quarks from different hadrons start to interact with each others. There is no successful model at the moment describing such state of matter since it is very difficult just to identify the relevant degrees of freedom. Many bodies interactions might be the answer but it seems that higher number of bodies interaction non perturbatively correct the picture. For even higher n_0, the relevant degrees of freedom would be a quasi particle model of quark pairing since hadrons starts to overlap and loose their meaning at that scale. Finally, for $40 \sim 100 n_0$, perturbative QCD is relevant to address the free quarks degrees of freedom. This is mainly the range of our focus here. Although, the density in NS in believed to be less than the domain of applicability of

pQCD, the density being of order 1 n_0 to $\sim 10n_0$ in the core. Upon using better resummation techniques, the domain of applicability of pQCD will be extended towards lower values of the baryon density and puts additional constraints on the equation of state [15]. Moreover, theoretical pure quark stars may exist and pQCD would be relevant for this deconfined state of matter.

7.1.1 Constraints on NS

Astrophysical observations taught us a lot about neutron stars. First, the existence of pulsars with pulse period smaller than one second implied that the star in question possesses a radius of order $10-100kms$. The reason why such stars are rotating so fast is that the angular momentum of the original massive star is conserved during the supernovae. Just like ice-skaters retract their arms to gain speed, the reduced radius of the star means an higher rotation speed. Since the star is stable, mechanical balance means :

$$\frac{G\,M\,m}{R^2} = m\,R\,\omega^2 \rightarrow \omega = \left(\frac{G\,M}{R^3}\right)^{1/2} \tag{7.1}$$

where m is a mass test at the surface of the star, R the radius of the star, M the mass of the star and G is Newton's gravitational constant. Therefore, a rapidly pulsating star must be very massive to conserve its mechanical balance. The maximal mass versus radius is an open question and directly related to the determination of a precise EoS. In a more refined approach of general relativity and gravitational waves, the first observed event of two merging neutron stars was GW170817 [2; 3], observed conjointly with EM waves [16]. From GW, it is possible to recover the tidal deformability of the star which reflects how easily a, more or less, compact star is deformed under an external gravitational field. It can be related to the radius of the star itself and gravitational Love number k_2 [17]:

$$\Lambda = \frac{2}{3} k_2 \frac{R^5}{m^5}. \tag{7.2}$$

The Love number is of order $k_2 \sim 0.2 - 0.3$ and depends on the stiffness of the EoS. Hence, measurement on the tidal deformability gives an upper bound for the maximum radius of the star [6]. Lastly, an important constraint concerns the speed of sound inside NS. Obviously, it must be less than one (in natural units) according to special relativity, but we also know that at asymptotically high baryon densities, the relevant degrees of freedom are free quarks, whose pressure is well-known to be $P_f = \frac{N_c\,N_f\,\mu_f^4}{12\pi^2}$, the pressure of an ideal Fermi gas. Relating this pressure to the energy density:

$$\varepsilon = -\mathcal{P} + \mu_f\,n_f, \quad n_f = \frac{\partial \mathcal{P}}{\partial \mu_f}, \tag{7.3}$$

this gives:

$$\varepsilon = 3\mathcal{P}. \tag{7.4}$$

In this limit, since for free quarks the QCD beta function is zero and the Fermi gas is conformally invariant. This conformal limit of $c_s^2 = 1/3$ is well accepted and since first perturbative corrections to the free pressure are negative, this conformal limit is believed to be reached from below. It remains an open question whether this conformal limit is an absolute limit in QCD, or if at some intermediate baryon densities, during a possible phase transition, it may be exceeded before going down again to approach the conformal limit from below. The second one being

preferred recently in order to have a sufficiently stiff EoS at intermediate baryon density to support the neutron star.

Following recent observations [18], it seems that the maximum radius for a NS is roughly $\sim$ 13kms while its maximum mass is $\sim$ 2.2 solar mass.

7.2 Equation of state for neutron stars

As a very good approximation, one often describes neutron stars as being completely cold, since only $10 - 100s$ after the birth of the star (after the supernovae), the temperature at the surface drops to few$\sim keV$ and it is three to six orders of magnitude below the typical chemical potential scale in low energy effective model of QCD or with respect to pQCD.

Neutrons stars are not made entirely of neutrons, a small fraction of protons and electrons are present. The reason for this is that a free neutron will undergo a weak decay, the so-called direct URCA process,

$$n \to p + e^- + \bar{\nu}_e. \tag{7.5}$$

The decay products have low energies ($m_n - m_p - m_e = 0.778MeV$) with most of that energy being carried away by the light electron and (nearly massless) neutrino. Because it is almost non-interacting with nuclear matter, a neutrino tends to escape from the neutron star and this is the major cooling mechanism as the neutron star is being formed in a supernova explosion. Since neutrons has a typical lifetime of about 15 minutes, there must be something that prevents this decay in the case of the star, and that is the presence of the protons and the electrons. If all the available low-energy levels for the decaying proton are already filled by the protons present in the star, then the Pauli exclusion principle takes over and prevents the decay from taking place. But, the reverse process, the electron capture, is also authorized by weak interactions,

$$p + e^- \to n + \nu_e. \tag{7.6}$$

To reach stability, the star must be at equilibrium with respect to these weak interactions. This equilibrium can be expressed in terms of the chemical potentials for the three particle species (four if including the neutrino, but since it barely interacts, it is negligible)

$$\mu_n = \mu_p + \mu_e. \tag{7.7}$$

Since we are interested in perturbative QCD approach, the relevant degrees of freedom for our approach are the quarks and not the nucleons that may be found in the core of the NS. In this approach, the previous URCA process now reads

$$\begin{aligned} d &\to n + e^- + \bar{\nu}_e \\ u + e^- &\to d + \nu_e \end{aligned} \tag{7.8}$$

which reflects in terms of chemical potential :

$$\mu_d = \mu_s = \mu_u + \mu_e. \tag{7.9}$$

Moreover, the NS must be electrically neutral, therefore we have one additional constraint on the density of quarks and electrons. Since the electric charges are $q_u = 2/3$, $q_d = q_s = -1/3$,

$q_e = -1$ (for quark u,d,s and e^-) then neutrality implies:

$$\frac{2}{3}n_u - \frac{1}{3}n_s - \frac{1}{3}n_d - n_e = 0 \tag{7.10}$$

At leading order, if we assume the masses to be negligible, since $\mathcal{P}_f = \frac{N_c N_f \mu_f^4}{12\pi^2}$ and $\mathcal{P}_e = \frac{\mu_e^4}{12\pi^2}$, using the second equality in Eqn.(7.3) leads to:

$$n_u = n_d = n_s, \quad n_e = 0 \tag{7.11}$$

and electrical neutrality is realized without electrons. This does not describe a realistic NS, so one must abandon the assumption that every particle are massless. Introducing the strange mass, $m_s \sim 93$MeV, as a first correction will allow electrons to be present in the star. Using Eqn.(7.10), μ_e can be expressed in terms of μ_B so one is left with only one parameter for the pQCD pressure: the baryon density μ_B.

Going to higher orders in perturbative calculations, one can evaluate corrections to the pressure and the energy density such as to evaluate the ratio :

$$\frac{\mathcal{P}}{\varepsilon} = \frac{1}{3} - \#_1\, \alpha_s + \dots \tag{7.12}$$

which is the equation of state, necessary for determination of the mass versus radius constraints of neutron stars. Hence, upon knowing exactly the equation of state, we characterize uniquely the structure of the neutron (or dwarf) stars. Alternatively, knowing the structure of the star (from astrophysical observations) means that, using reverse engineering, one can constrains the value of the equation of state.

7.2.1 Integration of the EoS

Assuming a static and spherically symmetric perfect fluid, then the general relativistic Tolman-Volkoff-Oppenheimer equation, that characterizes neutron stars, is :

$$\frac{d\mathcal{P}}{dr} = -\frac{G\epsilon(r)\mathcal{M}(r)}{c^2 r^2}\left[1 + \frac{p(r)}{\epsilon(r)}\right]\left[1 + \frac{4\pi r^3 p(r)}{\mathcal{M}(r)c^2}\right]\left[1 - \frac{2G\mathcal{M}(r)}{c^2 r}\right]^{-1} \tag{7.13}$$

Where G is Newton's gravitational constant, $\mathcal{M}(r)$ is the mass inside radius r, therefore $\mathcal{M}(R) = M$ is equal to the mass of the star M for a radius R of the star. The first two factors are corrections from special relativity – boost factor for the momentum and the space-time volume, respectively, while the third factor comes from General Relativity. The mass inside radius r is determined via :

$$\begin{aligned} \frac{d\mathcal{M}}{dr} &= 4\pi r^2 \rho(r) = \frac{4\pi r^2 \epsilon(r)}{c^2} \\ \mathcal{M}(r) &= 4\pi \int_0^r dr' r'^2 \rho(r') = 4\pi \int_0^r dr' r'^2 \frac{\epsilon(r')}{c^2}. \end{aligned} \tag{7.14}$$

Since the neutron star is a bounded sphere in vacuum, it satisfies the boundary condition: $\mathcal{P}(R) = 0$. Now, these equations can be integrated for a certain equation of state $\mathcal{P}(\mu_B)/\epsilon(\mu_B)$, for different μ_B, that will give different configurations (Mass versus Radius) for the star.

As a concrete example, we can use our previous result at leading order. Including the strange quark current mass:

$$
\begin{aligned}
P_{\rm LO}^{\rm RGOPT}(m,m_s,\mu,\mu_s,\mu_e) = &- N_c\frac{(m+m_s)^4}{8\pi^2}\left(\frac{3}{4}-L(m+m_s)\right)+N_c\frac{(m+m_s)^4}{(4\pi)^2 g(b_0-2\gamma_0)}\\
&-2\,N_c\frac{m(m+m_s)^3\,\gamma_0}{(4\pi)^2 g\,b_0(b_0-2\gamma_0)}-(m+m_s)^4 s_1\\
&-N_c(N_f-1)\frac{m^4}{8\pi^2}\left(\frac{3}{4}-L(m)\right)+N_c\,(N_f-1)\,\frac{m^4}{(8\pi)^2 g\,b_0}-(N_f-1)\,m^4\,s_1\\
&+P_s(m+m_s,\mu)+P_d(m,\mu)+P_u(m,\mu_u)+P_e(0,\mu_e).
\end{aligned}
\tag{7.15}
$$

Where,

$$
\begin{aligned}
P_f(m,\mu)\equiv\Theta(\mu^2-m^2)\frac{N_c}{12\pi^2}\Bigg\{&\mu\;p_F[m,\mu]\left(\mu^2-\frac{5}{2}m^2\right)+\frac{3}{2}m^4\ln\left(\frac{\mu+p_F[m,\mu]}{m}\right)\\
&+\frac{3}{2}m^4\ln\left(\frac{\mu+p_F[m,\mu]}{m}\right)\Bigg\},
\end{aligned}
\tag{7.16}
$$

and

$$
p_F[m,\mu]\equiv\sqrt{\mu^2-m^2}. \tag{7.17}
$$

Comparison of the result with the easier $m_s = 0$ case is displayed in fig(7.2). Using an equation of state coming from pQCD, is a crude approximation, for first application, giving an incomplete picture explaining why the tail of graph is off the charts with respect to [19]. A better approach would be to recombine with low energy effective model but this is currently outside our scope. We see quite clearly that ignoring the strange quark mass leads to non-physical description of the neutron star since the maximum mass/radius is well above the observed neutron star so far (see section 7.1.2). However, at leading order, for non zero strange current mass, the result is roughly in agreement with observations. This result has been crosschecked by the author as well as his coauthors [1]. This is part of an on-going project to be pursued to NLO and NNLO using the RGOPT approach. This sound result at LO is encouraging and motivates applications at higher orders that may lead to more precise determination of the EoS for neutron stars from the resummed perturbative side.

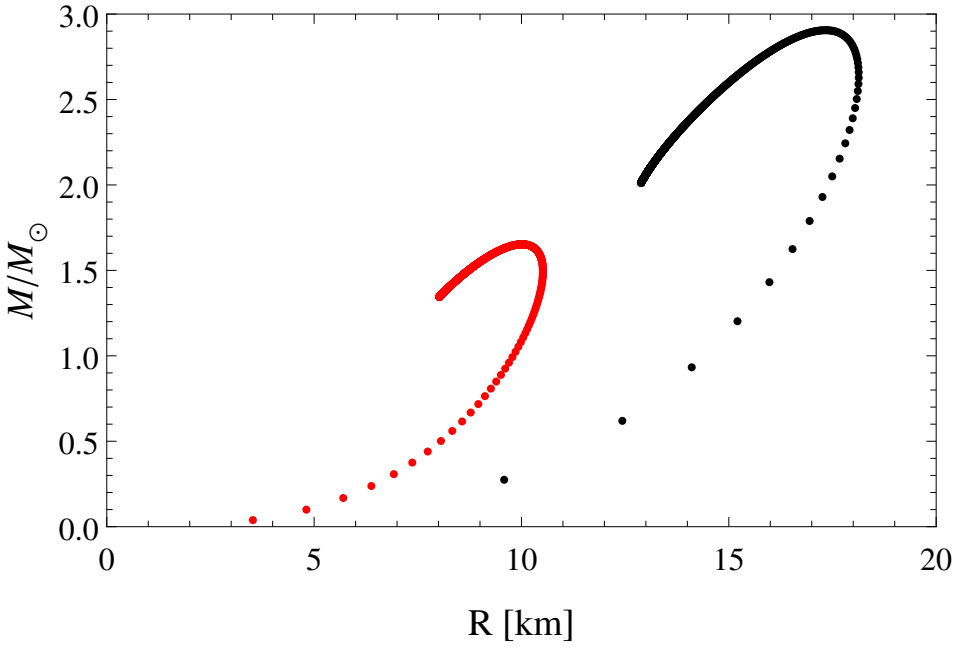

Figure 7.2: Mass versus radius curve for RGOPT improved QCD at leading order with $N_f = 2 + 1$. The red curve corresponds to $m_s \neq 0$ while the black one corresponds to $m_s = 0$.

7.3 Bibliography

[1] Loic Fernandez, Jean-Loic Kneur, Marcus B. Pinto, and Tulio E. Restrepo. In preparation.

[2] B. P. Abbott et al. Multi-messenger observations of a binary neutron star merger. *The Astrophysical Journal*, 848(2):L12, oct 2017.

[3] Abbott et al. GW170817: Observation of gravitational waves from a binary neutron star inspiral. *Phys. Rev. Lett.*, 119:161101, Oct 2017.

[4] Mark G. Alford, Andreas Schmitt, Krishna Rajagopal, and Thomas Schäfer. Color superconductivity in dense quark matter. *Rev. Mod. Phys.*, 80:1455–1515, Nov 2008.

[5] Joseph I. Kapusta. Quantum Chromodynamics at High Temperature. *Nucl. Phys. B*, 148:461–498, 1979.

[6] Eemeli Annala, Tyler Gorda, Aleksi Kurkela, Joonas Nättilä, and Aleksi Vuorinen. Evidence for quark-matter cores in massive neutron stars. *Nature Phys.*, 16(9):907–910, 2020, 1903.09121.

[7] Emmanuel Fonseca et al. The NANOGrav Nine-year Data Set: Mass and Geometric Measurements of Binary Millisecond Pulsars. *Astrophys. J.*, 832(2):167, 2016, 1603.00545.

[8] Paul Demorest, Tim Pennucci, Scott Ransom, Mallory Roberts, and Jason Hessels. Shapiro Delay Measurement of A Two Solar Mass Neutron Star. *Nature*, 467:1081–1083, 2010, 1010.5788.

[9] John Antoniadis et al. A Massive Pulsar in a Compact Relativistic Binary. *Science*, 340:6131, 2013, 1304.6875.

[10] Gordon Baym, Tetsuo Hatsuda, Toru Kojo, Philip D. Powell, Yifan Song, and Tatsuyuki Takatsuka. From hadrons to quarks in neutron stars: a review. *Rept. Prog. Phys.*, 81(5):056902, 2018, 1707.04966.

[11] C. Drischler, J. W. Holt, and C. Wellenhofer. Chiral Effective Field Theory and the High-Density Nuclear Equation of State. *Ann. Rev. Nucl. Part. Sci.*, 71:403–432, 2021, 2101.01709.

[12] Kenji Fukushima and Vladimir Skokov. Polyakov loop modeling for hot QCD. *Prog. Part. Nucl. Phys.*, 96:154–199, 2017, 1705.00718.

[13] Hubert Hansen, Rainer Stiele, and Pedro Costa. Quark and Polyakov-loop correlations in effective models at zero and nonvanishing density. *Phys. Rev. D*, 101(9):094001, 2020, 1904.08965.

[14] Antoine Pfaff, Hubert Hansen, and Francesca Gulminelli. Bayesian analysis of the properties of hybrid stars with the Nambu–Jona-Lasinio model. *Phys. Rev. C*, 105(3):035802, 2022, 2112.09595.

[15] Oleg Komoltsev and Aleksi Kurkela. How Perturbative QCD Constrains the Equation of State at Neutron-Star Densities. *Phys. Rev. Lett.*, 128(20):202701, 2022, 2111.05350.

[16] B. P. Abbott et al. Multi-messenger Observations of a Binary Neutron Star Merger. *Astrophys. J. Lett.*, 848(2):L12, 2017, 1710.05833.

[17] Katerina Chatziioannou. Neutron star tidal deformability and equation of state constraints. *Gen. Rel. Grav.*, 52(11):109, 2020, 2006.03168.

[18] M. C. Miller et al. The Radius of PSR J0740+6620 from NICER and XMM-Newton Data. *Astrophys. J. Lett.*, 918(2):L28, 2021, 2105.06979.

[19] Aleksi Kurkela, Paul Romatschke, and Aleksi Vuorinen. Cold Quark Matter. *Phys. Rev. D*, 81:105021, 2010, 0912.1856.

8

Summary

In this Thesis, we have discussed various aspects of the renormalization group properties applied in the context of thermal field theory. A review of the core concepts of renormalization was discussed in chapter 2, notably the concept of anomalous dimensions which is important for effective field theories, but also introducing the concept of vacuum energy, a mandatory piece of any massive quantum field theory in order to achieve renormalization group invariance. A brief introduction to the theory called Quantum Chromodynamics was discussed in chapter 4, introducing the core concepts and some technicals aspects required for calculation at finite temperature and density. Notably, the state-of-the art perturbative calculations for QCD in a medium and its current limitations has been over-viewed. Chapter 5 was dedicated to the theory of Hard Thermal Loops (HTL), which incorporates the long-distance physics that arises for QCD in a medium. We saw an EFT construction out of the HTL Lagrangian, at least for the leading order, while discussing the concepts for its generalization at next order. Defining such EFT permitted to resum exactly the so-called soft leading logarithm in QCD that involves $\alpha_s^2 \ln \alpha_s$. The procedure also resummed partially the next-to-leading logarithms and we paved the way for a full resummation of this last one once the mixed sector, appearing at α_s^3, will be determined. This result, published in Physical Review Letters, now replaced the previous ones as the new state-of-the-art calculation in Cold and Dense QCD, until the completion of the mixed sector, that is presumed to go even well beyond through other resummation of logarithm families, is achieved.

We have also explored applications of renormalization group properties in the context of a variational approach named Optimized Perturbation Theory (OPT). Specifically, application of the renormalization group optimized perturbation theory (RGOPT) in $\lambda\phi^4$ at finite temperature and zero chemical potential up to next-to-next-to-leading order was discussed and displayed great improvement in matter both of convergence, and remnant dependence in the renormalization scale, with respect to the naive perturbation series. This work was subject to a publication in Physical Review D. The RGOPT approach has also been applied to the specific case of Cold and Dense matter on the current quark mass contribution also displaying impressive improvements with respect to the naive expansion. This work shall be peer-reviewed soon.

The specific case of RGOPT resummation in the Hard Thermal Loop perturbation theory

framework for the gluons and its complications was considered, paving the way for, hopefully soon, application of the method once the mixed hard/soft sector will be completed. Finally, early results for the determination of an equation of state, relevant for neutron stars, using the RGOPT procedure at leading order for massive quarks was presented after a very brief overview of the main characteristics of Neutron Stars.

Next future work

The first work in line would be now to complete the evaluation of the two loop HTL diagram at zero temperature and finite chemical potential, introduced in chapter 7 and (almost) complete derivation in appendix B.2.2, to address a renormalization group improved version of Hard Thermal perturbation theory. In view of the result of RGOPT applied to the quark sector using the naive mass operator $m\bar{\psi}\psi$, it motivates us to consider instead the HTL resummed quark propagator to address carefully the degrees of freedom for quarks at high baryon densities and zero temperature. Once these results for the pressure obtained, the goal would be to obtain a realistic equation of state for perturbative QCD that would add constraints on the presently unknown range of 1 to 10 nuclear saturation density in the QCD phase diagram.

The second work in line, would be to address the case of finite temperature QCD using the RGOPT procedure at next-to-next-to-leading order using already known results in the literature for the gluon sector in order to (hopefully) decrease the large residual dependence in the renormalization scale observed in the literature.

Finally, the resummation techniques applied in the context of cold and dense QCD to the soft logarithms, call for even more resummation. Indeed, upon consideration of a more complete framework for HTL EFT up to and including α_s^3 order will allow to determine and resum the LL and NLL hard logarithms while also fully determining the so (newly-)called hybrid sector that involves $\sim \ln(\Lambda/2\mu)\ln(m_E/\mu)$. This sector amounts to a double resummation both in the hard and soft logarithm which is believed to greatly decrease the residual scale dependence of the pressure.

Appendices

A.1 QCD basics

A.1.1 Notations

Natural units are always assumed : $c = \hbar = k_B = 1$. Sum over repeated indices is implicit. In dimensional regularization, our notations for the sum integrals read:

$$D = d + 1 = 4 - 2\varepsilon,\ H(d) = \frac{2\pi^{d/2}}{\Gamma(d/2)(2\pi)^d},$$

$$\sum\!\!\!\!\!\!\int_{P/\{P\}} = \left(\frac{e^{\gamma_E}\Lambda^2}{4\pi}\right)^{\varepsilon} T \sum_{\omega_P/\tilde{\omega}_P} \int \frac{d^dP}{(2\pi)^d},$$

with $\omega_P/\tilde{\omega}_P$ the bosonic/fermionic Matsubara frequencies respectively.

A.1.2 Gell-Mann matrices

Gell-Mann matrices:

$$\begin{gathered}\lambda_1 = \begin{pmatrix} 0 & 1 & 0 \\ 1 & 0 & 0 \\ 0 & 0 & 0 \end{pmatrix} \quad \lambda_2 = \begin{pmatrix} 0 & -i & 0 \\ i & 0 & 0 \\ 0 & 0 & 0 \end{pmatrix} \quad \lambda_3 = \begin{pmatrix} 1 & 0 & 0 \\ 0 & -1 & 0 \\ 0 & 0 & 0 \end{pmatrix} \quad \lambda_4 = \begin{pmatrix} 0 & 0 & 1 \\ 0 & 0 & 0 \\ 1 & 0 & 0 \end{pmatrix} \\ \lambda_5 = \begin{pmatrix} 0 & 0 & -i \\ 0 & 0 & 0 \\ i & 0 & 0 \end{pmatrix} \quad \lambda_6 = \begin{pmatrix} 0 & 0 & 0 \\ 0 & 0 & 1 \\ 0 & 1 & 0 \end{pmatrix} \quad \lambda_7 = \begin{pmatrix} 0 & 0 & 0 \\ 0 & 0 & -i \\ 0 & i & 0 \end{pmatrix} \quad \lambda_8 = \frac{1}{\sqrt{3}} \begin{pmatrix} 1 & 0 & 0 \\ 0 & 1 & 0 \\ 0 & 0 & -2 \end{pmatrix}\end{gathered} \tag{1}$$

A.1.3 Euclidean Feynman rules (Standard QCD)

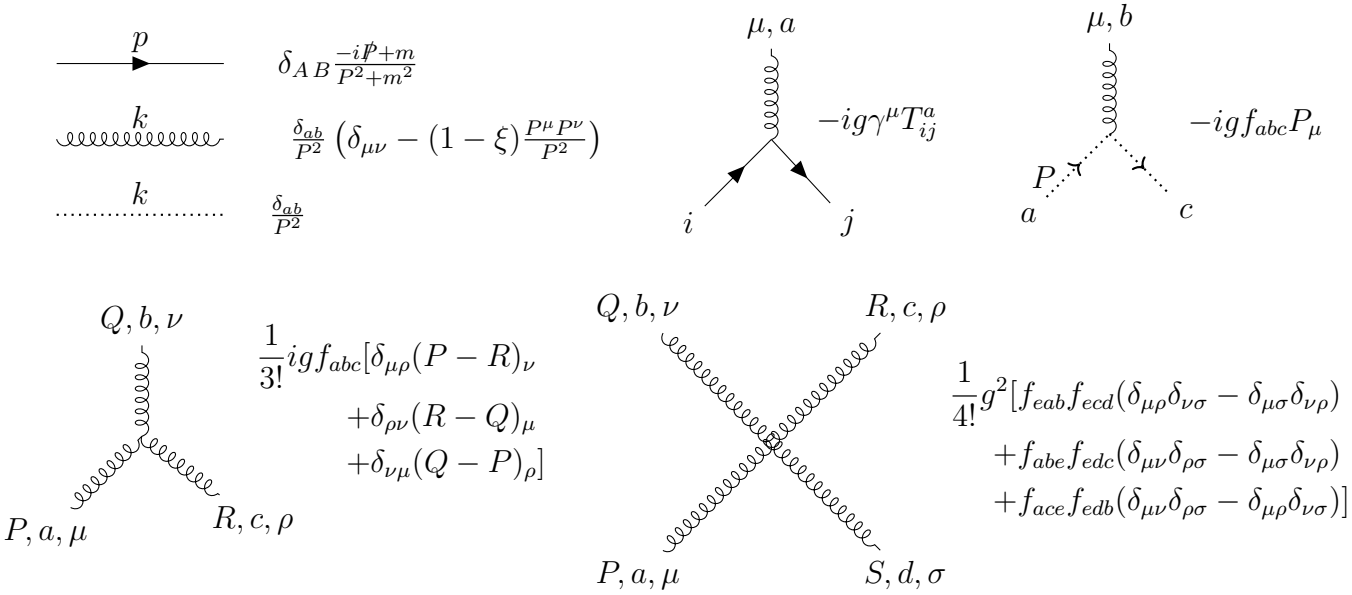

Every gluon impulsion face towards the vertices.

A.1.4 Sum integral basics

Consider the generic one loop sum integral over bosonic Matsubara frequencies:

$$\mathrm{I_B} \equiv T\sum_n \frac{f(i\omega_n,\vec{p})}{\omega_n^2+p^2}. \tag{2}$$

Assuming f to be regular in ω_n after analytic continuation, we identify $T\sum_n$ with the residue of the following weighting function (Bose-Einstein distribution):

$$n_B(ip) = \frac{1}{e^{i\beta p}-1}. \tag{3}$$

Using the residue theorem, this can be expressed as a contour integral represented on the left diagram in fig.(A.1). This same contour can be continuously transformed to the one on the right hand side using Cauchy theorem. To avoid the poles, the integration contours are shifted by $\pm i0^+$. Making a change of variable $p \to -p$ and using: $n_B(-ip) = -1 - n_B(ip)$, after some algebra we find:

$$\mathrm{I_B} = \oint_{\mathcal{C}} \frac{dp_0}{2\pi i}\frac{f(ip_0,\vec{p})}{p_0^2+p^2} i n_B(ip_0) = \int_{-\infty-i0^+}^{+\infty-i0^+}\frac{dp_0}{2\pi}\frac{f(ip_0,\vec{p})}{p_0^2+p^2} + \int_{-\infty-i0^+}^{\infty-i0^+}\frac{dp_0}{2\pi}\left[f(ip_0,\vec{p})+f(-ip_0,\vec{p})\right]\frac{n_B(ip_0)}{p_0^2+p^2}. \tag{4}$$

The first term is medium independent and is identified with the vacuum contribution, which goes through the renormalization procedure, while the second term is purely medium induced. For the second contribution, we close the contour in the lower half plane, where the Bose-Einstein distribution exponentially falls off, and encle the pole at $p_0 = -ip$. For the first one, however, one need to have more information on the convergence of the f function. Generally, f is just a propagator which thus satisfies Jordan's criteria. Usually, one prefers to recombine the p_0 integral with the d^dp integral such as to identify the generally well-known vacuum

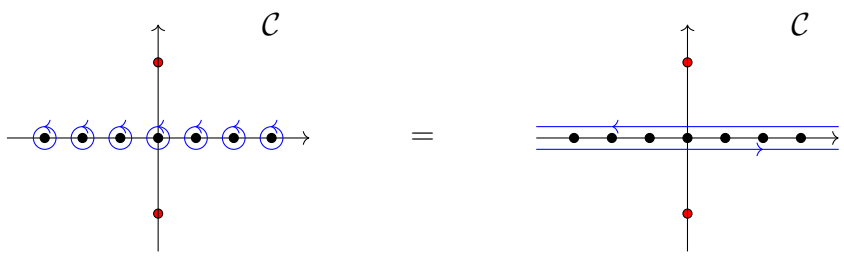

Figure A.1: Contour integration over bosonic Matsubara frequencies. Black dots are the pole of the Bose-Einstein distributions at $p_0 = \omega_B$. Red dots on the imaginary axis are the pole of the propagator in $p_0 = \pm ip$.

contributions. Here we will proceed to the p_0 integral instead. The residue theorem leads to:

$$\mathrm{I_B} = \frac{1}{2p}\left(f(p_0,\vec{p}) + n_B(p)\left(f(p_0,\vec{p}) + f(-p_0,\vec{p})\right)\right). \tag{5}$$

For the fermionic Matsubara frequencies, the method is very similar. Starting from:

$$\mathrm{I_F} = T\sum_{\{n\}} \frac{f(i\tilde{\omega}_n,\vec{p})}{(\tilde{\omega}_n)^2 + \vec{p}^2 + m^2} = T\sum_{\{n\}} \frac{-f(i\tilde{\omega}_n,\vec{p})}{(i\tilde{\omega}_n)^2 - \vec{p}^2 - m^2}, \tag{6}$$

and using the Fermi-Dirac distribution:

$$n_F(p) = \frac{1}{e^{\beta p}+1}, \tag{7}$$

as the weighting function ($E^2 = \vec{p}^2 + m^2$):

$$\begin{aligned}\mathrm{I_F} = -\int_{-i\infty}^{i\infty}\frac{dp_0}{2\pi i}\frac{f(p_0,\vec{p})}{p_0^2 - E^2} - \oint_{\mathcal{B}}\frac{dp_0}{2\pi i}\frac{f(p_0,\vec{p})}{p_0^2 - E^2} + \int_{-i\infty+0^+ +\mu}^{i\infty+0^+ +\mu}\frac{dp_0}{2\pi i}\frac{f(p_0,\vec{p})}{p_0^2 - E^2}n_F(p_0-\mu) \\ + \int_{-i\infty-0^+ +\mu}^{i\infty-0^+ +\mu}\frac{dp_0}{2\pi i}\frac{f(p_0,\vec{p})}{p_0^2 - E^2}n_F(\mu-p_0)\end{aligned} \tag{8}$$

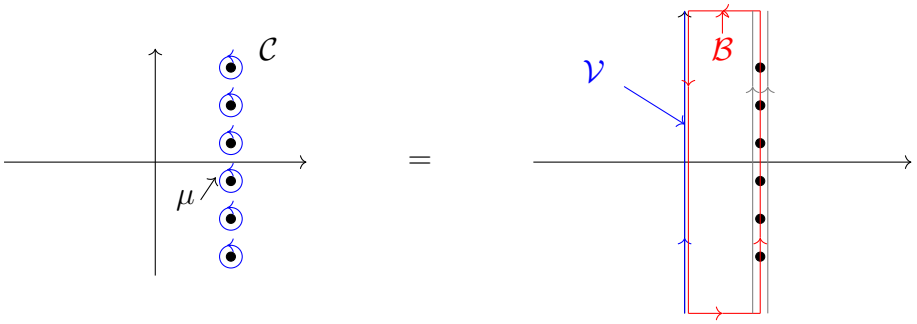

Figure A.2: Integral contour for fermionic Matsubara sum. While the gray contour, that run on both sides of the vertical axis at μ, are shifted from the pole by $\pm i0^+$, the red closed contour goes exactly through the poles and along the imaginary axis at $\mathrm{Re}(P_0) = 0$.

The first term in Eqn.(8) corresponds to the vacuum term, and can be evaluated rather simply from standard integration. In the present example, this vacuum contribution contains a divergence $\sim 1/\varepsilon$ which should be treated by renormalization. The second term is a pure

chemical potential contribution (zero temperature) whose contour is named $\mathcal{B}$ and is the red one. Finally, the last two are the mixed temperature/chemical-potential contributions that run both side of the imaginary axis at $\mathrm{Re}(P_0) = \mu$ and depicted in fig.(A.2) as the gray contours. Finally,

$$\mathrm{I_F} = \frac{1}{2E}\left(f(E,\vec{p}) - f(E,\vec{p})n_F(E-\mu) - f(-E,\vec{p})n_F(E+\mu)\right) \tag{9}$$

It then remains to integrate over $d^d\vec{p}$ (in dimenisonal regularization) which in general cannot be done analytically.

A.1.5 One loop gluon self-energy

We will review the calculation of the quark loop contribution to the gluon self-energy at finite temperature and density from which the expression of the Hard Thermal loop originates. Once having calculated the expression for this diagram, it can be easily generalized to the three others since most calculation steps are the same.

Figure A.3: Gluon self energy at leading order

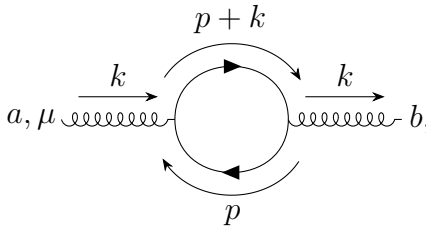

$$= \Pi_q^{\mu\nu} = g^2 T \sum_n \int \frac{d^3\vec{p}}{(2\pi)^3} N_f \,\mathrm{Tr}\left(\gamma^\mu \frac{-i\not{P}+m}{P^2+m}\gamma^\nu \frac{-i\not{P}-i\not{K}+m}{(P+K)^2+m^2}\right)$$

$$\times \sum_{a,b,j} \frac{1}{4}(\mathrm{T}^{\mathrm{a}}_{\mathrm{ji}})(\mathrm{T}^{\mathrm{b}}_{\mathrm{ij}}) \tag{10}$$

Note that one can evaluate the 00 component of this tensor only and the Ward identity will give the spatial components instead of proceeding to the full evaluation. The first step is to use Eqn.(9) and to drop the temperature independent term. This will leave only the matter part of interest. Without loss of generality, we will assume that there is no pole in the contour integral over $\mathcal{B}$ define in figure A.2 so that the calculation reduce to:

$$\Pi_q^{00} = g^2\frac{N_f}{2}\delta_{ab}\int\frac{d^3\vec{p}}{(2\pi)^3}\left\{\frac{-1}{2\pi i}\int_{-i\infty+0^+ +\mu}^{i\infty+0^+ +\mu} dp_0 \frac{1}{p_0^2-E_p^2}\frac{4\left[p_0^2+p_0k_0+E^2+\vec{p}\cdot\vec{k}\right]}{(p_0+k_0)^2-(\vec{p}+\vec{k})^2-m^2}\frac{1}{e^{\beta(p_0-\mu)}+1}\right.$$
$$\left. + \frac{-1}{2\pi i}\int_{-i\infty-0^+ +\mu}^{i\infty-0^+ +\mu} dp_0 \frac{1}{p_0^2-E_p^2}\frac{4\left[p_0^2+p_0k_0+E^2+\vec{p}\cdot\vec{k}\right]}{(p_0+k_0)^2-(\vec{p}+\vec{k})^2-m^2}\frac{1}{e^{\beta(\mu-p_0)}+1}\right\} \tag{11}$$

The next step is to evaluate the p_0 integral using the residue theorem, then for the two residues which contain $\vec{p}+\vec{k}$, proceed to a shift $\vec{p}\to\vec{p}-\vec{k}$. The four residues have the same structure where the only differences are $k_0 \to -k_0$, $n_F(E+\mu) \to n_F(E-\mu)$. Thus we can calculate one residue and in the end take $n_F(E\pm\mu) \to N_F(E) = n_F(E+\mu) + n_F(E-\mu)$, $f(k_0) \to 2\,\mathrm{Re}(f(k_0)) = [f(k_0)+f(-k_0)]$.

The first contribution is:

$$g^2\frac{N_f}{2}\delta_{ab}\int\frac{d^3\vec{p}}{(2\pi)^3}\frac{1}{2E}\frac{4[2E^2+E\,k_0+\vec{p}\cdot\vec{k}]}{(E+k_0)^2-(\vec{p}+\vec{k})^2-m^2}\left(\frac{1}{e^{\beta(E-\mu)}+1}\right),\quad E^2=\vec{p}^{\,2}+m^2 \tag{12}$$

Integration over the solid angle $\left(\vec{p}\cdot\vec{k}=|p||\omega|\,z\right)$ can be carried out, using the fact that $\int_{-1}^{1}dz\frac{1}{a+bz}=\frac{1}{b}\ln\left(\frac{a+b}{a-b}\right)$ and $\int_{-1}^{1}dz\frac{z}{a+bz}=\frac{2}{b}-\frac{a}{b^2}\ln\left(\frac{a+b}{a-b}\right)$ such that one finds ($k^2=k_0^2-\vec{k}^{\,2}$):

$$\Pi_q^{00}=-\frac{g^2}{\pi^2}\frac{N_f}{2}\delta_{ad}\int\frac{dp\,p^2}{E}n_F(E-\mu)\left\{\frac{1}{2}+\frac{1}{2}\ln\left(\frac{R_+}{R_-}\right)\frac{4Ek_0-4E^2-k^2}{4p\,\omega}\right\},\ R_\pm=\vec{k}^{\,2}-2k_0E\pm2p\,\omega, \tag{13}$$

Thus combining all the residues, the result for this graph is:

$$\Pi_q^{00}=-\frac{g^2}{\pi^2}\frac{N_f}{2}\delta_{ad}\ \mathrm{Re}\int\frac{dp\,p^2}{E}N_F(p)\left\{1+\frac{4Ek_0-4E^2-k^2}{4p\,\omega}\ln\left(\frac{R_+}{R_-}\right)\right\} \tag{14}$$

This integral is not solvable analytically in general but can be integrated numerically. Without demonstration (calculations are very similar but simpler than the previous one) the result for each graph reads:

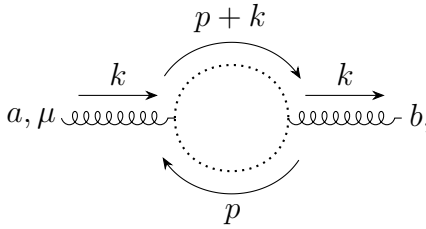

$$=\Pi_{gh.}^{00}=-g^2\frac{N_c\delta_{ab}}{(2\pi)^2}\,\mathrm{Re}\int\frac{dp}{\omega}\frac{1}{e^{\beta\,p}-1}\left\{(p^2-k_0p)\ln\left(\frac{K_+}{K_-}\right)\right\}$$

$$K_\pm=k^2-2k_0p\pm2p\,\omega$$

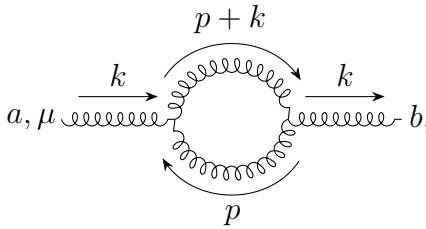

$$=g^2\frac{N_c\delta_{ab}}{(2\pi)^2}\,\mathrm{Re}\int\frac{dp\,2p}{e^{\beta p}-1}\left\{1+\frac{(10p^2+3{k_0}^2-10k_0p-6\omega^2)}{4p\omega}\ln\left(\frac{K_+}{K_-}\right)\right\}$$

$$=\Pi_{3gl.}^{00}$$

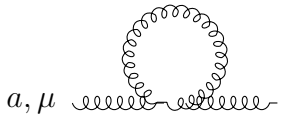

$$=\Pi_{4gl.}^{00}=-g^2 3\,N_c\delta_{ab}\int\frac{dp}{(2\pi)^2}\frac{2\,p}{e^{\beta p}-1} \tag{15}$$

Neglecting the quark masses and regarding the static infrared regime, namely, taking $k_0=0$ first then $\|\vec{k}\|=\omega\to0$) :

$$
\begin{aligned}
\Pi^{00}_{q.} &\to -\frac{g^2}{\pi^2}\frac{N_f}{2}\delta_{ad}\ \mathrm{Re}\int\frac{dp\,p^2}{p}N_F(p)\left\{1+\frac{-4p^2+\omega^2}{4p\,\omega}\left(\pm i\pi-\frac{\omega}{p}+\mathcal{O}(\frac{\omega^2}{p^2})\right)\right\}\\
\Pi^{00}_{gh.} &\to -g^2\frac{N_c\delta_{ab}}{(2\pi)^2}\,\mathrm{Re}\int\frac{dp}{\omega}\frac{1}{e^{\beta\,p}-1}\left\{(p^2)\left(\pm i\pi-\frac{\omega}{p}+\mathcal{O}(\frac{\omega^2}{p^2})\right)\right\}\\
\Pi^{00}_{3gl.} &\to g^2\frac{N_c\delta_{ab}}{(2\pi)^2}\,\mathrm{Re}\int\frac{dp\,2p}{e^{\beta p}-1}\left\{1+\frac{(10p^2-6\omega^2)}{4p\omega}\left(\pm i\pi-\frac{\omega}{p}+\mathcal{O}(\frac{\omega^2}{p^2})\right)\right\}\\
\Pi^{00}_{4gl.} &\to -g^2 3\,N_c\delta_{ab}\int\frac{dp}{(2\pi)^2}\frac{2p}{e^{\beta p}-1}
\end{aligned}
\tag{16}
$$

where the sign of $\pm i\pi$ depends on the relative magnitude of ω and p. Since the function Re kills this divergent contribution, in this limit the result is :

$$
\Pi^{00}_{\mathrm{matter}}=\frac{g^2T^2}{2\pi^2}\left\{-2N_f\int_0^\infty dp\,\left(\frac{p}{e^{\beta\,(p-\mu)}+1}+\frac{p}{e^{\beta\,(p+\mu)}+1}\right)+N_c\left(\frac{1}{2}-\frac{3}{2}-3\right)\int dp\,\frac{p}{e^{\beta\,p}-1}\right\}
\tag{17}
$$

therefore, we can identify the Debye mass for the gluon after the last integration :

$$
m_E^2=-\Pi^{00}_{\mathrm{matter}}=g^2\left\{\left(\frac{N_c}{3}+\frac{N_f}{6}\right)T^2+\frac{1}{2\pi^2}N_f\mu^2\right\}.
\tag{18}
$$

A.1.6 Massive pressure at NNLO for Cold and Dense

A.1.7 Evaluation of the NLO correction

Here we will outline the calculation of the massive quarks contribution to the pressure at next-to-leading order [1] for arbitrary temperature *and* chemical potential. Then, we will take the limit $T\to 0$. Since at $T=0$ only the quark loop is non zero, we will not discuss the other diagrams but the derivation is very similar (just like in the previous section) after scalarization. This contribution reads, for one flavor of quark:

$$
\begin{aligned}
&\mathcal{P}^{\mathrm{C.Q.M}}_{\mathrm{NLO}}(m,T,\mu)= \quad \text{  }\\
&=g^2d_A\sum\!\!\!\!\!\!\int_{\{P\},\{Q\},K}(2\pi)^d\delta^d(\vec{p}-\vec{q}-\vec{k})\delta_{n_p,n_k+n_q}\mathrm{Tr}\left\{\frac{\gamma^\nu(-i\not{P}+m)\gamma_\nu(-i\not{Q}+m))}{K^2(P^2+m^2)(Q^2+m^2)}\right\}
\end{aligned}
\tag{19}
$$

Evaluating the trace gives $(d-1)P\cdot Q+m^2(d+1)$. Using,

$$
P\cdot Q=\frac{-1}{2}\left(\overbrace{(P-Q)^2}^{=K^2}-(P^2+m^2)-(Q^2+m^2)+2m^2\right),
\tag{20}
$$

then,

$$
\begin{aligned}
&\mathcal{P}^{\mathrm{C.Q.M}}_{\mathrm{LO}}(m,T,\mu)=\\
&g^2d_A\sum\!\!\!\!\!\!\int_{\{P\},\{Q\},K}(2\pi)^d\delta^d(\cdots)\delta_{n_p,n_k+n_q}\left\{\frac{d-1}{2}\left(\frac{1}{K^2}(\frac{1}{Q^2+m^2}+\frac{1}{P^2+m^2})-\frac{1}{Q^2+m^2}\frac{1}{P^2+m^2}\right)\right.\\
&\left.+2m^2\frac{1}{K^2}\frac{1}{Q^2+m^2}\frac{1}{P^2+m^2}\right\}.
\end{aligned}
\tag{21}
$$

Introducing useful notations:

$$\mathcal{P}_{\mathrm{LO}}^{\mathrm{C.Q.M}}(m,T,\mu) = g^2 d_A \left\{ \frac{d-1}{2} \left(2I_b(T) - I_f(m,T,\mu)\right) I_f + 2m^2 H_f(m,T,\mu) \right\}, \tag{22}$$

with

$$I_b(T) = \sum\!\!\!\!\!\!\int_K \frac{1}{K^2}, \quad I_f(m,T,\mu) = \sum\!\!\!\!\!\!\int_{\{P\}} \frac{1}{P^2+m^2} \tag{23}$$

are one loop integrals while $H_f(m,T,\mu) = (2\pi)^d \delta^d(\vec{p}-\vec{q}-\vec{k}) \delta_{n_p, n_k+n_q} \frac{1}{K^2} \frac{1}{P^2+m^2} \frac{1}{Q^2+m^2}$ is a pure two loops integral. At this point an important comment is crucial. The order of evaluation of the multiple sums appearing in H_f leads to potentially different results. The root of the problem is that there is no unique analytic continuation of a function defined only on integers. The resolution of this ambiguity was given by Norton and Cornwall [2]. The idea is to transforms the Kronecker delta in H_f into a contour integral which leads to a factorization of the sum integrals. Reintroducing the factor $\beta = \frac{1}{T}$:

$$\beta\, \delta_{n_P, n_Q+n_K} = \int_0^\beta du\, e^{i\,u(P^0-Q^0-K^0)} = \frac{e^{i\,\beta(P^0-Q^0-K^0)-1}}{i(P^0-Q^0-K^0)}. \tag{24}$$

Where $P^0/Q^0 = \tilde{\omega}^F_{p/q} = (2n_{P/Q}+1)\pi T - i\mu$ and $K^0 = 2n_K ßT$. Since Q^0 and K^0 enters with a minus sign inside the exponential, to ensure that integrand in the contour integral over u falls off exponentially, we multiply by $-exp\, i\beta(Q^0 + i\mu + K^0)$ which is equal to one when Q^0 and K^0 take value on the bosonic/fermionic Matsubara frequencies respectively. This is a unique prescription that also ensures that the normal vacuum is recovered upon taking $T, \mu \to 0$. Defining,

$$I(P^0,Q^0,K^0) = \frac{e^{i\beta(Q^0+K^0)-\beta\mu} - e^{i\beta\, P^0-\mu\beta}}{i(P^0-Q^0-K^0)}, \tag{25}$$

which has no poles in $P^0,\ Q^0$ and K^0, then the sum in H_f factorizes. Using same contour tricks as in the first section of appendix A, one finds:

$$\begin{aligned} T\sum_{\{P\}} \frac{1}{P^2+m^2} I(P^0,Q^0,K^0) =& \frac{1}{2E_p}\left(I(iE_p,Q^0,K^0) - n_p^- I(-iE_p,Q^0,K^0) - n_p^+(iE_p,Q^0,K^0)\right). \\ T\sum_{K} \frac{1}{K^2} I(P^0,Q^0,K^0) =& \frac{1}{2\omega}(I(P^0,Q^0,i\omega) + n_B\, I(P^0,Q^0,i\omega) - n_B\, I(P^0,Q^0,-i\omega)) \end{aligned} \tag{26}$$

Where,

$$\begin{aligned} n_p^\pm \equiv& n_F^\pm(E_p) = \frac{1}{e^{\beta(E_p\pm\mu)}+1}, \quad E_p = \sqrt{\vec{p}^{\,2}+m^2}, \\ n_B \equiv& n_B(\omega) = \frac{1}{e^{\beta\omega}-1}, \quad \omega = \|\vec{k}^{\,2}\|. \end{aligned} \tag{27}$$

Proceeding to the evaluation of the three sums, then rewriting $I(P^0,Q^0,K^0)$ as

$$I(P^0,Q^0,K^0) = \frac{1}{i(P^0-Q^0-K^0)} \left(\left(\frac{1}{n_B(K^0)}+1\right)\left(\frac{1}{n_F^-(Q^0)}-1\right) - \left(\frac{1}{n_F^-(P^0)}-1\right)\right), \tag{28}$$

after lengthy algebra, most conveniently carried out by mathematica, one finds (with $N_p = n_p^+ + n_p^-$):

$$\begin{aligned} H_f(m,T,\mu) = \int_{\vec{p},\vec{q},\vec{k}} (2\pi)^d \delta^d(\vec{p}-\vec{q}-\vec{k}) \Bigg\{ & \frac{1}{4E_pE_q\omega(E_p+E_q+\omega)} + n_B \frac{E_p+E_q}{2E_pE_q\omega(((E_p+E_q)^2-\omega^2))} \\ & + n_B \left(N_p \frac{E_p^2+\omega^2-E_q^2}{2E_p\omega\left((E_p+E_q)^2-\omega^2\right)\left((E_p-E_q)^2-\omega^2\right)} + (p \leftrightarrow q) \right) \\ & - \left(N_p \frac{E_q+\omega}{4E_pE_q\omega((E_q+\omega)^2-E_p^2)} + (p \leftrightarrow q) \right) \\ & - \frac{n_p^-n_q^+ + n_q^-n_p^+}{4E_pE_q\left((E_p+E_q)^2-\omega^2\right)} - \frac{n_q^+n_p^+ + n_q^-n_p^-}{4E_pE_q\left((E_p-E_q)^2-\omega^2\right)} \Bigg\}. \end{aligned} \tag{29}$$

The two terms on the second line actually vanishes in dimensional regularization. This can be seen by expanding the numerator and denominator and realizing that it leads to a factor $P \cdot Q$ in the numerator which vanishes in the integration from $-\infty$ to ∞. The first term is the vacuum contribution, since no distribution multiplies it. This contribution is well known from QCD at $T = \mu = 0$ therefore we can reverse the machinery on P^0, Q^0, K^0 integral using,

$$I_3^0 \equiv \int_{-\infty}^{+\infty} \frac{dP^0}{2\pi} \int_{-\infty}^{+\infty} \frac{dQ^0}{2\pi} \frac{1}{((Q^0)^2+a^2)((P^0 \pm Q^0)^2+b^2)((Q^0)^2+c^2)} = \frac{1}{4(a\,b\,c)(a+b+c)}. \tag{30}$$

Such the vacuum contribution reads:

$$H_f^{\text{vac.}} \equiv H_f(m,0,0) = \int \frac{d^{d+1}P}{(2\pi)^{d+1}} \int \frac{d^{d+1}Q}{(2\pi)^{d+1}} \frac{1}{(P^2+m^2)(Q^2+m^2)(Q-P)^2}. \tag{31}$$

Terms on the third line can also be expressed in a simpler way using :

$$\begin{aligned} I_1^0 &\equiv \int_{-\infty}^{\infty} \frac{dP^0}{2\pi} \frac{1}{(P^0)^2+a^2} = \frac{1}{2a}, \\ I_2^0 &\equiv \int_{-\infty}^{\infty} \frac{dP^0}{2\pi} \frac{1}{((P^0)^2+a^2)((P^0 \pm Q^0)^2+b^2)} = \frac{a+b}{2a\,b} \frac{1}{((Q^0)^2+(a+b)^2}, \\ \Pi(Q^2,m_1^2,m_2^2) &\equiv \int \frac{d^{d+1}P}{(2\pi)^{d+1}} \frac{1}{(P^2+m_1^2)((P-Q)^2+m_2^2)}. \end{aligned} \tag{32}$$

In the end, terms on the third line simplify to $2I_f(T,\mu)\,\Pi(-m^2,m^2,0)$. Similarly, the second term on the first line identify to $I_b\,\Pi(0,m^2,m^2)$. The last two terms on the fourth line are pure two loops in medium contributions that are hardly possible to simplify. Only angular

integration can be readily carried out and leads to:

$$\begin{aligned}
&\int \frac{d^dP d^dQ}{(2\pi)^{2d}} \left\{ (n_p^+ n_q^+ + n_p^- n_q^-) \frac{1}{8E_pE_q(m^2 + \vec{p}\cdot\vec{q} - E_pE_q)} + (n_p^+ n_q^- + n_p^- n_q^+) \frac{1}{8E_pE_q(m^2 + \vec{p}\cdot\vec{q} + E_pE_q)} \right\} \\
&= \frac{1}{(2\pi)^4} \int_0^\infty dp\, p \int_0^\infty dq\, q \frac{1}{4E_pE_q} \left\{ (n_p^+ n_q^+ + n_p^- n_q^-) \ln\left(\frac{E_pE_q - p\,q - m^2}{E_pE_q + p\,q - m^2} \right) \right. \\
&\left. + (n_p^+ n_q^- + n_p^- n_q^+) \ln\left(\frac{E_pE_q + p\,q + m^2}{E_pE_q - p\,q + m^2} \right) \right\}, \\
&\equiv \frac{1}{4} J_3(m, T, \mu).
\end{aligned} \tag{33}$$

Collecting all the pieces, the final expression for the massive fermion loop contribution to the pressure is:

$$\begin{aligned}
\mathcal{P}_{\text{NLO}}^{\text{C.Q.M}} =& g^2 d_A \left\{ \frac{d-1}{2}(2I_b - I_f) I_f + 2m^2 \Big(H_f^{\text{vac.}} + I_b(T)\, \Pi(0, m^2, m^2) + 2I_f(T, \mu)\, \Pi(-m^2, m^2, 0) \right. \\
&\left. - \frac{1}{4} J_3(m, T, \mu) \Big) \right\}.
\end{aligned} \tag{34}$$

From this expression, the complete vacuum contribution can be readily extracted since we saw in the last section how vacuum contribution splits from in medium contributions: $I_b = I_b^{T=0} + I_b^{T\neq 0} = 0 + I_b^T$ and $I_f(m, T, \mu) = I_f^{T=\mu=0} + I_f'(m, T, \mu)$. Since we are ultimately interested in the cold and dense case, that means taking the limit $T \to 0$ where:

$$n_B \xrightarrow[T\to 0]{} 0, \quad n_p^- \xrightarrow[T\to 0]{} \theta(\mu - E_p), \quad n_p^+ \xrightarrow[T\to 0]{} 0. \tag{35}$$

The theta function, or Heaviside/step function, then cuts the momentum integration at the Fermi impulsion $p_F = \sqrt{\mu^2 - m^2}$ which becomes simpler to evaluate. The final result is given below in Eqn.(39).

Quark pressure

The expression for the NNLO pressure for one massive flavor of quark is:

$$P_{2,f}^{PT}(m, \mu) = P_{LO,f}^{PT}(m, \mu) + P_{NLO,f}^{PT}(m, \mu) + P_{NNLO,f}^{PT}(m, \mu) \tag{36}$$

With:

$$\begin{aligned}
P_{LO,f}^{PT}(m, \mu) = -N_c \frac{m^4}{8\pi^2}\left(\frac{3}{4} - L_m\right) + \Theta(\mu^2 - m^2) \frac{N_c}{12\pi^2} \Big[\mu\, p_F \left(\mu^2 - \frac{5}{2} m^2 \right) \\
+ \frac{3}{2} m^4 \ln\left(\frac{\mu + p_F}{m} \right) \Big]
\end{aligned} \tag{37}$$

$$p_F \equiv \sqrt{\mu^2 - m^2}, \quad L_m = \ln\left(\frac{m}{\Lambda}\right) \tag{38}$$

$$
\begin{aligned}
P^{PT}_{NLO,f}(m,\mu) = &-\frac{d_A\, g^2}{4(2\pi)^4} m^4 \left(3L_m^2 - 4L_m + \frac{9}{4}\right) \\
&- \Theta(\mu^2 - m^2)\frac{d_A\, g^2}{4(2\pi)^4}\left\{3\left[m^2 \ln\left(\frac{\mu + p_F}{m}\right) - \mu\ p_F\right]^2 - 2p_F^4\right\} \\
&- \Theta(\mu^2 - m^2)\frac{d_A\, g^2}{4(2\pi)^4)} m^2(4 - 6L_m)\left[\mu\ p_F - m^2 \ln\left(\frac{\mu + p_F}{m}\right)\right]
\end{aligned} \tag{39}
$$

$$
\begin{aligned}
P^{PT}_{NNLO,f}(m,\mu) = &+ \frac{g^4 m^4}{135(4\pi)^6}\left(\alpha_{0,2} + \alpha_{1,2}\ L_m + \alpha_{2,2}\ L_m^2 + \alpha_{3,2}\ L_m^3\right) \\
&+ \frac{g^4 d_A \mu^4}{(4\pi)^4 2\pi^2}\Theta(\mu^2 - m^2)\Bigg\{ - \hat{m}^2[(11C_A - 2N_f)z + 18C_F(2z - \hat{u})](L_m)^2 \\
&- \frac{1}{3}\Bigg[C_A\left(22\hat{u}^4 - \frac{185}{2}z\hat{m}^2 - 33z^2\right) + \frac{9C_F}{2}(16\hat{m}^2\hat{u}(1 - \hat{u}) \\
&- 3(7\hat{m}^2 - 8\hat{u})z - 24z^2) - N_f(4\hat{u}^4 - 13z\hat{m}^2 - 6z^2)\Bigg] L_m \\
&+ C_A\left(-\frac{11}{3}\ln\frac{\hat{m}}{2} - \frac{71}{9} + G_1(\hat{m})\right) \\
&+ C_F\left(\frac{17}{4} + G_2(\hat{m})\right) \\
&+ N_f\left(\frac{2}{3}\ln\frac{\hat{m}}{2} + \frac{11}{9} + G_3(\hat{m})\right) + G_4(\hat{m})\Bigg\},
\end{aligned} \tag{40}
$$

$$
\begin{aligned}
\alpha_{0,2} &= (357315 + 176\pi^4 + 960\pi^2(\log 2)^2 - 960(\log 2)^4 - 23040\ Li_4(1/2) + 12960\ \zeta(3) \\
&\quad + 90N_f(-393 + 224\ \zeta(3))) \\
\alpha_{1,2} &= 180(-3817 + 286N_f + 48\ \zeta(3)) \\
\alpha_{2,2} &= -720(-807 + 26N_f) \\
\alpha_{3,2} &= 2880(-81 + 2N_f)
\end{aligned}
$$

$$
\hat{m} = \frac{m}{\mu}\ ,\ L_m = \ln\frac{m}{\Lambda}\ ,\ \hat{u} = \frac{u}{\mu} = \frac{\sqrt{\mu^2 - m^2}}{\mu}\ ,\ z = \hat{u} - \hat{m}^2 \ln\frac{1 + \hat{u}}{\hat{m}}\ ,\ L = \ln\hat{m}
$$

$$
\begin{aligned}
G_1(\hat{m}) &= 32\pi^4\hat{m}^2(-0.01863 + 0.02038\hat{m}^2 - 0.039\hat{m}^2 L + 0.02581\hat{m}^2 L^2 - 0.03153\hat{m}^2 L^3 \\
&\quad + 0.01151\hat{m}^2 L^4) \\
G_2(\hat{m}) &= 32\pi^4\hat{m}^2(-0.1998 - 0.04797L + 0.1988\hat{m}^2 - 0.3569\hat{m}^2 L + 0.3043\hat{m}^2 L^2 \\
&\quad - 0.1611\hat{m}^2 L^3 + 0.09791\hat{m}^2 L^4) \\
G_3(\hat{m}) &= 32\pi^4\hat{m}^2(-0.05741 - 0.02679L - 0.002828L^2 + 0.05716\hat{m}^2 - 0.08777\hat{m}^2 L \\
&\quad + 0.0666\hat{m}^2 L^2 - 0.02381\hat{m}^2 L^3 + 0.01384\hat{m}^2 L^4) \\
G_4(\hat{m}) &= 32\pi^4\hat{m}^2(0.07823 + 0.0388L + 0.004873L^2 - 0.07822\hat{m}^2 \\
&\quad + 0.1183\hat{m}^2 L - 0.08755\hat{m}^2 L^2 + 0.03293\hat{m}^2 L^3 - 0.01644\hat{m}^2 L^4)
\end{aligned} \tag{41}
$$

Ring graph resummation in standard weak coupling expansion

The ring diagram with massive quarks was first evaluated in [3]. There, they used two massless flavours (up and down) and considered the strange quark to be massive. Introducing a global symmetry factor of nine to incorporate the physics of three massive quarks instead, the

contribution reads :

$$\Omega_{RING} = \frac{9\, d_A\, g^4\, \mu^4}{512\pi^6}\left(\mathrm{I}_{13}\left(2\ln\left(\frac{g}{(4\pi)}\right)-\frac{1}{2}\right)+\frac{1}{2}\left(\mathrm{I}_{20}+\frac{16}{3}(1-\ln 2)\ln(2)\mathrm{I}_{21}+\mathrm{I}_{22}\right)\right) \tag{42}$$

We checked that upon taking the massless limit, this correctly reproduce the expected coefficient at g^4 order in Eqn.(5.11). The integrals appearing here are :

$$\begin{aligned}
\mathrm{I}_{13}(m,\mu) =& \frac{8}{3}(1-\ln 2)\hat{p_F}^3 + 0.318\hat{p_F}^6 - 0.137\hat{p_F}^7 \\
\mathrm{I}_{20}(m,\mu) =& 3.84\hat{v} - 7.94\hat{v}^2 + 8.06\hat{p_F}^2 + \ln(\hat{v})(3.81\hat{v} + 9.7\hat{v}^2 - 7.42\hat{v}^2\ln(\hat{v})) \\
\mathrm{I}_{21}(m,\mu) =& -0.11\hat{v} + 1.11\hat{v}^2 + \ln(\hat{v})(-0.059\hat{v} - 2.07\hat{v}^2 + 0.4\hat{v}^2\ln(\hat{v})) \\
\mathrm{I}_{22}(m,\mu) =& -0.8255\hat{p_F}^2 - 0.03084\hat{p_F}^7 + 0.00161\hat{v}\ln(\hat{v}) \\
&+ \mathrm{I}_{13}(m,\mu)\left(2\ln\vec{\hat{\mu}}^2 + 2\ln\left(\frac{\tilde{\hat{\mu}}^4 + \tilde{\hat{\mu}}^2\mathrm{I}_{22\mathrm{h}2} + \mathrm{I}_{22\mathrm{h}3}(m,\mu)}{\tilde{\hat{\mu}}^4 + 0.5\tilde{\hat{\mu}}^2\mathrm{I}_{22\mathrm{h}2}(\mathrm{m},\mu)}\right)\right) \\
\mathrm{I}_{22\mathrm{h}2}(m,\mu) =& 1.313\hat{p_F} + 0.434\hat{p_F}^2 + 0.253\hat{p_F}^5 \\
\mathrm{I}_{22\mathrm{h}3}(m,\mu) =& 1.844\hat{v} - 0.844\hat{v}^2 + \ln(\hat{v})(0.194\hat{v} - 0.392\hat{v}^2 - 0.704\hat{v}^2\ln(\hat{v}))
\end{aligned} \tag{43}$$

Where $\hat{v} = 1 - \frac{m}{\mu}$, $\hat{p_F} = \frac{p_F}{\mu}$ and $\vec{\hat{\mu}} = \vec{\mu}/\mu$. The vector $\vec{\mu} = (\mu_1, \mu_2, ..., \mu_{N_l})$ in Eqn.(43), is the chemical potential vector for N_l massless flavors of quarks in their analysis. Additionally, $\hat{\vec{\mu}} = \vec{\mu}/\mu = 2$. For quarks with the same chemical potential, it reduces to $\vec{\hat{\mu}}^2 = 2$.

A.1.8 Anomalous dimensions

We give here the expression for the first coefficient of the beta, gamma functions as well as the subtraction coefficients related to the vacuum energy density anomalous dimension. Note that we do not need the 4-loop b_3 and γ_3 coefficients for our analysis but since they are known in the literature, we can use them to derive s_3, the $\mathcal{O}(g^4)$ subtraction coefficient. For the gamma function :

$$\gamma = \frac{d\ln m}{d\ln\Lambda} \tag{44}$$

$$\begin{aligned}
\gamma_0(N_f) =& \frac{1}{2\pi^2} \\
\gamma_1(N_f) =& \frac{1}{(2\pi)^4}\frac{1}{8}\left(\frac{202}{3} - \frac{20}{9}N_f\right) \\
\gamma_2(N_f) =& \frac{1}{32(2\pi)^6}\left(1249 + N_f\left(\frac{-2\,216}{27} - \frac{160}{3}\zeta(3)\right) - \frac{140}{81}N_f^2\right) \\
\gamma_3(N_f) =& \frac{1}{128(2\pi)^8}\Big(\frac{4\,603\,055}{162} + \frac{135\,680}{27}\zeta(3) - 8\,800\zeta(5) \\
&+ \Big(-\frac{91\,723}{27} - \frac{34\,192}{9}\zeta(3) + 880\zeta(4) + \frac{18\,400}{9}\zeta(5)\Big)N_f \\
&+ \Big(\frac{5\,242}{243} + \frac{800}{9}\zeta(3) - \frac{160}{3}\zeta(4)\Big)N_f^2 + \Big(-\frac{332}{243} + \frac{64}{27}\zeta(3)\Big)N_f^3\Big)
\end{aligned} \tag{45}$$

For the beta function :

$$\beta(g) = \frac{dg}{d\ln\Lambda} \tag{46}$$

$$
\begin{aligned}
b_0(N_f) =& \frac{1}{(4\pi)^2}\left(11-\frac{2}{3}N_f\right)\\
b_1(N_f) =& \frac{1}{(4\pi)^4}\left(102-\frac{38}{3}N_f\right)\\
b_2(N_f) =& \frac{1}{(4\pi)^6}\left(\frac{2\,857}{2}-\frac{5\,033}{18}N_f+\frac{325}{54}N_f^2\right)\\
b_3(N_f) =& \frac{1}{(4\pi)^8}\left(\frac{149\,753}{6}+3\,564\zeta(3)-\Big(\frac{1\,078\,361}{162}+\frac{6\,508}{27}\zeta(3)\Big)N_f\right.\\
&\left.+\Big(\frac{50\,065}{162}+\frac{64\,72}{81}\zeta(3)\Big)N_f^2+\frac{1\,093}{729}N_f^3\right)
\end{aligned}
\tag{47}
$$

Finally, the subtraction coefficients associated with the naive mass operator $m\bar{\psi}\psi$ for quarks:

$$
\begin{aligned}
s_0 =& \frac{-N_c}{(4\pi)^2(b_0-2\gamma_0)}\\
s_1 =& -\frac{N_c}{4}\left(\frac{b_1-2\gamma_1}{4(b_0-2\gamma_0)}-\frac{1}{12\pi^2}\right)\\
s_2 =& N_c\frac{112\,077+24\,519N_f+2\,101N_f^2+576(15-58N_f)\zeta(3)}{4*1\,152\pi^4(-81+2N_f)(15+2N_f)}\\
s_3 =& \frac{-32\,N_c}{128\pi^6}\frac{\left(2\,485.78+1\,045.17\,N_f+351.286\,N_f^2-8.6872\,N_f^3+0.0282158\,N_f^4\right)}{(-81+2N_f)(-57+2N_f)(15+2N_f)}
\end{aligned}
\tag{48}
$$

A.1.9 Running of $\alpha_s = g/4\pi$

At leading order, upon solving the beta function, the running of α_s reads ($g_i = g(M_i)$):

$$
\ln\left(\frac{M_h}{M_0}\right)=\frac{1}{2b_0}\left(\frac{1}{g_h^2}-\frac{1}{g_0^2}\right). \tag{49}
$$

Which, upon introducing the one-loop $\overline{\text{MS}}$ QCD scale,

$$
\Lambda_{\overline{\text{MS}}}^{\text{LO}} = M_0\, e^{-\frac{1}{2b_0\, g^2}}, \tag{50}
$$

one can express the coupling solely in function of this parameter and the renormalization scale M_h:

$$
g_h^2=\frac{1}{2b_0\,\ln\frac{M_h}{\Lambda_{\overline{\text{MS}}}^{\text{LO}}}}. \tag{51}
$$

At leading order, we use $\Lambda_{\overline{\text{MS}}}^{\text{LO}} = 176\,\text{MeV}$ which corresponds to $\alpha_s(M = 1.5\text{GeV}) = g/4\pi = 0.326$. At next-to-leading order:

$$
\Lambda_{\overline{\text{MS}}}^{\text{NLO}} = M_h e^{-1/(2b_0 g_h^2)}(b_0\, g_h^2/(1+b_1\, g_h^2/b_0))^{-\frac{b_1}{2(b_0)^g}}. \tag{52}
$$

We used $\Lambda_{\overline{\text{MS}}}^{\text{NLO}} = 320$ MeV. And finally, at NNLO:

$$
\Lambda_{\overline{\text{MS}}}^{\text{NNLO}} = M_h e^{-\frac{1}{2b_0 g}}\,(b_0 g)^{-\frac{b_1}{2b_0^2}}\;\; e^{-\frac{g}{2b_0}\left(\left(\frac{b_2}{b_0}-\frac{b_1^2}{b_0^2}\right)+\left(\frac{b_1^3}{2b_0^3}-\frac{b_1 b_2}{b_0^2}\right)g\right)}. \tag{53}
$$

With $\Lambda_{\overline{\text{MS}}}^{\text{NNLO}} = 334$ MeV.

B.2 Hard Thermal Loop framework

We detail the HTL formalism introduced first in chapter 5. Note that the two following subsections B.2.1 and B.2.2 has different conventions that should not be mixed. Each sections are self-consistent. The first one, following [4], is used in our work on the determination and resummation of the LL and NLL series seen in chapter 5, while the second is important for the evaluation of the HTL two loop diagram discussed in chapter 6 and follows the notation of [5]. We only detail the convention we used for our work on the LL and NLL series in section B.2.1.

B.2.1 One-loop $T = 0$ HTL pressure calculation

The one-loop HTL graph of Fig.(5.5) gives for the free energy :

$$\mathcal{F}_{\rm LO}^{\rm HTL} = \frac{-d_A}{2}\int_K ((d-1)\ln[\Delta_T(K)] + \ln[\Delta_L(K)])\,, \tag{54}$$

where $K^\mu = (K^0, \vec{k})$ is an Euclidean vector in $d+1$ dimensions. The propagator $\Delta_{T,L}$ depends on the gluon self-energy:

$$\Delta_{T,L}(K) \equiv \frac{1}{K^2 + \Pi_{T,L}}, \tag{55}$$

The scalar functions Π_T and Π_L being the transverse and longitudinal components of the one-loop HTL self-energy tensor :

$$\Pi^{\mu\nu}(K) = T^{\mu\nu}(\hat{K})\Pi_T(K) + L^{\mu\nu}(\hat{K})\Pi_L(K), \tag{56}$$

where the T, L projection operators are :

$$\begin{aligned} T^{\mu\nu}(\hat{K}) &\equiv \delta^{\mu i}\delta^{\nu j}\left(\delta^{ij} - \hat{k}^i\hat{k}^j\right) \\ L^{\mu\nu}(\hat{K}) &\equiv \delta^{\mu\nu} - \hat{K}^\mu\hat{K}^\nu - T^{\mu\nu}(\hat{K}). \end{aligned} \tag{57}$$

The HTL gluon self-energy is :

$$\Pi^{\mu\nu}(K) = m_g^2\int_{\hat{\mathbf{v}}}\left(\delta^{\mu 0}\delta^{\nu 0} - \frac{iK_0}{K\cdot V}V^\mu V^\nu\right). \tag{58}$$

Where $V^\mu \equiv (-i, \hat{\mathbf{v}})$ is a light-like vector, with $\hat{\mathbf{v}}$ a d-dimensional unit vector. The integration measure in d dimensions is defined as

$$\int_{\hat{\mathbf{v}}} \equiv \frac{h(d)}{2}\int_0^\pi d\theta_v sin^{d-2}(\theta_v) = \frac{h(d)}{2}\int_{-1}^1 dz_v(1-z_v^2)^{\frac{d-3}{2}}, \quad h(d) \equiv \frac{\Gamma(\frac{d}{2})}{\Gamma(\frac{3}{2})\Gamma(\frac{d-1}{2})} \tag{59}$$

where $z_v \equiv \hat{\mathbf{k}} \cdot \hat{\mathbf{v}}$. Taking the trace and 00 components of Eqn.(56), and Eqn.(58) with appropriate d-dimensional measures, leads to

$$\begin{aligned}
\Pi^{\mu\mu}(K) &= m_g^2 \int_{\hat{\mathbf{v}}} \delta^{00} = m_E^2 \\
\Pi^{00}(K) &= m_g^2 \left[1 + \int_{\hat{\mathbf{v}}} \frac{iK_0}{-iK_0 + |\hat{\mathbf{k}}| z_v} \right] \\
&= m_g^2 \left[1 - {}_2F_1 \left(\frac{1}{2}, 1, \frac{d}{2}; -\frac{|\hat{\mathbf{k}}|2}{K_0^2} \right) \right],
\end{aligned} \tag{60}$$

where ${}_2F_1$ is the Hypergeometric function, and where the final equality assumes $|\hat{\mathbf{k}}|/K_0 \in \mathbb{R}$ and $\mathrm{Re(d)} > 1$. Following notations of [4], we define

$$\begin{aligned}
\eta_a(x) &\equiv \frac{\partial}{\partial z} {}_2F_1 \left(\frac{1}{2}, 1, z; x \right) \Big|_{z=a} \\
\kappa_a(x) &\equiv \frac{\partial^2}{\partial^2 z} {}_2F_1 \left(\frac{1}{2}, 1, z; x \right) \Big|_{z=a}
\end{aligned} \tag{61}$$

which gives a compact expression for the ε expansion for the Π^{00} integral:

$$\Pi^{00}(K) = m_g^2 \left[1 + iK_0 \mathcal{L}(K) + \eta_{3/2} \left(-\frac{|\hat{\mathbf{k}}|^2}{K_0^2} \right) \varepsilon - \frac{1}{2} \kappa_{3/2} \left(-\frac{|\hat{\mathbf{k}}|^2}{K_0^2} \right) \varepsilon^2 + \mathcal{O}(\varepsilon) \right] \tag{62}$$

with the notation

$$\mathcal{L}(K) \equiv -\frac{1}{2|\hat{\mathbf{k}}|} \ln \left(\frac{iK_0 + |\hat{\mathbf{k}}|}{iK_0 - |\hat{\mathbf{k}}|} \right). \tag{63}$$

The scalar functions Π_T and Π_L, expanded up to $\mathcal{O}(\varepsilon^2)$, can be expressed as

$$\Pi_I(K) = \Pi_{I,0}(K) + \varepsilon\, \Pi_{I,1}(K) + \varepsilon^2\, \Pi_{I,2}(K) + \mathcal{O}(\varepsilon^3), \quad I \in \{T, L\} \tag{64}$$

where the coefficients above are given by

$$\begin{aligned}
\Pi_{L,0}(K) &= m_E^2 \frac{K^2}{|\hat{\mathbf{k}}|^2} \left[1 + iK_0 \mathcal{L}(K) \right], \\
\Pi_{L,1}(K) &= m_E^2 \frac{K^2}{|\hat{\mathbf{k}}|^2} \eta_{3/2} \left(-\frac{|\hat{\mathbf{k}}|^2}{K_0^2} \right), \\
\Pi_{L,2}(K) &= -m_E^2 \frac{K^2}{2|\hat{\mathbf{k}}|^2} \kappa_{3/2} \left(-\frac{|\hat{\mathbf{k}}|^2}{K_0^2} \right), \\
\Pi_{T,n}(K) &= \frac{1}{2} \left[m_E^2 - \sum_{i=0}^{n} \Pi_{L,i}(K) \right]
\end{aligned} \tag{65}$$

For computation, it turns out to be convenient to express these expressions in terms of the polar angle $\phi_K \equiv \|\mathbf{k}\|/K^0$.

$$\begin{aligned}\Pi_T(\phi_K) &= \frac{m_g^2}{2}\cot(\phi_K)\left[\arctan[\tan(\phi_K)]\csc^2(\phi_K) - \cot(\phi_K)\right] + \mathcal{O}(\varepsilon),\\ \Pi_L(\phi_K) &= m_g^2\csc^2(\phi_k)\left[1 - \arctan[\tan(\phi_K)]\cot(\phi_K)\right] + \mathcal{O}(\varepsilon).\end{aligned} \tag{66}$$

Note that $\arctan[\tan(\phi_K)] = \phi_K - \pi\cdot\theta(\phi_K - \pi/2)$ where θ denotes the Heaviside step function.

B.2.2 HTL two loop diagram

Fermion diagram at zero temperature and finite chemical potential.

Following Andersen et al. [5], the fermion diagram in fig5.4b reads in the mass expansion m_g (after using simplifications notably through Ward identities) :

$$\begin{aligned}\mathcal{P}_{3qg}^{(hh)} =& -\frac{d_A N_f}{2} m_g^2 g^2 \sum\!\!\!\!\!\!\int_{\{PQ\}}\left[\frac{d+1}{d-1}\frac{1}{P^2Q^2r^2} - \frac{4d}{d-1}\frac{q^2}{P^2Q^2r^4} - \frac{2d}{d-1}\frac{P\cdot Q}{P^2Q^2r^4}\right]\mathcal{I}_R\\ &- \frac{d_A N_f}{2} m_g^2 g^2 \sum\!\!\!\!\!\!\int_{\{PQ\}}\left[\frac{3-d}{d-1}\frac{1}{P^2Q^2R^2} + \frac{2d}{d-1}\frac{P\cdot Q}{P^2Q^2r^4} - \frac{d+2}{d-1}\frac{1}{P^2Q^2r^2}\right.\\ &\left. + \frac{4d}{d-1}\frac{q^2}{P^2Q^2r^4} - \frac{4}{d-1}\frac{q^2}{P^2Q^2r^2R^2}\right] + \mathcal{O}(g^2m_g^4).\end{aligned} \tag{67}$$

where we only selected the $g^2\, m_g^2$ term relevant for the discussion. The factor $\mathcal{I}_P$ reads:

$$\mathcal{I}_P = \frac{w(\varepsilon)}{2}\int_{-1}^{-1} dc(1-c^2)^{-\varepsilon}\frac{iP_0}{iP_0 - p\,c} = \frac{w(\varepsilon)}{2}\left\langle\frac{iP_0}{iP_0 - p\,c}\right\rangle_c, \qquad w(\varepsilon) = 2^{2\varepsilon}\frac{\Gamma(2-2\varepsilon)}{\Gamma(1-\varepsilon^2)}. \tag{68}$$

Every integrals appearing here were evaluated in [5] at finite temperature and zero chemical potential, then, in the limit $T \gg \mu$ using an expansion in μ/T in [6]. Here, however, we need these integrals in the strict $T \to 0$ and $\mu \neq 0$ limit. This means reevaluating the master integrals for strictly zero temperature and finite chemical potential. The major difference with the non-zero temperature evaluation lies in the fact that the previous change of variable $(p, q) \to (s, \beta)$ (see below), leads now to a non-trivial new integration boundary on the variable s : $\int_0^{\frac{1}{1+\sqrt{1-\beta}}}$. At non zero temperature, the boundary is ∞. The dependence on the s variable factorize trivially in calculations and thus we are left with basically the same master integrals but with an additional term $(\frac{1}{1+\sqrt{1-\beta}})^\alpha$ that we treat using Mellin-Barnes (MB) transformations. More information on MB and the vocabulary that we will use can be found in appendix C. Using the two identities $\left\langle\frac{\mathcal{I}_R}{r^2}\right\rangle = \left\langle\frac{1}{r^2}\right\rangle - \left\langle\frac{c^2}{R_c^2}\right\rangle$, $\left\langle\frac{\mathcal{I}_R}{r^4}\right\rangle = \left\langle\frac{1}{r^4}\right\rangle - \left\langle\frac{c^2}{R_c^2r^2}\right\rangle$, where $R_c^2 = r_0^2 + c^2r^2$, Eqn.(67) simplifies to:

$$\begin{aligned}\mathcal{P}_{3qg}^{(hh)} =& -\frac{d_A N_f}{2} m_E^2 g^2 \sum\!\!\!\!\!\!\int_{\{PQ\}}\left[\frac{d+1}{d-1}\frac{1}{P^2Q^2r^2} - \frac{d+1}{d-1}\left\langle\frac{c^2}{P^2Q^2R_c^2}\right\rangle_c + \frac{4d}{d-1}\left\langle\frac{q^2c^2}{P^2Q^2r^2R_c^2}\right\rangle_c\right.\\ &+ \frac{2d}{d-1}\left\langle\frac{P\cdot Q\,c^2}{P^2Q^2r^2R_c^2}\right\rangle_c\\ &\left. + \frac{3-d}{d-1}\frac{1}{P^2Q^2R^2} - \frac{d+2}{d-1}\frac{1}{P^2Q^2r^2} - \frac{4}{d-1}\frac{q^2}{P^2Q^2R^2r^2}\right].\end{aligned} \tag{69}$$

In $\overline{\rm MS}$ it reads for the final result:

$$\mathcal{P}_{3qg}^{(hh)} = -\frac{d_A N_f m_E^2 g^2 \mu^2}{256\,\pi^4}\left(\frac{M}{2\mu}\right)^{4\varepsilon}\left(\frac{1}{\varepsilon}+\mathcal{O}(\varepsilon^0)\right) \tag{70}$$

obtained from Eqn.(69) with:

$$I_1 \equiv \sum\!\!\!\!\!\!\int_{\{PQ\}} \frac{1}{P^2Q^2R^2} = \frac{\mu^2}{64\pi^4}\left(\frac{M}{2\mu}\right)^{4\varepsilon}\left(\frac{1}{\varepsilon}+6\right) \tag{71}$$

$$I_2 \equiv \sum\!\!\!\!\!\!\int_{\{PQ\}} \frac{1}{P^2Q^2r^2} = -\frac{\mu^2}{32\pi^4}\left(\frac{M}{2\mu}\right)^{4\varepsilon}\left(\frac{1}{\varepsilon}+8-2\ln 2\right) \tag{72}$$

$$I_3 \equiv \sum\!\!\!\!\!\!\int_{\{PQ\}} \frac{q^2}{P^2Q^2r^2R^2} = \frac{\mu^2}{768\pi^4}\left(\frac{M}{2\mu}\right)^{4\varepsilon}\left(\frac{1}{\varepsilon}\left(15-12\ln 2\right)+84-\pi^2-48\ln 2\right) \tag{73}$$

$$I_4 \equiv \sum\!\!\!\!\!\!\int_{\{PQ\}} \left\langle \frac{c^2}{P^2Q^2R_c^2}\right\rangle_c = \frac{\mu^2}{32\pi^4}\left(\frac{M}{2\mu}\right)^{4\varepsilon}\left(\frac{1}{\varepsilon}\left(-1+\ln 2\right)-8+\frac{5\pi^2}{24}+4\ln 2\right) \tag{74}$$

$$I_5 \equiv \sum\!\!\!\!\!\!\int_{\{PQ\}} \left\langle \frac{c^2q^2}{P^2Q^2R_c^2r^2}\right\rangle_c = \frac{\mu^2}{768\pi^4}\left(\frac{M}{2\mu}\right)^{4\varepsilon}\left(\frac{1}{\varepsilon}\left(-1+4\ln 2\right)+\mathcal{O}(\varepsilon^0)\right) \tag{75}$$

$$I_6 \equiv \sum\!\!\!\!\!\!\int_{\{PQ\}} \left\langle \frac{c^2\,P\cdot Q}{P^2Q^2R_c^2r^2}\right\rangle_c = \frac{\mu^2}{128\pi^4}\left(\frac{M}{2\mu}\right)^{4\varepsilon}\left(\frac{1}{\varepsilon}+10-2\ln 2\right). \tag{76}$$

Following [5], it is straightforward to derive I_1, I_2 and I_4 as long as we incorporates the modifications in the boundary integration on "s" after the change of variable from (p,q) to (s,β). For the three other integrals, some 2-cut parts need to be reevaluated as explained previously. We call 0-cut, 1-cut and 2-cut integrals, the integrals with 0,1 or 2 factor of n_F^- respectively. The sum can be carried, using the formula (B.39) of [5], for example:

$$\sum\!\!\!\!\!\!\int_{\{PQ\}} \frac{1}{P^2Q^2(R_0^2+r^2c^2)} = -\int_{\mathbf{p}}\frac{n_F(p)}{p}2\,\mathrm{Re}\int_Q \frac{1}{Q^2(R_0^2+r^2c^2}\bigg|_{P_0=-ip+0^+} + \int_{\mathbf{pq}}\frac{n_F(p)n_F(q)}{p\,q}\,\mathrm{Re}\,\frac{r^2c^2-p^2-q^2}{\Delta(p+i0^+,q,r\,c)}. \tag{77}$$

Where integral over 4-momentum $\int_Q$are carried at $T=\mu=0$. More precisely, at zero temperature, the integrals decomposition reads:

$$I_1 = \sum\!\!\!\!\!\!\int_{\{PQ\}} \frac{1}{P^2Q^2R^2} = \int_{\mathbf{p\,q}}\left(\frac{\theta(\mu-p)\theta(\mu-q)}{4p\,q}\right)\frac{2p\,q}{\Delta(p,q,r)} \tag{78}$$

$$I_2 = \sum\!\!\!\!\!\!\int_{\{PQ\}} \frac{1}{P^2Q^2r^2} = -2\int_{\mathbf{p}}\frac{\theta(\mu-p)}{2p}\int_Q\frac{1}{Q^2r^2} + \int_{\mathbf{p\,q}}\frac{\theta(\mu-p)\theta(\mu-q)}{4p\,q}\frac{1}{r^2} \tag{79}$$

$$\begin{aligned} I_3 =& \sum\!\!\!\!\!\!\int_{\{PQ\}} \frac{q^2}{P^2Q^2r^2R^2} = -\int_{\mathbf{p}}\frac{\theta(\mu-p)}{2p}\int_Q\frac{1}{Q^2R^2}\left(\frac{q^2}{r^2}+\frac{p^2}{q^2}\right)\bigg|_{P_0=-ip+0^+} \\ &+\int_{\mathbf{p\,q}}\frac{\theta(\mu-p)\,\theta(\mu-q)}{4p\,q}\frac{p^2}{r^2}\frac{r^2-p^2-q^2}{\Delta(p,q,r)}, \end{aligned} \tag{80}$$

$$
\begin{aligned}
I_4 =& \sum\!\!\!\!\!\!\int_{\{PQ\}} \left\langle \frac{c^2}{P^2Q^2R_c^2} \right\rangle_c = -2\int_{\mathbf{p}} \frac{\theta(\mu-p)}{2p} \,\mathrm{Re}\int_Q \frac{1}{Q^2} \left\langle \frac{c^2}{R_c^2} \right\rangle_c \Big|_{P_0=-ip+0^+} \\
&+ \int_{\mathbf{p}\,\mathbf{q}} \frac{\theta(\mu-p)\theta(\mu-q)}{4p\,q} \,\mathrm{Re}\left\langle \frac{c^2(r^2c^2-p^2-q^2)}{\Delta(p,q,r\,c)} \right\rangle_c
\end{aligned} \tag{81}
$$

$$
\begin{aligned}
I_5 = \sum\!\!\!\!\!\!\int_{\{PQ\}} \left\langle \frac{c^2\,q^2}{P^2Q^2R_c^2r^2} \right\rangle_c =& -\int_{\mathbf{p}} \frac{\theta(\mu-p)}{2p} \left\langle \mathrm{Re}\int_Q \frac{c^2(p^2+q^2)}{Q^2r^2(R_0^2+r^2c^2)}\Big|_{P_0=-ip+0^+} \right\rangle_c \\
&+ \int_{\mathbf{p}\,\mathbf{q}} \frac{\theta(\mu-p)\theta(\mu-q)}{4p\,q} \frac{q^2}{r^2} \left\langle \mathrm{Re}\,\frac{c^2(r^2c^2-p^2-q^2)}{\Delta(p+i0^+,q,r\,c)} \right\rangle_c .
\end{aligned} \tag{82}
$$

Where $\Delta(p,q,r) = p^4+q^4+r^4-2(p^2q^2+q^2r^2+p^2r^2) = -4p^2q^2(1-x^2)$ and x is the angle between p and q. For I_6, we proceed first with some algebra simplifications:

$$
\begin{aligned}
I_6 =& \sum\!\!\!\!\!\!\int_{\{PQ\}} \left\langle \frac{c^2\,P\cdot Q}{P^2Q^2R_c^2r^2} \right\rangle_c = \sum\!\!\!\!\!\!\int_{\{PQ\}} \left\langle \frac{c^2}{2P^2Q^2R_c^2} \right\rangle_c + \sum\!\!\!\!\!\!\int_{\{PQ\}} \left\langle \frac{c^2}{2P^2Q^2r^2} \right\rangle_c \\
&- \sum\!\!\!\!\!\!\int_{\{PQ\}} \left\langle \frac{c^4}{2P^2Q^2R_c^2} \right\rangle_c - \sum\!\!\!\!\!\!\int_{\{Q\}} \sum\!\!\!\!\!\!\int_{R_\mu} \left\langle \frac{c^2}{Q^2R_c^2r^2} \right\rangle_c ,
\end{aligned} \tag{83}
$$

where R_μ means bosonic Matsubara frequencies shifted by $-2i\mu$. This term is straightforward to evaluate, it leads to modified Bose-Einstein distribution whose limit when $T\to 0, \mu\neq 0$ is non-zero, but the result is a pure imaginary contribution. The first term in (83) is $I_4/2$ while the second is $\langle c^2\rangle_c I_2/2$. Finally, the last term decompose into:

$$
\begin{aligned}
\sum\!\!\!\!\!\!\int_{\{PQ\}} \frac{c^4}{P^2Q^2R_c^2} =& -2\int_{\mathbf{p}} \frac{\theta(\mu-p)}{2p} \left\langle \mathrm{Re}\int_Q \frac{c^4}{Q^2(R_0^2+c^2r^2)}\Big|_{P_0=-ip} \right\rangle_c \\
&+ \int_{\mathbf{p}\,\mathbf{q}} \frac{\theta(\mu-p)\theta(\mu-q)}{4p\,q} \,\mathrm{Re}\left\langle \frac{c^4(r^2c^2-p^2-q^2)}{\Delta(p,q,r\,c)} \right\rangle_c .
\end{aligned} \tag{84}
$$

All one-cut integrals and two-cut integrals are given below giving back (71)-(76).

One-cut formula

$$
\int_Q \frac{1}{Q^2r^2} \frac{1}{(4\pi)^2} M^{2\varepsilon} p^{-2\varepsilon} 2 \left(\frac{1}{\varepsilon} + 4 - 2\ln 2 \right) \tag{85}
$$

$$
\int_Q \frac{q^2}{Q^2R^2r^2}\Big|_{P_0=-ip} = \frac{1}{(4\pi)^2} \mu^{2\varepsilon} p^{-2\varepsilon} (-1) \left(\frac{1}{\varepsilon^2} + \frac{1-2\ln 2}{\varepsilon} + 10 - 2\ln 2 + 2\ln^2 2 - \frac{7\pi^2}{12} \right) \tag{86}
$$

$$
\int_Q \frac{1}{Q^2R^2q^2} = \frac{1}{(\pi)^2} \mu^{2\varepsilon} p^{-2-2\varepsilon} \left(\frac{1}{\varepsilon} - 2 - 2\ln 2 \right) \tag{87}
$$

$$
\mathrm{Re}\int_Q \frac{1}{Q^2} \left\langle \frac{c^2}{R_c^2} \right\rangle_c = \frac{1}{(4\pi)^2} M^{2\varepsilon} p^{-2\varepsilon} \left(\frac{2(1-\ln 2)}{\varepsilon} + 4\left(2 - \ln 2 + \ln^2 2\right) - \frac{\pi^2}{2} \right) \tag{88}
$$

$$
\mathrm{Re}\int_Q \frac{1}{Q^2r^2} \left\langle \frac{c^2}{R_c^2} \right\rangle_c = \frac{1}{(4\pi)^2} \mu^{2\varepsilon} p^{-2-2\varepsilon} \left(-\frac{1}{4} \right) \left(\frac{1}{\varepsilon} + \frac{4}{3} + \frac{2}{3}\ln 2 \right) \tag{89}
$$

$$
\mathrm{Re}\int_Q \frac{q^2}{Q^2r^2} \left\langle \frac{c^2}{R_c^2} \right\rangle_c = \frac{1}{(4\pi)^2} \mu^{2\varepsilon} p^{-2\varepsilon} \left(\frac{13-16\ln 2}{12\varepsilon} + \frac{29}{9} - \frac{19}{18}\ln 2 + \frac{8}{3}\ln^2 2 - \frac{4}{9}\pi^2 \right) \tag{90}
$$

$$\mathrm{Re}\int_Q \frac{1}{Q^2}\left\langle \frac{c^4}{R_c^2}\right\rangle_c = \frac{1}{(4\pi)^2}\mu^{2\varepsilon}p^{-2\varepsilon}\left(\frac{5-6\ln 2}{3\varepsilon}+\frac{52}{9}-2\ln 2+4\ln^2 2-\frac{\pi^2}{2}\right) \tag{91}$$

Two-cut integrals

The two-cut integrals appearing in I_1, I_2 are straightforward to evaluate and with (85) it gives back (71) and (72). The 2-cut integrals appearing in I_4 can be analytically integrated over x and c giving:

$$\begin{aligned} I_{4,2c} &= \int_{\mathbf{pq}} \frac{\theta(\mu-p)\theta(\mu-q)}{4p\,q}\,\mathrm{Re}\left\langle \frac{c^2(c^2r^2-p^2-q^2)}{\Delta(p,q,r\,c)}\right\rangle_c \\ &= \left(\frac{\mu^2}{16\pi^4}\right)\left(\frac{-1}{8}\right)\int_0^1 dp\int_0^1 dq\,\left(\ln\gamma+\frac{(1-\gamma)}{\sqrt{\gamma}}\ln\left(\frac{1+\sqrt{\gamma}}{1-\sqrt{\gamma}}\right)\right), \end{aligned} \tag{92}$$

with $\gamma=\left(\frac{p-q}{p+q}\right)^2$. The remaining integrals gives $(\frac{\pi^2}{6}-4\ln 2)$, so we end up with:

$$I_{4,2c} = -\frac{\mu^2}{768\pi^4}\left(\pi^2-24\ln 2\right). \tag{93}$$

However, $I_{3,2c}$ and $I_{5,2c}$ possesses at least one degree of divergence in ε thus cannot be integrated numerically. We will proceed with the evaluation of $I_{3,2c}$, being the easiest one, and give instructions for the evaluation of $I_{5,2c}$ (the latter being the most complicated one). Using,

$$\left\langle \frac{q^2}{r^2}\frac{(r^2-p^2-q^2)}{\Delta(p,q,r)}\right\rangle_x = -\frac{1}{2\varepsilon}\left\langle\frac{q^2}{r^4}\right\rangle_x, \tag{94}$$

we have

$$\begin{aligned} I_{3,2c} &\equiv \int\frac{d^dp\,d^dq}{(2\pi)^{2d}}\frac{\theta(\mu-p)\theta(\mu-q)}{4p\,q}\left(\frac{-1}{2\varepsilon}\right)\left\langle\frac{q^2}{r^4}\right\rangle_x \\ &= -\left(\frac{\Omega_d}{(2\pi)^d}\right)^2\frac{\mu^{2-4\varepsilon}}{128\varepsilon}\frac{w(\varepsilon)}{2}\int_{-1}^1 dz\,(1-z^2)^{-\varepsilon}\int_0^1 d\beta\int_0^{\frac{1}{1+\sqrt{1-\beta}}} ds\,s^{1-4\varepsilon}\beta^{1-2\varepsilon}(1-\beta)^{-1/2}\frac{2-\beta}{8(1-y\,\beta)^2} \end{aligned} \tag{95}$$

where we proceeded to the change of variable $(p,q)\to(s,\beta)$ with $s=\frac{p+q}{2}$, $\beta=\frac{p\,q}{s^2}$, $y=\frac{1-z}{2}$. This change of variable leads to a non-trivial upper-bound of integration at zero temperature. One must make the difference between the two regions of integration $p<q$ and $p>q$ where $(p=s_+,q=s_-)$ and $(p=s_-,q=s_+)$, $s_\pm=s(1\pm\sqrt{1-\beta})$. In Eqn.(95), it leads to the suppression of a term $\propto(1-\sqrt{1-\beta})$ and an overall factor of two. Now, one can proceed to the trivial "s" integral. The "s" integration leads to a factor of $(1+\sqrt{1-\beta})^{4\varepsilon-2}$ which we simplify using Mellin-Barnes transformation (see appendix C). From now on, "s" will designate the MB variable:

$$\left(1+\sqrt{1-\beta}\right)^{4\varepsilon-2} = \frac{1}{\Gamma(2-4\varepsilon)}\int_{\mathcal{C}} ds\,\Gamma(-s)\Gamma(2-4\varepsilon+s)(1-\beta)^{s/2}. \tag{96}$$

Once implemented into (95), the β integral can be recognized as an Hypergeometric function ${}_2F_1$:

$$I_{3,2c} = \left(\frac{\Omega_d}{(2\pi)^d}\right)^2 \frac{\mu^{2-4\varepsilon}}{128\varepsilon(2-4\varepsilon)} \frac{w(\varepsilon)}{2} \int_{-1}^{1} dz \int_{\mathcal{C}} ds \frac{(1-z^2)^{-\varepsilon}\Gamma(-s)\Gamma(\frac{1}{2}+\frac{s}{2})\Gamma(2+s-4\varepsilon)}{128\,\varepsilon(-1+2\varepsilon)\Gamma(2-4\varepsilon)} \times \left(\frac{\Gamma(2-2\varepsilon)}{\Gamma(\frac{5}{2}+\frac{s}{2}-2\varepsilon)}\, {}_2F_1\left(\begin{matrix}2,\ 2-2\varepsilon \\ \frac{5}{2}+\frac{s}{2}-2\varepsilon\end{matrix}\middle| y\right) - \frac{\Gamma(3-2\varepsilon)}{2\Gamma(\frac{7}{2}+\frac{s}{2}-2\varepsilon)}\, {}_2F_1\left(\begin{matrix}2,\ 3-2\varepsilon \\ \frac{7}{2}+\frac{s}{2}-2\varepsilon\end{matrix}\middle| y\right) \right). \tag{97}$$

Using the change of variable $z = 1-2t$, $t = y$, we recognize, via (123), the integral over t as a ${}_3F_2$ at unity. Using (127), both Hypergeometric can be simplified to ${}_2F_1$ and then one can use Gauss's summation theorem (125) to further simplify to gamma functions:

$$I_{3,2c} = -\left(\frac{\Omega_d}{(2\pi)^d}\right)^2 \frac{\mu^{2-4\varepsilon}}{\varepsilon} \frac{1}{\Gamma(\frac{3}{2}-2\varepsilon)} \int_{\mathcal{C}} ds \frac{2^{-5+s}\left((1+s)^2-4(2+s)\varepsilon+4\varepsilon^2\right)\Gamma(-s)\Gamma(\frac{1+s}{2})\Gamma(1+\frac{s}{2}-2\varepsilon)}{(-1+s-2\varepsilon)(1+s-2\varepsilon)(3+s-2\varepsilon)}. \tag{98}$$

We choose to close the contour on the right enclosing the poles of $\Gamma(-s)$, a rising gamma, and $\frac{1}{-1+s-2\varepsilon}$ which comes from a lowering gamma. Thus, using residue theorem, we have to sum over all poles of $\Gamma(-s)$ and subtract the spurious pole in $s = 1+2\varepsilon$ which pinches the contour in the $\varepsilon \to 0$ limit (see figC.4). Evaluating first the pole in $s = 0, 1, 1+2\varepsilon$ we find:

$$\begin{aligned} s=0:&\ \frac{1}{192\pi^4\varepsilon} + \frac{2-24\ln 2}{576\pi^4} \\ s=1:&\ -\frac{1}{256\pi^4\varepsilon^2} + \frac{-5+8\ln 2}{512\pi^4\varepsilon} + \frac{-17+2\pi^2+40\ln 2-32\ln^2 2}{1024\pi^2} \\ s=1+2\varepsilon:&\ -\frac{1}{256\pi^4\varepsilon^2} + \frac{-3+4\ln 2}{256\pi^4\varepsilon} + \frac{-96+5\pi^2+72\ln 2-48\ln^2 2}{1536\pi^4}. \end{aligned} \tag{99}$$

Now, we can expand (98) in series of ε:

$$\begin{aligned} I^{\varepsilon}_{3,2c} = csc(\pi s)\Bigg(&\frac{(1+s)}{64\pi^3(-3+2s+s^2)\varepsilon} \\ &+ \frac{(-1+s(13+4s)(-1+s+s^2)-(-1+s)(1+s)^2(3+s)\mathcal{H}(\frac{s}{2}))}{32\pi^3(-1+s)^2(1+s)(3+s)^2}\Bigg) \\ &+ csc(\pi s)\frac{-4s(2+s)(-2+s(2+s))\ln(2)+12\ln 2}{32\pi^3(-1+s)^2(1+s)(3+s)^2}. \end{aligned} \tag{100}$$

The pole in this expression now only comes from $\csc(\pi s)$ whose residue are: $\csc(\pi s) = \frac{(-1)^s}{\pi}$. Evaluating the sum from 2 to infinity can be done using mathematica. The sum over harmonic numbers is in general not recognized but using its integral representation:

$$\mathcal{H}(z) = \int_0^1 dx\, \frac{1-x^z}{1-x}, \tag{101}$$

it can be easily evaluated. Note that the same trick can be used for digamma functions which also appear recurrently:

$$\psi(0,z) = \mathcal{H}(z-1) - \gamma_E. \tag{102}$$

The results for the sum from 2 to infinity then reads:

$$\sum_{s=2}^{\infty} \mathrm{Res}(I_{3,2c}) = \frac{42 - 144\ln 2}{9216\pi^4\varepsilon} + \frac{-23 - 552\ln 2 + 576\ln^2 2}{9216\pi^4}. \tag{103}$$

Grouping up the results, and reintroducing the factor μ, $\overline{MS}$ and $2^{4\varepsilon}$:

$$I_{3,2c} = \mu^2 \left(\frac{M}{2\mu}\right)^{4\varepsilon} \left(\frac{-1}{128\pi^4\varepsilon^2} - \frac{3+4\ln 2}{256\pi^4\varepsilon} + \frac{\pi^2 - 3(5+4\ln 2)}{192\pi^4}\right). \tag{104}$$

Adding (104), (86) and (87) we find (80) where the divergence proportional to ε^{-2} cancel out which is a non-trivial crosscheck. We found the integral $I_{6,2c}$ to have no divergence at all, so the evaluation can be carried out numerically.

$$I_{6,2c} \equiv \int_{\mathbf{pq}} \frac{\theta(\mu-p)\theta(\mu-q)}{4p\,q}\,\mathrm{Re}\left\langle \frac{c^4(r^2c^2 - p^2 - q^2)}{\Delta(p,q,r\,c)} \right\rangle_c \tag{105}$$

However, using MB method, we manage to find an analytic expression in perfect agreement. The first step is to simplify the quotient:

$$\frac{r^2c^2 - p^2 - q^2}{\Delta(p + i0^+, q, r\,c)} = -\frac{1}{2}\sum_{\pm} \frac{1}{(p + i0^+ \pm q)^2 - r^2c^2}, \tag{106}$$

then to integrate over c :

$$\left\langle \frac{c^4}{(p + i0^+ \pm q)^2 - r^2c^2} \right\rangle_c = \frac{3}{(3-2\varepsilon)(5-2\varepsilon)} \frac{1}{(p + i0^+ \pm q)^2}\, {}_2F_1\left(\begin{matrix}\frac{5}{2},\ 1\\ \frac{7}{2} - \varepsilon\end{matrix}\,\middle|\, \frac{r^2}{(p + i0^+ \pm q)^2}\right). \tag{107}$$

In the case $(p + q + i0^+)$, the 0^+ is not needed, but it is required for the case $(p - q)$. Then we proceed to the change of variable (s, β) which send the argument of the Hypergeometric to $1 - y\,\beta$. Using then (124) we can reproduce the same steps as for $I_{3,2c}$. Unfortunately, all the Hypergeometric functions do not disappear this time and we are left with remaining ${}_3F_2$. However, using (128) we can recast these Hypergeometric in a much more convenient form. For example:

$${}_3F_2\left(\begin{matrix}\frac{5}{2},\ 1,\ 1-\varepsilon\\ 1+\varepsilon,\ \frac{3-s}{2}\end{matrix}\,\middle|\, 1\right) = \frac{\Gamma(\frac{3}{2} - \frac{s}{2})\Gamma(-2 - \frac{s}{2} + 2\varepsilon)}{\Gamma(-1 - \frac{s}{2})\Gamma(\frac{1}{2} - \frac{s}{2} + 2\varepsilon)}\, {}_3F_2\left(\begin{matrix}\frac{5}{2},\ \varepsilon,\ 2\varepsilon\\ 1+\varepsilon,\ \frac{1}{2} - \frac{s}{2} + 2\varepsilon\end{matrix}\,\middle|\, 1\right). \tag{108}$$

The ratio test for these Hypergeometric reads respectively: $\mathcal{S}_{(1)} = 4\varepsilon - 4 - s$ and $\mathcal{S}_{(2)} = 2 + s$, thus, we factorized a part of the divergence (in the variable s) in the gamma function that multiplies the Hypergeometric, but the remaining ${}_3F_2$ still has a divergence. The trick is that this new Hypergeometric possesses two arguments of order $\mathcal{O}(\varepsilon)$, then the associated pochhammer contributes as $\Gamma(\varepsilon)^{-1}\Gamma(2\varepsilon)^{-1}$. Except for the case $k = 0$ in the series representation of the hypergeometric. Then, only the term $k = 0$ (which is equal to one) contributes to the order

$\mathcal{O}(\varepsilon^0)$. So we can rewrite the Hypergeometric as:

$$ {}_3F_2\left(\begin{matrix}\frac{5}{2},\ 1,\ 1-\varepsilon \\ 1+\varepsilon,\ \frac{3-s}{2}\end{matrix}\middle|\, 1\right) = \frac{\Gamma(\frac{3}{2}-\frac{s}{2})\Gamma(-2-\frac{s}{2}+2\varepsilon)}{\Gamma(-1-\frac{s}{2})\Gamma(\frac{1}{2}-\frac{s}{2}+2\varepsilon)} \times \left(1+\mathcal{O}(\varepsilon^2)\right). \tag{109} $$

As the global coefficient of this Hypergeometric is not of order $\mathcal{O}(\varepsilon^{-2})$ the first order in ε is enough for our current order of interest in ε. This trick will also be used for $I_{5,2c}$ as explained below. Equipped with these transformations, it is pretty much similar to $I_{3,2c}$ and so we end up with the results (separating the case $(p+q)$ from $(p-q)$ using the upper index $\pm$):

$$ \begin{aligned} I^{+}_{6,2c} =& \mu^2 \left(\frac{6-\pi^2+4\ln 2}{384\pi^4}\right) \\ I^{-}_{6,2c} =& \mu^2 \left(\frac{-4+\pi^2}{768\pi^4}\right) \\ I_{6,2c} = I^{+}_{6,2c} + I^{-}_{6,2c} =& \mu^2 \left(\frac{8-\pi^2+8\ln 2}{768\pi^4}\right). \end{aligned} \tag{110} $$

Attempting to solve $I_{5,2c}$ now, require first to simplify the quotient

$$ I_{5,2c} \equiv \int_{\mathbf{p}\,\mathbf{q}} \frac{\theta(\mu-p)\theta(\mu-q)}{4p\,q}\frac{q^2}{r^2}\,\mathrm{Re}\left\langle \frac{c^2(r^2c^2-p^2-q^2)}{\Delta(p,q,r\,c)}\right\rangle_c, \tag{111} $$

first by rewriting $q^2 = \frac{r^2+q^2-p^2-2\mathbf{p}\cdot\mathbf{q}}{2} = \frac{1}{2} - \frac{\mathbf{p}\cdot\mathbf{q}}{r^2}$, where we dropped the q^2-p^2 integral as it is purely imaginary. Then we use the identities

$$ \begin{aligned} \left\langle c^2\frac{\mathbf{p}\cdot\mathbf{q}}{r^2}\frac{(r^2c^2-p^2-q^2)}{\Delta(p,q,r\,c)}\right\rangle_{c,x} =& -\frac{p^2+q^2}{p^2-q^2}\langle c^2\rangle_c - \frac{1}{2}\sum_{\pm}\frac{1}{(p\pm q)^2}\left\langle\frac{c^4\,\mathbf{p}\cdot\mathbf{q}}{(p\pm q)^2-r^2c^2}\right\rangle_{c,x} \\ \left\langle\frac{c^2(r^2c^2-p^2-q^2)}{\Delta(p,q,r\,c)}\right\rangle_{c,x} =& -\frac{c^2}{2}\sum_{\pm}\frac{1}{(p+i\varepsilon\pm q)^2-r^2c^2}, \end{aligned} \tag{112} $$

to get, using $\langle c^2\rangle = \frac{1}{3-2\varepsilon}$:

$$ \begin{aligned} I_{5,2c} = \left(\frac{\Omega_d}{(2\pi)^d}\right)^2 \int_0^\mu dp \int_0^\mu dq \frac{1}{4p\,q}(p\,q)^{1-2\varepsilon}\Bigg(& -\frac{c^2}{4}\left\langle\sum_{\pm}\frac{1}{(p+i\varepsilon\pm q)^2-r^2c^2}\right\rangle_{c,x} \\ & + \frac{p^2+q^2}{(p-q+i\varepsilon)^2}\frac{1}{3-2\varepsilon}\left\langle\frac{\mathbf{p}\cdot\mathbf{q}}{r^2}\right\rangle_x \\ & + \frac{1}{2}\sum_{\pm}\frac{1}{(p+i\varepsilon\pm q)^2}\left\langle\frac{c^4\,\mathbf{p}\cdot\mathbf{q}}{(p\pm q)^2-r^2c^2}\right\rangle_{c,x}\Bigg). \end{aligned} \tag{113} $$

In this equation, the second term ($I^{pq}_{5,2c}$) and the case $(p-q)$ of the last term ($I^{c^4,-}_{5,2c}$) are divergent whereas all others ($I^{c^4,+}_{5,2c}$,$I^{c^2,\pm}_{5,2c}$) are finite and can be evaluated numerically or using

MB transformation. They read:

$$\begin{aligned} I_{5,2c}^{c^2,+} &= \mu^2 \left(\frac{12\ln 2 - \pi^2}{768\pi^4} \right) \\ I_{5,2c}^{c^2,-} &= \frac{\mu^2}{1536\pi^2} \\ I_{5,2c}^{c^4,+} &= \mu^2 \left(\frac{\pi^2 - 6(-5 + 2\ln^2 2 + 8\ln 2)}{4608\pi^4} \right). \end{aligned} \tag{114}$$

The integral $I_{5,2c}^{pq}$ can be readily evaluated following the same steps as for $I_{3,2c}$ using first:

$$\left\langle \frac{\mathbf{p}\cdot\mathbf{q}}{r^2} \right\rangle_x = \frac{1}{8}\beta \left({}_2F_1\left(\begin{matrix} 1-\varepsilon,\ 1 \\ 3-2\varepsilon \end{matrix} \middle| 1 \right) - {}_2F_1\left(\begin{matrix} 2-\varepsilon,\ 1 \\ 3-2\varepsilon \end{matrix} \middle| 1 \right) \right). \tag{115}$$

We find after all integration:

$$I_{5,2c}^{pq} = -\mu^2 \left(\frac{M}{2\mu} \right)^{4\varepsilon} \left(\frac{1}{384\pi^4\varepsilon^2} + \frac{11}{1152\pi^4\varepsilon} + \frac{422 - 21\pi^2}{6912\pi^4} \right). \tag{116}$$

The very last contribution, $I_{5,2c}^{c^4,-}$, remains uncertain at the moment. While we obtained with certainty the order $\mathcal{O}(\varepsilon^{-2})$ and $\mathcal{O}(\varepsilon^{-1})$, the finite coefficient gives unnatural number that has not been fully crosschecked yet. At the moment, we have:

$$I_{5,2c}^{c^4,-} = \mu^2 \left(\frac{M}{2\mu} \right)^{4\varepsilon} \left(\frac{1}{384\pi^4\varepsilon^2} + \frac{17 - 6\ln 2}{1152\pi^4\varepsilon} + \mathcal{O}(\varepsilon^0) \right). \tag{117}$$

Finally,

$$I_{5,2c} = \mu^2 \left(\frac{M}{2\mu} \right)^{4\varepsilon} \left(\frac{1 - \ln 2}{192\pi^4\varepsilon} + \mathcal{O}(\varepsilon^0) \right). \tag{118}$$

Notice again, the non-trivial check that $\mathcal{O}(\varepsilon^{-2})$ disappears.

C.3 Mellin-Barnes transformation, contour integration and Hypergeometric functions

Mellin-Barnes transformation is a generalization of the binomial theorem, it allows to separate terms of the forms $(x+y)^\nu$ into $y^s x^{\nu-s}$ much more easier to handle with dimensional regularization. Concretely,

$$(x+y)^\nu = \frac{1}{\Gamma(-\nu)} \frac{1}{2\pi i} \int_{\mathcal{C}} ds\, \frac{y^s}{x^{-\nu+s}} \Gamma(-s)\Gamma(-\nu+s). \tag{119}$$

See for example [7] for a complete overview of the Mellin transform and generalized Hypergeometric functions. We will call *lowering gammas*, the gamma functions with pole going from zero to minus infinity in the left complex plane, such as $\Gamma(s)$, in opposition to *rising gammas*, such as $\Gamma(-s)$, whose poles go from zero to infinity in the right complex plane. The contour of integration $\mathcal{C}$ has to be chosen such that it separates the poles of rising and lowering gammas, see C.4. The coefficient of the all-order expansion is encoded in the pole of the gamma

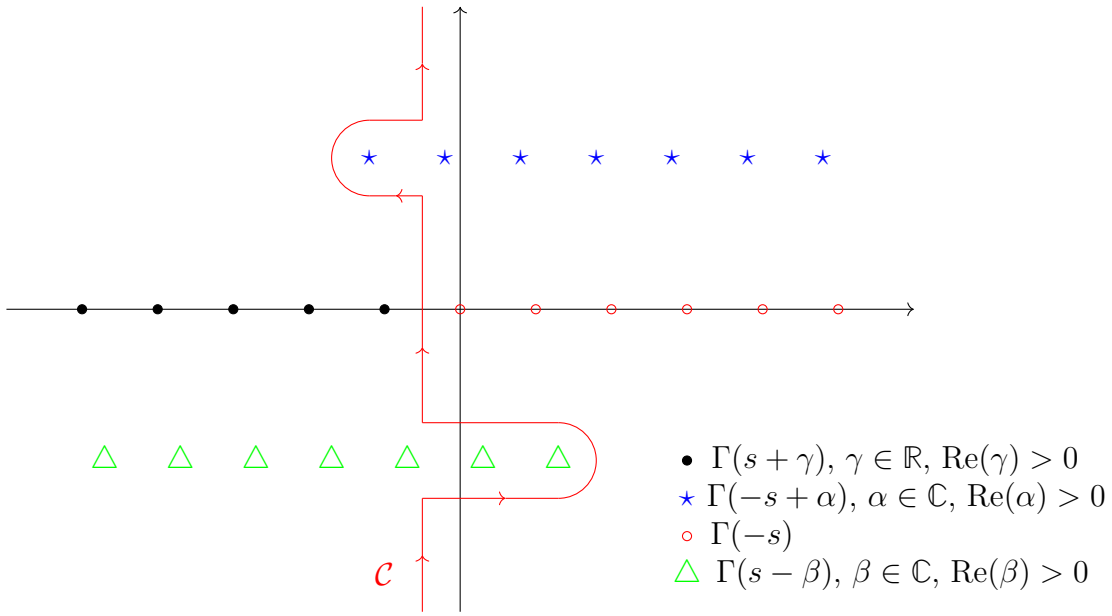

Figure C.4: General contour of integration for a Mellin-Barnes transformation

functions that we need to carefully integrate. To choose on which side one should close the contour entirely depends on the convergence properties of the integrand. In the trivial example in Eqn.(119), if $x \leq y$, one has to close the contour on the left, while for $x \geq y$ it needs to closed on the right. However, as the MB integral will be the last one to be carried out, the integrand will become far more complicated and we will have to study the convergence properties of the Hypergeometric and gamma functions that will appear. More information on Hypergeometric functions can be found below. On the example drown above, it was asserted that all poles from the different gamma functions could be well separated at all time so that the definition of the contour is unambiguous. But it could happen that the first pole of a rising and a lowering gamma are only separated by ε, the dimensional regularization parameter. Concretely, the situation drown on fig. C.4 for the two series of gammas $\Gamma(-s)$ and $\Gamma(s-\beta)$ with $\beta \to 1+2\varepsilon$. As long as $\varepsilon \neq 0$, the contour, even though being wiggly, can be defined, but it is no longer the case in the limit $\varepsilon \to 0$. In this case, the pole of the lowering gamma is pinching the contour on the first two poles of the rising gamma. The commutativity of the Mellin-Barnes integral and the limit is lost. One must then identify these *spurious* poles, that cross the contour, and integrate them before the limit is taken or before the expansion in ε. Finally, upon choosing the side of the complex plane in which one will close the contour, one has to subtract the contribution of these spurious poles. In this example, if we close the contour to the right, it would means taking the residue of the first two poles of $\Gamma(-1+s+2\varepsilon)$ and subtracting them to the contribution of the poles of $\Gamma(-s)$.

C.3.1 Hypergeometric Functions

The generalized Hypergeometric function ${}_pF_q(z)$ is an analytic function of one variable with $p+q$ parameter. Its most common representation is the generalized Hypergeometric series

$$ {}_pF_q(z) \equiv {}_pF_q\left(\begin{matrix}\alpha_1,\ \alpha_2,\ \ldots,\ \alpha_p \\ \beta_1,\ \ldots,\ \beta_q\end{matrix}\middle| z\right) = \sum_{n=0}^{\infty} \frac{(\alpha_1)_n (\alpha_2)_n \ldots (\alpha_p)_n}{(\beta_1)_n \ldots (\beta_q)_n} \frac{z^n}{n!}, \tag{120} $$

where $(a)_b$ is the Pochhammer's symbol:

$$(a)_b = \frac{\Gamma(a+b)}{\Gamma(b)}. \tag{121}$$

Obviously, if an upward parameter is equal to a downard parameter, they cancel out. The series is defined on the disk $|z| < 1$ and by analytic continuation elsewhere. On the circle $|z| = 1$, it converges if $p \leq q$, diverges for $p \geq q+2$, and the convergence for $p = q+1$ is dictated by the ratio test

$$\mathcal{S} = \sum_{i=1}^{q} \beta_i - \sum_{i=1}^{p} \alpha_i. \tag{122}$$

The series converges only for $\mathrm{Re}(\mathcal{S}) > 0$. Hypergeometric functions of order (p, q) can be related to an higher order $(p+1, q+1)$ one by integration:

$${}_{p+1}F_{q+1}\left(\begin{matrix}\alpha_1,\ \alpha_2,\ \ldots,\ \alpha_p,\ \nu \\ \beta_1,\ \ldots,\ \beta_q,\ \mu+\nu\end{matrix}\middle|\, z\right) = \int_0^1 dt\, t^{\nu-1}\,(1-t)^{\mu-1}\,{}_pF_q\left(\begin{matrix}\alpha_1,\ \ldots,\ \alpha_p \\ \beta_1,\ \ldots,\ \beta_q\end{matrix}\middle|\, t\,z\right). \tag{123}$$

Hypergeometric at $z = x$ can be related to other Hypergeometric at $z = 1-x$:

$$\begin{aligned}{}_2F_1\left(\begin{matrix}\alpha_1,\ \alpha_2 \\ \beta_1\end{matrix}\middle|\, x\right) &= \frac{\Gamma(\beta_1)\Gamma(\beta_1-\alpha_1-\alpha_2)}{\Gamma(\beta_1-\alpha_1)\Gamma(\beta_1-\alpha_2)}\,{}_2F_1\left(\begin{matrix}\alpha_1,\ \alpha_2 \\ \alpha 1+\alpha_2+1-\beta_2\end{matrix}\middle|\, 1-x\right) \\ &+ \frac{\Gamma(\beta_1)\Gamma(\alpha_1+\alpha_2-\beta_1)}{\Gamma(\alpha_1)\Gamma\alpha_2)}(1-x)^{\beta_1-\alpha_1-\alpha_2}\,{}_2F_1\left(\begin{matrix}\beta_1-\alpha_1,\ \beta_1-\alpha_2 \\ 1+\beta_1-\alpha_1-\alpha_2\end{matrix}\middle|\, 1-x\right)\end{aligned} \tag{124}$$

The particular Hypergeometric function ${}_2F_1(z)$, the Gauss series, can be cast in analytical functions for some specific values of the parameter and/or the argument. The one of interest for us is Gauss's summation theorem

$${}_2F_1\left(\begin{matrix}a,\ b \\ c\end{matrix}\middle|\, 1\right) = \frac{\Gamma(c)\Gamma(c-a-b)}{\Gamma(c-a)\Gamma(c-b)}, \tag{125}$$

which is used extensively in our calculations. Such relation also exist for Hypergeometric ${}_3F_2$ at unity but it involves Clebsch-Gordan coefficients which are unpractical for summation. We are not aware of such relations for higher order Hypergeometric functions. The MB framework requires to perform summation of Hypergeometric function of the form:

$$\sum_{s=0}^{\infty} \frac{\left(\prod_i\ \Gamma(\alpha_i+s)\right)\,{}_pF_q\left(\begin{smallmatrix}a_1,\,a_2,\,\ldots,\,a_p \\ b_1,\,\ldots,\,b_{p-1},\,c+s\end{smallmatrix}\middle|\, 1\right)}{\prod_i \Gamma(\beta_i+s)}, \tag{126}$$

which, to the best of our knowledge, is impossible to perform. Thus motivating the introduction of the following transformation formula on Hypergeometric to cast them into a summable form. The first one relates Hypergeometric (p, q) at unity to a $(p-1, q-1)$, also at unity, for contiguous

parameters:

$$
{}_pF_q\left(\begin{matrix}\alpha_1,\ \ldots,\ \alpha_{f-1},\ c+1,\ \alpha_f,\ \ldots,\ \alpha_j\\ \beta_1,\ \ldots,\ \beta_{k-1},\ c,\ \beta_k,\ \ldots,\ \beta_l\end{matrix}\middle|\,1\right) = {}_{p-1}F_{q-1}\left(\begin{matrix}\alpha_1,\ \ldots,\ \alpha_{f-1},\ \alpha_f,\ \ldots,\ \alpha_j\\ \beta_1,\ \ldots,\ \beta_{k-1},\ \beta_k,\ \ldots,\ \beta_n\end{matrix}\middle|\,1\right)
$$
$$
+\frac{\prod_{i=1}^{j}\alpha_i}{c\prod_{p=1}^{n}\beta_p}\,{}_{p-1}F_{q-1}\left(\begin{matrix}\alpha_1+1,\ \ldots,\ \alpha_{f-1}+1,\ \alpha_f+1,\ \ldots,\ \alpha_j+1\\ \beta_1+1,\ \ldots,\ \beta_{k-1}+1,\ \beta_k+1,\ \ldots,\ \beta_n+1\end{matrix}\middle|\,1\right). \tag{127}
$$

The two following relations allow one to transform $(3,2)$ Hypergeometric function into another $(3,2)$ with different parameters:

$$
{}_3F_2\left(\begin{matrix}\alpha_1,\ \alpha_2,\ \alpha_3\\ \beta_1,\ \beta_2\end{matrix}\middle|\,1\right) = \frac{\Gamma(\beta_2)\Gamma(\mathcal{S})}{\Gamma(\beta_2-\alpha_1)\Gamma(\beta_1+\beta_2-\alpha_2-\alpha_3)}\,{}_3F_2\left(\begin{matrix}\alpha_1,\ \beta_1-\alpha_2,\ \beta_1-\alpha_3\\ \beta_1,\ \beta_1+\beta_2-\alpha_2-\alpha_3\end{matrix}\middle|\,1\right)
$$

$$
{}_3F_2\left(\begin{matrix}\alpha_1,\ \alpha_2,\ \alpha_3\\ \beta_1,\ \beta_2\end{matrix}\middle|\,1\right) = \frac{\Gamma(\beta_1)\Gamma(\beta_2)\Gamma(\mathcal{S})}{\Gamma(\alpha_1)\Gamma(\beta_1+\beta_2-\alpha_1-\alpha_2)\Gamma(\beta_1+\beta_2-\alpha_1-\alpha_3)}\times \qquad ,
$$
$$
\times\,{}_3F_2\left(\begin{matrix}\beta_1-\alpha_1,\ \beta_2-\alpha_1,\ \mathcal{S}\\ \beta_1+\beta_2-\alpha_1-\alpha_2,\ \beta_1+\beta_2-\alpha_1-\alpha_3\end{matrix}\middle|\,1\right) \tag{128}
$$

where $\mathcal{S}$ is the test ratio variable defined in Eq.(122). These transformations are allowed only for $\mathrm{Re}(\mathcal{S}) > 0$, otherwise the Hypergeometric may not be well-defined. For $\mathrm{Re}(\mathcal{S}) = -1$ or $\mathrm{Re}(\mathcal{S}) = 0$, it is possible to extract the singularity to define the Hypergeometric. In the calculation pursued in appendix B.2.2, contour integration over these kind of Hypergeometric functions appeared. The Mellin-Barnes variable appears into the parameters α_i, β_j and thus the ratio test variable $\mathcal{S}$ depends on s. In this manner, it allows one to factorise the divergence of the Hypergeometric into poles of gamma functions such as $\Gamma(\mathcal{S})$ that can be easily integrated.

D.4 Thermal integral appearing in $\lambda\phi^4$ model

$$
K_2(\frac{m}{T}) = -\frac{32}{T^4}\int_0^\infty dp\,p\ \frac{n(E_p)}{E_p}\int_0^p dq\,q\ \frac{n(E_q)}{E_q}\int_{p-q}^{p+q} dk\,k\sum_{\sigma=-1,+1} f_2(E_\sigma,k) \tag{129}
$$

$$
K_3(\frac{m}{T}) = \frac{96}{T^4}\int_0^\infty dp\,p\ \frac{n(E_p)}{E_p}\int_0^p dq\,q\ \frac{n(E_q)}{E_q}\int_0^q dr\,r\ \frac{n(E_r)}{E_r}
$$
$$
\times\sum_{\sigma,\tau=-1,+1}\{f_3(E_{\sigma\tau},p+q+r) - f_3(E_{\sigma\tau},p+q-r) - f_3(E_{\sigma\tau},p-q+r) + f_3(E_{\sigma\tau},p-q-r)\}, \tag{130}
$$

where

$$
\begin{aligned}
f_2(E,k) &= \left(\frac{E^2-M_k^2}{E^2-k^2}\right)^{\frac{1}{2}} \ln\frac{(E^2-k^2)^{\frac{1}{2}}+(E^2-M_k^2)^{\frac{1}{2}}}{(E^2-k^2)^{\frac{1}{2}}-(E^2-M_k^2)^{\frac{1}{2}}} \quad , \quad k^2 < E^2-4m^2 \\
&= 2\left(\frac{M_k^2-E^2}{E^2-k^2}\right)^{\frac{1}{2}} \arctan\left(\frac{E^2-k^2}{M_k^2-E^2}\right)^{\frac{1}{2}} \quad , \quad E^2-4m^2 < k^2 < E^2 \\
&= \left(\frac{M_k^2-E^2}{k^2-E^2}\right)^{\frac{1}{2}} \ln\frac{(M_k^2-E^2)^{\frac{1}{2}}+(k^2-E^2)^{\frac{1}{2}}}{(M_k^2-E^2)^{\frac{1}{2}}-(k^2-E^2)^{\frac{1}{2}}} \quad , \quad E^2 < k^2
\end{aligned}
\tag{131}
$$

$$
\begin{aligned}
f_3(E,p) &= p\ln\frac{m^2-E^2+p^2}{m^2} + 2(m^2-E^2)^{\frac{1}{2}} \arctan\frac{p}{(m^2-E^2)^{\frac{1}{2}}} \quad , \; E^2 < m^2 \\
&= p\ln\frac{\left|E^2-m^2-p^2\right|}{m^2} + \left(E^2-m^2\right)^{\frac{1}{2}} \ln\frac{(E^2-m^2)^{\frac{1}{2}}+p}{\left|(E^2-m^2)^{\frac{1}{2}}-p\right|} \quad , \; E^2 > m^2
\end{aligned}
\tag{132}
$$

and

$$
\begin{aligned}
M_k^2 &= 4m^2+k^2 \\
E_\sigma(p,q) &= \sqrt{p^2+m^2}+\sigma\sqrt{q^2+m^2} \\
E_{\sigma\tau}(p,q,r) &= \sqrt{p^2+m^2}+\sigma\sqrt{q^2+m^2}+\tau\sqrt{r^2+m^2}\,.
\end{aligned}
\tag{133}
$$

In the limit $x \equiv m/T \to 0$ these can be expressed analytically as:

$$
K_2(x) \simeq \frac{(4\pi)^4}{72}\left(\ln x + \frac{1}{2} + \frac{\zeta'(-1)}{\zeta(-1)}\right) - 372.65\, x\,(\ln x + 1.4658)\,, \tag{134}
$$

$$
K_3(x) \simeq \frac{(4\pi)^4}{48}\left(-\frac{7}{15} + \frac{\zeta'(-1)}{\zeta(-1)} - \frac{\zeta'(-3)}{\zeta(-3)}\right) + 1600.0\, x\,(\ln x + 1.3045)\,. \tag{135}
$$

In the numerics we rather use the exact expressions Eqs.(129), (130).

D.5 Bibliography

[1] Joseph I. Kapusta. Quantum Chromodynamics at High Temperature. *Nucl. Phys. B*, 148:461–498, 1979.

[2] R.E Norton and J.M Cornwall. On the formalism of relativistic many body theory. *Annals of Physics*, 91(1):106–156, 1975.

[3] Aleksi Kurkela, Paul Romatschke, and Aleksi Vuorinen. Cold Quark Matter. *Phys. Rev. D*, 81:105021, 2010, 0912.1856.

[4] Tyler Gorda, Aleksi Kurkela, Risto Paatelainen, Saga Säppi, and Aleksi Vuorinen. Cold quark matter at N3LO: Soft contributions. *Phys. Rev. D*, 104(7):074015, 2021, 2103.07427.

[5] Jens O. Andersen, Emmanuel Petitgirard, and Michael Strickland. Two loop HTL thermodynamics with quarks. *Phys. Rev. D*, 70:045001, 2004, hep-ph/0302069.

[6] Najmul Haque, Aritra Bandyopadhyay, Jens O. Andersen, Munshi G. Mustafa, Michael Strickland, and Nan Su. Three-loop HTLpt thermodynamics at finite temperature and chemical potential. *JHEP*, 05:027, 2014, 1402.6907.

[7] L.J. Slater. *Generalized Hypergeometric Functions.* Cambridge University Press, 1966.